Revolutionizing High Ammonia Waste Stream Treatment: Advanced Efficacy of the Novel Granular Sludge Reactor

by

Xin Zou

A thesis submitted in partial fulfillment of the requirements for the degree of

Doctor of Philosophy

in

Environmental Engineering

Department of Civil and. Environmental Engineering
University of Alberta

ABSTRACT

High ammonia waste streams, containing both inorganic and organic nitrogen (N), can lead to algae outgrowth and the formation of disinfection byproducts if not properly treated. These waste streams are traditionally combined with municipal wastewaters for treatment. However, their high ammonia content can compromise the effectiveness of the wastewater treatment plants (WWTPs), leading to more stringent discharge limits for these sidestreams and industrial wastewaters. This thesis aims to develop a highly efficient technology for treating ammonia rich waste streams and to optimize the operation strategies for treating wastewaters with varied carbon to nitrogen (C/N) and alkalinity to nitrogen (Alk/N) ratios.

Aerobic granular sludge (AGS) is featured by its superior biomass retention, high biomass density, excellent settling capacity, and resilience to toxic environments and shock loadings. These attributes make it a promising alternative for high ammonia wastewater treatment, especially those from industrial sources or those contaminated with recalcitrant compounds. Although AGS is a well-established technology for treating municipal wastewaters with low ammonia content and a C/N ratio around 10, its application to high ammonia wastewater has been rarely explored. High ammonia waste streams, often characterized by low C/N and Alk/N ratios, pose significant challenges for AGS application, including slow granulation, granule instability, and limited N removal capacity.

This thesis first examined the impact of C/N ratios and influent solid content on N removal performance and granule structural and functional stability (Chapters 4 and 5). The results demonstrated that high ammonia conditions with low C/N ratios are conducive to the enrichment

of highly efficient autotrophic ammonia oxidizing bacteria (AAOB), achieving higher ammonia removal compared to high C/N conditions, where heterotrophic ammonia oxidizing bacteria (HAOB) was dominated. Subsequent tests on high ammonia wastewater with varied C/N and low Alk/N ratios in the AGS system indicated that a C/N ratio over 6 is required for high N removal. Low N removal was observed under conditions of low C/N and Alk/N ratios, likely due to an insufficient denitrification process and low alkalinity availability (Chapter 6). Additionally, a thorough microbial analysis showed that granules contributed more than flocs to N reduction under high C/N conditions, whereas flocs contributed more under low C/N conditions (Chapter 7).

Based on these findings, a new granular sludge reactor (GSR) was developed and tested for its effectiveness in treating high ammonia, low C/N waste streams. The GSR demonstrated an outstanding N removal capacity of up to 4.2 kg N/(m^3·d) and a rapid startup for treating wastewaters rich in recalcitrant compounds, as well as efficacy in organic N removal (Chapter 8, 9 and 10). In the GSR, the retention of highly active flocs and small granule, alongside strategies to facilitate the denitrification process for alkalinity recovery, contributed to such high N removal capacity. Furthermore, the GSR proved its capability in N removal and granule stability when using high COD wastewater as carbon source for the denitrification process, highlighting its promising upscaling potential (Chapter 11).

In summary, this thesis has elucidated the impact of waste streams' characteristics on AGS treatment performance and identified the critical parameters controlling the enhancement of high ammonia waste stream treatment. Through a deep understanding of the influence of C/N ratios

and detailed microbial analysis of the roles of granules and flocs, significant insights were gained. The newly developed GSR has opened up new opportunities for the enhanced removal of both inorganic and organic N from high ammonia waste streams.

PREFACE

This thesis is an original work conducted by Xin Zou under the supervision of Prof. Dr. Yang Liu at the University of Alberta. Xin Zou conducted all experiments and was responsible for conceptualization, methodology, investigation, formal analysis, data curation, visualization, and writing the original draft. Dr. Yang Liu contributed to the conceptualization, project administration, supervision, funding acquisition, and the review and editing of the manuscript. Contributions from colleagues are acknowledged as follows:

Chapter 4: (A version of this chapter has been published)

Zou, X., Gao, M., Mohammed, A., & Liu, Y. (2023). Responses of various carbon to nitrogen ratios to microbial communities, kinetics, and nitrogen metabolic pathways in aerobic granular sludge reactor. *Bioresource Technology*, *367*, 128225.
https://doi.org/10.1016/j.biortech.2022.128225

Author contribution statement:

Xin Zou: Conceptualization, Methodology, Software, Formal analysis, Writing - original draft. Mengjiao Gao: Writing - review & editing, Methodology. Abdul Mohammed: Writing - review & editing, Supervision. Yang Liu: Conceptualization, Writing - review & editing, Supervision, Project administration, Funding acquisition.

Chapter 5: (A version of this chapter has been published)

Zou, X., Gao, M., Sun, H., Zhang, Y., Yao, Y., Guo, H., & Liu, Y. (2024). Influence of residual anaerobic granular sludge (AnGS) from anaerobically digested molasses wastewater in aerobic granular sludge reactor. *Science of the Total Environment*, *949*, 175206.

Author contribution statement:

Xin Zou: Conceptualization, Methodology, Formal analysis, Investigation, Visualization, Writing - original draft. Yiduo Yao: Methodology, Investigation. Yang Lu: Formal analysis. Lu Kong: Investigation. Mengjiao Gao: Formal analysis. Yihui Zhang: Investigation. Hengbo Guo: Investigation. Yang Liu: Conceptualization, Writing - review & editing, Supervision, Project administration, Funding acquisition.

Chapter 6: (A version of this chapter has been submitted for journal publication)
Author contribution statement:
Xin Zou: Conceptualization, Methodology, Formal analysis, Investigation, Visualization, Writing - original draft. Yiduo Yao: Methodology, Investigation. Lu Kong: Investigation. Yang Lu: Formal analysis. Mengjiao Gao: Formal analysis. Yihui Zhang: Investigation. Hengbo Guo: Investigation. Yang Liu: Conceptualization, Writing - review & editing, Supervision, Project administration, Funding acquisition.

Chapter 7: (A version of this chapter has been submitted to journal publication)
Author contribution statement:
Xin Zou: Conceptualization, Methodology, Formal analysis, Investigation, Visualization, Writing - original draft. Yang Lu: Formal analysis. Yang Liu: Conceptualization, Writing - review & editing, Supervision, Project administration, Funding acquisition.

Chapter 8: (A version of this chapter has been published)
Zou, X., Gao, M., Yao, Y., Zhang, Y., Guo, H., & Liu, Y. (2024). Efficient nitrogen removal from ammonia rich wastewater using aerobic granular sludge (AGS) reactor: Selection and enrichment of effective microbial community. *Environmental Research*, *251*, 118573. https://doi.org/10.1016/j.envres.2024.118573
Author contribution statement:
Xin Zou: Conceptualization, Methodology, Formal analysis, Investigation, Visualization, Writing - original draft. Mengjiao Gao: Formal analysis. Yiduo Yao: Methodology, Investigation. Yihui Zhang: Investigation. Hengbo Guo: Investigation. Yang Liu: Conceptualization, Writing - review & editing, Supervision, Project administration, Funding acquisition.

Chapter 9: (A version of this chapter has been published)
Zou, X., Mohammed, A., Gao, M., & Liu, Y. (2022). Mature landfill leachate treatment using granular sludge-based reactor (GSR) via nitritation/denitritation: Process startup and optimization. *Science of the Total Environment*, *844*, 157078. https://doi.org/10.1016/j.scitotenv.2022.157078
Author contribution statement:

Xin Zou: Conceptualization, Methodology, Software, Formal analysis, Writing - original draft. Abdul Mohammed: Writing - review & editing, Supervision. Mengjiao Gao: Writing - review & editing, Methodology. Yang Liu: Conceptualization, Writing - review & editing, Supervision, Project administration.

Chapter 10: (A version of this chapter has been published)

Zou, X., Zhang, Y., Gao, M., Yao, Y., Guo, H., & Liu, Y. (2024). Enhancing biological dissolved organic nitrogen removal in landfill leachate wastewater: The role of sodium acetate co-metabolism. *Chemical Engineering Journal*, *479*, 147714.
https://doi.org/10.1016/j.cej.2023.147714

Author contribution statement:

Xin Zou: Conceptualization, Methodology, Formal analysis, Investigation, Visualization, Writing - original draft. Yihui Zhang: Methodology, Formal analysis. Mengjiao Gao: Methodology, Writing - review & editing. Yiduo Yao: Investigation. Hengbo Guo: Investigation. Yang Liu: Conceptualization, Writing - review & editing, Supervision, Project administration, Funding acquisition.

Chapter 11: (A version of this chapter has been published)

Zou, X., Yao, Y., Gao, M., Zhang, Y., Guo, H., & Liu, Y. (2024). Treatment of high ammonia anaerobically digested molasses wastewater using aerobic granular sludge reactor. *Bioresource Technology*, 131056.
https://doi.org/10.1016/j.biortech.2024.131056

Author contribution statement:

Xin Zou: Conceptualization, Methodology, Formal analysis, Investigation, Visualization, Writing - original draft. Mengjiao Gao: Methodology, Investigation. Huijuan Sun: Formal analysis. Yihui Zhang: Investigation. Yiduo Yao: Investigation. Hengbo Guo: Investigation. Yang Liu: Conceptualization, Writing - review & editing, Supervision, Project administration, Funding acquisition.

Other publications during candidature:

1. **Zou, X.**, Zhou, Y., Gao, M., Yang, S., Mohammed, A., & Liu, Y. (2022). Effective N2O emission control during the nitritation/denitritation treatment of ammonia rich wastewater. *Journal of Environmental Chemical Engineering*, 10(2), 107234.

2. Gao, M., Guo, B., **Zou, X.**, Guo, H., Yao, Y., Chen, Y., Guo, J., & Liu, Y. (2024). Mechanisms of anammox granular sludge reactor effluent as biostimulant: Shaping microenvironment for anammox metabolism. *Bioresource Technology*, 130962.

3. Guo, H., Gao, M., Yao, Y., **Zou, X.**, Zhang, Y., Huang, W., & Liu, Y. (2024). Enhancing anammox process with granular activated carbon: A study on Microbial Extracellular Secretions (MESs). *Science of The Total Environment*, 926, 171980.

4. Gao, M., **Zou, X.**, Dang, H., Guo, H., Yao, Y., Chen, Y., Guo, J., & Liu, Y. (2024). Enhancing anammox process at moderate temperature via employing anammox granular sludge reactor effluent addition. *Process Safety and Environmental Protection*, 182, 894-902.

5. Gao, M., Dang, H., **Zou, X.**, Yu, N., Guo, H., Yao, Y., & Liu, Y. (2023). Deciphering the role of granular activated carbon (GAC) in anammox: Effects on microbial succession and communication. *Water Research*, 233, 119753.

6. Gao, M., **Zou, X.**, Dang, H., Mohammed, A. N., Yang, S., Zhou, Y., Yao Y., Guo H., & Liu, Y. (2023). Exploring interactions between quorum sensing communication and microbial development in anammox membrane bioreactor. *Journal of Environmental Chemical Engineering*, 109339.

7. Guo, H., Gao, M., Lee, K., Yao, Y., **Zou, X.**, Zhang, Y., Huang, W., & Liu, Y. (2023). Rapid enrichment of anammox bacteria for low-strength wastewater treatment: Role of influent nitrite and nitrate ratios in sequencing batch reactors (SBRs). *Journal of Environmental Chemical Engineering*, 11(6), 111434.

DEDICATION

To my dear parents

Laichang & Qingping

To my beloved families and friends

To peace and love

"Those who contemplate the beauty of the earth find reserves of strength that will endure as long as life lasts. There is something infinitely healing in the repeated refrains of nature -- the assurance that dawn comes after night, and spring after winter."

— Rachel Carson, Silent Spring

ACKNOWLEDGEMENTS

The story starts in the summer of 2015 when I coincidentally read "*Silent Spring*" by Rachel Carson. This book illuminated the importance of a sustainable environment, sparking a connection between me and the environmental studies.

Since 2017, I had dedicated nearly seven years to wastewater nutrient removal. My unexpected journey into granular sludge processes began in the autumn of 2020. Look back the four years, I am proud of my progress in problem solving and self-studying skills and the days and nights spent in the lab. The pandemic overlapped with much of my PhD journey, making it a challenging time. My accomplishments over the past four years would not have been possible without the support of my supervisor, colleagues, friends, families, and the countless medical staff, scientists, and volunteers.

My supervisor, Prof. Yang Liu, has been a perfect role model for my future career and life. Dr. Liu's sharp mind, dedication to practical applications, and unwavering commitment to excellence have been inspiring. I am fortunate to have worked with such an outstanding and inspiring supervisor from the beginning of my academic career. Under Dr. Liu's supervision, I kept push myself to think more clearly, logically, and creatively. Beyond her academic prowess, Dr. Liu's kindness and resilience taught me to remain modest and resilient in the face of setbacks. I deeply grateful for Dr. Liu's guidance throughout this journey.

I would like to extend my thanks to my colleagues and friends. Dr. Huixin Zhang and Dr. Huijuan Sun, thank you for your strong support in lab-scale and pilot-scale projects. Dr. Lei Zhang, Dr. Yingdi Zhang, Dr. Najiaowa Yu, Dr. Qi Huang, Dr. David Zhao, Dr. Mostafa Khalil, Anqi Mou, Xinya Yang, Yiyang Yuan, Lu Kong, Chengyuan Li and Carlo B. Bais, thank you for being reliable and helpful lab mates. My dearest friends Yihui Zhang, Hengbo Guo, Mozhu Li, Dr. Jia Li, Dr. Lingjun Meng and Dr Zhexuan An, thank you for your emotional support and for cheering me up with your bright spirits. Anita, thank you for your warm spirit and care, your support has been invaluable.

Special thanks to my dearest sisters in Edmonton, Dr. Mengjiao Gao, Danqin Shangguan and Yiduo Yao. I am thankful for your companionship during late nights and all the laughter we shared. These four years are memorable and filled with shared setbacks, achievements, happiness, and sadness. I was also impressed by Mengjiao's agile mind, logical thinking, and indomitable spirit. She taught me how to communicate my ideals effectively and guide me to become a well-trained PhD candidate. Thank you for always standing by my side and showing your support. Fan Zhang, thank you for taking care of me during my busiest times and making me feel at home. Helei Hu, Yaolu Li and Huaike Su, thank you for your online companionship and for being present during every important moment in my life.

Thanks to the financial support from the Natural Sciences and Engineering Research Council of Canada (NSERC) Discovery Project, the Natural Sciences and Engineering Research Council of Canada (NSERC) Alliance Project, the City of Calgary, the City of Edmonton, Alberta Innovates, the Regional District of Nanaimo, the Canada Research Chair (CRC) in Future Water Services (Liu, Y.), and the China Scholarship Council (CSC) Ph.D. scholarship (Zou, X. & Guo, H.). The authors also acknowledge the support provided by Advancing Canadian Water Assets (ACWA) (Liu, Y.).

Last but not least, I would like to express my deepest gratitude to my parents. It is your guidance, unconditional love and support that make me who I am now.

TABLE OF CONTENTS

LIST OF TABLES

LIST OF FIGURES

LIST OF ABBREVIATIONS

N	Nitrogen
TDN	Total dissolved nitrogen
DON	Dissolved organic nitrogen
WWTPs	Wastewater treatment plants
Nit/DNit	Nitritation/denitritation
AAOB	Autotrophic ammonia oxidizing bacteria
COD	Chemical oxygen demand
CAS	Conventional activated sludge
AGS	Aerobic granular sludge
TIN	Total inorganic nitrogen
C/N	Carbon to nitrogen
GSR	Granular sludge reactor
Alk/N	Alkalinity to nitrogen
TKN	Total Kjeldahl Nitrogen
NOB	Nitrite oxidizing bacteria
SOAD	Sulfide-oxidizing autotrophic denitrification
Anammox	Anaerobic ammonia oxidation
Nif/DNif	Nitrification/denitrification
HNAD	Heterotrophic nitrification aerobic denitrification
HNADMs	Heterotrophic nitrification aerobic denitrification microorganisms
SVI	Sludge volume index
sCOD	soluble chemical oxygen demand
MLSS	Mixed liquor suspended solids
MLVSS	Mixed liquor volatile suspended solids
bCOD	Biodegradable chemical oxygen demand
HAOB	Heterotrophic ammonia oxidizing bacteria
DO	Dissolved oxygen
SBR	Sequencing batch reactors
SRT	Solid retention time

EPS	Extracellular polymeric substances
FA	Free ammonia
amo	Ammonia monooxygenase
hao	Hydroxylamine oxidoreductase
nxr	Nitrite oxidoreductase
nar	Nitrate reductases
nir	Nitrite reductase
nor	Nitric oxide reductase
nosZ	Nitrous oxide reductase
NAR	Nitrite accumulation rate
S-EPS	Soluble extracellular polymeric substance
L-EPS	Loosely bound extracellular polymeric substance
T-EPS	Tightly bound extracellular polymeric substance
ASVs	Amplicon sequence variants
HRT	Hydraulic retention time
PAOs	Polyphosphate accumulating organisms
GAOs	Glycogen accumulating organisms
NSR	Nitrite oxidoreductase
qPCR	quantitative polymerase chain reaction
TN	Total nitrogen
BOD	Biochemical oxygen demand
TS	Total solids
TSS	Total suspended solids
DOM	Dissolved organic matter
BNR	Biological nutrient removal
SMPs	Soluble microbial products
bsCOD	biodegradable soluble COD
DPAOs	Denitrifying polyphosphate accumulating organisms

Chapter 1. Introduction

1.1 Background and motivations

In high ammonia waste streams that sourced from municipal (i.e., anaerobically digested sludge supernatant) and industrial (i.e., anaerobically digested molasses wastewater) sectors, inorganic nitrogen (N) constitutes approximately 75% of the total dissolved nitrogen (TDN), with dissolved organic nitrogen (DON) making up the remaining 25%. These wastewaters, such as anaerobically digested sludge supernatant, are characterized by small volumes and high ammonia concentrations, which accounts for only 1% of the total plant influent flow but contributes 20 to 40% of the total N load. Conventionally, these high ammonia waste streams are integrated with mainstream wastewater treatment systems before discharging. This paradigm can destabilize mainstream treatment performance due to the significant ammonia loading and the potential formation of toxic disinfection by-products [1].

The removal of inorganic N has been extensively studied. For the treatment of high ammonia waste streams, nitritation/denitritation (Nit/DNit) is more economically favourable compared to the traditional nitrification/denitrification (Nif/DNif) process. Nit/DNit converts ammonia to nitrite, which is then directly denitrified to nitrogen gas ($NH_4^+ \rightarrow NO_2^- \rightarrow N_2$), whereas the traditional Nif/DNif process involves additional steps for nitrite oxidation to nitrate and nitrate reduction ($NH_4^+ \rightarrow NO_2^- \rightarrow NO_3^- \rightarrow NO_2^- \rightarrow N_2$). Nit/DNit approach can save up to 25% in energy for oxygen supply and 40% in chemical demand. However, the retention of autotrophic ammonia oxidizing bacteria (AAOB), which are slow-growing microorganisms crucial for the Nit/DNit process, remains a major challenge that limits the overall treatment capacity.

Studies on organic N removal are scarce in the literature. It has been reported that N-containing organics can be degraded through hydrolysis and fermentation (decarboxylation and deamination) by extracellular enzymes. In conventional anaerobic/anoxic/oxic treatment systems, the anaerobic zone, with the presence of chemical oxygen demand (COD), has been identified as the primary contributor to DON removal, a process that generally involves hydrolysis and fermentation [2, 3]. The reported approaches for DON removal primarily rely on membrane filtration (i.e.,

ultrafiltration, and nanofiltration) [4], which can impose substantial operational and maintenance costs as well as significant energy requirements.

In comparison to existing conventional activated sludge (CAS) system, an emerging biofilm-based technology, the aerobic granular sludge (AGS) system offers substantial advantages. The AGS system is a self-immobilizing microbial aggregate without the requirement for external supporting material, significantly enhancing biomass retention, which benefits the retention of AAOB. The AGS system is featured by its exceptional biomass retention, high biomass density, superior settling capacity, and resilience to toxic environments and shock loadings, making it a superior, low footprint alternative for high ammonia wastewater treatment [5]. The nature of AGS promotes the growth of diverse anaerobic, anoxic, facultative, and aerobic microorganisms, potentially enhancing the simultaneous removal of COD, inorganic N and organic N. Besides the aforementioned attractive aspects of adopting AGS in high ammonia wastewater treatment, two critical issues still need to be addressed: the varied wastewater characteristics, particularly the deficiency of alkalinity, and the limited biodegradable organics observed in some anaerobically digested high ammonia wastewaters.

A sufficient alkalinity to N (Alk/N) ratio of 7.14 is essential to achieve complete ammonia oxidation, as pH drops during this process, and AAOB activity ceased when pH falls below 7 [6]. While external alkalinity can be supplied to support the treatment of low Alk/N wastewaters, it can also be replenished through denitritation or denitrification processes. These processes, therefore, play a crucial role in treating low Alk/N wastewaters. However, existing AGS systems often exhibit low denitrification efficiencies, which hinders their application for the treatment of high ammonia waste streams.

AGS technology is typically applied for the treatment of high C/N wastewater with a ratio of 10. The C/N ratio plays a key role in the granulation process and AGS stability. A low C/N ratio was reported to extend the granulation process, and a C/N ratio over 10 or below 1 might adversely impact the N removal performance and granule stability [7]. Additionally, a high C/N ratio might facilitate the denitrification process, while the competition between heterotrophic and autotrophic microorganisms might adversely affect the ammonia removal performance. To date, no study has

employed AGS system for organic N removal from high ammonia waste streams, and only limited studies have explored the feasibility and efficacy of AGS in inorganic nitrogen removal from high ammonia waste streams with concentrations over 400 mg N/L [8-12]. Among the reported studies, thorough investigation into the impact of C/N ratios on granular sludge-based systems and the pathways for inorganic and organic N removal are underexplored.

In the current study, a new granular sludge reactor design, referred to as the granular sludge reactor (GSR), was developed to address the issues mentioned above. Unlike conventional AGS studies, which predominantly rely on continuous aeration, this newly proposed design introduced an anoxic phase with additional COD to enhance inorganic and organic N removal and optimize COD utilization in high ammonia waste streams. Over the past four years, 12 reactors were operated to address the aims of this thesis and to provide important mechanistic understanding and practical guidance for upscale application of the GSR technology for the treatment of ammonia rich waste streams.

1.2 Research objectives

The primary aim of this thesis is to develop a highly efficient technology for the treatment of ammonia rich waste streams and to optimize the operation strategy for treating waste streams with varied C/N and Alk/N ratios. This objective was accomplished through three specific objectives:

Objective 1. Evaluate the influence of waste stream characteristics (C/N ratios and residual solid content) on N removal pathways and granular stability.

Objective 2. Identify the critical process controls in AGS treating high ammonia waste streams with varied C/N ratios.

Objective 3. Apply and optimize the newly developed GSR for the removal of inorganic and organic N from high ammonia waste streams.

1.3 Thesis outline

This thesis consists of twelve chapters.

Chapter 1 provides a brief introduction of the background, research objectives and approaches, and an outline of this thesis.

Chapter 2 offers a comprehensive literature review related to the objectives.

Chapter 3 lists the general materials and methods adopted in this thesis.

Chapters 4-5 address the Objective 1, investigating the impact of waste stream characteristics, including C/N ratios and solid content, on N removal pathways and granule stability in AGS. These chapters provide information on the selection of N removal pathway that guide the following studies. Specifically, Chapter 4 examines the impact of C/N ratios on ammonia oxidation pathways and their contributions to N removal capacity, based on specific microbial activity tests and microbial community results. The potential mechanism for the community and N pathway shifts were proposed. Chapter 5 explores the impact of influent solids on AGS, focusing on granular sludge functional and structural stability and N removal efficiency.

Chapters 6-7 tackle Objective 2, exploring key control parameters in high ammonia waste stream treatment and guiding the development of the newly proposed GSR. Chapter 6 highlights the limitation of AGS in treating high ammonia, low alkalinity waste streams under varied C/N ratios, with a detailed microbial community analysis. Chapter 7 investigates the contributions of granules and flocs to N removal capacity under varied C/N ratios. A systematic microbial community analysis was conducted to identify divergences between granules and flocs and their responses during C/N ratio shifts.

Chapters 8-11 address Objective 3, evaluating the efficacy of the newly developed GSR for inorganic and organic N removal from high ammonia waste streams. Chapter 8 focuses on inorganic N removal from high ammonia waste streams with low C/N and low Alk/N ratios. Chapter 9 assesses the GSR efficacy in the treatment of high ammonia, low C/N ratio and heavy metal contaminated wastewater, with a specific focus on inorganic N removal. Chapter 10 investigates the dissolved organic nitrogen (DON) removal in high ammonia waste streams. Chapter 11 evaluates the feasibility of utilizing high COD waste streams as a replacement for commercial carbon source in N removal within the GSR.

Chapter 12 concludes the research findings and achievements, offering recommendations for future research.

Chapter 2. Literature Review

2.1 Nitrogen fractions in high ammonia waste streams

The high ammonia waste streams that are mentioned in this thesis primarily originated from aerobic or anaerobic digestion processes. These waste streams are characterized by high ammonia, over 400 mg/L, and have varied biodegradable COD (bCOD) levels, with bCOD/N ratios ranging from 0.1 to 10 [6, 13]. Alongside the high ammonia level, DON compounds are released into the liquid phase during anaerobic digestion. The inorganic N fraction comprises ammonia, nitrite and nitrate, while organic N consist of a complex matrix of various compounds. This includes biodegradable compounds like amino acids, proteins and amino sugars, and nonbiodegradable compounds, such as humic acids and fulvic acids [6, 14, 15]. Approximately 50% of the released DON is recalcitrant, making it challenging for wastewater treatment plants (WWTPs) to meet stringent discharge limits, with Total Kjeldahl Nitrogen (TKN) concentrations below 50 mg/L. This highlights the need for effective technology to treat such high ammonia waste streams.

2.2 Biological processes for inorganic nitrogen removal from high ammonia waste streams

Biological processes for treating high ammonia waste streams can be categorized based on different C/N ratios, as the C/N ratio is a critical factor influencing N removal performance. Previous studies have not clearly defined high and low C/N ratios. Therefore, in this thesis, a C/N ratio lower than 3 is considered low, and a C/N ratio over 3 is considered high. This classification is based on the C/N ratio required for the completion of the denitrification process.

2.2.1 Inorganic nitrogen removal from low C/N ratio waste streams

2.2.1.1 Conventional nitrification/denitrification

High ammonia wastewater is traditionally being treated by combining with domestic wastewater and through nitrification/denitrification process. Nitrification process involves ammonia oxidation to nitrite (by autotrophic ammonia oxidizing bacteria (AAOB)) and then nitrite oxidation to nitrate (by nitrite oxidizing bacteria (NOB)) under aerobic condition ($NH_4^+ \rightarrow NO_2^- \rightarrow NO_3^-$). Denitrification process comprises nitrate reduction to nitrite followed by nitrite reduction

to nitric oxide, nitrous oxide, then to nitrogen gas ($NO_3^- \rightarrow NO_2^- \rightarrow NO \rightarrow N_2O \rightarrow N_2$) with the presence of organic carbon as electron donor.

2.2.1.2 Nitritation/denitritation

Nitritation/denitritation (Nit/DNit) converts ammonia to nitrite (Reaction 2.1) and then directly denitrifies to nitrogen gas without producing nitrate (Reaction 2.2). Compared to the conventional Nif/DNif process, Nit/DNit can reduce oxygen demand and carbon demand by 25% and 40%, respectively [16]. High ammonia waste streams, such as centrate, mature landfill leachate, and various industrial wastewaters, often lack sufficient alkalinity and biodegradable organic carbon, which are essential for efficient ammonia removal. As a result, Nif/DNif process typically require intensive energy inputs for aeration and chemical additions for alkalinity and external carbon sources. Aeration is one of the most energy-intensive processes in WWTPs [17]. Therefore, Nit/DNit has emerged as a superior alternative to the conventional process, especially for the treatment of high ammonia waste streams.

$$2NH_4^+ + 3O_2 \rightarrow 2NO_2^- + 4H^+ + 2H_2O \qquad \text{Reaction 2.1}$$

$$2NO_2^- + CH_3COO^- \rightarrow N_2 + 2CO_2 + H_2O + OH^- \qquad \text{Reaction 2.2}$$

2.2.1.3 Autotrophic nitrogen removal processes

The autotrophic N removal processes potentially occurring in the treatment of high ammonia, low C/N ratio wastewaters involve anaerobic ammonia oxidation (anammox) and sulfide-oxidizing autotrophic denitrification (SOAD). The anammox process converts ammonia and nitrite to nitrogen gas, saving 60% of aeration consumption and eliminating the need for organic carbon [18]. This process is typically combined with nitritation. However, the slow growth and high sensitivity of anammox bacteria to nitrite, oxygen and temperature limit their practical applications [19, 20].

The sulfide-oxidizing autotrophic denitrification (SOAD) process utilizes sulfide or thiosulfate as an electron donor for denitrification. This process is independent of organic carbon, and thus saving the chemical costs. The presence of sulfide in industrial and sewer discharges has been documented [21], suggesting that this process might be feasible when treating high ammonia digestate.

2.2.2 Inorganic nitrogen removal from high C/N ratio waste streams

The conventional Nif/DNif and Nit/DNit processes are also capable of performing N removal under high COD conditions, whereas anammox process is likely inhibited under high COD conditions [22]. Additionally, heterotrophic nitrification aerobic denitrification (HNAD), firstly reported in 1988 [23], can also facilitate N removal from high COD wastewaters. During the HNAD process, heterotrophic nitrification aerobic denitrification microorganisms (HNADMs) oxidizes ammonia in the presence of COD and perform denitrification under aerobic conditions [24]. This process can be carried out by a single microorganism, which directly converts ammonia to N_2 [25, 26].

2.3 Biological processes for organic nitrogen removal from high ammonia waste streams

Most research on DON removal has focused on physical and chemical methods [27, 28]. These methods often include coagulation, nanofiltration, advanced oxidation, and adsorption [4, 29, 30]. Generally, biological process showed limited capability for DON removal. Most biodegradable organic N is converted to ammonia via hydrolysis and acidogenesis during anaerobic digestion. In mainstream treatment systems, the anaerobic zone showed high DON removal (~68%), while limited removal or even production of DON was observed in the anoxic phase [3, 15]. In the aerobic phase, elevated DON concentrations were obtained [3]. Further, the denitrification process has been reported as sink and source of DON, with the influence of C/N ratios on DON being controversial [31, 32]. Although DON is recognized as one of the most problematic constituents in the discharge of leachate into WWTPs due to its recalcitrate nature, successful strategies for DON removal remain scarce.

2.4 Biological technologies for high ammonia waste stream treatment

For inorganic N removal from high ammonia waste streams with varied C/N ratios, Nit/DNit is preferred process due to its robustness against operational variations and cost-effectiveness. This process involves autotrophic ammonia oxidizing bacteria (AAOB) and denitrifiers. The key to achieve high Nit/DNit capacity is the retention of slow growing AAOB.

2.4.1 Conventional activated sludge technology

For sewage treatment in WWTPs, conventional activated sludge (CAS) technology necessitates a large footprint. This is due to the poor settleability and low biomass density, typically ranging from 3 to 5 g/L for CAS [33]. Consequently, a large secondary settling tank is required to ensure sufficient retention of microbes.

2.4.2 Emerging biofilm-based technology: aerobic granular sludge

Towards a more energy efficient treatment system, biofilm-based technologies have emerged to create more compact WWTPs. These technologies rely on the immobilization of microbes on carriers or retaining microbes in the system via membrane separation [33]. However, they are limited by biofilm mass transfer and high maintenance costs.

In the late 1990s, aerobic granular sludge (AGS) technology was discovered. AGS is a unique biofilm-based microbial consortium without the need for a supporting material, advancing as a compelling alternative to activated sludge systems for wastewater treatment. Generally, a sludge size over 0.2 mm and sludge volume index (SVI) below 80 mL/g was considered granular sludge, otherwise classified as suspended sludge or flocs. AGS is featured by its outstanding biomass density, settling capacity, biomass retention, microbial diversity, tolerance to toxic compounds, and ability to withstand shock loadings [34]. These features enable wastewater treatment plants to save on land requirements (such as settling tank) and capital costs relevant to WWTP operation [35]. Moreover, AGS enhances industrial wastewater treatment performance and stability [36]. The superior biomass retention of AGS supports the growth of AAOB, thereby potentially achieving high N removal capacity with this technology. However, previous studies have primarily focused on COD removal, while N removal studies have been limited [37].

2.5 Aerobic granular sludge technology: status and challenges

Driven by the increasing need for sustainability and stringent discharge standards, research has focused on elevating hydraulic loads without increasing reactor volume. Treatment systems have now shifted towards implementing AGS technology in municipal and industrial wastewater treatment.

2.5.1 Aerobic granular sludge in low ammonia wastewater treatment – a well-established technology

AGS technology has been adopted for the treatment of municipal wastewaters, which typically have ammonia concentrations ranging from 30 to 50 mg/L and biodegradable COD (bCOD) concentrations around 200 to 500 mg/L [38]. The high C/N ratios approximately 10 in municipal wastewaters are favourable for the granulation process. The first full scale AGS installation was accomplished using Nereda® biotechnology. By 2021, 88 full scale AGS-based WWTPs had been constructed, with 80 applied to municipal wastewater treatment by the Nereda® and S:Select® brands [5]. The Nereda® AGS system operates with simultaneous fill and draw, continuous aeration and settling. The N loading rate that achieved in this system ranges from 0.4 to 1.2 kg/(m^3·d) [39, 40]. Key factors driving successful AGS implementation include rapid granulation and long-term stability.

2.5.2 Aerobic granular sludge in high ammonia waste stream treatment: status

To date, only six studies have adopted AGS for the treatment of landfill leachate and industrial wastewater with ammonia concentrations over 400 mg/L and C/N ratios ranging from 0.4 to 13.7 (Table 2.1). With high C/N ratios (over 3), ammonia removal efficiencies ranged from 50% to 99%, while efficiencies of 84% to 88% were achieved with low C/N ratios (below 3). Under both high and low C/N conditions, TIN removal efficiencies were below 75%. Among these, only one study investigated the applicability of AGS for high ammonia, low C/N wastewater treatment.

Table 2.1 Reported studies using aerobic granular sludge system for the treatment of high ammonia waste streams.

Reactor type	Waste streams	NH_4^+-N concentration (mg/L)	C/N ratio	Treatment process	NH_4^+-N removal efficiency	TIN removal efficiency	N loading rate (kg/(m3·d))	Reference
AGS	Landfill leachate	366	13.7	Nif/DNif	95%	75%	0.4	[12]
AGS	Swine slurry	1823	7.5	Nif/DNif	< 50%	< 50%	1.0	[41]
AGS	Livestock	650	3	-	-	73%	-	[11]
AGS	Synthetic	120-500	1.6-6.8	Nit or Nif	99%	23%	0.7	[42]
AGS	Synthetic	< 500	2	Nit	84%	40%	1.6	[43]
AGS-Fenton-AS	Landfill leachate	512	0.4	Nit/DNit	88%	75%	-	[8]

2.5.3 Aerobic granular sludge in high ammonia waste stream treatment: challenges

The primary challenges for adopting AGS technology for the treatment of high ammonia, low COD wastewaters can be attributed to the following two aspects:

I. Slow granule formation and granule instability

High ammonia levels elevated free ammonia (FA) concentration, which has been reported to negatively affect the granulation process. This is due to the reduced extracellular polymeric substance (EPS) production and lowered hydrophobicity, which hindered cell attachments [44]. Low C/N condition limit the growth of heterotrophic bacteria, the main contributors to EPS production, leading to the formation of loosely structured granular sludge. Additionally, the residual solids in wastewater potentially influencing the granule stability.

II. Limited nitrogen removal

Achieving high N removal in high ammonia waste streams hinges on maintaining appropriate Alk/N and C/N ratios. These ratios are critical for efficient N oxidation and reduction. The Alk/N ratios are vital because pH decreases during ammonia oxidation. To maintain a pH range of 7.5 to 8.0, which is suitable for ammonia oxidation, an Alk/N ratio of 7.14 is necessary [6]. Most high ammonia wastewaters have an Alk/N ratio below 7, leading to suboptimal conditions for ammonia oxidation. C/N ratios are crucial for N removal efficiency and alkalinity generation. During the denitrification process, alkalinity could be generated, which can help balance pH levels in the system. A combined Nit/DNit process can reduce the need for external alkalinity supplementation. However, strategies to enhance the denitrification process and integrate Nit/DNit into AGS system for treating high ammonia, low C/N waste streams remains unclear.

2.6 Key factors to maintain granule structure during the treatment of high ammonia waste streams

Granulation begins with cell to cell adhesion, forming aggregates through physical and chemical forces such as van der waals, and ionic attractions. This initial stage is followed by the development phase, where EPS and quorum sensing molecules (signaling molecules for cell to cell communication) secretion promote the growth of granular sludge (Figure 2.1). The final maturation process is facilitated by applied selection forces [5]. Key selection forces of significant importance are detailed below:

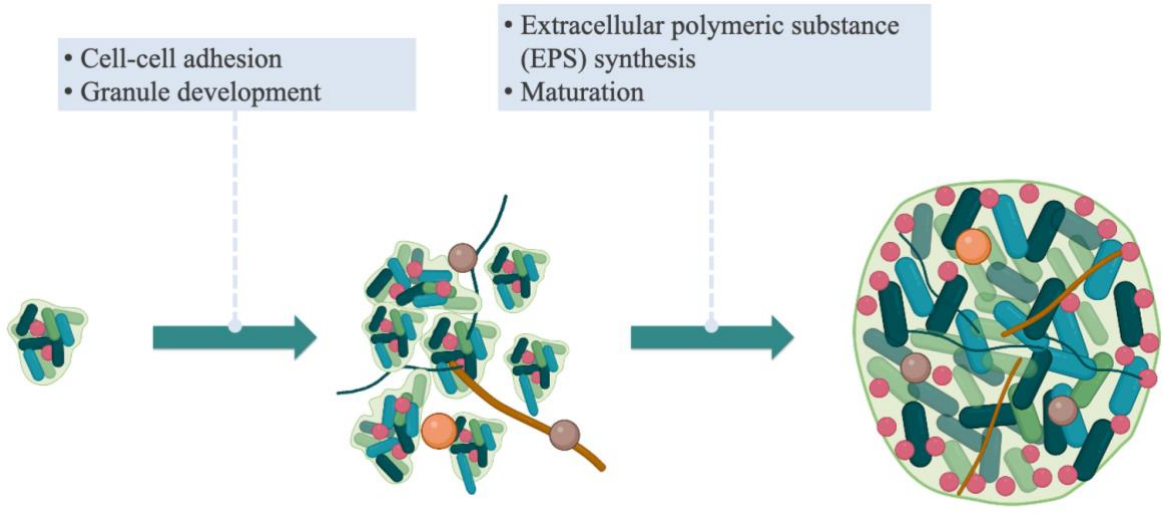

Figure 2.1 Granule formation mechanisms.

2.6.1 Carbon to nitrogen ratios

C/N ratios have been reported to influence granule formation, size, and stability [45]. The availability of bCOD influences the growth of functional microbes that critical to granule formation, particularly those responsible for EPS production [46]. Previous studies have demonstrated that granular sludge disintegrates at C/N ratio over 10 and below 1 [46, 47]. A C/N ratio over 8 favours the growth of fast-growing, heterotrophic, EPS producing microbes, which likely form fluffy and large granules. In contrast, a lower C/N ratio enriches slow-growing microbes, resulting in small and dense granules [47].

2.6.2 Organic loading rate

Similar to C/N ratios, organic loading rate (OLR) also plays a pivotal role in the granulation process. AGS can be cultivated at high OLR up to 15 kg COD/(m^3·d), which can accelerate granulation [48]. However, granules cultivated under such high OLR are less stable and prone to disintegrate over time. In contrast, the granule cultivation period is longer with low OLR, but the cultivated granules are examined to be more stable in structure and performance [47].

2.6.3 Hydrodynamic shear force

Hydrodynamic shear force, primarily provided by aeration and represented as up-flow superficial velocity, significantly impacts granule structure and shape [38]. A shear force over 1.2 cm/s is necessary for AGS formation [49]. Higher shear forces promote the formation of thin and dense granular sludge. Maintaining high shear force is beneficial for eliminating filamentous outgrowth, thereby enhancing granule stability [50]. Additionally, hydrodynamic shear force stimulates the secretion of EPS, which are crucial for cell to cell interactions and granule development.

2.6.4 Settling period

The settling period is an important selection force that manipulates the proportion of flocs (size below 0.2 mm) and large granules (size over 0.2 mm). With a short settling duration (2 to 10 min), flocs are likely washed out due to their slow settling capacity, allowing only large granules to be retained in the system [51]. Conversely, a long settling time allows flocs to remain in the system alongside large granules. Short settling times are commonly used in AGS studies to select for the fast settling and dense granules.

2.6.5 Microbial selection

Previous studies have indicated that controlling the microbial growth rates at a low level is the key to stabilizing granules [52]. Studies widely reported stable granular sludge with the enrichment of polyphosphate accumulating organisms (PAOs), glycogen accumulating organisms (GAOs) and nitrifying microorganisms like AAOB [52, 53]. These microorganisms help control the size of the granular sludge when treating high COD wastewater, thereby preventing the formation of large granules that are prone to disintegration into flocs over time, which can deteriorate treatment performance.

2.6.6 Feeding regime

Slow anaerobic feeding has been widely recognized to benefit AGS formation compared to pulse injection, primarily due to the enrichment of slow growing microorganisms, such as GAOs and PAOs [38]. These microorganisms convert available carbon to storage polymers, leaving limited bCOD for the growth of fast growing heterotrophic bacteria, especially filamentous bacteria that

can cause granule disintegration, in the subsequent aerobic phase [48]. Aerated feeding and fast static feeding can achieve rapid granulation but are suitable only for studies focusing on organic removal. Under these conditions, heterotrophic bacteria outcompete autotrophic N removal bacteria [54].

2.6.7 Carbon source

The most commonly used carbon source in granule cultivation studies are sodium acetate, glucose, ethanol and propionate. Different carbon sources can influence the microbial community and granule structure. Sodium acetate has been identified as the ideal carbon source for granule cultivation and N removal, outperforming propionate, glucose, and ethanol. Granules cultivated with ethanol have stability concerns, while those formed with propionate and glucose require a longer time for granulation [55, 56].

2.6.8 Influent solid content

Suspended solids in influent wastewaters minimally impacted granulation time but varied in granule size. Higher suspended solid content formed dense granular sludge, enhancing settling capacity and microbial activities [57]. However, excessive suspended solids may negatively affect sludge retention due to living space competition, leading to sludge washout [58].

2.7 Strategies to enhance nitrogen removal during high ammonia waste stream treatment

2.7.1 Strategies under high ammonia and high COD conditions

Poor ammonia and TIN removal have been reported in previous AGS studies treating high ammonia, high COD waste streams. This might be due to the competition between heterotrophic bacteria and autotrophic ammonia oxidizing bacteria (AAOB) for oxygen and space. Enhance the retention of AAOB can improve ammonia removal efficiency. Bioaugmentation can elevate the ammonia removal efficiency up to 86% [59]. Slow step feeding of high COD wastewater has also been tested and proven effective for improving ammonia removal. This strategy allows the

consumption of COD during the feeding phase, resulting in less residual COD when the reactor transitions to the aerobic phase [60].

2.7.2 Strategies under high ammonia and low COD conditions

To date, strategies for achieving high TIN removal in AGS system are limited. Only one study has reported 75% TIN removal in low C/N wastewaters, utilizing a combination with Fenton process [8]. Even for high C/N wastewaters, TIN removal efficiencies have ranged from 23% to 75% [11, 12, 41, 42], indicating inefficient COD utilization in AGS system. Apart from AGS studies, strategies such as supplying external carbon source during the anoxic phase to facilitate TIN removal are commonly used to enhance TIN removal [61]. Additionally, high COD waste streams can serve as an alternative for commercial carbon sources for denitrification [62].

2.8 Full-scale technologies for high ammonia waste stream treatment

Until now, several commercialized technologies have been developed for high ammonia wastewater treatment, such as SHARON, DEMON® and ANITA™Mox. The SHARON process uses Nit/DNit process, while DEMON® and ANITA™Mox employ the nitritation/anammox process [63, 64]. Among these, ANITA™Mox, which utilizes attached growth sludge, shows the highest N loading rate at 1 to 1.2 kg N/(m^3·d), followed by SHARON and DEMON®, both exhibiting N loading rates ranging from 0.2 to 0.6 kg N/(m^3·d). These technologies are typically operated at temperatures above 25 ^oC. Granular sludge-based technology has yet to be applied to treat such waste streams.

Chapter 3. Materials and Methods

This chapter elucidates the general materials and methods used in Chapter 4 to Chapter 11. Specific methodologies unique to each chapter will be addressed within their corresponding chapters.

3.1 Analytical procedures

The performance evaluation of the reactor was carried out by analyzing influent and effluent samples every two days. Upon collection, these samples were immediately filtered using 0.45 μm filters to determine concentrations of NH_4^+-N, NO_2^--N, NO_3^--N, and soluble COD (sCOD). The measurement of NH_4^+-N, NO_2^--N and NO_3^--N were analyzed by HACH Nessler reagent, NitriVer® 2 nitrite reagent, and TNT 835 nitrate reagent (HACH, Germany), respectively. Additionally, parameters such as sCOD, biomass density and properties including mixed liquor suspended solids (MLSS), mixed liquor volatile suspended solids (MLVSS), and sludge volume index for 5 min (SVI_5) and 30 min (SVI_{30}), were assessed according to the Standard Method [65]. Additionally, the biodegradable COD (bCOD) was measured following the standard method for ultimate biochemical oxygen demand measurement [65]. The changes in granular sludge sizes were monitored using ImageJ software.

3.2 Cycle tests

Cycle tests were performed at the end of each stage to assess the transformation of N compounds throughout a typical cycle. The anoxic feeding phase was not included as it was difficult to collect representative samples due to the lack of mixing in this period. Besides of that, sampling occurred in all other stages in a cycle. Collected samples were filtered (0.45 μm filters) and analyzed for NH_4^+-N, NO_2^--N, NO_3^--N and sCOD according to Section 3.1.

3.3 Microbial activity test

Batch tests were carried out to evaluate the specific activities of different N pathways, encompassing ammonia oxidation by autotrophic ammonia oxidizing bacteria (AAOB) and heterotrophic ammonia oxidizing bacteria (HAOB), nitrite oxidation by nitrite oxidizing bacteria (NOB), and nitrite reduction and nitrate reduction by denitrifying bacteria. These batch tests were

performed in triplicate at the temperature that used in respective studies. For all the tests, the sludge samples were collected at the steady state of each stage and specifically under aerobic phase to ensure a homogeneous environment. The MLVSS concentration in batch tests was consistently maintained at 4 g/L, with an initial pH set to approximately 7.5. The results were expressed as g N/(g VSS·d).

AAOB, HAOB and NOB activity tests were conducted under aerobic conditions using 30 mL mixed liquor (containing centrifuged sludge and synthetic medium) in 160 mL serum bottles. The growth medium for AAOB activity tests contained 400 mg/L NH_4^+-N and 2800 mg $CaCO_3$/L alkalinity. The growth medium used for HAOB activity tests contained 400 mg/L NH_4^+-N, 2800 mg $CaCO_3$/L alkalinity, 1200 mg/L COD, and 50 mg/L allylthiourea (ATU). ATU was used as an inhibitor of AAOB [66]. The substrate for NOB activity tests contained 200 mg/L NO_2^--N and 1400 mg $CaCO_3$/L. The pH was adjusted to around 7.5, and the bottles were then tightly sealed with rubber stopper and aluminum cap and shaken at 160 rpm. Sampling occurred at 15 min intervals for a duration of an hour. These samples were then filtered and analyzed for NH_4^+-N to ascertain AAOB and HAOB activities via the rate of NH_4^+-N reduction, and for NO_3^--N to determine NOB activity based on the rate of NO_3^--N production.

Denitritation and denitrification activity tests were conducted under anoxic environment using 80 mL mixed liquor in 120 mL serum bottles. The medium for denitritation activity tests contained 200 mg/L NO_2^--N, 1400 mg $CaCO_3$/L, and 2000 mg/L COD, and for denitrification activity tests contained 100 mg/L NO_3^--N, 700 mg $CaCO_3$/L, and 1000 mg/L COD. Prior to the tests, the pH of the mixed liquor was adjusted to around 7.5, followed by a nitrogen gas purge for 10 min to ensure anoxic environment. The bottles were then sealed and shaken at 180 rpm. Samples were collected every 10 min for 40 min. These samples were filtered and analyzed for NO_2^--N and NO_3^--N to determine the denitritation and denitrification activities according to the slope of NO_2^--N and NO_3^--N reduction, respectively, versus time.

3.4 Extracellular polymeric substances extraction

Extracellular polymeric substances (EPS) extraction utilized the modified formaldehyde-sodium hydroxide method [67]. In detail, 10 mL samples were taken from the reactor; after supernatant

removal, it was resuspended to 10 mL using ultrapure water, followed by centrifugation at 4 ºC and 2000 g for 15 min. The resultant supernatant was passed through 0.22 µm filters, designating it as soluble EPS (S-EPS). The pellets were subsequently resuspended in 10 mL of ultrapure water, with an addition of 0.06 mL of 36.5% formaldehyde, and stored at 4 ºC for an hour. Post-centrifugation (4 ºC, 5000 g, 15 min), the supernatant was filtered (0.22 µm) and termed as loosely bound EPS (L-EPS). The pellets were then resuspended in ultrapure water to 10 mL with the addition of 4 mL 1N sodium hydroxide, incubated at 4 ºC for 3 hrs, followed by centrifugation at 4 ºC and 6000 g for 15 min. The supernatant was filtered (0.22 µm) to yield tightly bound EPS (T-EPS). All EPS samples (S-EPS, L-EPS and T-EPS) were dialyzed for 24 hours using Spectra/Por® dialysis membrane, 3.5 kD (Spectrum Laboratories, Inc.). Protein quantification employed the modified Lowry method [68], while polysaccharide content was determined using the phenol-sulphuric acid method [69-71].

Chapter 4. Influence of Carbon to Nitrogen Ratios to Ammonia Oxidation Pathways in Aerobic Granular Sludge Reactor[1]

4.1 Introduction

In biological wastewater treatment, nitrogen removal relies on autotrophic nitrification (conducted by autotrophic ammonia and nitrite oxidizing bacteria, AAOB, and NOB) and anoxic denitrification [72]. It has been reported that the autotrophic nitrification process would be negatively affected if high COD were present, mainly due to the oxygen competition among autotrophic and heterotrophic microorganisms [73]. In addition, heterotrophic nitrification aerobic denitrification (HNAD) [23], may also carry out ammonia oxidation and denitrification in the presence of COD and oxygen [24]. Microorganisms such as *Paracoccus*, *Alcaligenes*, *Aeromonas*, *Bacillus*, *Acinetobacter*, and *Pseudomonas* are known HNADMs, capable to perform HNAD [34]. This process was found to be affected by a range of operation factors (such as dissolved oxygen (DO), C/N ratio, temperature, and salinity) [24], in which C/N ratio has been recently studied and shown to impact the N metabolic pathway (autotrophic or heterotrophic nitrification) [25, 73, 74]. However, the underlying mechanisms of the C/N ratio in the succession of N metabolic pathways were still unclear, especially the role of ammonia in the system. Further, due to the lack of information about specific microbial activities regarding autotrophic and heterotrophic nitrification at different C/N ratios, their contributions to ammonia oxidation in a co-existing system have been overlooked.

The C/N ratio has also been reported as a crucial factor impacting granule formation, size, and structural stability [45]. Previous studies employed a relatively high C/N ratio (~8) to cultivate AGS [75]; while high C/N ratio might adversely impact the N removal processes and; granule disintegration was reported at a low C/N condition (C/N at 1) [7]. As N contaminated wastewater characteristics can vary significantly depending on C/N ratio, the impact of C/N on N removal of wastewaters and granule stability in AGS systems need to be demonstrated.

[1] A version of this chapter has been published: Zou, X., Gao, M., Mohammed, A., & Liu, Y. (2023). Responses of various carbon to nitrogen ratios to microbial communities, kinetics, and nitrogen metabolic pathways in aerobic granular sludge reactor. *Bioresource Technology*, *367*, 128225. https://doi.org/10.1016/j.biortech.2022.128225

In this chapter, various C/N ratios (with different N levels) were tested for their impacts on the dominant N metabolic pathways in the following aspects: the specific microbial activities associated with nitrogen transformation, the dynamics of microbial community composition and the relative abundance of functional genes. Potential mechanisms that contribute to the succession of microbial communities were proposed. This study helps to better understand the contribution of AAOB and HAOB in different C/N conditions and provides an insight on the selection and enrichment of specific microbes for more efficient ammonia removal in future studies.

4.2 Methods and materials

4.2.1 Reactor configuration and operation

A 1.8 L aerobic granular sludge (AGS) reactor (diameter: 6 cm, height: 69 cm) was used to treat wastewater in a sequencing batch mode (Figure 4.1). Air was introduced at 2.4 cm/s at the bottom of the reactor through an air diffuser. Synthetic wastewater was introduced at the bottom of the reactor. The reactor was operated for 280 days in four stages at 20 ˚C, each stage characterized by a different C/N ratio. The reactor was operated with a 50% feed exchange ratio and 4 h per cycle. Each cycle comprised 60 min anoxic feeding, 170 min aeration, 5 min settling, 3 min decanting, and 2 min idling. Pre-programmed timers automatically controlled the SBR operation sequences. Solid retention time (SRT) was not controlled in this study; sludge removal occurred only through effluent discharge.

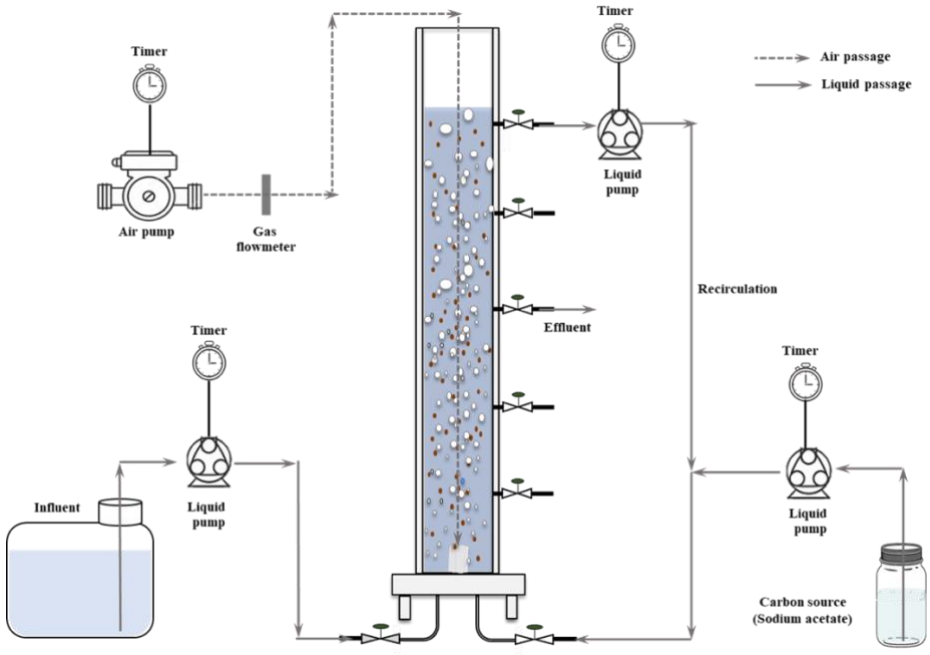

Figure 4.1 Schematic of the granular sludge reactor.

4.2.2 Seed sludge and synthetic reactor feed

Dried AGS from a former AGS cultivation reactor using synthetic wastewater was used as the inoculum for a fast reactor startup. The mixed liquor volatile solids (10 g/L) in the suspended sludge were used to inoculate the AGS reactor. Various NH_4^+-N concentrations (100, 200, and 400 mg/L, in the form of ammonium chloride) and 1200 mg/L COD (using sodium acetate anhydrous) were used as the synthetic wastewater reactor feed in Stage I to Stage IV (detailed information is shown in Table 4.1). Carbon dioxide in the air was the inorganic carbon source for the growth of nitrifying bacteria in all stages. In Stages III and IV, extra alkalinity (using sodium bicarbonate) was supplied to maintain the pH to above 7; and 2800 and 1400 mg $CaCO_3$/L alkalinity were added to the reactor feed, respectively. Per liter, the synthetic wastewater also contained 0.05 g KH_2PO_4, 0.06 g K_2HPO_4, 0.03 g $CaCl_2 \cdot 2H_2O$, 0.025 g $MgSO_4 \cdot 7H_2O$, 0.02 g $FeSO_4 \cdot 7H_2O$, and micro-nutrients prepared according to previous study [76].

Table 4.1 Aerobic granular sludge reactor feed characteristics.

Stages	COD (mg/L)	NH_4^+-N (mg/L)	C/N ratio	Alkalinity supplied (mg/L)
I	1200	100	12	0
II	1200	200	6	0
III	1200	400	3	2800
IV	1200	200	6	1400

4.2.3 DNA extraction and microbial analysis

DNA was extracted in duplicate samples taken from reactor sludge at each stage (Stage I to Stage IV) using DNeasy PowerSoil® DNA Isolation Kits (QIAGEN, Hilden, Germany) following the protocol provided. Extracted DNA was checked for quality using NanoDrop™ One (ThermoFisher Waltham, MA), and sequenced on the Illumina Miseq platform at Génome Québec Innovation Centre (Montréal, QC, Canada). The raw sequence data were processed on the QIIME2 platform using the DADA2 algorithm for low-quality sequences and chimera removal [77] and assigned taxonomy based on the GreenGene database (version13_8) with 99% similarity [78, 79]. The Phylogenetic Investigation of Communities by Reconstruction of Unobserved States 2 (PICRUSt2) pipeline was used to predict the abundance of functional genes for nitrogen conversion in different C/N ratios based on the Kyoto Encyclopedia of Genes and Genomes (KEGG) database [80]. The genes of core enzymes that related to ammonia oxidation and N removal were identified based on the KEGG pathway maps of nitrogen metabolism. The raw sequencing data was submitted to the National Center for Biotechnology Information (NCBI) GenBank (PRJNA887036).

4.2.4 Statistical analysis

The significance of the results was measured using the T-test in Microsoft® Excel® software, version 2109. A P-value < 0.05 was considered to be significant. RStudio, version 3.6.3, packages "vegan" and "ggplot" were used to perform canonical correspondence analysis (CCA) [81].

4.3 Results and discussion

4.3.1 Sludge characteristics

Figure 4.2a shows the dynamics of MLSS and MLVSS throughout the reactor operation. MLSS and MLVSS concentrations dropped in the first week of operation due to the sludge lost during

seed sludge rehydration. Afterwards, both MLSS and MLVSS gradually increased, and reached 10 g/L and 6 g/L at the end of Stage I, respectively. As influent NH_4^+-N concentration increased from 100 (Stage I) to 200 mg/L (Stage II), MLSS and MLVSS concentrations decreased to 7 and 5 g/L, respectively, and the sludge granular size decreased from 4.1 ± 1.0 mm to 2.2 ± 0.6 mm (Figure 4.3). A drastic reduction in biomass concentration (MLSS and MLVSS) was observed in the first two weeks after the influent NH_4^+-N level further increased from 200 mg/L (Stage II) to 400 mg/L (Stage III). However, after the initial two weeks, the biomass concentration increased over a short time to 10 g/L MLSS and 9 g/L MLVSS, which was accompanied by a slight reduction in sludge granule size (to 2.0 ± 0.6 mm). In Stage IV, MLSS and MLVSS continuously increased from 10 and 8 g/L to 18 and 15 g/L, respectively. Granule size was further reduced to 0.7 ± 0.4 mm (Figure 4.3). The decrease in granule size from Stage I to IV could be attributed to a reduced production of extracellular polymeric substances (EPS) by heterotrophic microorganisms due to the lower C/N ratios [82, 83]. In addition to the lower C/N ratios, higher FA concentrations might also contribute to the smaller granule size due to its adverse impact on cell hydrophobicity and EPS production [84].

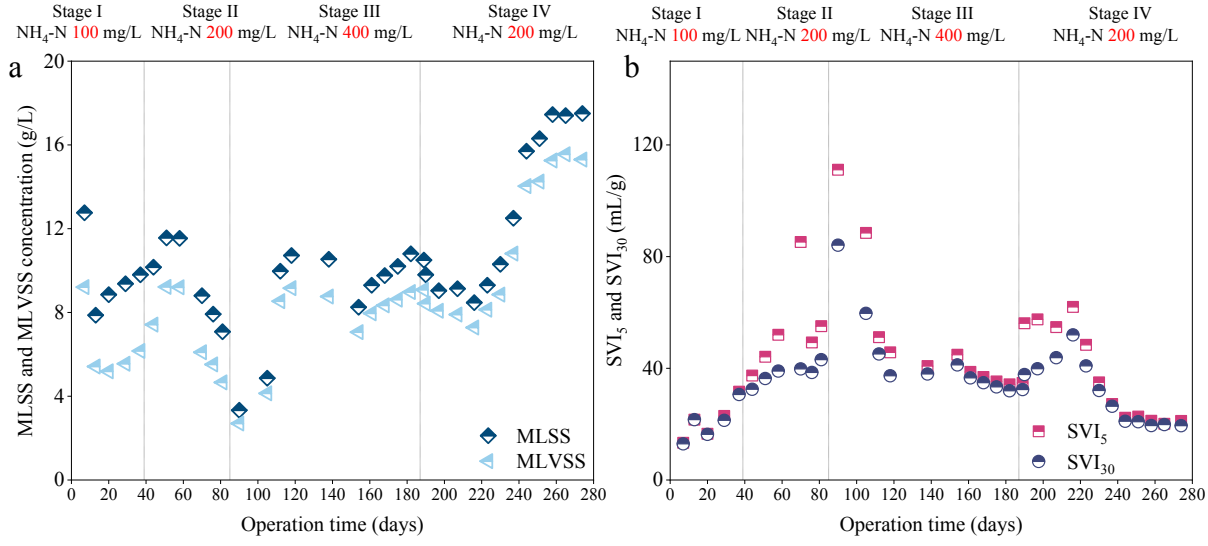

Figure 4.2 Sludge characteristics at each stage of wastewater treatment: (a) concentrations of mixed liquor suspended solids (MLSS) and mixed liquor volatile suspended solids (MLVSS); (b) sludge volume index (SVI) values at 5 min and 30 min.

Figure 4.2b presents the sludge volume indexes SVI_5 and SVI_{30} at different stages of wastewater treatment. Throughout the reactor operation, SVI values were maintained below 60 mL/g, except during the beginning of Stage III when considerable biomass washout was observed. These data suggest that the settling capacity and the stability of the granular sludge were maintained in the reactor even at a low C/N ratio of 3, although gradually reduced granule sizes were noticed. The SVI values in this study are in the commonly reported SVI range for AGS, below 80 mL/g [85].

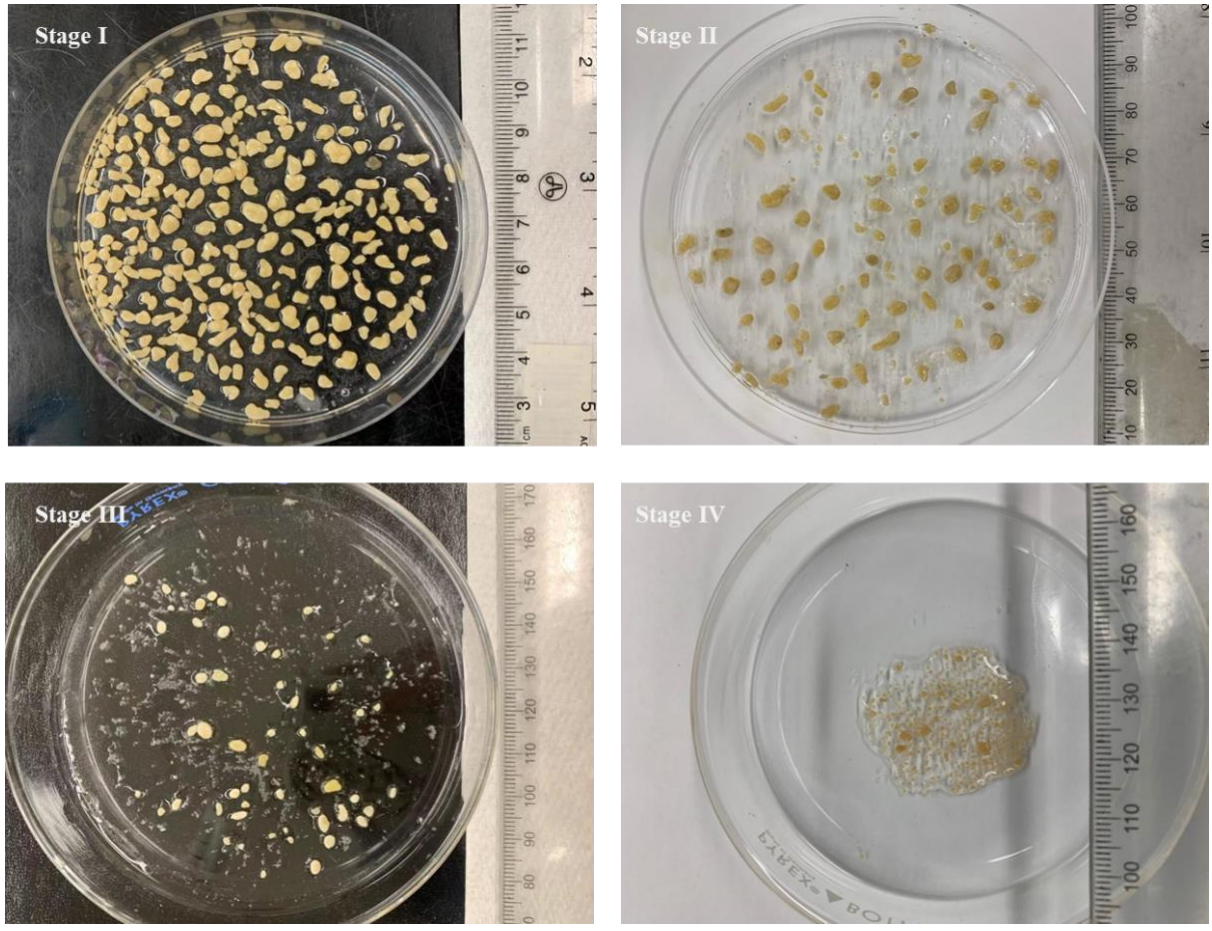

Figure 4.3 Granular sludge morphology in Stages I to IV under different carbon to nitrogen condition.

4.3.2 Nitrogen removal

Figure 4.4a shows NH_4^+-N, NO_2^--N, and NO_3^--N concentrations in reactor effluent at influent concentrations of 1200 mg/L COD and NH_4^+-N concentrations of 100 (Stage I; C/N = 12), 200 (Stage II; C/N = 6), 400 (Stage III; C/N = 3), and 200 (Stage IV; C/N = 6) mg/L, respectively.

Figure 4.4b shows NH_4^+-N and total inorganic nitrogen (TIN) removal efficiencies. In Stage I, with a C/N ratio of 12, NH_4^+-N, NO_2^--N, and NO_3^--N in the effluents were 51 ± 1.0 mg/L, 1 ± 0.5 mg/L, and 0.1 ± 0.1 mg/L, respectively, indicating 49 ± 0.5% NH_4^+-N and 46 ± 1.5% TIN removals. In Stage II, the C/N ratio decreased to 6, and the effluent contained 142 ± 2.4 mg/L NH_4^+-N, 1 ± 0.8 mg/L NO_2^--N, and 0.1 ± 0.1 mg/L NO_3^--N, indicating NH_4^+-N and TIN removal efficiencies of 28 ± 2.4% and 28 ± 2.3%, respectively. It is noteworthy that TIN removal was constrained by the limited ammonia removal capacity in Stages I and II with no NO_x (i.e., NO_2^- and NO_3^-) accumulation. The low ammonia removal was likely due to the wash out of the slow growing ammonia oxidizing bacteria, since heterotrophic bacteria had a faster sludge growth rate [86]. Meanwhile fast settling sludge selection force was applied throughout the operation. There are three possible mechanisms that contributed to the low effluent NO_x, including simultaneous nitrification and denitrification (SND); NH_4^+-N uptake for cell growth [25, 87] instead of oxidization and; heterotrophic nitrification aerobic denitrification (HNAD), which happened in the presence of COD and oxygen, converting ammonia to N_2 directly [25, 34]. Further research is needed to investigate the sludge production that accounted for N removal to gain a better understanding on N mass balance. Ammonia removal mechanisms in Stage I and Stage II were further assessed in cycle tests, activity tests, and microbial community analysis.

With a C/N ratio of 3 in Stage III, effluent NH_4^+-N concentrations were gradually reduced from 325 mg/L to ~1 mg/L as NO_2^--N accumulated after 18 days of acclimation. Effluent NH_4^+-N, NO_2^--N, and NO_3^--N concentrations stabilized at 1 ± 0.7 mg/L, 213 ± 6.2 mg/L, and 4 ± 1.8 mg/L, respectively, and the removals of 99 ± 0.3% NH_4^+-N and 45 ± 1.1% TIN were achieved over 98 days of reactor operation. High ammonia removal efficiency and NO_x (i.e., NO_2^- and NO_3^-) accumulation indicated that ammonia oxidation capacity was stimulated by lower C/N ratio as previously reported [83]. The accumulated NO_2^--N accounted for 90% of the oxidized nitrogen, indicating NOB was suppressed in this stage, which was due to the high free ammonia content (FA, up to 30 mg/L) at the initial condition of each cycle. As reported, the NOB activity could be successfully suppressed at 0.1-1 mg/L FA [88]. Although the C/N ratio again increased in Stage IV to 6, NH_4^+-N removal and TIN removal efficiencies were maintained at 99 ± 0.2% and 65 ± 0.9%, respectively (Figure 4.4b). NO_2^--N (51 ± 0.3 mg/L) and NO_3^--N (18 ± 1.3 mg/L) accumulated in the effluent, suggesting that ammonia oxidizing bacteria that enriched in Stage III

probably had the capacity to sustain some level of COD fluctuation and was competitive to the heterotrophic bacteria for N source in this condition. The slight increase in effluent NO_3^--N concentration was due to lower (compared to Stage III) influent NH_4^+-N and FA concentrations (up to 15 mg/L), and as reported NOB could gradually recover from FA inhibition [89]. Figure 4.4c shows a consistently high COD removal (98 ± 1.5%) from the AGS reactor, with influent 1200 mg/L COD (representing the COD concentration in the feed) and effluent 34 ± 9.5 mg/L COD throughout Stage I to Stage IV, regardless of the changes in influent NH_4^+-N concentration.

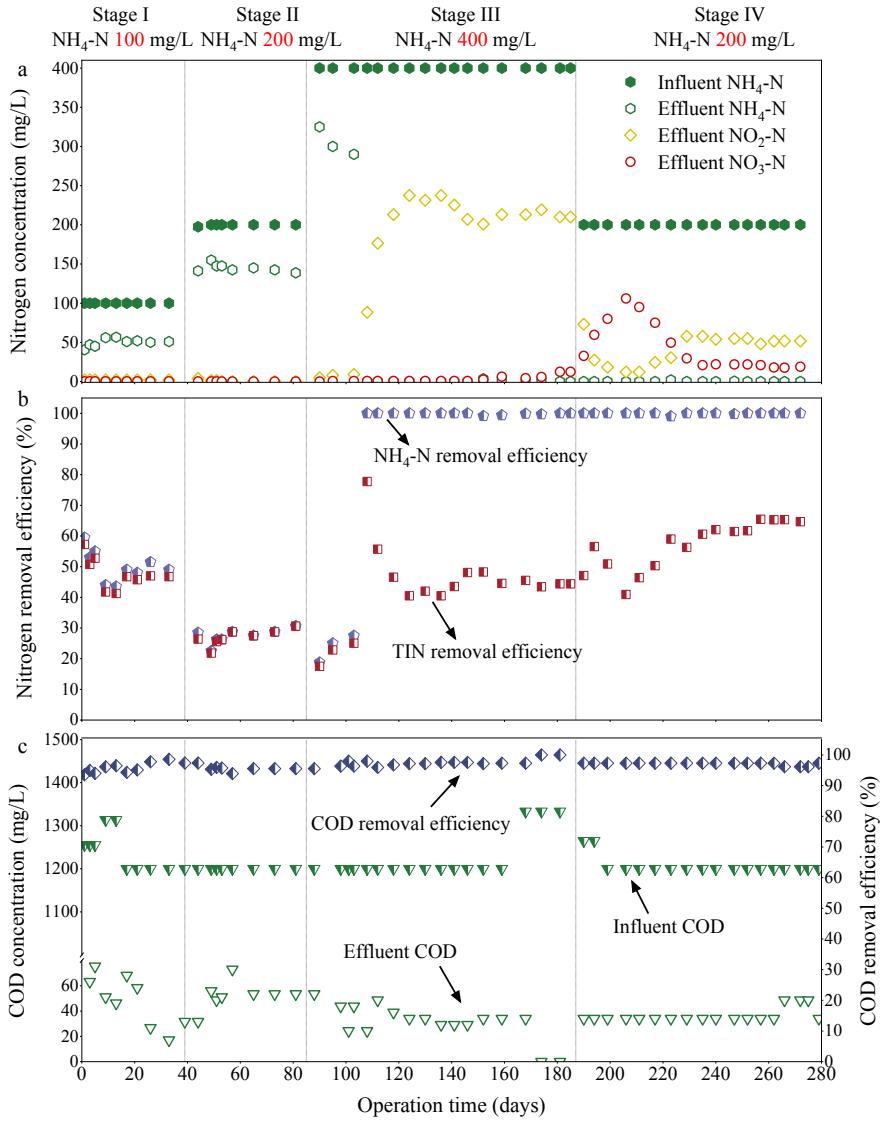

Figure 4.4 AGS reactor performance in Stage I to Stage IV: (a) influent and effluent nitrogen concentrations (NH_4^+-N, NO_2^--N, NO_3^--N); (b) NH_4^+-N and total inorganic nitrogen (TIN) removal efficiencies; (c) influent and effluent COD concentrations and removal efficiencies.

4.4 Microbial kinetics

To get a deeper understanding of the contribution on nitrogen removal from potential nitrogen metabolic pathways, specific microbial activities (Figure 4.5) including the activities of AAOB, HAOB, NOB, and denitritation and denitrification were conducted in each stage.

4.4.1 Specific microbial activities associated with nitrogen oxidation

Figure 4.5a shows the highest AAOB activity of 0.24 g N/(g VSS·d) in Stage III at 400 mg/L NH_4^+-N, followed by an AAOB activity of 0.22 g N/(g VSS·d) in Stage IV, suggesting higher AAOB activities were obtained under higher ammonia concentration. In comparison, significantly lower AAOB activities of 0.006 g N/(g VSS·d) in Stage I and 0.008 g N/(g VSS·d) in Stage II were observed ($p<0.01$). The AAOB activities at Stages III and IV were in the range of reported values (0.07-0.68 g N/(g VSS·d)), while those at Stages I and II were comparatively low [88, 90].

HAOB activities in Stage I (0.02 g N/(g VSS·d)) and Stage II (0.04 g N/(g VSS·d)) were higher than AAOB activities (Figure 4.5a), suggesting that heterotrophic nitrification was likely the dominant N transformation pathway in Stage I and Stage II. HAOB activities further increased to 0.09 g N/(g VSS·d) and 0.13 g N/(g VSS·d) in Stage III and Stage IV, respectively. However, compared to the AAOB activity in Stages III and IV, that ammonia oxidation rate was about 3 times higher than HAOB ammonia oxidation rate, indicating autotrophic ammonia oxidation was the dominant ammonia transformation pathway in Stage III and Stage IV. The HAOB activities obtained in this study were comparable to reported HAOB activities [72]. Results indicated that the significantly increased ammonia removal capacity in Stage III and Stage IV was mainly contributed by AAOB. It should be noted that the comparison between specific AAOB and HAOB activities have not been reported previously.

Limited NOB activity was detected in Stages I, II, and III: 0.008 g N/(g VSS·d), 0.012 g N/(g VSS·d), and 0.01 g N/(g VSS·d), respectively (Figure 4.5a). Higher NOB activity (0.16 g N/(g VSS·d)) was observed in Stage IV. The low NOB activities in Stage I and Stage II could be attributed to a lack of substrate for NOB to grow (i.e., NO_2^-), since heterotrophic nitrification commonly co-occurs with aerobic denitrification [91]. The limited NOB activity in Stage III was

mainly due to the inhibition from the high free ammonia (FA, up to 30 mg/L) at the initial condition of each operation cycle [92]. The increase in NOB activity in Stage IV agrees with the nitrate production and accumulation in the performance results.

4.4.2 Specific microbial activities associated with nitrogen removal

The limited denitritation (0.08 and 0.07 g N/(g VSS·d)) and denitrification (0.06 and 0.06 g N/(g VSS·d)) in Stage I and Stage II, respectively (Figure 4.5b), were likely a result of the trace NO_2^--N and NO_3^--N accumulation, which served as substrates for the respective processes. With the production and accumulation of NO_2^--N and NO_3^--N, denitritation activity increased significantly ($p<0.01$) to 1.29 g N/(g VSS·d) (Stage III) and to 1.33 g N/(g VSS·d) (Stage IV), and denitrification activity also increased significantly ($p<0.01$) to 0.73 g N/(g VSS·d) (Stage III) and to 0.84 g N/(g VSS·d) (Stage IV). Similar to results reported in Peng and Zhu [93], the NO_2^--N removal rate was about 2 times higher than the NO_3^--N removal rate.

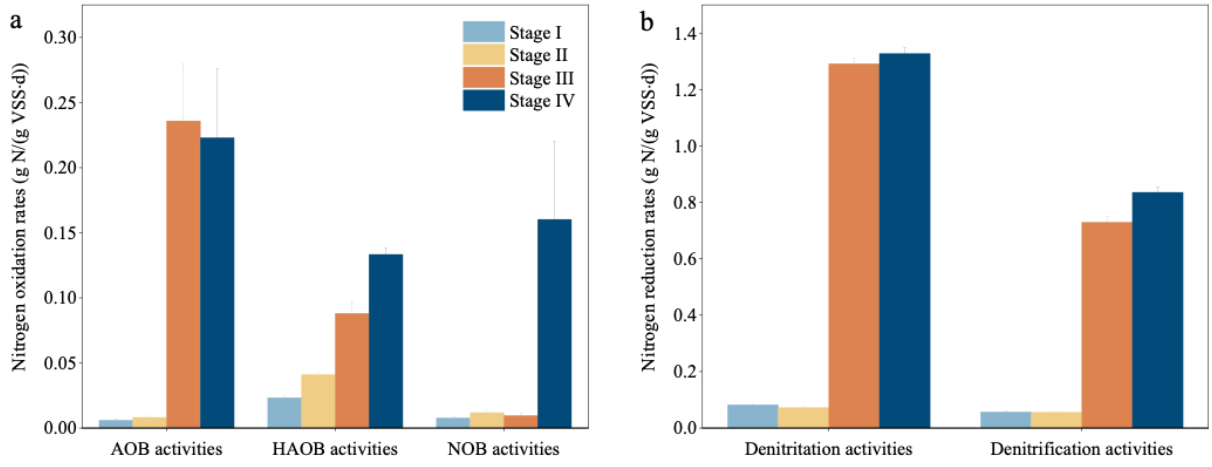

Figure 4.5 Stage I to Stage IV: (a) Nitrogen oxidation rates of autotrophic ammonia oxidizing bacteria (AAOB), heterotrophic ammonia oxidizing bacteria (HAOB), and nitrite oxidizing bacteria (NOB); (b) Nitrogen removal rates of denitritation and denitrification.

4.4.3 Cycle tests at different carbon to nitrogen ratios

Cycle tests were performed to investigate the oxidation states of nitrogen in a typical cycle at each stage, as shown in Figure 4.6. The cycle tests were started once aeration began. In Stages I and II (Figure 4.6a and Figure 4.6b), low NH_4^+-N removals were observed (20–22.5 mg/L, calculated based on the difference of NH_4^+-N concentrations at the beginning and end of the cycle), and trace

levels of NO_2^--N and NO_3^--N were detected throughout the cycle test. The initial COD concentration of 535-620 mg/L, which was half of the influent COD concentration due to the 50% exchange ratio, was depleted within an hour. The cycle tests in Stage I and Stage II confirmed the absence of NO_x accumulation throughout the cycles, suggesting that nitritation/nitrification and denitritation/denitrification happened simultaneously in the presence of oxygen. This observation may be attributed to the nature of granular sludge, which provided an anoxic environment for denitrification in the inner granules. Aerobic denitrification, which commonly co-occurs with heterotrophic nitrification might also contribute to simultaneous nitrogen removal [24]. As mentioned in Section 3.3, the activity test results showed the heterotrophic nitrification was the core N transformation pathway in Stages I and II. In addition to simultaneous N removal, N assimilation by bacteria can also contribute to TIN loss, which requires future studies to quantify.

Figure 4.6c shows a typical cycle test in Stage III. Within 100 min, ~160 mg/L initial NH_4^+-N was completely consumed. NO_2^--N accumulated from 55 mg/L (at the beginning of the cycle) to 216 mg/L, and trace NO_3^--N was produced (up to 5 mg/L). The initial COD of 311 mg/L in the cycle was relatively low compared to the COD concentrations in Stage I and Stage II. The initial NO_2^--N concentration (55 mg/L) was lower than the theoretical initial NO_2^--N concentration (108 mg/L, which was calculated based on the leftover NO_2^--N concentration (216 mg/L) at the end of previous cycle and the 50% feed exchange ratio). The lower COD and NO_2^--N concentrations at the beginning of the cycle could be attributed to anoxic denitritation, which removed the leftover NO_2^--N with the introduced COD in the anoxic feeding period. Accumulated NO_2^--N accounted for 98% of the NH_4^+-N oxidized, again suggesting that simultaneous denitrification or aerobic denitrification was limited in Stage III, which might be attributed to the limited COD level in the aerobic phase and the reduced granule sizes. TIN removal in this stage was mainly contributed by denitritation during the anoxic feeding period.

Figure 4.6d shows a typical cycle in Stage IV. Ammonia was completely oxidized within 100 min, and the NO_x-N accumulation was 85% of oxidized NH_4^+-N. The remaining 15% NH_4^+-N might be associated with simultaneous nitrification denitrification (SND) and aerobic denitrification. Compared to Stage III, lower NO_2^--N accumulation was observed; this could be attributed to the reduced influent ammonia concentration and the higher C/N ratio that enhanced the denitritation.

Aerobic denitrification has been reported previously with C/N ratios from 5 to 10 [94-96], and the C/N ratio of 6 in this stage was within this range. The COD was 453 mg/L at the beginning of the cycle and that was completely consumed in an hour. Heterotrophic denitrification was also noticeable during the anoxic feeding period, which consumed all the leftover NO_2^--N and NO_3^--N with influent COD. The NO_3^--N concentration was consistently lower than the NO_2^--N concentration, indicating NOB inhibition was still observed in Stage IV.

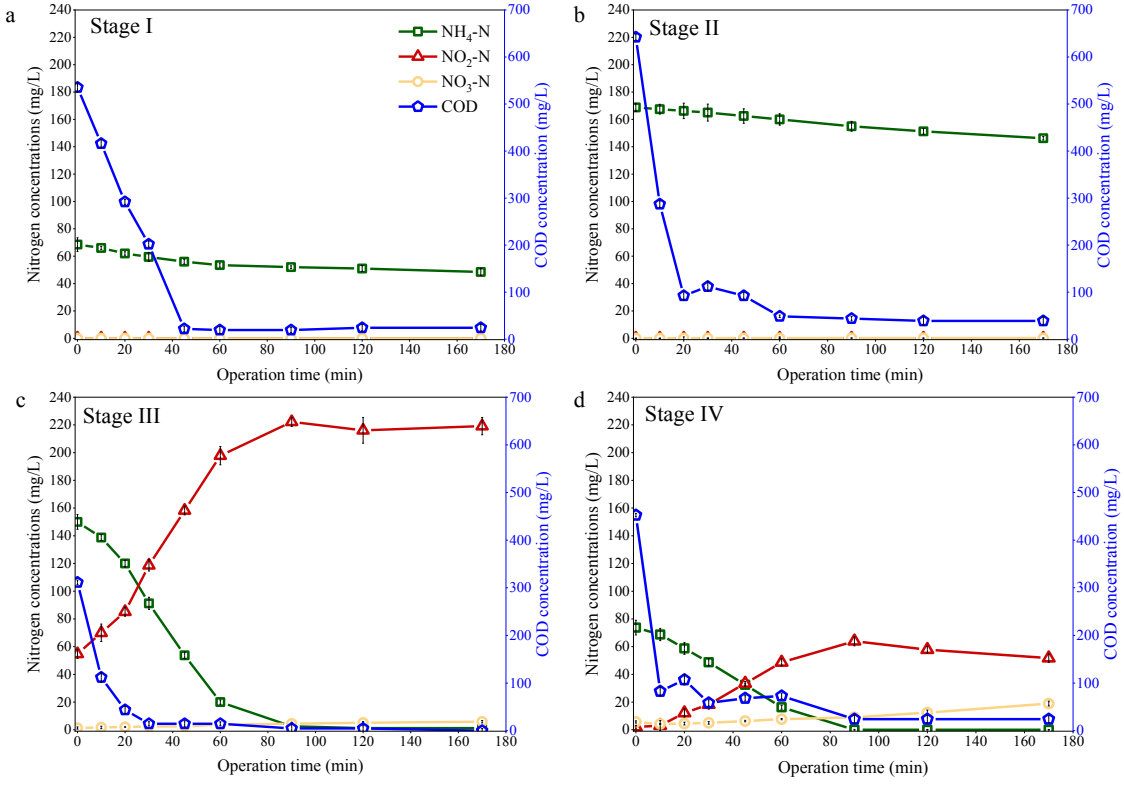

Figure 4.6 NH_4^+-N, NO_2^--N, NO_3^--N, and COD profiles in cycle tests: (a) Stage I (100 mg/L), (b) Stage II (200 mg/L), (c) Stage III (400 mg/L), (d) Stage IV (200 mg/L).

4.4.4 Microbial community dynamics

At the phylum level (Figure 4.7a), Proteobacteria accounted for the greatest proportion among all four stages, occupying 78% in Stage I, 88% in Stage II, 87% in Stage III and 91% in Stage IV. AAOB (i.e., *Nitrosomonas*) and denitrifiers (i.e., *Thauera*, *Paracoccus*) belong to the phylum Proteobacteria. Bacteroidetes is also a major phylum among all stages, accounting for 2%, 3%, 3% and 1%, respectively. Actinobacteria accounted for 19% in Stage I and gradually reduced to 0.1% in Stage IV. Chloroflexi and WPS-2 have the highest proportion in Stage III, at 7% and 2%,

respectively. Proteobacteria, Bacteroidetes, Actinobacteria and Chloroflexi have been reported as being involved in the N, organics and phosphorus removal, and granulation process [97]. Previous study reported that mature granules had a reduced relative abundance of Actinobacteria, which emphasizes the stability of granules over time [98].

Further analysis was conducted at the genus level (with relative abundances > 0.1%) in Stage I to Stage IV, as shown in Figure 4.7b. The dominant genera (> 1%) in all stages were heterotrophs [99, 100]; their high redundancy ensured stable COD removal efficiencies at various ammonia concentrations.

4.4.4.1 Microbial genera affiliated with heterotrophic nitrifying microorganisms

The dominant genera *Thauera* and *Paracoccus* are heterotrophic microorganisms capable of performing denitrification. *Thauera* and *Paracoccus* are commonly found in core communities in laboratory and full scale AGS systems [25, 101]. The relative abundance of *Thauera* was reduced dramatically from Stage I (64%) to Stage IV (1%), whereas the relative abundance of *Paracoccus* increased substantially from Stage I (3%) to Stage IV (80%). This observation indicated that the C/N ratio had a critical impact on bacterial population selection in the AGS system. The increase in the relative abundance of *Paracoccus* could be explained by its preference for high COD and high N environments [102, 103]. Previous studies have indicated that *Paracoccus* has a higher substrate uptake rate than *Thauera* [47, 104] and can perform nitrification and denitrification even at FA concentrations of 184 mg/L [25]. These characteristics support its dominance in this study. Further, *Paracoccus* has been reported to be capable to perform HNAD [25], thus the enrichment of *Paracoccus* agrees with the gradual increase of HAOB activities. Huang, Cui, Yan and Cui [34] also reported a high *Paracoccus* abundance (56% of the microbial community) at COD 600 mg/L with C/N ratio at ~2.7. This result emphasizes the high COD and ammonia content probably favours the growth of *Paracoccus*. However, contradictory results were reported previously, which indicated the abundance of *Paracoccus* increased as nitrogen level decreased [75]. Therefore, the impacts of ammonia concentration, the C/N ratio, and reactor operation on the enrichment of *Paracoccus* need further investigation.

The abundance of *Azoarcus* and unclassified genera in the Comamonadaceae and Rhodocyclaceae families was reduced to < 1% from Stage I to II, which may be attributed to their preference for high COD and limited nitrogen as demonstrated by Sarkar and Reinhold-Hurek [105] and Wang, Geng, Ren, Guo, Wang and Wang [100]. The relative abundance of *Corynebacterium* and *Flavobacterium* decreased to 0.1% in Stages III and IV, which was speculated to be the result of FA inhibition. The abundance of unclassified genera affiliated with the class Betaproteobacteria increased from 2% (Stage I) to 38% (Stage II), while its abundance reduced to < 0.1% in Stage III and increased again in Stage IV (1%), considering the FA levels in each stage, it is speculated that the population shift might be also due to the elevated FA level in Stage III. Further study is needed to understand the underlying mechanism of the observed population shift. In contrast, the relative abundance of unclassified genera in families A4b, Crymorphaceae, and Pseudomonadaceae, and in phylum WPS-2 increased as the ammonia level increased.

4.4.4.2 Microbial genera affiliated with autotrophic nitrifying microorganisms

The core autotrophic nitrification microorganisms in this reactor were *Nitrosomonas* (0.3% in Stage III) and unclassified genera affiliated with the Nitrosomondaceae family (0.2% at Stage IV), which have been previously reported as a representative AAOB [106] (Figure 4.7). The ammonia removal efficiencies in Stage III and Stage IV (Figure 4.4b) were likely enhanced by the enrichment of these autotrophic nitrifying bacteria (*Nitrosomonas* and unclassified genera in the Nitrosomondaceae family), even though their relative abundances were low (< 1%). In addition, the specific microbial activities result also suggest that autotrophic nitrifying bacteria with low abundance was the major contributor to the ammonia oxidation, even though highly abundant genus was found to be affiliated to heterotrophic nitrification. Similar observations had been reported previously [106].

The dominant genus for nitrite oxidation was *Nitrobacter*, which was observed in Stage III and Stage IV and accounted for 0.1% of the microbial community in both stages. The limited NOB activity in Stage III with 0.1% relative abundance of *Nitrobacter* was likely due to FA inhibition. Limited NOB activities have been observed in nitritation reactors, even though NOB were present in the microbial communities of these reactors [92, 107]. The development of autotrophic nitrifying bacteria (AAOB and NOB) supports the succession of the dominant nitrogen metabolic

pathway from heterotrophic nitrification in Stage I and Stage II to autotrophic nitrification in Stage III and Stage IV. To better understand the dynamics of microbial community and verify the shift in N metabolic pathway, functional genes expression studies should be incorporated in future studies.

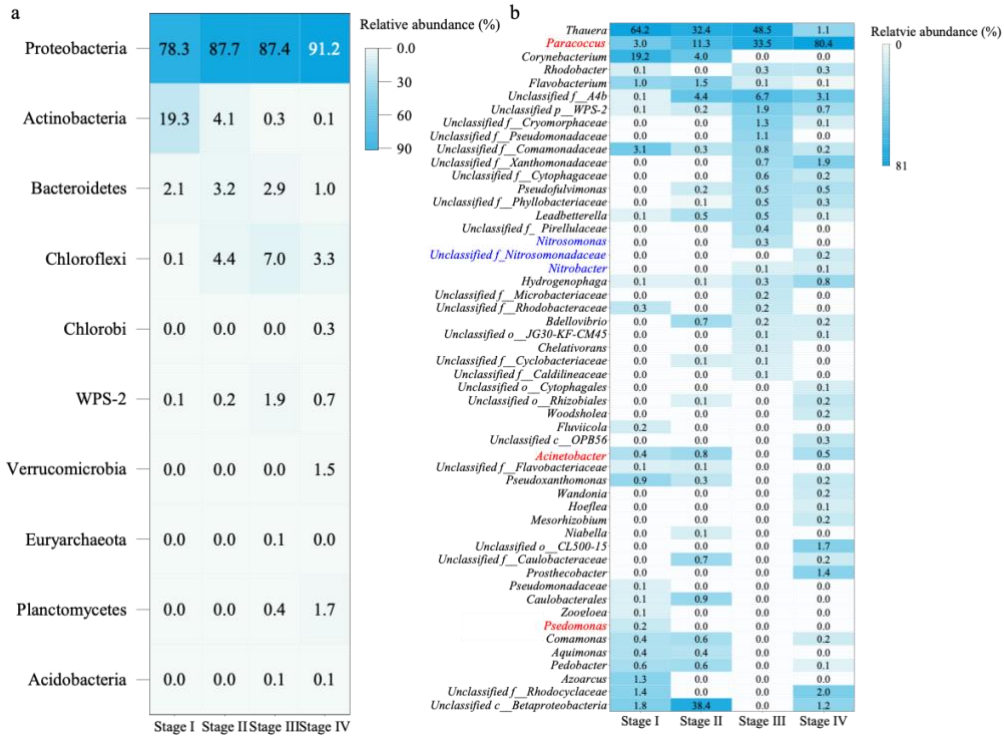

Figure 4.7 Microbial relative abundances at the (a) phylum (> 0.1%) and (b) genus level (> 0.1%) at each stage. Unidentified genera are shown at family (Unclassified f_), order (Unclassified o_), class (Unclassified c_) and phylum (Unclassified p_) levels. Blue colored genera were affiliated with autotrophic nitrifying microorganism; red colored genera were commonly classified heterotrophic nitrifying microorganism.

4.4.4.3 Microbial functional genes prediction: nitrogen metabolism

Genes of core enzymes associated with ammonia oxidation (ammonia monooxygenase (*amoABC*) and hydroxylamine oxidoreductase (*hao*)) were identified in Stage III and Stage IV (Figure 4.8), while the relative abundance of those enzymes in Stages I and II were limited. This result supports the observation on the stimulation of autotrophic nitrification in Stages III and IV. The relative abundance of nitrite oxidoreductase genes (*nxrAB*) and nitrate reductases genes (*narGH*/*napAB*) were reduced in Stages III and IV (Figure 4.8). The *napAB* genes have been reported to be key genes participating in denitrification and nitrate respiration under aerobic conditions; also, these genes were commonly used to identify aerobic denitrifying bacteria [108]. It was speculated that

aerobic denitrification might be the core denitrifying process in Stages I and II, due to the highly abundant *napAB* genes. The reduction in *napAB* genes' abundance in Stages III and IV indicates the reduced dominance of aerobic denitrification compared to anoxic denitrification. The highest relative abundance of nitrite reductase (*nirSK*) genes was observed in Stage III, followed by that observed in Stage IV (Figure 4.8); this might be correlated to the substrate (NO_2^-) availability, which showed a higher concentration in Stage III. Nitric oxide reductase (*norBC*) and nitrous oxide reductase (*nosZ*) showed relatively higher abundance, supporting the denitrification capacity in the current system.

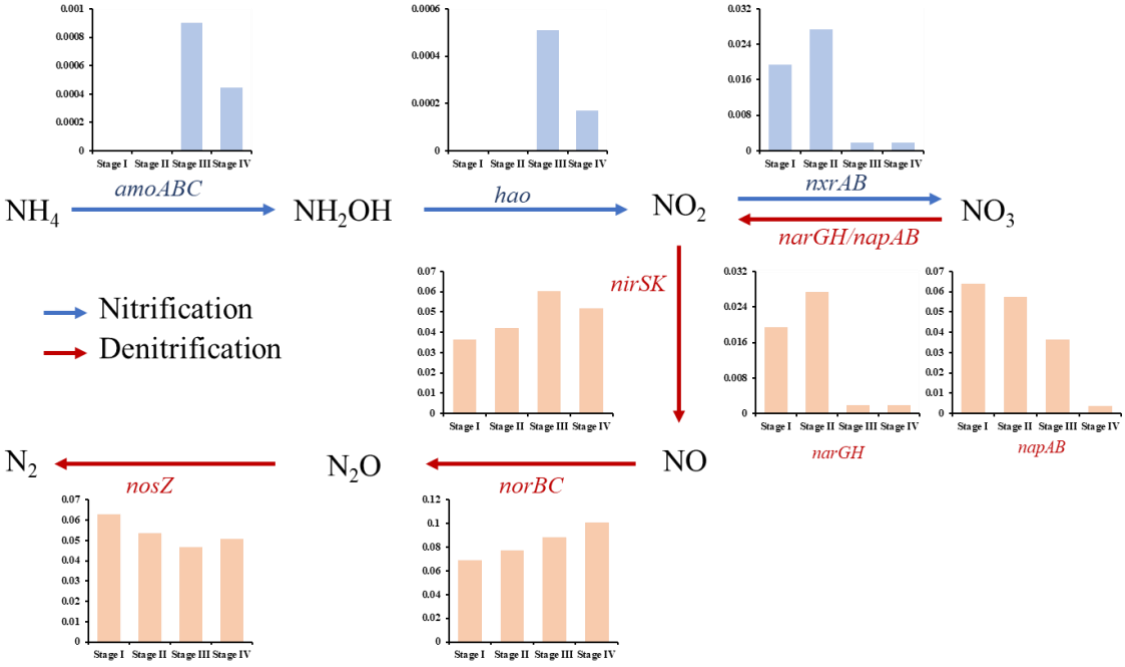

Figure 4.8 Predicted relative abundances of functional genes related to nitrification (*amoABC*, *hao*, *nxrAB*) and denitrification (*narGH*/*napAB*, *nirSK*, *norBC*, *nosZ*) in each stage.

4.4.5 Mechanisms of microbial succession in ammonia oxidation

In this study, heterotrophic nitrification coexists with autotrophic nitrification. Heterotrophic nitrification was the dominant nitrogen metabolic pathway in Stage I and Stage II. The limited autotrophic nitrification contribution in the first two stages to ammonia oxidation was likely due to the selection pressure from high C/N ratio. A high C/N ratio stimulated the growth of heterotrophic bacteria, which competed for the space with autotrophic bacteria, and may have resulted in difficulties in cultivating slow growing bacteria (i.e., AAOB).

The current results indicate that with consistent COD concentration, the autotrophic ammonia oxidation pathway was triggered in Stage III (with 400 mg/L NH_4^+-N) and autotrophic ammonia oxidation outcompeted heterotrophic nitrification in Stage III and IV as the major nitrogen metabolic pathway. The most reported explanation for higher ammonia oxidation efficiency at lower C/N ratios was the reduced competition between heterotrophs and AAOB for space and oxygen [75, 82, 83, 109]. However, oxygen competition might not be the reason in this case, since the COD was completely consumed within an hour, and there was a ~110 min aerobic condition in absence of COD. Further, the space competition from the growth of heterotrophs to AAOB in this study could not explain the AAOB growth stimulation in Stage III, because the COD concentration in the feed remained the same throughout operation, and the growth of heterotrophs and space competition might be similar in all four stages.

4.4.5.1 Proposed mechanism for the development of autotrophic ammonia oxidation

The free ammonia (FA) inhibition on heterotrophic bacteria [84] was proposed as the potential mechanism that triggered the microbial succession associated with nitrogen transformation. It has been reported that AGS formed only when the FA concentration was less than 23.5 mg/L [84]. The FA concentrations in Stage I to IV were 11, 21, 30, and 15 mg/L respectively, indicating the FA level in Stage III might inhibit the EPS production microbes, most likely heterotrophic bacteria, and thus, AAOB could grow and be retained in the reactor. Therefore, in addition to the C/N ratio, ammonia and FA concentrations were crucial for the shifts in the N metabolic pathway.

FA has been reported to adversely impact the energy metabolism of microorganisms. In detail, FA could passively diffuse into the cell and result in proton imbalance. To balance the pH, cells need to consume more energy to pump protons in and potassium out, and which would cause potassium deficiency and further affect enzyme activities [110]. Therefore, higher FA conditions could increase the required energy for cell maintenance and cause lower cell activity and yield. These might be the mechanism of FA inhibition on some heterotrophic bacteria in this study. Future research is needed to investigate the potential FA inhibition impact on the growth of autotrophic and heterotrophic bacteria.

4.5 Conclusions

This chapter demonstrated that high ammonia and low C/N conditions are conducive to high ammonia removal in AGS system, suggesting AGS's capacity for high ammonia wastewater treatment. Elevated ammonia concentration with a low C/N ratio at 3 stimulated the growth of AAOB (*Nitrosomonas*), which enhanced ammonia removal efficiencies from 28% (C/N = 6) to 100%. Although the abundance of AAOB was low (0.3%), their activity was 2.7-fold higher than that of HAOB. Heterotrophic nitrification was the dominant nitrogen transformation pathway at high C/N ratios (12 and 6). Stable granular sludge was achieved throughout the operation. Current study believed that FA inhibition on heterotrophic bacteria and nitrogen competition between AAOB and heterotrophic bacteria played a key role for the development of autotrophic nitrogen transformation pathway.

Chapter 5. Influence of Residual Sludge Content from Anaerobically Digested Sludge Wastewater on Aerobic Granular Sludge Reactor[2]

5.1 Introduction

Chapter 4 has demonstrated the influence of varied C/N ratios in high ammonia wastewaters on N removal pathways, revealing a shift in nitrification pathways between heterotrophic and autotrophic nitrification. Chapter 4 suggested that high ammonia conditions select for highly active AAOB, leading to higher ammonia removal efficiency. However, given that anaerobically digested sludge wastewaters often contain residual sludge, its potential impact on the efficacy of downstream reactors warrants further investigation.

Recently, upflow anaerobic sludge blanket (UASB) reactors, employing anaerobic granular sludge (AnGS), are extensively utilized for energy and nutrient recovery from high strength industrial wastewaters and waste activated sludge [111, 112]. To date, no study has systematically investigated the impact of residual AnGS, particularly at a high concentration of 1.8 g/L, on the performance of AGS systems with a specific focus on N reduction.

AnGS addition has been primarily confined to AGS start-up [113], rather than continuous addition. Previous studies have investigated the treatment of wastewater with high solid content (below 0.7 g/L), results have been controversial. It has been reported that influent solids negatively impacted oxygen transfer, the retention of microbes, reactor stability and effluent quality [6, 57, 114]. In contrast, other studies documented enhanced settling efficiency, shortened granulation time, and improved N reduction during the treatment of high solid wastewater [57, 58]. The discrepancy in reported results highlights the need for a systematic investigation into the impact of residual solids (AnGS) in wastewater on the performance of nitrogen removal reactors, providing insights for its prospective deployment.

[2] A version of this chapter has been published: Zou, X., Gao, M., Sun, H., Zhang, Y., Yao, Y., Guo, H., & Liu, Y. (2024). Influence of residual anaerobic granular sludge (AnGS) from anaerobically digested molasses wastewater in aerobic granular sludge reactor. *Science of the Total Environment*, *949*, 175206.

This chapter aims to evaluate the impact of AnGS introduction on nitrogen removal from anaerobically digested molasses wastewater. An AGS reactor was employed to treat wastewater with residual AnGS of 1.8 g/L and settled wastewater with minimal AnGS content of 0.3 g/L. A comprehensive investigation was carried out into its impacts on treatment performance, AGS structural stability, and microbial community dynamics, coupled with mass balance model, as well as the persistence of observed effects when AnGS was eliminated from the wastewater. This chapter offers insights into the treatment of AnGS contained wastewaters in future studies.

5.2 Methods and materials

5.2.1 Reactor setup and operation

A cylindrical AGS reactor with a 3 L capacity was employed to treat anaerobically digested molasses wastewater over a period of 110 days at 20 ^{o}C. The reactor was initially seeded with nitrifying granular sludge from an AGS reactor treating high ammonium wastewater. To start-up the reactor, the low AnGS wastewater was introduced into the reactor for 18 days. Once the reactor stabilized, high AnGS wastewater was introduced into the AGS reactor, marking the Stage I operation. The sequencing batch AGS operated with 50% exchange ratio. An upflow superficial velocity of 1.2 cm/s was maintained by a fine bubble air diffuser positioned at the reactor's base. Programmable timers were utilized for automatic control of the reactor's operations. The reactor was operated at a cycle time of 4 hours, including 1 hour for feeding, which is known to benefit granule stability [115], 2.75 hours for aerobic phase, and 5 minutes each for settling and discharging phases. The reactor operation could be divided into two stages, Stage I used the mixed anaerobically digested molasses wastewater with AnGS content at 1.8 g/L (the high AnGS condition); Stage II fed with the settled anaerobically digested molasses wastewater with minimal AnGS content at around 0.3 g/L (the low AnGS condition). The dissolved oxygen (DO) concentrations were within the range of 1.0 to 1.2 mg/L in both stages. The solid retention time (SRT) was not manually controlled in this study.

5.2.2 Calculation methods

Nitrite accumulation rate (NAR) was employed in this study to evaluate the activities of AAOB and NOB in the AGS, determined according to Equation 5.1. SRT was adopted and calculated

based on Equation 5.2. to help with the understanding of the influence of AnGS introduction on the AGS.

$$NAR = \frac{C_{NO_2^- - N}}{C_{NO_2^- - N} + C_{NO_3^- - N}} \times 100\% \quad \text{Equation 5.1}$$

where $C_{NO_2^- - N}$ and $C_{NO_3^- - N}$ represent the NO_2^--N and NO_3^--N concentrations in the AGS treated effluent.

$$SRT = \frac{MLSS_R \times V_R}{MLSS_E \times V_E} \quad \text{Equation 5.2}$$

where $MLSS_R$ and V_R refer to the MLSS concentration in the AGS and volume of the AGS reactor, respectively. $MLSS_E$ and V_E refer to the effluent MLSS concentration and volume. No manual sludge discharge was performed in the AGS.

5.2.3 Microbial community analysis

DNA from the sludge samples from Stage I, II, and AnGS were extracted for analysis using DNeasy PowerSoil Pro Kit (QIAGEN, Hilden, Germany). The extracted DNA was amplified using the universal primer pair 515 F/806 R. These samples were then dispatched for amplicon sequencing on the Illumina Miseq PE250 platform at Genome Quebec (Montréal, QC, Canada). Data processing, including taxonomy assignment, was executed in the Qiime2 pipeline using the DADA2 algorithm and the GreenGenes database (version 13_8) with a 97% similarity [116]. Biodiversity and richness, such as Shannon, Simpson and Chao1 indexes were calculated, and Principal Coordinate analysis (PCoA) were employed to assess the community differences between the AnGS and AGS sludge samples from Stages I and II. These analyses carried out based on the genus level abundance data using the "ggplot2", "ade4" and "vegan" packages in R.

5.2.4 Microbial immigration dynamics analysis

A mass balance model was employed to analyze the contribution of influent AnGS to the microbial communities in AGS in Stage I [117, 118]. Based on previous study, Equation 5.3 to Equation 5.7 were used:

$$\frac{dN_x}{dt} = \mu_x N_x + n_{x,influent} - n_{x,effluent} - n_{x,waste} \quad \text{Equation 5.3}$$

Assume steady state condition,

$$0 = \mu_x N_x + n_{x,influent} - n_{x,effluent} \quad \text{Equation 5.4}$$

$$\mu_x = \frac{n_{x,effluent} - n_{x,influent}}{N_x}$$ Equation 5.5

$$\mu_x = \frac{n_{x,effluent}}{N_x} - \frac{n_{x,influent}}{N_x}$$ Equation 5.6

The cell concentration is assumed to be proportional to the volatile suspended solid (VSS) concentration [118],

$$\mu_x = \frac{1}{SRT} - \frac{P_{x,influent} \times VSS_{influent} \times Q_{influent}}{P_{x,AGS} \times VSS_{AGS} \times V_{AGS}}$$ Equation 5.7

where N_x represents cell number of specific microorganisms in the AGS, t denotes the operation duration (d), μ_x is the net growth rate of microorganisms (1/d), $n_{x,influent}$ and $n_{x,effluent}$ represent the cell number of microbial x entering and exiting the system per day (1/d), respectively. The $n_{x,waste}$ is the cell number of microbes x wasted from the system, which is 0 in this study, since the sludge only wasted with the effluent discharging. $P_{x,influent}$ represents the relative abundance of microbe x in all OTUs in influent, $VSS_{influent}$ represents the VSS concentration in the influent (g/L), $Q_{influent}$ denotes the daily volume of the influent (L/d), $P_{x,AGS}$ represents the relative abundance of microbe x in all OTUs in AGS reactor, VSS_{AGS} represents the VSS concentration in the AGS reactor (g/L) and V_{AGS} represents the volume of the AGS reactor (L). Positive μ values represent actively growing microorganisms in AGS, while negative values indicate inactive immigrant in the AGS.

5.2.5 Statistical analysis

The determination of result significance was conducted using the p-value obtained from T-test (Microsoft Excel), with a p-value below 0.05 indicating statistical significance.

5.3 Results

5.3.1 Reactor performance

5.3.1.1 Nitrogen and COD removal

Figure 5.1 elucidates the transformation of N, COD and their respective removal efficiencies in the AGS for the treatment of anaerobically digested molasses wastewater over 110 days. In Stages I and II, with influent NH_4^+-N concentrations ranged from 350 to 470 mg/L, effluent concentrations of NH_4^+-N maintained at below 1 mg/L, that was an over 99% ammonium removal (Figure 5.1a and Figure 5.1b). The average NO_2^--N and NO_3^--N concentrations in Stage I (the high AnGS condition) effluent were 130 mg/L and 260 mg/L, respectively, that was a 10% TIN removal

(Figure 5.1a and Figure 5.1b). In contrast, Stage II (the low AnGS condition) achieved an 8% TIN removal with effluent NO_2^--N and NO_3^--N concentrations at 6 mg/L and 390 mg/L, respectively. Figure 5.1c indicates the nitrite accumulation rate over the operation period. An average nitrite accumulation of 30% was attained in Stage I (the high AnGS condition). However, after one week of operation in Stage II (the low AnGS condition), the nitrite accumulation reduced and stabilized at 1%. Nitrite accumulation was observed immediately upon introducing high AnGS content influent wastewater, indicating a quick response to the reduced SRT. Figure 5.1d shows the sCOD levels in Stage I influent and effluent were 2953 mg/L and 2634 mg/L, respectively, that was a sCOD removal efficiency of 11%. Interestingly, the sCOD removal efficiency experienced an improvement to 20% in Stage II. The decreased nitrite accumulation and higher sCOD removal in Stage II might be attributed to the elimination of AnGS from influent wastewater, which likely disintegrated and hydrolysed, interfered the system and resulting in a higher COD in Stage I's effluent. The residual recalcitrant COD in the effluent should be further treated, potentially using advanced oxidation or photocatalytic processes [119, 120]. The hydrolysis of AnGS may also introduce ammonium and organic nitrogen into the system. Based on the consistently high ammonium removal efficiency, the produced ammonium likely being completely oxidized, but the organic nitrogen needs to be further tested and treated in future studies.

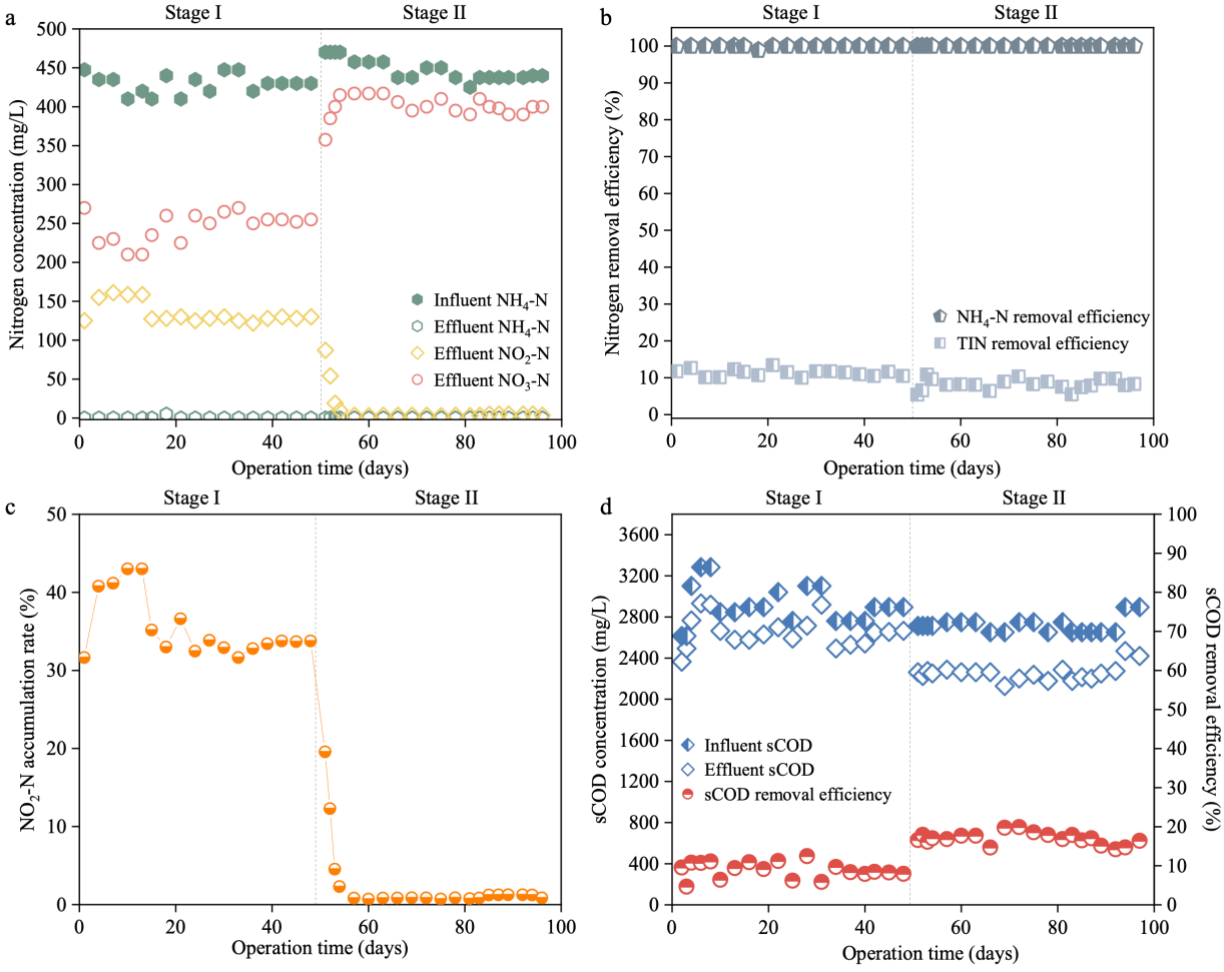

Figure 5.1 Reactor performance over stage I (the high AnGS condition) and stage II (the low AnGS condition), including a) NH_4^+-N, NO_2^--N and NO_3^--N concentrations in influent and effluent; b) NH_4^+-N and TIN removal efficiencies; c) NO_2^--N accumulation rates; and d) sCOD concentrations and removal efficiencies in influent and effluent.

5.3.1.2 Effluent solid content

The effluent solid concentration in Stage I (the high AnGS condition) was 2.6 g/L, while that in Stage II (the low AnGS condition) was 0.3 g/L. The effluent solids, predominantly in flocculant form, were likely derived from disintegrated AnGS and detachment of microorganisms from AGS's surface. Solids were discharged exclusively during effluent decanting. The SRT, determined by the effluent solid content, was 7 days in Stage I and 80 days in Stage II. This trend indicated that elevated AnGS introduction may compromise the stability of the AGS, leading to increase sludge disintegration and loss.

5.3.2 Sludge characteristics

Figure 5.2 presents values on biomass content and SVI over the operation period. In Figure 5.2a, it's shown that the MLSS and MLVSS concentrations were 10 g/L and 8 g/L in Stage I (the high AnGS condition). Elevated MLSS and MLVSS concentrations were noticed in Stage II (the low AnGS condition), with an average of 12 g/L MLSS and 9 g/L MLVSS. Figure 5.2b illustrates the SVI_5 and SVI_{30} dynamics in response to AnGS introduction. The SVI_5 was 68 mL/g in Stage I, then gradually decreased and stabilized at 46 mL/g in Stage II. The SVI_{30} was higher in Stage I at 40 mL/g, and then gradually settled at 25 mL/g in Stage II. Compared to Stage II (low AnGS condition), the high AnGS addition in Stage I likely caused increased friction between AnGS and AGS, leading to granule disintegration. This resulted in increased floc presence in the reactor, contributing to higher SVI values and lower biomass concentrations due to sludge washout. Previous study has also observed the disintegration of AnGS when added into AGS reactor [51]. Additionally, the AnGS might elevate organic loading in the system, which might result in subsequent oxygen competition and may hinder the aerobic metabolism and leading to structural breakdown.

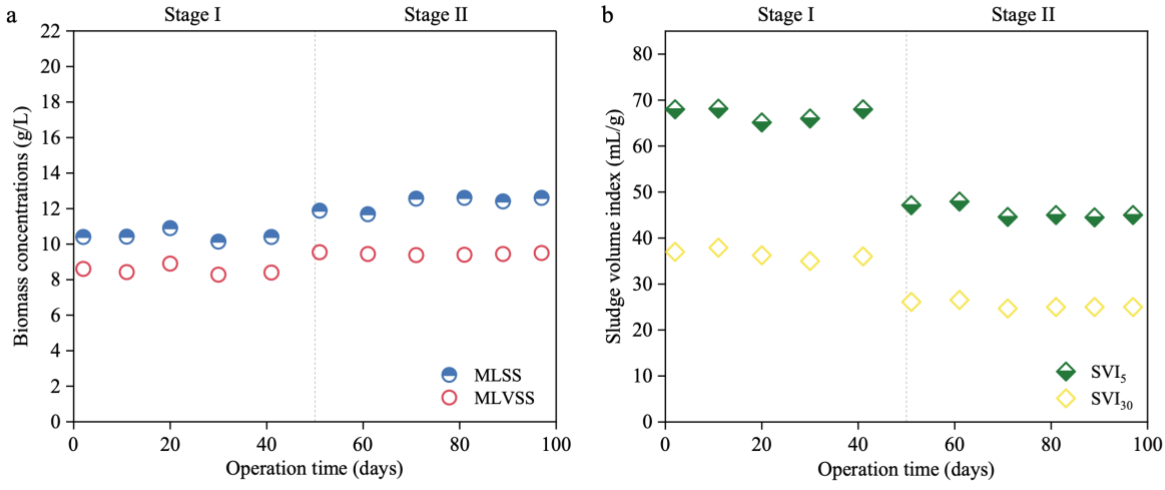

Figure 5.2 Dynamics of a) mixed liquor suspended solids (MLSS) and mixed liquor volatile suspended solids (MLVSS) concentrations, and b) sludge volume index (SVI_5 and SVI_{30}) across reactor operation.

The size of the AGS in Stage I (the high AnGS condition) was 0.6 ± 0.3 mm, with notable presence of AnGS that acted as a nucleus within these granules. The granule size in Stage II (the low AnGS

condition) slightly increased to 0.7 ± 0.5 mm. The morphology of AGS in Stages I and II can be found in Figure 5.3. The observed smaller AGS in Stage I is likely due to the sludge detachment from granule surface through the friction between AnGS and AGS. Consequently, more intact granular sludge was preserved in the system. Similar observation has been documented previously [121]. Further, the presence of AnGS in the core of AGS implies that the retained AnGS or AnGS aggregates potentially contributed to support granule formation in AGS.

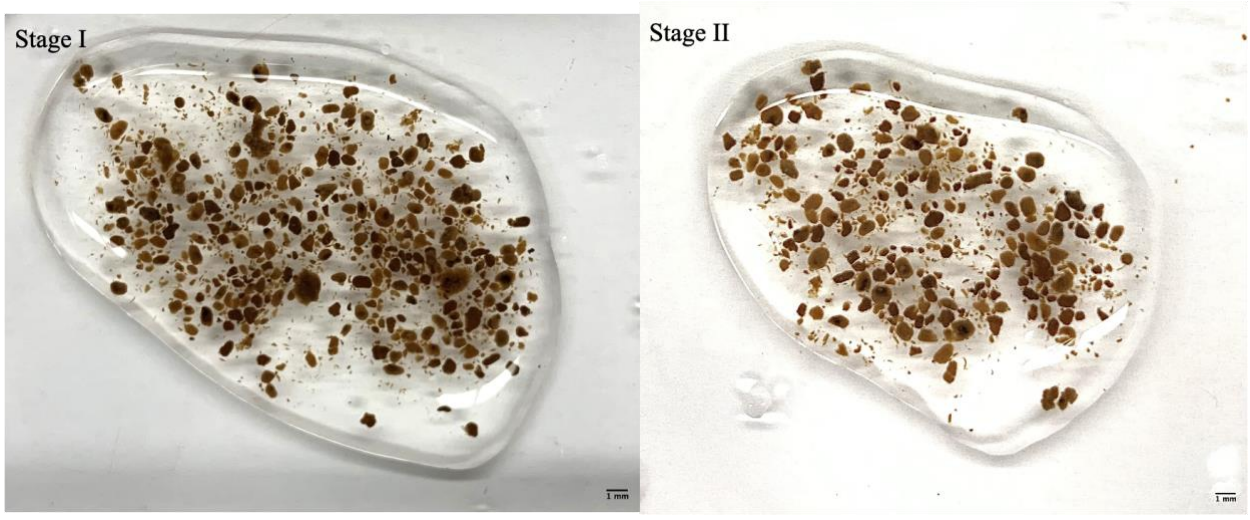

Figure 5.3 Morphology of granular sludge in Stage I and Stage II.

5.3.3 Microbial kinetics

Figure 5.4 illustrates the rates of ammonium oxidation and nitrite oxidation, serving as indicators of autotrophic ammonia oxidizing bacteria (AAOB) and nitrite oxidizing bacteria (NOB) activity, respectively, during Stages I and II. Initially, in Stage I, AAOB activity was recorded at 0.22 g N/(g VSS·d). This rate increased significantly ($p<0.05$) to 0.32 g N/(g VSS·d) in Stage II, a rise that can be attributed to an extended SRT promoting AAOB retention. The AAOB activities achieved in current study fall within the range of previously reported values, which varied from 0.08 to 0.65 g N/(g VSS·d) [122-126]. Significantly ($p<0.05$) increased activity of NOB was also observed from 0.19 g N/(g VSS·d) in Stage I to 0.31 g N/(g VSS·d) in Stage II. Further, the NOB activity in Stage I was lower than the AAOB activity, which explained the elevated nitrite accumulation in Stage I. Notably, the NOB activities observed in this study were higher compared to those reported in previous studies [126, 127]. This may be attributed to the well-cultivated seed

sludge that originated from a high ammonia wastewater treatment system, and the start-up phase, which allowed the microbes to pre-adapt to the wastewater.

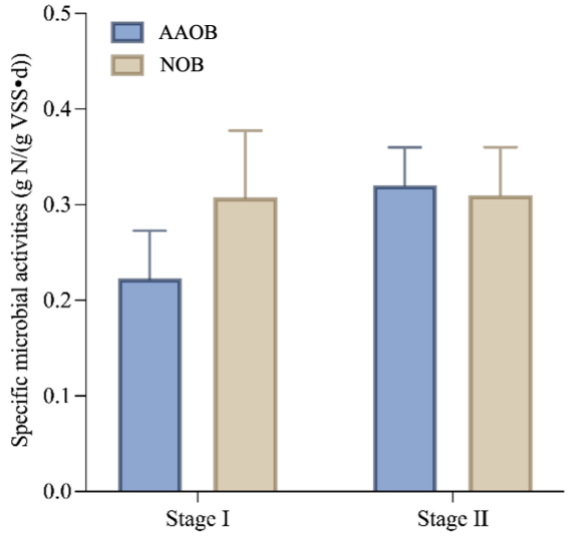

Figure 5.4 Specific microbial activities of autotrophic ammonia oxidizing bacteria (AAOB) and nitrite oxidizing bacteria (NOB) across the reactor operation.

5.3.4 Microbial community dynamics

To assess the influence of AnGS introduction on microbial community assembly within the AGS, a detailed microbial analysis was carried out.

5.3.4.1 Microbial community at phylum level

Figure 5.5a displays the microbial composition at phylum level in sludge samples from Stage I, II and AnGS. In Stage I, Proteobacteria, Synergistetes and Actinobacteria were the top three phyla, with relative abundances at 32%, 17% and 14%, respectively. In Stage II, Proteobacteria remained the most abundant phylum, constituting 54% of the microbial community, followed by Actinobacteria and Thermi, both accounting for 14% of the microbial community. The predominance of Proteobacteria and Actinobacteria underscores the capacity of the system to remove nitrogen and degrade complex organic matter [128, 129]. The microbial community in the AnGS was mainly composed of the phylum Synergistets at 33%, Firmicutes at 16%, Verrucomicrobia at 12% and Euryarchaeota at 11%, which were commonly reported in anaerobic digestion studies [130, 131]. The significant presence of Synergistets in Stage I, at 17%, likely due to the introduction and retention of AnGS. In contrast, the relative abundance of Synergistetes

dropped to less than 1% in Stage II once AnGS was removed from the feed. Stage I also showed a higher relative abundance of KSB3, Euryarchaeota and Firmicutes, which were the dominant microorganism in AnGS. These observations align with the previously reported studies, showing the influence of externally introduced microbes were more significant under short SRT condition like Stage I in current study than that under long SRT condition [132].

5.3.4.2 Microbial community at genus level

Figure 5.5b depicts the divergency of microbial composition at the genus level in sludge samples from Stage I, II and AnGS. In Stage I, the dominant genus was *HA73*, accounting for 13.7% of the community, followed by *Leucobacter* (6.9%) and *Steroidobacter* (6.2%). Stage II's microbial community was most abundant in genus *B-42* at 14.2%, followed by *Leucobacter* at 8.7% and *Nitrosomonas* at 7.8%. The predominant genera in AnGS were *HA73* at 30.1%, *R4-41B* at 10.9%, and genera in phylum KSB3 at 9.1%.

Development of genera associated with nitrogen oxidation

The genera predominantly involved in ammonium oxidation were *Nitrosomonas* and genera belonging to the family Nitrosomonadaceae. *Nitrosomonas*, commonly found in wastewater treatment systems, displayed 0.3% of the microbial community in Stage I, substantially increasing to 7.8% in Stage II. Likewise, the relative abundance of genera affiliated to family Nitrosomonadaceae rose from 2.3% in Stage I to 5.2% in Stage II. *Nitrosomonas*, an r-strategist, proliferate more rapidly under high ammonium conditions compared to K-strategist, which explains its increased dominance in the reactor [6, 133]. The increased relative abundance of AAOB in Stage II was consistent with the elevated specific AAOB activity. *Nitrobacter* was the dominant NOB in the AGS, accounted for 0.6% in Stage I and increased to 3.1% in Stage II. The elevated relative abundances of *Nitrosomonas* and *Nitrobacter* in Stage II were likely attributed to the extended SRT, facilitates the retention of these slow growing bacteria. Moreover, the reduced abundance of *Nitrobacter* in Stage I was consistent with the observed increase in nitrite accumulation. It is reasonable that the relative abundance of these genera was limited in the AnGS.

Development of genera associated with nitrogen reduction

Genera *Paracoccus* and *Thauera* are frequently reported as dominant denitrifiers in wastewater treatment systems [134, 135]. However, their relative abundances were merely 1% in Stages I and II, likely due to the low availability of biodegradable sCOD necessary for the growth of denitrifiers. In contrast, *Steroidobacter*, which had capability to perform denitrification using steroid as the organic carbon source [136]. The higher abundance of this genus in Stage I aligns with the activity and TIN removal performance result.

Besides heterotrophic denitrifiers, this study observed the presence of *Thiobacillus*, a functional microorganism recognized in sulfide-oxidizing autotrophic denitrification (SOAD) studies [137, 138]. *Thiobacillus* can use sulfide or thiosulfate as electron donors to remove N, a process typically observed under anoxic conditions [139, 140]. However, this microbe has also been detected in Nif/DNif biofilm reactors [141]. With the distinct layer structure in AGS, the SOAD process could potentially occur in the inner core of the AGS. *Thiobacillus* was undetectable in the AnGS, but showed 1% relative abundance in Stage I and 4% in Stage II. The absence of *Thiobacillus* in AnGS suggests that its emergence in Stages I and II was not due to the introduction of AnGS. The presence of sulfide in industrial and sewer discharges has been documented previously [21]. The hypothesis is that the slow feeding of sulfide-containing digested wastewater stimulated the growth of *Thiobacillus*. This suggests the possibility of autotrophic denitrification occurring in the AGS, contributing to nitrogen removal alongside with heterotrophic denitrification process. Further research, involving the measurement of influent wastewater sulfide concentration and the specific activity of this process, is required to ascertain the specific contribution of SOAD to the overall nitrogen removal in this system.

Development of genera associated with COD degradation

In Stage I, the dominated genera related to COD degradation were primarily sourced from AnGS, including *HA73*, genera belonging to order Bacteroidales, those affiliated with Clostridiales, and those belonging to the family Coriobacteriaceae. These microorganisms are capable of performing hydrolysis and fermentation processes [142-145]. In comparison, the predominant COD degradation genera in Stage II likely had a broad enzymatic capacity to degrade complex organic

compounds, involving genera from the order Burkholderiales, order JG30-KF-CM45, and family Phyllobacteriaceae [146, 147]. *B-42* and *Leucobacter* were present in both stages. *B-42*, belonging to the family Trueperaceae, has been reported to degrade organics under extreme environments [148]. Genus *Leucobacter* is known for its ability to degrade complex organics [149].

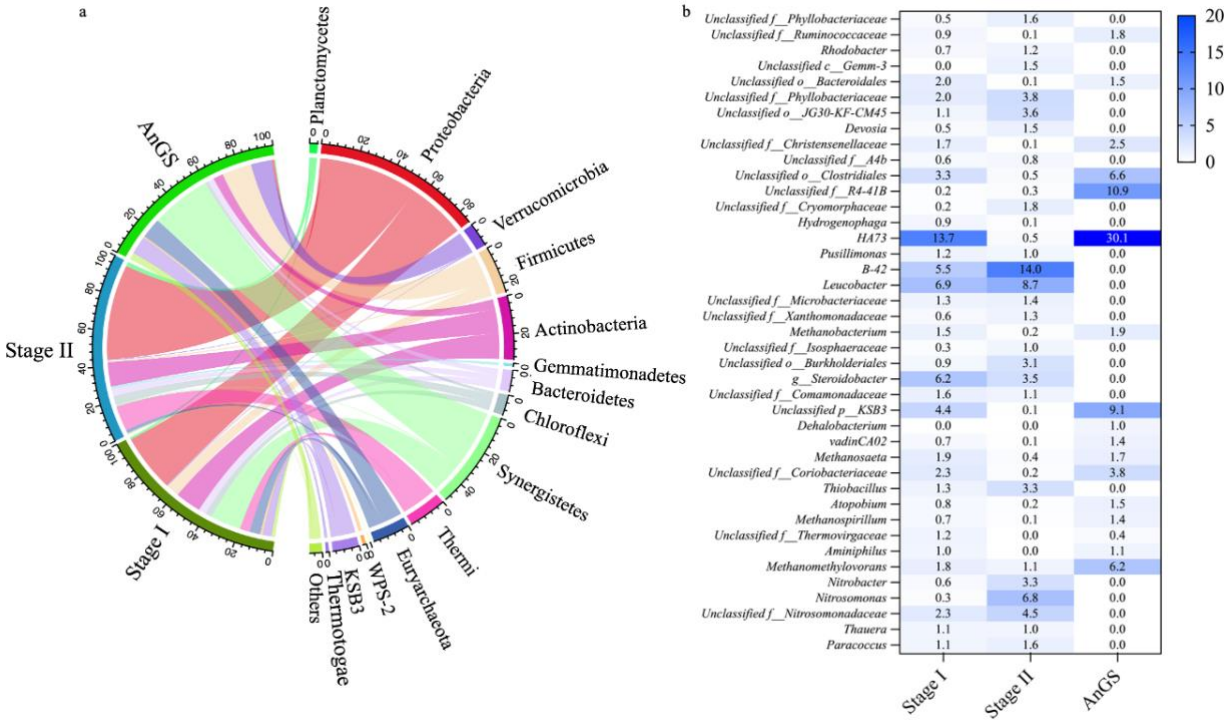

Figure 5.5 Development of microbial community at a) phylum level and b) genus level (relative abundance over 1%) in sludge samples from Stages I, II and anaerobic granular sludge; Unidentified genera were named at family (Unclassified f_), order (Unclassified o_), class (Unclassified c_) and phylum (Unclassified p_) levels.

5.3.4.3 Microbial Diversity and relationship

Figure 5.6a shows the microbial diversity and richness across Stage I, II and AnGS. The Shannon and Simpson indexes, which represent the diversity of the microbial community, indicated a decrease in diversity from Stage I to Stage II. The Chao1 index, reflecting the richness of the microbial community, showed that Stage I exhibited the highest richness compared to Stage II and AnGS. This suggests that the introduction of AnGS potentially contributed to a more varied and abundant microbial community.

Principal coordinate analysis (PCoA) result was depicted in Figure 5.6b. The analysis revealed that PCoA1 axis explained 94% of the variance in the samples. Observations along the PCoA1 axis indicate that the AnGS and sludge samples from Stages I were more closely grouped, suggesting a higher degree of similarities in their microbial communities. This pattern supports the observation of AnGS retention in the system and their disappearance over the operation.

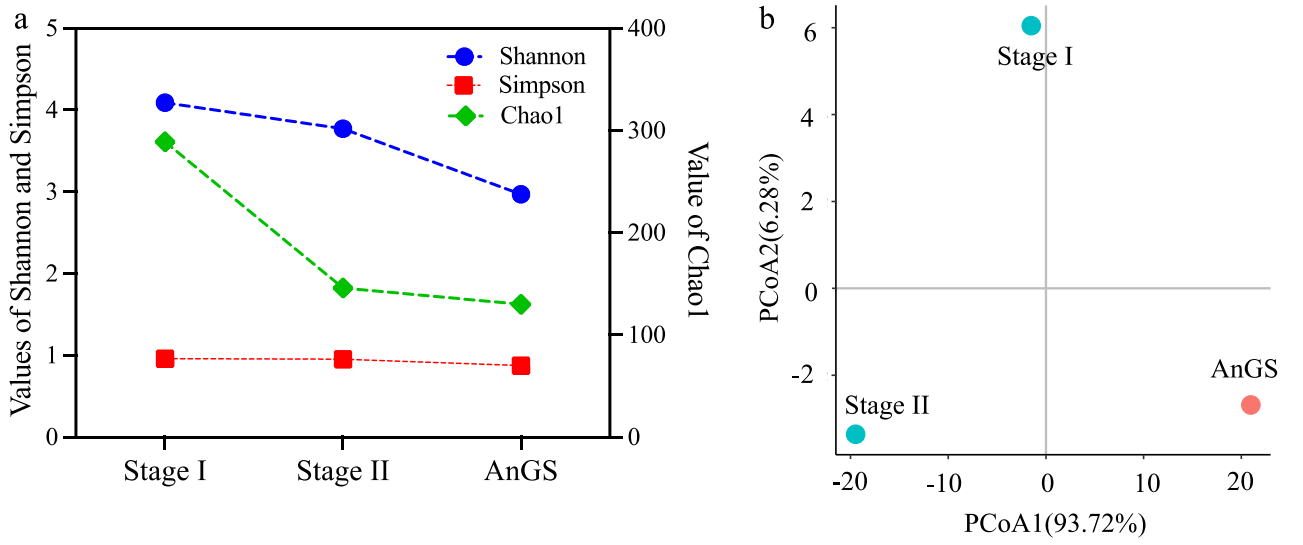

Figure 5.6 Diversity and relationship of sludge samples from Stages I, II and anaerobic granular sludge, a) microorganism biodiversity and richness indexes and b) principal coordinated analysis (PCoA).

5.3.4.4 Microbial immigration evaluation

Mass balance model analysis was performed at genus level for Stage I sludge sample. As delineated in Table 5.1, all dominant genera in AnGS, defined as having a relative abundance over 1%, exhibited inactive in the AGS, indicated by negative growth rates (μ). This implies that the microbial immigration from AnGS to AGS might have a minimal impact on its microbial composition. The mass balance analysis excluded Stage II, attributed to the minimal presence of AnGS in the feed, presumed to exert an insignificant impact on the AGS.

Table 5.1 Microbial immigration model analysis result.

Genera	μ-Stage I, 1/d
Unclassified_f_Ruminococcaceae	-0.495149797
Unclassified_o_Bacteroidales	-0.059086722
Unclassified_f_Christensenellaceae	-0.322450432
Unclassified_o_Clostridiales	-0.47202298
Unclassified_f_R4-41B	-20.57198295
HA73	-0.550018837
Methanobacterium	-0.248584211
Unclassified_p_KSB3	-0.512367734
Dehalobacterium	-7.230361211
vadinCA02	-0.435011622
Methanosaeta	-0.100266086
Unclassified_f_Coriobacteriaceae	-0.370009285
Atopobium	-0.476062795
Methanospirillum	-0.463983174
Aminiphilus	-0.182765381
Methanomethylovorans	-0.989219733

5.4 Discussion

5.4.1 Positive impacts from the introduction of AnGS

5.4.1.1 AnGS elevated nitrite accumulation via SRT control

Elevated nitrite accumulation was observed in Stage I (the high AnGS condition) at 30% compared to Stage II (the low AnGS condition) at 1%. This implies that the nitrite oxidation process was partially inhibited in Stage I. This observation has never been reported in AGS studies treating high solid content wastewaters. Potential factors that might lead to nitrite accumulation include inhibition by free ammonia and free nitrous acid, low temperatures, low DO and short SRT [150]. In current study, the reduced SRT is identified as a primary factor for nitrite accumulation, since the ammonium concentration, temperature and DO were maintained the same throughout the operation period. The consistent DO concentration, ranging from 1.0 to 1.2 mg/L, throughout the operation, indicated that the influent solids had no significant negative impact on oxygen transfer in this study. The SRT in Stage I was 7 days and in Stage II was 80 days. AAOB requires an SRT of 8 days [6], while NOB need over 10 days [151-153] to be retained in the reactor. This probably explained the reduced nitrite oxidation in Stage I. Although the SRT in Stage I was also lower than

the SRT required for AAOB retention, high ammonia removal was still observed. This could be attributed to the granular structure effectively retaining AAOB in the system and its higher affinity for oxygen compared to NOB. The introduction of AnGS at a concentration of 1.8 g/L had no significant effect on the ammonium oxidation process. However, a decline in ammonium oxidation efficiency may occur with the introduction of higher concentrations of AnGS into the AGS.

The nitrite accumulation reduced the oxygen and chemical demand for nitrogen removal via Nit/DNit, which involves oxidizing ammonium to nitrite and then reducing to nitrogen gas. This is more economically favourable than conventional nitrification/denitrification, which converts ammonium to nitrite, then to nitrate, and followed by nitrate reduction to nitrite and finally to nitrogen gas. The accumulation of nitrite benefits the subsequent nitrogen reduction unit. Although nitrite accumulation was achieved in current study, the low bCOD in the wastewater limited the TIN removal. Further treatments involving denitrification process should be performed prior to the discharge. However, the increased nitrite concentration in the AGS and effluent potentially induces higher N_2O emissions. Higher nitrite concentrations have been reported to stimulate N_2O production under both aerobic and anoxic conditions, particularly when biodegradable COD is limited in the AGS [154]. The production of N_2O should be further investigated and addressed before application.

5.4.1.2 AnGS enhanced the TIN removal via sludge hydrolysis

The introduction of AnGS led to an increase in TIN removal, from 8% in Stage II (the low AnGS condition) to 11% in Stage I (the high AnGS condition). This enhancement in TIN removal in Stage I might be attributed to the elevated nitrite accumulation, which consumes less COD to perform N reduction compared to nitrate denitrification. The hydrolyzation of AnGS contributed additional COD, thereby supporting the denitrification process.

AnGS comprised mainly particulate organic matter and inert solids, with the organic fraction constituted a significant portion, accounting for 83% of the solid content. These characteristics indicate that the AnGS has the potential to be hydrolyzed and provide extra COD to facilitate denitrification process. However, its hydrolysis might be constrained under 4 hours cycle time,

therefore, a prolonged anoxic feeding phase could be provided to facilitate hydrolysis and potentially enhancing denitrification efficiency.

5.4.1.3 AnGS enhanced performance through supporting granulation

Even with the introduction and resultant disturbance by AnGS, intact AGS was observed, which is playing a crucial role in sustaining high ammonium removal efficiency in both stages. Previous study has also reported stable granule structure under long term operation when treating high solids content wastewater [58]. Two primary mechanisms by which AnGS supports granulation were proposed.

Firstly, AnGS may have served as a core for granulation. Most of the introduced AnGS were gradually disintegrated into flocs or aggregates, which then provided a growth niche for microorganisms to attach on, and thus support the granulation process in the AGS system. This observation aligns with previous studies demonstrating rapid AGS cultivation upon introducing either intact or crushed granular sludge [155].

Secondly, it is speculated that introducing mature granular sludge, which has been recognized as a strategy for introducing quorum sensing (QS) molecules, particularly N-acylhomoserine lactones (AHLs) and autoinducer-2 (AI-2) molecules, might contribute to enhanced granulation [155]. These molecules are known to stimulate the secretion of extracellular polymeric substances (EPS), thereby facilitating the granulation process. Further, a short term QS introduction has been documented to have long term positive impact on the AGS [156], which may have contributed to the enhanced settling capacity and elevated biomass content in Stage II. Further studies employing QS molecules, scanning electron microscopy (SEM) and EPS analysis are needed to support this hypothesis [157].

5.4.2 Negative impacts from the introduction of AnGS

5.4.2.1 AnGS negatively affected the effluent biomass content via sludge disintegration

The introduction of AnGS into the AGS resulted in an elevated effluent solids concentration. The effluent from the AGS primarily comprised of flocs, which were likely derived from AnGS disintegration, as well as the biomass detachment from AGS's surface. Given that the AnGS

exhibited an average size at 1 mm with high density and good settling properties, it suggests that while AnGS was initially retained within the system, over time, it gradually disintegrated, either flowing out with the effluent or undergoing degradation within the system. Biomass detachment has also been documented in prior study treating high suspended solid wastewater [58]. Consequently, a post-treatment process is necessary to reduce the solids in the effluent to comply with discharge limit. It has also been reported that influent solids larger than 0.2 mm were likely retained in the system, either by trapped by AGS or through self-settling, while solids smaller than 0.1 mm were likely washed out, contributing to higher effluent solid concentrations [158]. This aligns with the observation in this study.

5.4.2.2 AnGS negatively affected the sCOD removal via the production of non-biodegradable sCOD

The addition of AnGS increased effluent sCOD concentration from ~2300 mg/L in Stage II (low AnGS condition) to ~2600 mg/L in Stage I (high AnGS condition). The sCOD removal efficiency was 11% in Stage I and 20% in Stage II. The elevated sCOD concentration in the effluent in Stage I might be attributed to the production of unbiodegradable COD from sludge hydrolysis [159]. During sludge hydrolysis, soluble microbial by-products and EPS are hydrolysed into small molecules, potentially supporting TIN removal. Concurrently, recalcitrant molecules, such as humic acid, are produced, which likely contribute to the increased effluent sCOD. The treatment of remaining TIN in the treated wastewater warrants further investigation, such as bypassing high COD molasses wastewater (before anaerobic digestion) into the reactor or introducing the anaerobically digested molasses wastewater stepwise to effectively utilize the available biodegradable sCOD in the wastewater.

5.4.2.3 AnGS negatively affected the specific microbial activities

With high AnGS addition, the specific microbial activities of AAOB and NOB were lower compared to those under low AnGS addition conditions. The reduction was likely due to the washout of functional microbes under reduced SRT and the detachment from granules caused by friction between AnGS and AGS. The diminished activities indicate a lower treatment capacity and reduced resilience to environmental shocks.

5.4.3 AnGS's influence on AGS performance through bioaugmentation

Bioaugmentation is an approach aimed at enhancing the degradation of pollutants through the introduction of specific microbes. The continuous introduction of AnGS was expected to bioaugment the system with facultative bacteria. However, mass balance model analysis revealed that the microorganisms present in AnGS experienced negative growth within the AGS, suggesting a lack of bioaugmentation effect from AnGS introduction. The detection of dominant genera from AnGS in Stage I sludge likely attributed to the continuous introduction and retention of AnGS. In contrast, a much lower relative abundance of these genera was noted in Stage II, at < 2%, supporting that the microorganisms from AnGS did not survive in AGS, and showed limited effect on microbial development.

5.4.4 Implications and perspectives

In future applications, such wastewater treatment can be tailored to specific requirements. For ammonium removal alone, a buffering tank can be applied for solids removal before introducing the wastewater into the AGS system. For nitrogen removal, the wastewater can be directly introduced into the reactor to remove nitrogen through the nitritation/denitritation pathway. This study demonstrated the feasibility of AnGS addition for facilitating nitrite accumulation, saving both oxygen and chemical inputs compared to nitrification/denitrification. Currently, strategies like free ammonia and free nitrous acid inhibition are used to eliminate NOB and achieve nitrite accumulation [160, 161]. The introduction of AnGS could simultaneously promote granulation and nitrite accumulation. The removal of oxidized nitrogen could utilize COD from AnGS hydrolysis with extended hydrolysis time or by adding high COD molasses wastewater before anaerobic digestion. However, the dosing concentration and frequency of AnGS should be considered. Additionally, the elevated effluent solids content necessitates additional units to address this concern.

5.5 Conclusion

The introduction of AnGS into the nitrogen removal AGS showed both positive and negative impacts on system performance. A stable ammonia removal efficiency of 99% was consistently achieved, unaffected by the introduction of AnGS at a concentration of 1.8 g/L. AnGS addition

led to an increase in nitrite accumulation from 1% (the low AnGS condition) to 30% (the high AnGS condition), and an improvement in TIN removal efficiency from 8% to 11%. In contrast, elevated effluent sCOD concentration was noted under the high AnGS condition, alongside an increase in effluent solid content. The positive impacts on N removal from AnGS introduction can be attributed to its facilitation of sludge granulation by acting as nucleus. The negative impacts from AnGS attributable to the disturbance of the system, disintegration of AnGS, and detachment of biomass from AGS's surface. Furthermore, the mass balance model analysis indicated that the addition of AnGS did not enhance the AGS microbial community through bioaugmentation. The results in current chapter provide a comprehensive insight into the potential effects of treating anaerobic digestate containing AnGS, outlining the complexities and considerations necessary for optimizing N removal processes in such system.

Chapter 6. Feasibility of Aerobic Granular Sludge (AGS) Reactor for High Ammonia Low Alkalinity Centrate Treatment under Various Carbon to Nitrogen Ratios: pH adjustment potential[3]

6.1 Introduction

Chapter 4 has demonstrated that high ammonia levels and low C/N ratios enriched and selected for highly active AAOB, significantly improving ammonia removal efficiency under alkalinity sufficient conditions. However, the feasibility of AGS and influence of varied bCOD content on high ammonia, low alkalinity centrate treatment has not yet been evaluated. Additionally, the combined effects of C/N ratios and Alk/N ratios remains underexplored.

High ammonia conditions promote the proliferation of slow growing bacteria such as ammonia oxidizing bacteria (AOB) and nitrite oxidizing bacteria (NOB). These bacteria have been reported to enhance the stability of granular sludge due to their ability to form dense structures [162, 163]. While high ammonia concentrations can increase the complexity of microbial community, they may also inhibit certain microorganisms responsible for the production of EPS, which are crucial for the granulation process [134, 163]. Additionally, the potential of C/N ratios on pH adjustmentt, compensating for the lack of alkalinity in the wastewater, is pivotal for high ammonia removal but has not yet been assessed. Consequently, a systematic investigation is needed to elucidate the influence of C/N ratios on treatment of high ammonia wastewaters using AGS reactors.

This chapter investigated the effects of varying C/N ratios on the overall performance of an AGS treating high ammonia, low alkalinity digested sludge centrate. The primary objectives were to provide a comprehensive analysis of the resultant changes across varying C/N ratios, uncover the underlying mechanisms governing these changes, and thereby identified the control parameters to optimizing the treatment of such wastewaters. The investigation focused on the evaluation of treatment performance, granule stability, microbial specific activity, and microbial community shift.

[3] A version of this chapter has been submitted for journal publication in June 2024.

6.2 Methods and materials

6.2.1 Source of wastewater and inoculum

Raw digested sludge centrate was periodically collected from an autothermal thermophilic aerobic digestion facility in Canada. The wastewater exhibited NH_4^+-N concentrations ranging between 769 and 952 mg/L, with limited NO_2^--N and NO_3^--N concentrations below 6 ± 3 mg/L, and an alkalinity between 1760 and 2330 mg $CaCO_3$/L, that is an Alk/N ratio of 2.3 to 2.7 (Table 6.1). The soluble chemical oxygen demand (sCOD) concentration varied from 2136 to 7897 mg/L across different batches, resulting in an average C/N ratio in the wastewater of between 2.8 to 8.3. The biodegradable proportion of sCOD ranges from 1016 to 6722 mg/L. Before undergoing the AGS treatment, the wastewater samples were stored at a temperature of 4 °C. The AGS treatment utilized an inoculum derived from well-cultivated granular sludge from an AGS treating high ammonia, low biodegradable COD (bCOD) liquid waste [164].

Table 6.1 Influent centrate physiochemical characteristics

Stages	NH_4^+-N concentrations (mg/L)	Alkalinity concentrations (mg/L)	Soluble COD concentrations (mg/L)	Biodegradable soluble COD concentrations (mg/L)	C/N ratios
I	952 ± 37	2250	7897 ± 90	6722 ± 167	8.3 ± 0.2
II	887 ± 31	2000	5878 ± 436	4563 ± 555	6.6 ± 0.5
III	858 ± 39	2330	3635 ± 245	2496 ± 407	4.2 ± 0.3
IV	769 ± 18	2120	2136 ± 251	1016 ± 171	2.8 ± 0.3

6.2.2 Reactor setup and operation

A 3 L cylindrical AGS with dimensions of 90 cm in height and 8 cm in diameter was utilized to treat high ammonia digested sludge centrate. The reactor was operated at 30 °C in sequencing batch mode to mimic the environment in wastewater treatment plant. The reactor operation could be divided into four stages with varying carbon to nitrogen (C/N) ratios: 8-9 in Stage I, 6-7 in Stage II, 4-5 in Stage III and 2-3 in Stage IV. Each stage featured an operational cycle adjusted for duration: 8 hours for Stage I, 6 hours for Stage II, 5 hours for Stage III and 4 hours for Stage IV. These cycles consisted of a 30 min anoxic feeding period, 30 min for settling, 10 min for decanting and the remaining time dedicated to aeration. Aeration was facilitated by an air diffuser located at the bottom of the reactor, achieving an upflow superficial velocity of 1.0 cm/s. The operational sequences of the reactor were regulated using programmable timers, with a 40% feed exchange rate per cycle.

6.2.3 Sludge characteristics

The extraction and measurement of soluble extracellular polymeric substance (S-EPS), loosely bound EPS (L-EPS) and tightly bound EPS (T-EPS) were conducted according to methods detailed in Chapter 3. Additionally, the changes in granular sludge sizes throughout the operation period were monitored using ImageJ software.

6.2.4 Microbial community analysis

DNA extraction was performed on seed sludge and sludge samples collected at Stages I to IV, using DNeasy PowerSoil Pro Kit (QIAGEN, Hilden, Germany). Amplification of the extracted DNA was performed with the universal primer pair 515 F/806 R, then sending the samples for amplicon sequencing on the Illumina Miseq PE250 platform at Genome Quebec (Montréal, QC, Canada). The processing of sequencing data, including the assignment of taxonomy, was conducted utilizing the DADA2 algorithm and referencing the Silva database (v138.1) with a 99% similarity [77, 165]. Alpha diversity and redundancy, as well as Principal Component Analysis (PCA) were evaluated using *ampvis2* in R [166].

6.2.5 Statistical analysis

The determination of result significance was conducted using the p-value obtained from T-test (Microsoft Excel), with a p value below 0.05 indicating statistical significance.

6.3 Results

6.3.1 Reactor performance

Figure 6.1 elucidates the reactor's efficacy in treating digested sludge centrate under varying C/N ratios. Figure 6.1a presents the dynamics of N compounds (NH_4^+-N, NO_2^--N and NO_3^--N) in the influent and effluent. Notably, the influent NH_4^+-N concentration ranged from 1000 to 780 mg/L, while effluent NH_4^+-N levels exhibited a progressive increase from 35 mg/L in Stage I to 50 mg/L in Stage II, 137 mg/L in Stage III and to 220 mg/L in Stage IV (Figure 6.1a). Effluent pH values were below 7 across the reactor operation. This upward trend in effluent ammonia could be attributed to the inadequate alkalinity for complete ammonia oxidation. An alkalinity to NH_4^+-N

ratio of 7.14 indicates a requisite alkalinity over 5500 mg/L as $CaCO_3$, beyond the 2000 mg/L alkalinity provided by the influent. Alternatively, COD could be leveraged to the denitrification process to replenish alkalinity internally. As the C/N ratio reduced from 9 to 2, the effluent nitrite concentration escalated from 82 mg/L (Stage I) to 105 mg/L (Stage II), 140 mg/L (Stage III) and reached 210 mg/L (Stage IV), indicating a diminished denitrification capacity and, consequently, a decrease in alkalinity recovery potential. In Stage I, with the highest C/N ratio of 8-9, an ammonia removal efficiency over 94% and a TIN removal of 86% were achieved (Figure 6.1b). A reduction in the C/N ratio to 6-7 resulted in reduced TIN removal to 79%, while maintaining stable ammonia removal at 94%. However, the reduction in the C/N ratio to 4-5 in Stages III and 2-3 in Stage IV compromised the denitritation process, thereby restricting the alkalinity recovery and leading to reduced ammonia and TIN removal efficiencies to 82% and 65% in Stage III and 72% and 44% in Stage IV (as shown in Figure 6.1b). Nitrate concentrations in the treated effluent maintained below 12 mg/L, likely due to suppressed NOB activity by high free ammonia concentration (up to 78 mg/L), surpassing the known NOB threshold (0.1-1 mg/L) [150].

Figure 6.1c reveals the sCOD concentration in the influent and effluent, as well as the removal efficiencies across stages. Influent sCOD levels varied considerably from 7897 mg/L in Stage I to 5878 in Stage II, 3635 mg/L in Stage III and 2136 in Stage IV, while effluent sCOD concentrations stabilized at approximately 1179 mg/L. This consistency in effluent sCOD suggests that it might primarily consist of the unbiodegradable proportion of influent sCOD, indicating that the biodegradable sCOD removal capacity was unaffected by the fluctuated C/N ratio. The sCOD removal efficiency dropped from 82% (Stage I) to 75% (Stage II), 62% (Stage III) and to 50% (Stage IV) due to the decreased available biodegradable sCOD in the centrate.

Figure 6.1d addresses the reduction in dissolved organic nitrogen (DON) throughout the operation period. The quantity of DON removed from AGS treatment was gradually reduced from 270 mg/L in Stage I to 244 mg/L in Stage II, 177 mg/L in Stage III and to 169 mg/L in Stage IV. The reduction in DON removal may result from reduced DON concentration in the influent centrate and the reduced C/N ratio, which has been reported to have positive relationship with DON reduction [124].

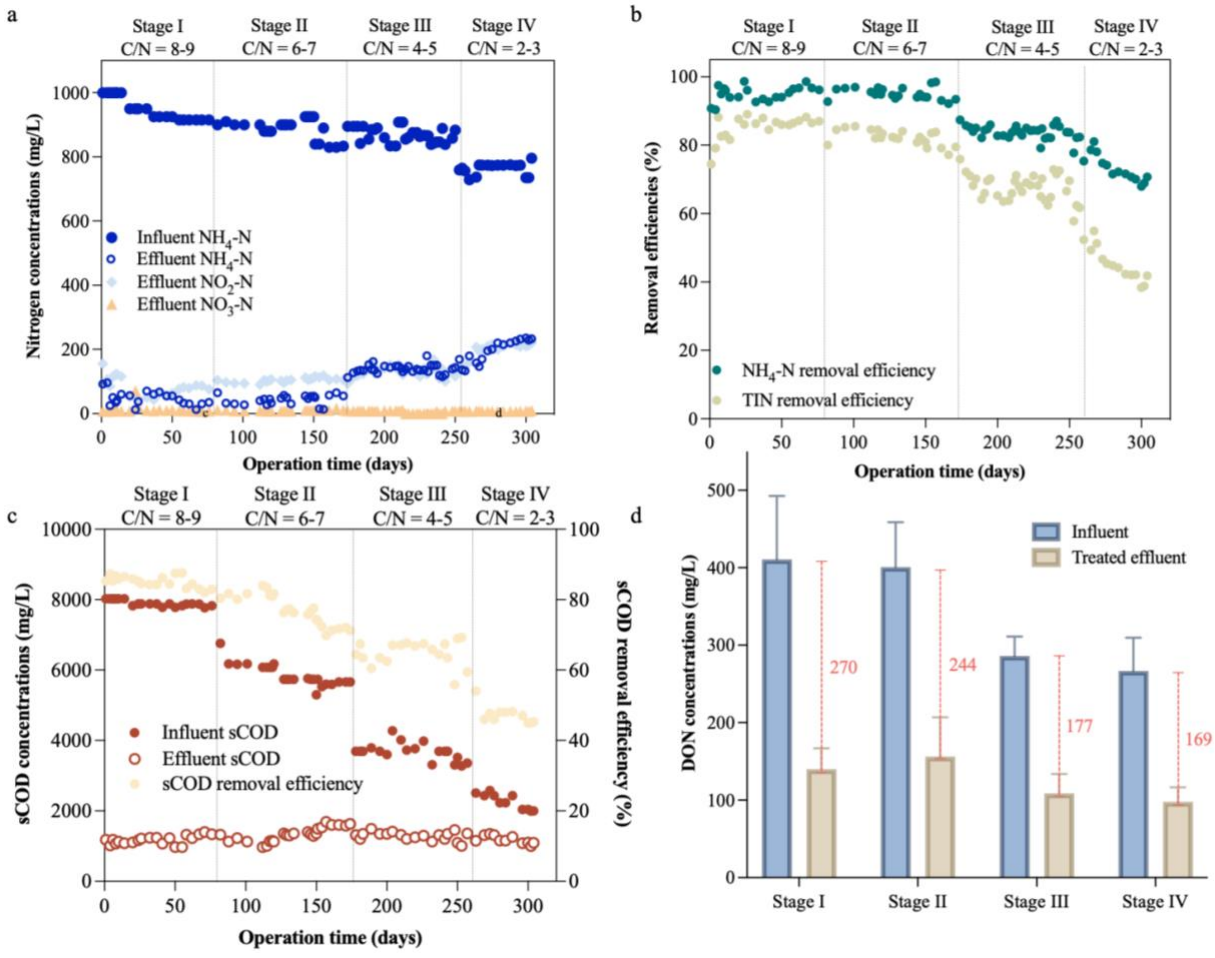

Figure 6.1 Reactor performance across the operation period, including a) concentrations of influent NH_4^+-N and effluent NH_4^+-N, NO_2^--N and NO_3^--N, b) removal efficiencies of NH_4^+-N and total inorganic nitrogen (TIN), c) concentrations of influent and effluent sCOD and its removal efficiency, and d) the concentrations of dissolved organic nitrogen (DON) in influent and treated effluent and the reduction of DON after treatment.

6.3.2 Sludge characteristics

6.3.2.1 Biomass concentration

Figure 6.2a illustrates the concentration of MLSS and MLVSS at different stages. The seed sludge had a concentration of 12 g/L MLSS and 10 g/L MLVSS. During Stage I, there was a noticeable increase, reaching peaks of 14 g/L for MLSS and 13 g/L for MLVSS. In Stage II, the concentrations of MLSS and MLVSS stabilized at 14 g/L and 12 g/L, respectively. A remarkable decreased was observed initially in Stage III, with values dropping to 9 g/L MLSS and 9 g/L MLVSS, before recovering to 13 g/L MLSS and 12 g/L MLVSS. This pattern of reduction

followed by an increase was also seen when the C/N reduced to 2-3, with biomass eventually reaching 13 g/L MLSS and 12 g/L MLVSS. This observation suggests a dynamic response of the biomass and adaptation to the operation conditions.

Figure 6.2b shows the SVI values at each stage. The seed sludge presented SVI_5 and SVI_{30} values at 80 and 47 mL/g, respectively. In Stage I, the SVI_{30} value increased to 68 mL/g, indicating a deterioration in the sludge settling ability. In Stage II, the SVI_5 and SVI_{30} improved and stabilized at 68 mL/g and 43 mL/g, respectively. In Stage III, the SVI_5 and SVI_{30} values temporarily spiked to 101 mL/g and 66 mL/g, respectively, then decreased to 73 mL/g and 40 mL/g. Similarly, the values increased to 87 mL/g for SVI_5 and 73 mL/g for SVI_{30} in Stage IV, which subsequently dropped to 71 mL/g and 44 mL/g, respectively.

Figure 6.2 highlights the optimal sludge concentration and settling capacity were observed at Stage II, corresponding to a C/N ratio of 6-7. The elevated SVI_5 and SVI_{30} values in Stage I might be attributed to the high C/N ratio, adversely impacting sludge structural stability and granulation, as noted by Wang et al. [46]. The observed decrease and subsequent improvement in MLSS, MLVSS and sludge settling capacity when C/N ratio dropped to 4-5 (Stage III) and 2-3 (Stage IV) imply that lower C/N ratio (< 5) initially disturb the system, causing granule structure instability, however, stabilization was achievable over time. The SVI_{30}/SVI_5 serve as a granulation indicator showing 90% in Stage I, 63% in Stage II, 55% in Stage III and 60% in Stage IV. This trend indicates a higher proportion of sludge in flocs form as the C/N ratio reduced [75].

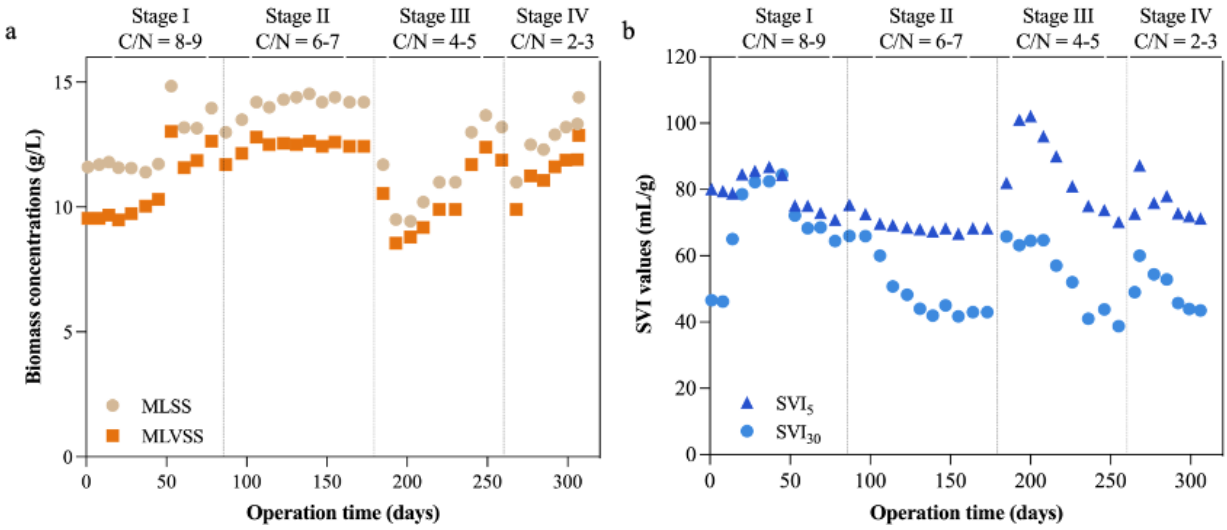

Figure 6.2 Biomass concentrations and settling capacity under different C/N ratios, including a) mixed liquor suspended solids (MLSS) and mixed liquor volatile suspended solids (MLVSS), and b) sludge volume indexes of 5 minutes (SVI_5) and 30 minutes (SVI_{30}).

6.3.2.2 Granular sludge size and EPS production

Figure 6.3 illustrates the dynamics of sludge size and EPS secretion under varied C/N ratios. Figure 6.3a depicts the change of granular sludge size, indicating a peak average size of 2.8 mm in Stage III, which slightly decreased to 2.7 mm at Stage IV, followed by 1.8 mm in Stage II, 1.3 mm in Stage I, and the smallest size was found in the seed sludge. Granular sludge morphologies under different C/N ratios were shown in Figure 6.4. The relatively small granule obtained in Stages I and II were likely due to the low dissolved oxygen (DO) levels and the need for a longer time for granule maturation under high ammonia conditions. The elevated COD and ammonia concentrations during these stages heightened oxygen demand, thereby lowering DO levels in the bulk liquid compared to later stages. Low DO levels constrained oxygen penetration into the granules and prompting microbes to form smaller aggregates for better substrate access [167]. Previous study has also documented reduced granular sludge size at high C/N at 9-10 and the granules were fluffy and loose in morphology [46]. Although, reduced granular sludge sizes were often reported with lower C/N condition [134, 168], but stable granular sludge was observed in Stages III and IV, which might potentially be correlated with EPS content and microbial composition.

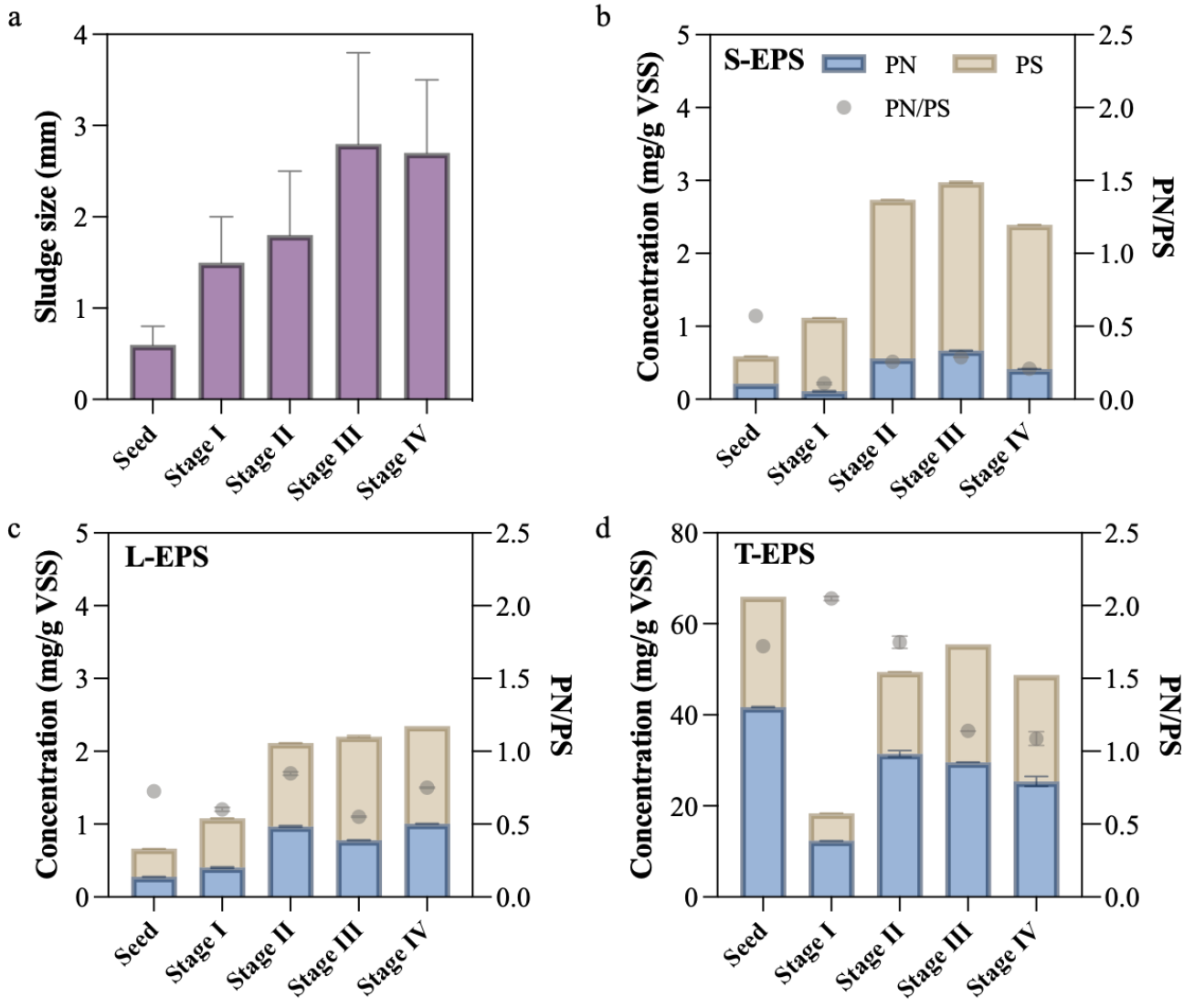

Figure 6.3 Sludge characteristics, including a) sludge size and b) concentrations of soluble extracellular polymeric substances (S-EPS) and its protein to polysaccharide ratios (PN/PS), c) concentrations of loosely bound EPS (L-EPS) and its protein to polysaccharide ratios (PN/PS), and d) concentrations of tightly bound EPS (T-EPS) and its protein to polysaccharide ratios (PN/PS) across the reactor operation.

EPS is crucial for the granulation process and stability of granular sludge, which comprises protein, polysaccharide, and other substances. The concentrations of S-EPS (Figure 6.3b), L-EPS (Figure 6.3c) and T-EPS (Figure 6.3d) revealed positive correlation with granular sludge size, except that in seed sludge. Lower overall EPS content that observed in Stages I and II aligned with the formation of smaller granular sludge. Further, the overall EPS contents in Stage IV was at the

same level as Stage III, which supports the observation of stable granule structure under reduced C/N conditions. T-EPS was the most abundant substance, followed by S-EPS and then L-EPS, aligning with the findings from previous granular study [169]. The protein to polysaccharide (PN/PS) ratio was less than 1 for S-EPS and L-EPS but exceeded 1 for T-EPS. L-EPS, rich in polysaccharide, is less conducive to flocculation and granulation [170], and high L-EPS levels can lead to sludge bulking and granule instability [171]. In contrary, the higher protein content observed in T-EPS is indicative of well-settling, stable granular sludge. This could be attributed to the negatively charged amino acids that involved in protein, which are adept at forming electrostatic bonds with multivalent cations, thereby enhance the stabilization of granule structure [172]. It is noticeable that all the lowest concentrations of S-EPS, L-EPS and T-EPS were observed in Stage I, with a significant increase by Stage II and stabilized afterwards. This observation suggests that a C/N ratio over 8 may impede EPS secretion.

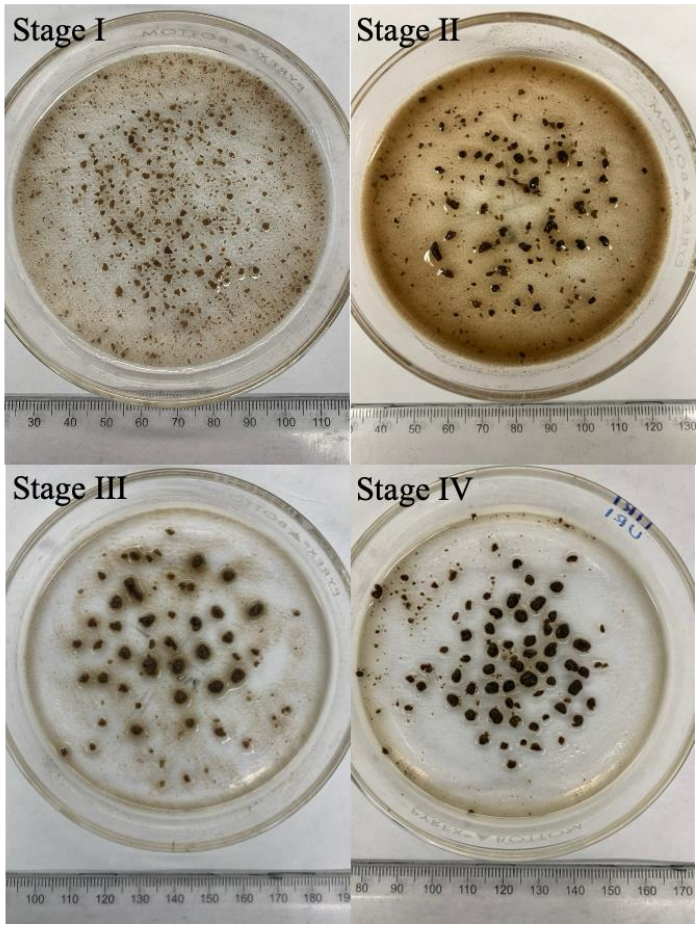

Figure 6.4 Morphology of aerobic granular sludge in each stage.

6.3.3 Microbial kinetics

6.3.3.1 Specific activites of ammonia oxidizing bacteria and nitrite oxidizing bacteria

Figure 6.5 elucidates the specific microbial activities, including AAOB, HAOB, NOB, denitritation and denitrification under various C/N ratios. Figure 6.5a shows the rates of ammonia and nitrite oxidation across reactor operation, highlighting that AAOB activity consistently outperformed HAOB activity. The highest AAOB activity was observed in the seed sludge at 0.38 g N/(g VSS·d). The lowest AAOB activity occurred in Stage I at 0.27 g N/(g VSS·d), which might be attributed to a microbial adaptation phase to the high COD environment. Subsequently, the AAOB activity elevated to 0.30 g N/(g VSS·d) in Stage II, 0.29 g N/(g VSS·d) in Stage III and reached 0.33 g N/(g VSS·d) in Stage IV. The gradual increase in AAOB activity may indicate their preference to low C/N condition and suggest that the low ammonia reduction in performance results of Stages III and IV unlikely due to the microbial activity. The AAOB activities obtained in current study aligns with the values reported in previous studies, ranging from 0.07 to 0.64 g N/(g VSS·d) [122, 123, 125, 126, 164].

According to Figure 6.5a, HAOB activity was notably low in the seed sludge and reached peak values in Stage I at 0.10 g N/(g VSS·d). Subsequently, the activity gradually reduced to 0.08 g N/(g VSS·d) in Stages II and III and further to 0.03 g N/(g VSS·d) in Stage IV, indicating a decline in HAOB activity as the C/N ratio decreased. Additionally, NOB activity remained minimal throughout the operation, with values not exceeding 0.006 g N/(g VSS·d). This limited NOB activity explained the observed low accumulation of nitrate in the AGS effluent.

6.3.3.2 Specific activities of denitritation and denitrification

Figure 6.5b depicts the specific activities of denitritation and denitrification across operation period. The highest denitritation and denitrification activities were obtained in Stage I, with denitritation reaching 4.2 g N/(g VSS·d) and denitrification achieving 1.6 g N/(g VSS·d). As the C/N ratio reduced, a gradual decrease in both activities was observed and obtained the lowest values in Stage IV, with 1.3 g N/(g VSS·d) for denitritation activity and 0.4 g N/(g VSS·d) for denitrification activity. This suggest that specific denitritation and denitrification activities were positively correlated to the C/N ratio.

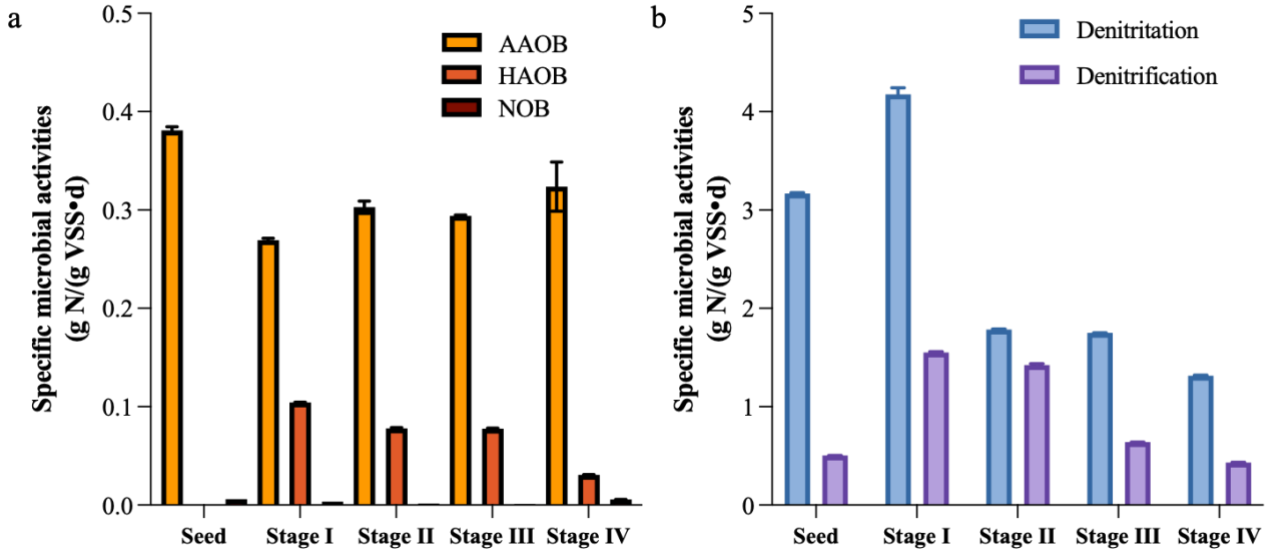

Figure 6.5 Specific microbial activities, including a) autotrophic ammonia oxidizing bacteria (AAOB), heterotrophic ammonia oxidizing bacteria (HAOB) and nitrite oxidizing bacteria (NOB); and b) denitritation and denitrification, under different C/N ratios.

6.3.4 Microbial response to different C/N ratios

6.3.4.1 Microbial diversity and richness

Figure 6.6 shows the diversity and richness of the microbial community in the course of 310 days, utilizing Shannon (Figure 6.6a) and Simpson (Figure 6.6b) indices for diversity and Chao1 (Figure 6.6c) for richness assessment. According to Figure 6.6, seed sludge exhibited the least microbial diversity and richness. As the C/N ratio decreased, an enhancement in microbial diversity was observed. An exception was noted in Stage III, which might be due to the microbial sensitivity to C/N ratios below 5. This aligns with the previously noticed reduction in biomass content in Stage III. The highest microbial richness was observed at Stage IV, which reduced with higher C/N ratios. Stages I and II exhibited similar richness levels, indicating the pivotal role of C/N ratios lower than 5 in driving the microbial community's succession. The observation of highest diversity and richness in Stage IV might be attributed to the large granule size, which likely harbors more diverse microbial communities, aligning with previous studies [173, 174].

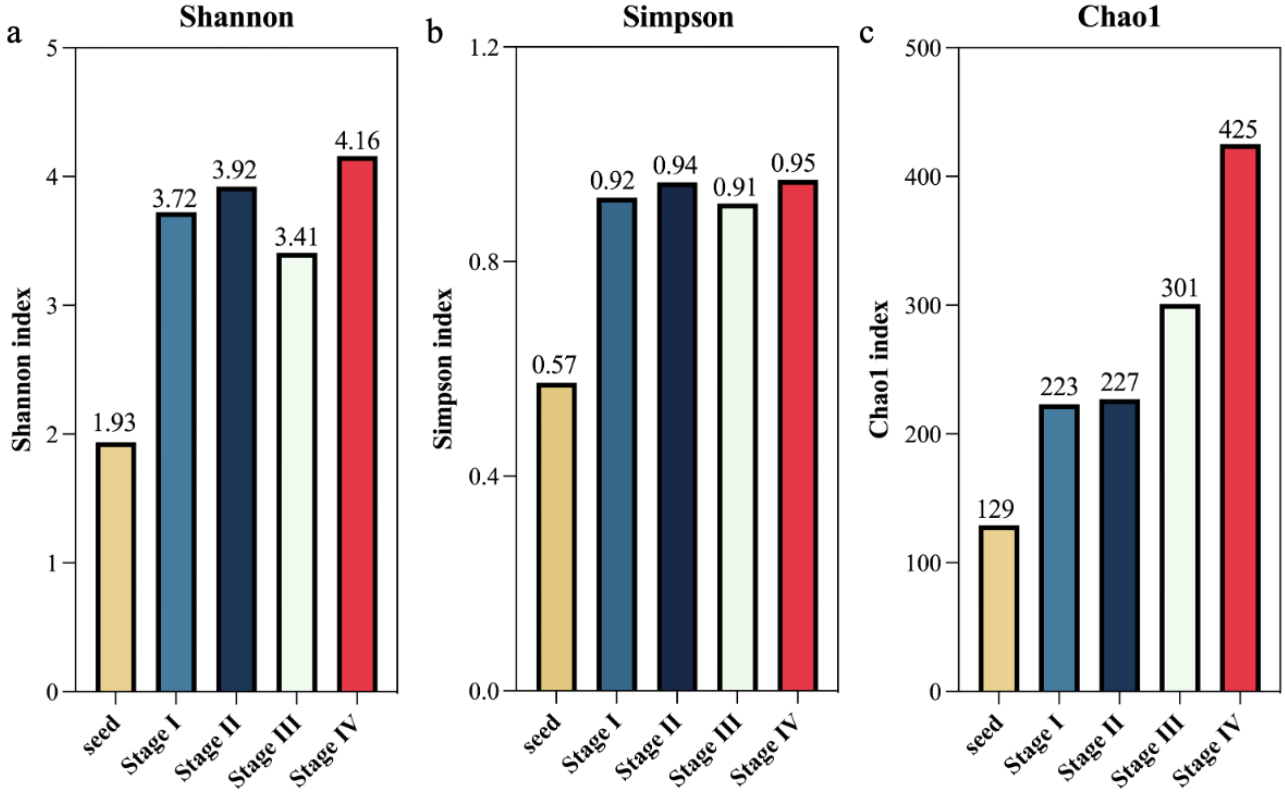

Figure 6.6 Community diversity and richness indices, including a) Shannon, b) Simpson and c) Chao1 in seed sludge and sludge sampled at each stage.

6.3.4.2 Microbial composition

Microbial dynamics at phylum level

Figure 6.7a reveals the microbial composition at phylum level in the seed sludge and at different stages. Proteobacteria was predominant in all samples, with its prevalence decreasing from 82% in the seed sludge to 54% in Stage I, 41% in Stages II and III and 28% in Stage IV. Given the crucial role of Phylum Proteobacteria in N and C cycling, this reduction in relative abundance may indicate a diminished N and C reduction capability [175], which matches the reactor performance results.

Distinct preferences for specific C/N ratios were observed among various microbial phyla. The relative abundance of Bacteroidota was the highest at 14% in Stages I and II, subsequently reduced to 7% in Stages III and IV. The phyla Chloroflexi accounted for 13% in Stage IV, in contrast to less than 7% in earlier stages. Deinococcota constituted 17% of the community at Stage IV, while

less than 2% was detected in other stages. The phylum Actinobacteriota was most prevalent in Stage III, accounting for 27% of the microbial community, compared to 2% in seed sludge, 7% in Stage I and 10% in Stages II and IV. Additionally, the Planctomycetota showed its highest relative abundance at 23% in Stage II, with 15% in Stage I, 14% in Stage III and 18% in Stage IV.

These observations implies that Proteobacteria favor higher C/N ratios, while Bacteroidota and planctomycetota showed a preference for C/N ratio over 6. Actinobacteriota thrived at a C/N ratio of 4-5, and C/N ratio below 3 are conducive to the growth of Chloroflexi and Deinococcota. It has been documented that Bacteroidota and Actinobacteriota, being heterotrophic bacteria, rely on the availability of organic carbon for survival [176, 177]. In contrast, Chloroflexi and Deinococcota, often associated with biofilm formation, are typically found in biofilm-based systems, and prefer lower C/N conditions [178-180].

Microbial dynamics at genus level

Figure 6.7b illustrates the top 30 genera within the system across the reactor operation. In the seed sludge, *Thauera* was markedly dominant, accounting 66% to the microbial community. This was followed by *Nitrosomonas* at 4.5%, a genus affiliated with phylum WPS-2 at 3.5%, a genus within the family NS9_marine group at 2.6%, and *Truepera* at 2.4%. The microbial shift at genus level across Stage I to IV was detailed based on functions.

I. Genus associated with nitrification processes

The autotrophic nitrification process was predominantly facilitated by the genus *Nitrosomonas*. The relative abundance of *Nitrosomonas* reduced from 4.5% in the seed to 1% in Stages I, II and III, then increased to 1.5% in Stage IV. This observation implies that low C/N conditions favoured the growth of *Nitrosomonas*, aligning with findings reported previously [134]. Additionally, the increased relative abundance of *Nitrosomonas* confirmed that the low ammonia reduction was unlikely due to the changes in abundance of functional microorganisms. Furthermore, the genus *Corynebacterium*, notable for its ability to conduct N fixation [181], peaked at 22% in Stage III. This marked presence contrasts with its relatively minor abundance in Stage II at 2% and less than 1% in Stages I and IV. Additionally, *Paracoccus* has also been recorded for its potential to perform heterotrophic nitrification [26], showing less than 2% abundance in Stages I to III and only 0.1%

in Stage IV. With the same level of relative abundance of *Paracoccus* in Stages I to III, the specific HAOB activity test showed a highest value at Stage I, suggesting a higher C/N ratio could possibly enhance its specific activity, which requires further studies.

II. Genus associated with denitrification processes

As the C/N ratio decreased, most of the genera associated with the heterotrophic denitrification process experienced a decline in relative abundance. *Thauera*, a key denitrifier within the system, had a relative abundance reduced from 66% in the seed sludge to 39% in Stage I, 25% in Stage II, 17% in Stage III and down to 6.5% in Stage IV. *Paracoccus*, another recognized denitrifier, showed limited abundance in the system (< 2%). The unidentified NS9 marine group, regarded as primary heterotrophic denitrifier in previous N removal study [151], was only detected in Stages I and II. In contrast, *Ottowia*, a traditional denitrifier [182], showed limited abundance (0.4%) in Stage I but increased to around 2% in subsequent stages. *Rubinisphaera* and *Advenella* were also the heterotrophic denitrification bacteria, which have been reported to play roles in power generation within microbial fuel cells [183, 184], both only observed in Stage I (2.7% and 1.3%) and Stage II (0.6% and 1.8%).

Further, with the decreased C/N ratios, *Psudomonas*, recently reported as capable for performing aerobic denitrification, increased in abundance from 0.1% in Stage I to 3.4% in Stage IV, aligning with findings that low COD environment favored the growth of aerobic denitrifiers [185]. Interestingly, the genus *Thermus* was scarcely detected in Stages I to III but sored to 16% in Stage IV, which could possibly be attributed to the selection of microorganism capable of secreting various enzymes for the decomposition and utilization of macromolecular organic matter in conditions with limited easily biodegradable COD [186].

III. Genus associated with autotrophic nitrogen removal processes

Microorganisms capable of autotrophic nitrogen removal processes, including anaerobic ammonium oxidation (anammox) and Fe (III) reduction coupled to anaerobic ammonium oxidation (Feammox), were unexpectedly proliferated even under relatively high COD condition. Specifically, the genus *Candidatus Anammoximicrobium* showed limited abundance in Stages I and II but increased to 0.6% and 3.2% of the microbial community in Stages III and IV,

respectively. The existence of *Candidatus Anammoximicrobium* suggests that a low C/N condition with residue ammonia and nitrite is preferred for its growth, and it demonstrated its adaptability across a C/N ratio range from 4 to 5. This genus has been documented in previous anammox studies under COD rich condition [187, 188]. Genus *Alicycliphilus* was known for iron metabolism, has also been identified as capable of performing Feammox [189]. The relative abundance of *Alicycliphilus* reached 13% in Stage III, followed by 3% in Stage II, 2.5% in Stage IV and 2.3% in Stage I. Its high abundance obtained in Stage III can be attributed to both the high remaining ammonia levels and the conducive environment provided by large granular size, offering an optimal habitat for *Alicycliphilus* growth. Furthermore, the genus *Limnobacter*, known for its occurrence in bio-electrochemical systems with anammox process [190], contributed to 0.7%, 0.9%, 0.5% and 1.8% in Stages I to IV. This trend suggests *Limnobacter*'s role in facilitating extracellular electron transfer for enhancing nitrogen removal in the granular sludge system.

IV. Genus associated with COD reduction

The relative abundance of genus that participate in organic carbon oxidation, such as *Taibaiella* and *Paludisphaera*, were experienced a gradual reduction from 4.3% to 1.5% and from 2.6% to 0.5%, respectively, from Stage I to IV. In addition, results showed the sensitivity of aerobic heterotrophic bacteria, such as *Persicitalea* and *Leucobacter*, to the changes in the C/N ratio. As the C/N ratio decreased to 5 from Stage II to Stage III, a notable decline in their relative abundance was observed, with *Persicitalea* decreasing from 4.3% to 1.5% and *Leucobacter* from 2.1% to 1.6%. The genus *Truepera* survived at Stage IV with a relative abundance of 1.3%, which could possibly attributed to its ability to metabolize a variety of organic compounds for growth [146].

V. Genus associated with granulation process

Filamentous bacteria play a crucial role in the granulation process and granule stability, serving as the structural backbone within the granule. Among these, the genus *Isosphaera* was identified as the predominant filamentous bacterium in AGS [191], exhibiting a higher relative abundance in Stages II (14%), III (12%) and IV (12%) than in Stage I (4.5%). In addition to that, other filamentous bacteria, such as genus *Litorilinea* and genera associated with family Caldilineaceae, were present and reached peak abundance in Stage IV. Importantly, no negative impacts on granule stability were observed with the increase in these genera. The growing prevalence of filamentous

bacteria in Stage IV suggests a selection process favouring microbes capable of thriving in low COD, high ammonia conditions and potentially contributing to the structural integrity of granules. The beneficial role of filamentous bacteria in the treatment of low strength wastewater has been documented previously [192]. Additionally, the existence of slow growing microbes that enriched with high ammonia across all stages, like *Nitrosomonas*, might also play a role in supporting granule integrity and stability during C/N shifts [115].

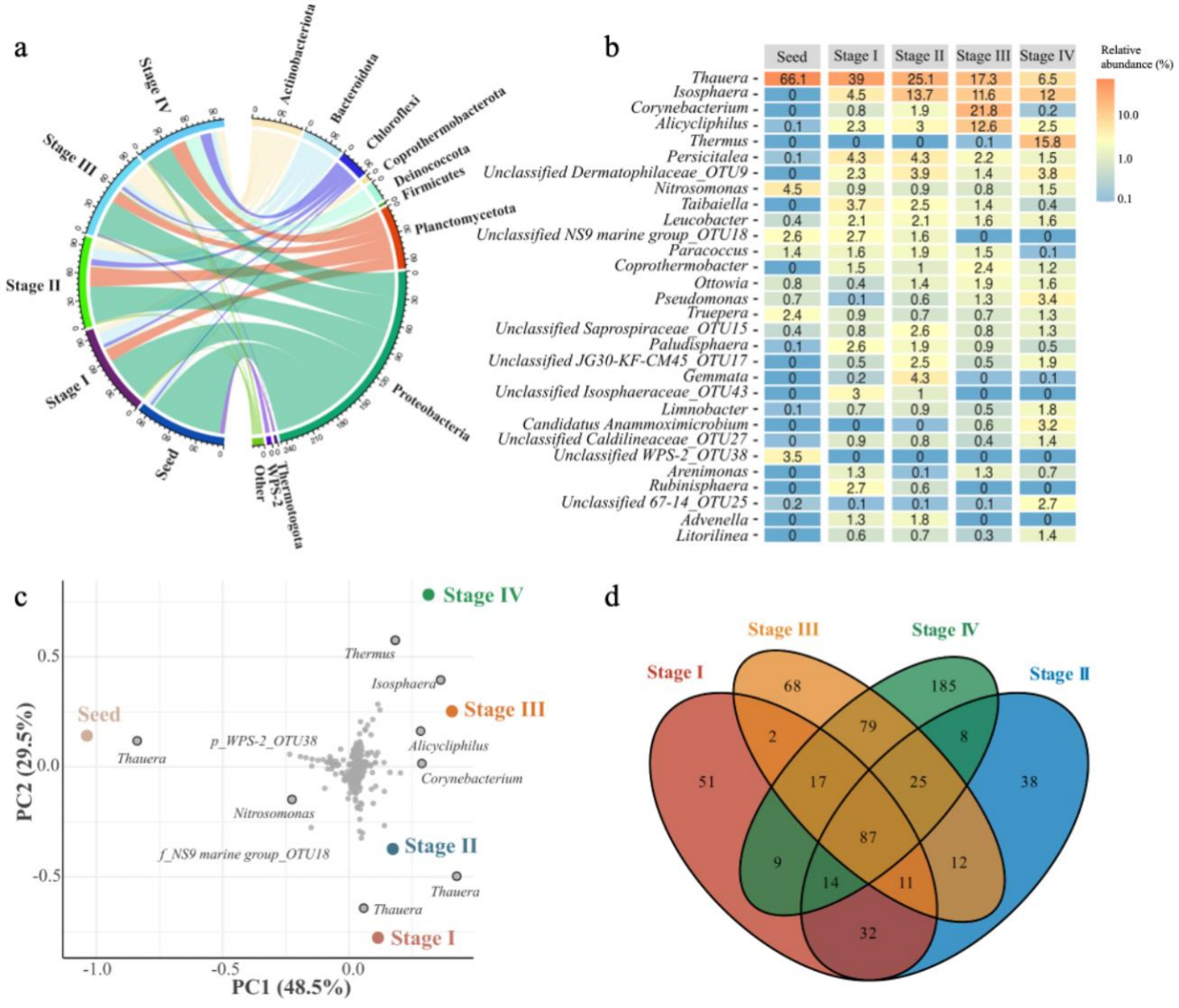

Figure 6.7 Microbial community dynamics at a) phylum level and b) the top 30 genera in seed sludge and in Stages I to IV; and c) principal component analysis (PCA) of microbial community in seed sludge and in Stages I to IV; and d) Venn diagram of amplicon sequence variants obtained at each stage.

6.3.4.3 Microbial divergency at different C/N ratios

Figure 6.7c reveals the divergencies of microbial community among seed sludge and sludge sampled at different C/N ratios. The PCA results, with PC1 explained 48.5% of the variance and PC2 explained 29.5%, collectively explained 78% of the total variance. The substantial separation of the seed sludge along the PC1 axis underscores a divergence in microbial community composition from that observed in subsequent stages. Furthermore, the PC2 axis reveals a progressive shift in the microbial community from Stage I to IV.

In Figure 6.7c, specific genera responsible for the observed divergence among different samples were identified. The genus *Nitrosomonas*, known for its role in autotrophic nitrification, was present in all sludge samples. Initially, *Thauera*, a genus involved in heterotrophic denitrification, dominated the microbial community in the seed sludge and Stages I and II. However, as the system transitioned to Stages III and IV, the prevailing genera shifted towards *Alicycliphilus*, *Isosphaera* and *Thermus*. These genera are implicated in autotrophic nitrogen removal processes, degradation and utilization of macromolecular organic matter for nitrogen removal, and the enhancement of granule structure, particularly under low C/N condition. This shifts in dominance suggests the system's adaptation and re-establishment of microbial community to the changing operational conditions.

Figure 6.7d shows that 87 amplicon sequence variants (ASVs) shared across all four stages. Predominantly, these shared ASVs were dominated by heterotrophic bacteria, denitrifiers and filamentous bacteria. Heterotrophic and filamentous bacteria were posited as pivotal to the granulation process, attributed largely to their EPS production capabilities and structural support to the granular sludge. This capacity for EPS production and structural reinforcement is crucial for maintaining a stable granule structure under low C/N condition. The stage specific unique ASVs were 51 in Stage I, 38 in Stage II, 68 in Stage III and a marked increase to 185 in Stage IV, implying the major microbial shift was observed under C/N ratio decreased to 2 to 3.

6.4 Conclusion

This chapter comprehensively evaluated the impact of varying C/N ratios, from 9 to 2, on the performance, granule characteristics and microbial dynamics over time. The reduction in C/N ratio

constrained N removal efficiencies due to alkalinity deficiency, evidenced by a decrease in ammonia removal efficiency from 94% to 72%, and TIN removal efficiency from 86% to 44%. No negative impact was observed on COD removal efficiency and granule stability as the C/N ratio reduced. Additionally, the reduction in C/N ratio induced a microbial community shift from one predominantly comprising heterotrophic denitrification bacteria, that utilizing easily biodegradable COD, to a more diverse community characterized by a combination of autotrophic N removal bacteria and heterotrophic bacteria adept at consuming macromolecular organics. Unexpected enrichment of microorganisms performing Anammox (genus *Candidatus anammoximicrobium*) and Feammox (*Alicycliphilus*) were observed. The high ammonia induced selection and enrichment of slow growing autotrophic bacteria and heterotrophic bacteria might contribute to the integrity and stability of granules during C/N shifts. The specific microbial activity reflected this microbial succession, with enhanced AAOB and diminished HAOB, denitritation, denitrification activities as the C/N ratio decreased. Granular sludge was observed throughout the reactor operation with an average size ranging from 1.3 mm to 2.8 mm. This chapter elucidates that a C/N ratio over 6 is necessary for high N removal in AGS systems treating high ammonia, low Alk/N wastewaters. Poor N removal under low C/N conditions was primarily due to limited denitrification and insufficient alkalinity recovery potential. Therefore, controlling parameters for optimizing the denitrification process, particularly for alkalinity recovery and COD utilization, are crucial for enhancing N removal in low C/N, low Alk/N ratio waste streams. These parameters should be considered when developing a new technology.

Chapter 7. Divergences of Granules and Flocs Microbial Communities and Contributions to Nitrogen Removal under Varied Carbon to Nitrogen Ratios[4]

7.1 Introduction

Chapter 6 has identified that parameters controlling denitrification efficiency are crucial for complete ammonia removal in the treatment of high ammonia waste streams with low C/N and low Alk/N ratios. To enhance system treatment capacity, it is equally important to identify the controlling parameters for selecting and enriching highly active sludge forms.

Typically, granules and flocs co-exist within granular sludge-based systems. This coexistence contributed to high N removal efficiencies, often exceeding 80% [193, 194]. Granules create varied microenvironments, encompassing aerobic, anoxic, and anaerobic conditions [195]. Additionally, the extended solid retention time in granular sludge aids the retention of slow growing microorganisms, particularly autotrophic ammonia oxidizing bacteria (AAOB), which are responsible for ammonia oxidation process [196]. In contrast, flocs are characterized by less limitation in oxygen and substrate diffusion, giving them a competitive edge for ammonia oxidation and reduction. These features often result in distinct microbial niches within granules and flocs. While the contributions of granules and flocs to N and organic removal have been studied, the results remain controversial [194, 197]. Moreover, most microbial community studies in granules and flocs have focused on low ammonia wastewater treatment with NH_4^+-N levels below 100 mg/L [197, 198], leaving a gap in understanding for systems treating high ammonia waste streams.

In AGS systems, variations in the C/N ratio can lead to granule instability, deteriorated treatment performance, and shifts in N removal pathways [46, 199]. The impacts of C/N ratios on the microbial communities within granules and flocs, and their respective contributions to N removal, remain inadequately explored. This information is critical for selecting the appropriate sludge form to optimize performance during the treatment of wastewaters with varying C/N ratios.

[4] A version of this chapter has been submitted for journal publication in July 2024.

In this chapter, an AGS reactor was employed to treat high ammonia centrate with varied C/N ratios through Nit/DNit. The primary objective is to demonstrate the divergences between granules and flocs under different C/N ratios, with a focus on specific microbial activities, contributions to N removal processes, and the dynamics of core microorganisms shared by granules and flocs, as well as granule specific and floc specific microorganisms.

7.2 Methods and materials

7.2.1 Source of wastewater

The high ammonia centrate was sourced from the effluent of a full-scale aerobic digester facility in British Columbia, Canada. Sampling was conducted periodically, and the collected centrate was stored at 4 ^{o}C before undergoing biotreatment. The concentrations of NH_4^+-N, NO_2^--N, NO_3^--N and alkalinity in the centrate were 865 ± 20 mg/L, 6 ± 3 mg/L, 6 ± 3 mg/L and 2217 ± 110 mg $CaCO_3$/L, respectively. The level of chemical oxygen demand (COD) varied from 1810 mg/L to 5300 mg/L, with the biodegradable portion ranging from 916 to 4236 mg/L.

7.2.2 Reactor operation

A cylindrical AGS reactor with an effective volume of 3 L was operated at 30 ^{o}C for high ammonia centrate treatment. The reactor operation was divided based on varied C/N ratios, with an average value at 6 in Stage I, 4 in Stage II and 2 in Stage III. The AGS operated on a 4-hour cycle, corresponding to an HRT of 10 hours. Each cycle consisted of 30 minutes of anoxic feeding, 160 minutes of aeration, 30 minutes of settling, and 10 minutes of decanting. The time-based phase change was automatically controlled by programmable timers. An upflow superficial velocity of 1.0 cm/s was maintained using a fine bubble air diffuser.

7.2.3 DNA extraction and 16s rRNA sequencing

Granules and flocs were sampled separately from 2 mL mixed liquor at the steady state of Stages I, II and III. Granules and flocs were separated using a 0.2 μm sieve. Granules were washed three times with phosphate buffered saline (PBS). Flocs proportions were centrifuged at 3,000 g for 10 min, then the supernatant was discarded, and the remaining pellet was used for DNA extraction. DNA extraction was performed in duplicate using the DNeasy PowerSoil Pro Kit (QIAGEN,

Hilden, Germany). Subsequently, the extracted DNA was stored at -20 °C after the quality check using NanoDrop One (ThermoFisher, Waltham, MA). The 16S rRNA gene amplification was conducted using the universal primer pair 515 F (5′-ACACTGACGACATGGTTCTACAGTGYCAGCMGCCGCGGTAA-3′) and 806 R (5′-TACGGTAGCAGAGACTTGGTCTGGACTACNVGGGTWTCTAAT-3′). Amplicon sequencing was conducted on the Illumina Miseq PE250 platform at Genome Quebec (Montréal, QC, Canada).

7.2.4 Bioinformatics analysis

The raw sequencing data was processed utilizing the DADA2 algorithm in R [77] to filter low quality sequences and chimeras and merge forward and reverse sequences. Taxonomy was assigned according to Silva reference database (version 138.1) [165]. Alpha-diversity analysis, core operational taxonomic units (OTUs) analysis and principal component analysis (PCA) were performed using the *ampvis2* package in R. The core OTUs analysis sorted the microorganisms into three categories: core, granule specific and floc specific microorganisms. An Upset plot was employed to analysis the shared and unique microorganisms at the genus level among different sludge forms (granules and flocs) and C/N ratios. Statistical analysis of taxonomic and functional profiles (STAMP) software (version 2.1.3) was utilized to evaluate the differences in proportions between samples [200]. Two-sided G test (w/Yates') + Fisher's test was used for statistical analysis, and the Storey false discovery rate (FDR) method was applied for multiple test correction. A p-value below 0.05 was considered statistically significant.

7.3 Results

7.3.1 Reactor performance

Table 7.1 presents the chemical characteristics of the influent raw wastewater and the effluent from the AGS process. The autothermal thermophilic sludge aerobic digestion centrate primarily contained NH_4^+-N, with a concentration ranging from 769 to 887 mg/L; alkalinity below 2330 mg/L; and soluble COD (sCOD) varying between 2136 mg/L to 5878 mg/L. These fluctuations in influent sCOD content resulted in different C/N ratios across the stages: 6 in Stage I, 4 in Stage II and 2 in Stage III.

Effluent NH_4^+-N concentrations increased progressively, from 124 mg/L in Stage I to 160 mg/L in Stage II, and 230 mg/L in Stage III. This corresponds to NH_4^+-N removal efficiencies of 86%, 79% and 68%, respectively. The elevated effluent NH_4^+-N concentrations was attributable to the lack of alkalinity in the centrate to facilitate complete ammonia oxidation, which is evidenced by the low pH in effluent. With below 6 mg/L NO_2^--N in the centrate, effluent NO_2^--N concentrations rose from 132 mg/L in Stage I to 206 mg/L in Stage II, and 243 mg/L in Stage III, due to the reduced biodegradable sCOD. Both influent and effluent NO_3^--N levels remained minimal, under 7 mg/L. The consistently low NO_3^--N concentration in the effluent is likely due to the inhibition effect of free ammonia, which could reach levels up to 78 mg/L, surpassing the threshold for NOB (0.1-1 mg/L) [150]. This corresponds to TIN removal efficiencies of 70%, 60% and 44% in Stages I, II, and III, respectively. Effluent sCOD levels remained stable between 1160 and 1360 mg/L, despite variations in influent sCOD. The remaining sCOD likely comprising primarily non-biodegradable COD, ranging from 890 to 1500 mg/L in the wastewater. The corresponding sCOD removal efficiencies were 75% in Stage I, 62% in Stage II, and 50% in Stage III.

Table 7.1 Characteristics of influent and treated effluent at Stages I, II and III.

Influent parameters	Stage I	Stage II	Stage III
C/N ratios	6± 0.5	4 ± 0.3	2 ± 0.8
NH_4^+-N concentration (mg/L)	887 ± 31	858 ± 39	850 ± 18
NO_2^--N concentration (mg/L)	6 ± 2	6 ± 2	6 ± 2
NO_3^--N concentration (mg/L)	3 ± 1	3 ± 1	3 ± 1
sCOD concentration (mg/L)	5300 ± 436	3635 ± 245	1810 ± 251
Biodegradable sCOD concentration (mg/L)	4236 ± 555	2496 ± 407	916 ± 171
Alkalinity	2200	2330	2120
Effluent parameters			
pH	6 ± 1	6 ± 1	6 ± 1
NH_4^+-N concentration (mg/L)	124 ± 17	160 ± 5	230 ± 25
NO_2^--N concentration (mg/L)	132 ± 16	206 ± 48	243 ± 22
NO_3^--N concentration (mg/L)	7 ± 1	7 ± 1	7 ± 1
sCOD concentration (mg/L)	1361 ± 92	1230 ± 62	1160 ± 38
NH_4^+-N removal efficiency (%)	86 ± 5	79 ± 7	68 ± 4
TIN removal efficiency (%)	70 ± 3	60 ± 5	44 ± 8
sCOD removal efficiency (%)	75 ± 6	62 ± 5	50 ± 5

7.3.2 Sludge characteristics

Table 7.2 presents the biomass concentration and sludge characteristics throughout the three stages. The MLSS concentration increased from 11 g/L in Stage I to 13 g/L in both Stages II and III. Similarly, the MLVSS content rose from 10 g/L in Stage I to 12 g/L in Stages II and III. Stable

SVI values were observed, ranging from 40 to 44 mL/g. The granular sludge structure was maintained and showing a size at 2.6 mm in Stage I, 2.8 mm in Stage II, and 2.7 mm in Stage III. The smaller granular sludge size observed in Stage I could be attributed to the low dissolved oxygen concentration (~0.8 mg/L). This low concentration was a result of the high COD and ammonia content in the bulk, which consumed a significant amount of dissolved oxygen, likely inducing microorganisms to form smaller granules to ensure oxygen diffusion. Similar observation has been reported in previous study [167]. Additionally, a reduction in granule size from Stage II to III might be due to the reduced availability of COD for extracellular polymeric substances (EPS) production. Granular sludge (> 0.2 mm in size) volatile solids accounted for 62% of the total MLVSS in Stage I, 69% in Stage II and 71% in Stage III. Accordingly, the flocs volatile solids contributed 38%, 31% and 29% to the total MLVSS in Stages I, II, and III, respectively. Previous study has also suggested a 35% flocs proportion for higher N removal in a flocs-granules coexisted system [201].

Table 7.2 Biomass concentrations and sludge characteristics.

Biomass characteristics	Stage I	Stage II	Stage III
MLSS (g/L)	11 ± 0.3	13 ± 0.5	13 ± 0.3
MLVSS (g/L)	10 ± 0.3	12 ± 0.4	12 ± 0.2
SVI_{30} (mL/g)	43 ± 1.0	40 ± 2.0	44 ± 1.0
Granular sludge/MLVSS (%)	62 ± 0.2	69 ± 0.4	71 ± 0.4
Flocs/MLVSS (%)	38 ± 0.3	31 ± 0.3	29 ± 0.2
Granular sludge size (mm)	2.6 ± 1.0	2.8 ± 0.9	2.7 ± 1.2

7.3.3 Microbial kinetics

Figure 7.1 illustrates the specific microbial activities of AAOB, HAOB, NOB, denitritation and denitrification in granules and flocs under varied C/N ratios and their contributions to the respective N oxidation and reduction capacities. Flocs consistently exhibited higher specific microbial activities for all five activity tests compared to granules.

7.3.3.1 Ammonia and nitrite oxidation rate

The ammonia oxidation rate was used to illustrate the activities of AAOB and HAOB. In granules, AAOB activities gradually reduced from 0.24 g N/(g VSS·d) in Stage I to 0.19 g N/(g VSS·d) in Stage II and 0.14 g N/(g VSS·d) in Stage III (Figure 7.1a). Conversely, AAOB activities in flocs increased from 0.25 g N/(g VSS·d) in Stage I to 0.31 g N/(g VSS·d) in Stage II, reaching 0.34 g N/(g VSS·d) in Stage III. The AAOB activities obtained in current study fall within the reported

range of 0.07 to 0.64 g N/(g VSS·d) [122, 123, 125, 126, 164]. These observations suggest that as the C/N ratio decreased, flocs may be more conducive to the growth of AAOB compared to granules. Although AAOB activity increased with the reduced C/N ratio, the higher biomass content in granules compared to flocs (Table 7.2) resulted in a higher partition of autotrophic ammonia oxidation contribution in granules at 61% in Stage I and 58% in Stage II, while equal contributions were observed in Stage III.

Compared to AAOB activities, HAOB and NOB activities were significantly lower ($p<0.05$). Both granules and flocs exhibited decreasing HAOB activities with reduced C/N ratios from Stage I to III (Figure 7.1b). In granules, HAOB activities decreased substantially from 0.1 g N/(g VSS·d) in Stage I to 0.07 g N/(g VSS·d) in Stage II and 0.03 g N/(g VSS·d) in Stage III. In flocs, HAOB activities declined from 0.11 g N/(g VSS·d) (Stages I and II) to 0.09 g N/(g VSS·d) (Stage III). The contribution of heterotrophic ammonia oxidation from granules reduced from 60% in Stage I to 45% in Stage III, while the contribution from flocs increased.

NOB activities, presented as nitrite oxidation rate, were below 0.002 g N/(g VSS·d) in granules (Figure 7.1c). In flocs, NOB activities elevated slightly from 0.001 g N/(g VSS·d) in Stage I to 0.005 g N/(g VSS·d) in Stage III. These low values explain the absence of nitrate in the effluent throughout the three stages. The contribution of granules to nitrite oxidation gradually decreased from 64% in Stage I to 37% in Stage III, while contribution from flocs elevated.

7.3.3.2 Nitrite and nitrate reduction rate

Denitritation activities, indicated by nitrite reduction rate, and denitrification activities, indicated by nitrate reduction rate, both decreased stepwise with reduced C/N ratios. From Stage I to Stage III, denitritation activities in granules decreased from 2.6 to 1.8 to 1.1 g N/(g VSS·d), while in flocs, the activities reduced from 2.7 to 2.5 to 2.3 g N/(g VSS·d). Denitrification activities were consistently lower than denitritation activities, showing up to a 10-fold difference, likely due to substrate limitations. Denitrification activities remained relatively stable across the three stages, ranging from 0.28 to 0.32 g N/(g VSS·d) in granules and 0.30 to 0.35 g N/(g VSS·d) in flocs. In both nitrite and nitrate reduction capacities, granules consistently outperformed flocs. The

contribution from granules to nitrite reduction decreased from 62% to 53% as the C/N ratio reduced, while the contribution to nitrate reduction in granules elevated from 60% to 70%.

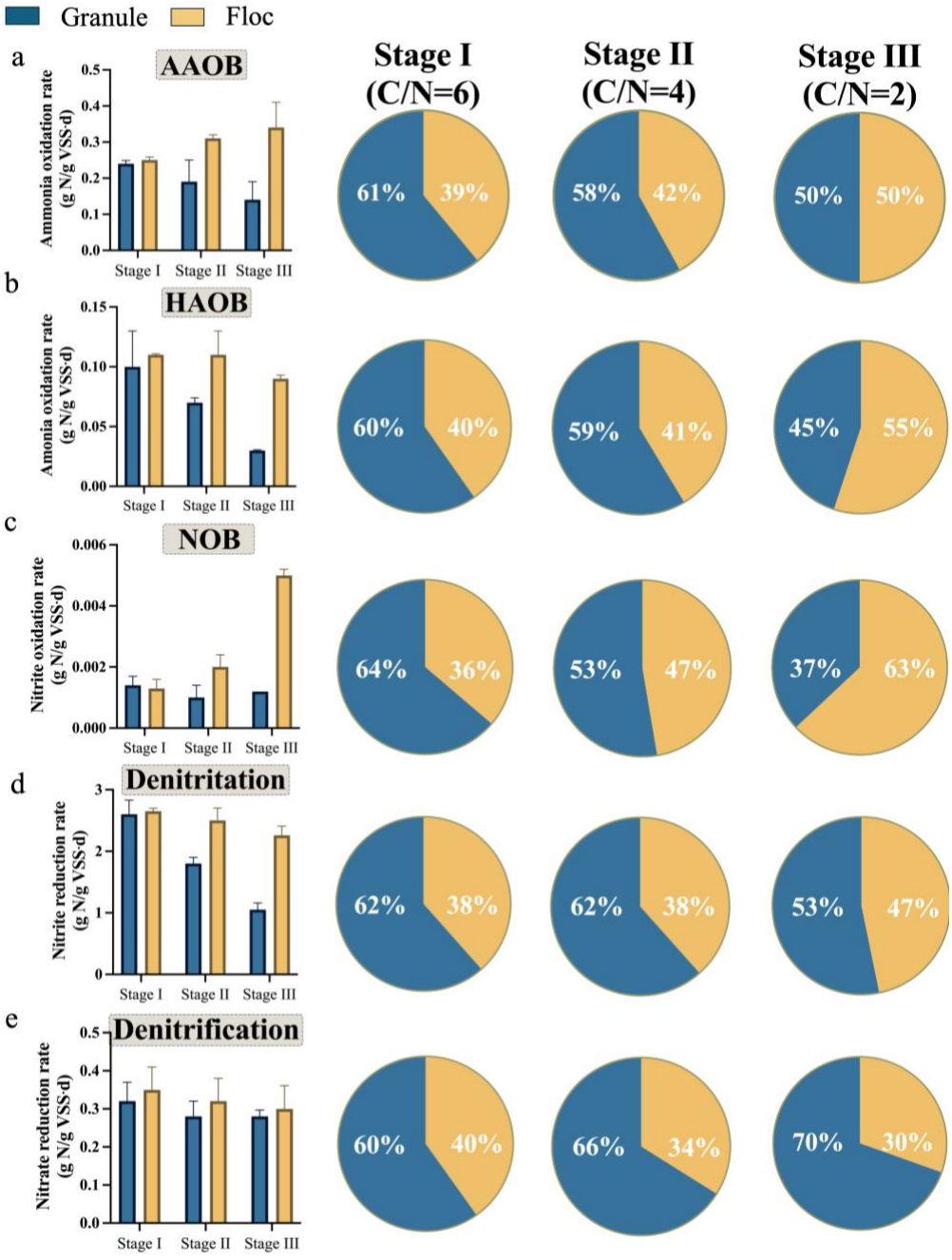

Figure 7.1 Specific microbial activities in granules and flocs and their contributions to the corresponded process in the system across Stage I to III, including a) autotrophic ammonia oxidizing bacteria (AAOB) activity and their contributions to autotrophic ammonia oxidation, b) heterotrophic ammonia oxidizing bacteria (HAOB) activity and their contributions to heterotrophic ammonia oxidation, c) nitrite oxidizing bacteria (NOB) activity and their contributions to nitrite oxidation, d) denitritation activity and their contribution to nitrite reduction and e) denitrification activity and their contributions to nitrate reduction.

7.3.4 Microbial community dynamics

7.3.4.1 Microbial diversity and richness

The evaluation of microbial community diversity and richness in granules and flocs under different C/N ratios is shown in Figure 7.2. Diversity was evaluated using the Shannon (Figure 7.2a) and Simpson (Figure 7.2b) indices, while richness was assessed using the Chao1 index (Figure 7.2c). Elevated microbial diversity was observed in granules compared to flocs at all stages. Decreasing C/N ratios had minimal impact on granule diversity. but negatively affected floc diversity. Granules in Stages I and II displayed higher richness levels compared to flocs, but in Stage III, flocs exhibited greater richness.

Figure 7.2d illustrates the number of shared amplicon sequencing variants (ASVs) among granules and flocs across the three stages. Granules and flocs shared 55 ASVs across all stages. Granules shared 11 ASVs across stages, while flocs shared 7 ASVs. In Stage III, granules and flocs shared the highest number of ASVs of 20, followed by 16 in Stage I and 5 in Stage II. Stage III flocs had the highest number of unique ASVs at 85, whereas Stage III granules had the lowest at 36. Both granules and flocs in Stages I and II had approximately 45 unique ASVs. These observations suggest that low C/N ratios may induce substantial shifts in the microbial community, particularly in flocs, evidenced by enhanced microbial richness and higher unique sequences in Stage III flocs compared to granules.

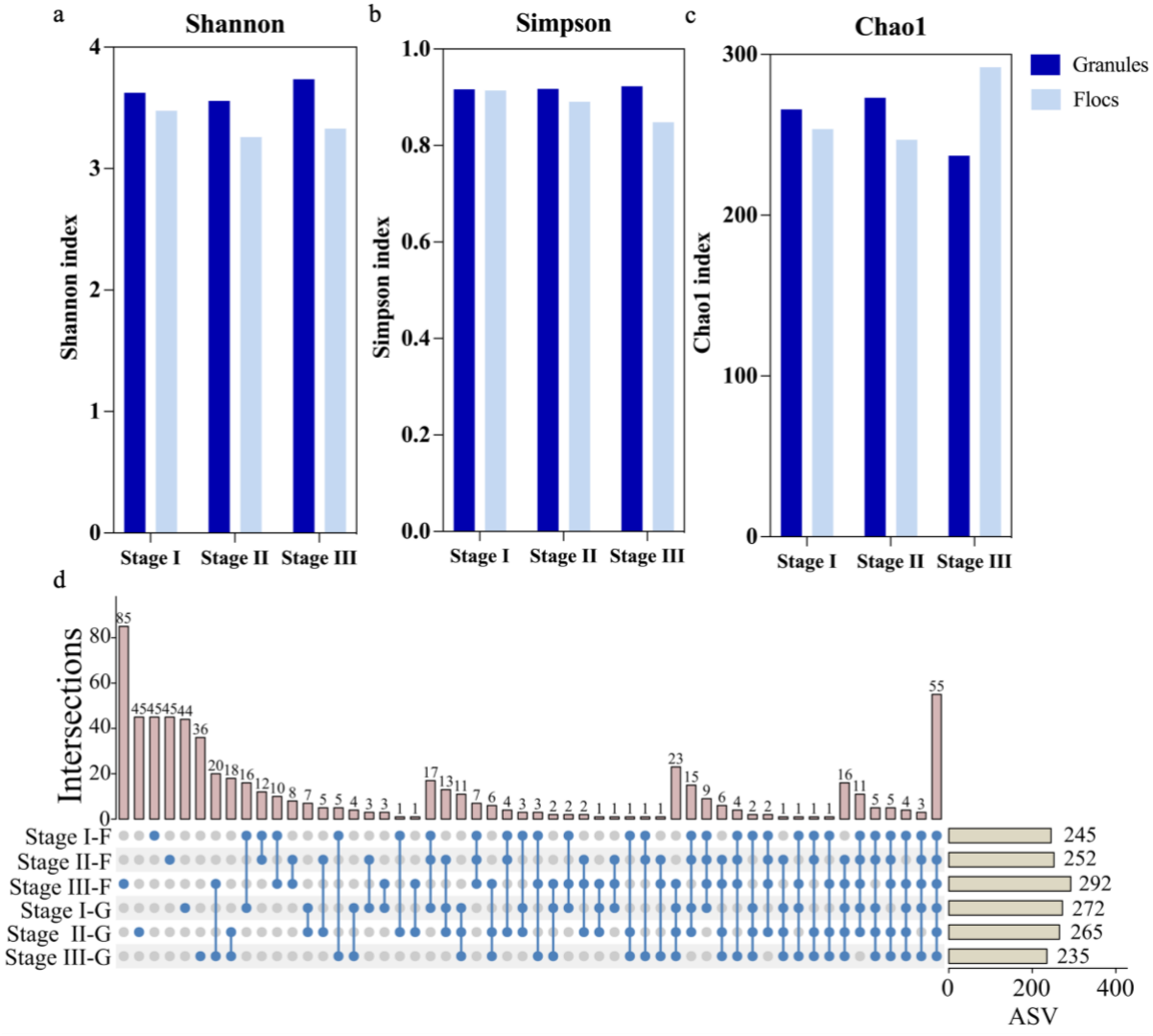

Figure 7.2 Dynamics of microbial diversity and richness, encompassing a) Shannon b) Simpson and c) Chao1 indice; and d) Upset plot for granules (Stage I-G, Stage II-G, Stage III-G) and flocs (Stage I-F, Stage II-F, Stage III-F) under each stage.

7.3.4.2 Microbial community at phylum level

To understand the divergences in granules and flocs and the shifts in the microbial community under varied C/N ratios, a phylum level microbial analysis was performed (Figure 7.3a). Proteobacteria was the most abundant phylum in all sludge samples, accounting for 44% in Stage I granules, 45% in Stage I flocs, 34% in Stage II granules, 44% in Stage II flocs, 27% in Stage III granules, and 29% in Stage III flocs. Comparable relative abundances of Proteobacteria were observed in granules and flocs within the same stage. Microorganisms affiliated with Proteobacteria are known to participate in N removal processes [202]. With the reduced C/N ratios,

Proteobacteria showed a stepwise decrease in both granules and flocs, aligning with the reduced N removal performance and decreased specific microbial activities, particularly denitritation and denitrification activities.

In addition to Proteobacteria, Actinobacteriota and Plantomycetota were among the top three phyla throughout the reactor operation. Previous studies have documented that many microorganisms in these phyla are capable of organic and N degradation [203, 204]. The relative abundance of Actinobacteriota decreased with the reduction in C/N ratios, with a considerable reduction observed in Stage III. Actinobacteriota decreased from 25% in Stage I granules and 28% in Stage I flocs to 20% in Stage II granules and 28% in Stage II flocs, and further to 17% in Stage III granules and 4% in Stage III flocs. Conversely, the relative abundance of Plantomycetota gradually increased in granules, from 14% in Stage I to 26% in Stage II, reaching 34% in Stage III. In contrast, the abundance of Plantomycetota remained relatively stable in flocs, at 8% in Stage I, 11% in Stage II, and 7% in Stage III. This suggests that microorganisms affiliated with Plantomycetota likely prefer to reside in granules and thrive in environments with low C/N ratios.

Similar to the shifts observed in Planctomycetota, the phylum Choloroflexi, widely known as filamentous bacteria, showed higher abundance in granules compared to flocs. The relative abundance of Chloroflexi increased as the C/N ratio decreased, accounting for 8% in Stage I granules and 1% in Stage I flocs, then rising to 13% in Stage II granules and 2% in Stage II flocs, and finally reaching 14% in Stage III granule and 4% in Stage III flocs. Additionally, a significant increment in the abundance of Deinococcota was observed in Stage III flocs, rising from 1% in Stages I and II to 38% in Stage III, while its relative abundance remained below 2% in granules. The Deinococcota potentially perform thermophilic organic degradation and denitrification [146, 205].

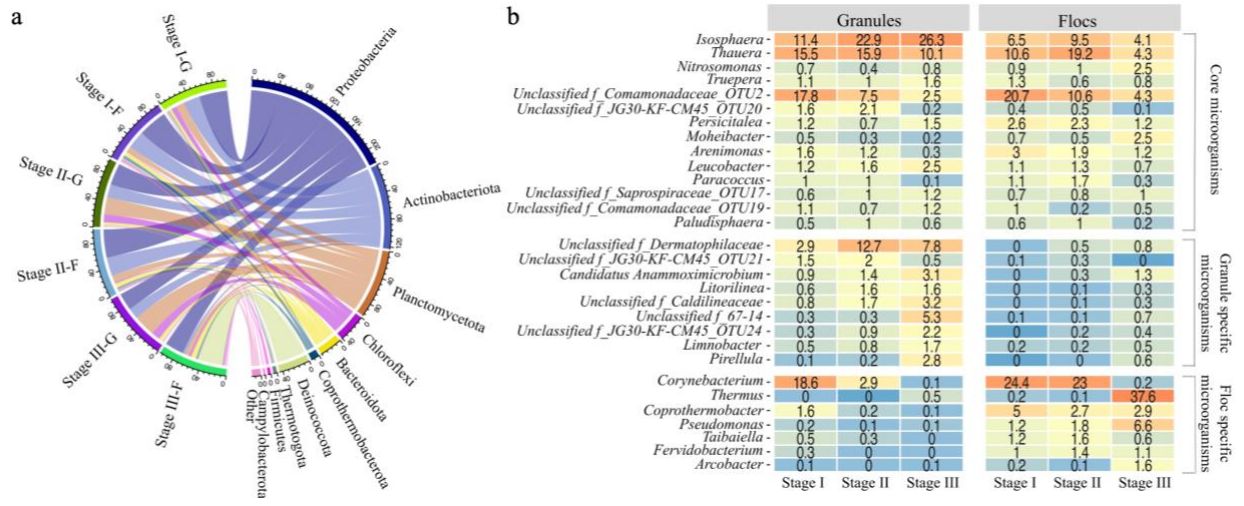

Figure 7.3 Microbial community composition at a) phylum and b) genus levels. Stage I-G represents Stage I granules and Stage I-F indicates Stage I flocs. Top 30 genus were presented, and being divided into three categories, including core microorganisms (shared by both granules and flocs), granule specific microorganisms (mainly dominated in granules), and floc specific microorganisms (mainly dominated in flocs). The unspecified genera were shown at family level (Unclassified f_).

7.3.4.3 Microbial community at genus level

To gain deeper insights, genus level microbial analysis was performed, revealing the dynamics of the top 30 abundant genera in granules and flocs (Figure 7.3b). These genera were categorized as core, granule specific and floc specific microorganisms.

Core microorganisms

Core microorganisms are present in both granules and flocs. The most abundant genera in this group were *Isosphaera*, *Thauera* and genus affiliated with the family Commamonadaceae across all C/N ratios.

In granules, the relative abundance of *Isosphaera* increased from 11% in Stage I to 23% in Stage II and 26% in Stage III, while in flocs, it changed from 7% to 10% to 4%. Known for its filamentous structure and role in organic degradation and biofilm formation, *Isosphaera* is crucial in maintaining granule structure and stability [191, 206, 207]. *Thauera*, a heterotrophic denitrifier capable of degrading aromatic compounds and producing polysaccharide, plays a key role in initial cell aggregation [208]. In granules, the proportion of *Thauera* reduced from 16% in Stages

I and II to 10% in Stage III. In flocs, *Thauera* abundance increased from 11% in Stage I to 19% in Stage II, then dropped to 4% in Stage III. Genera affiliated with the family Comamonadaceae, are documented as aerobic heterotrophic bacteria with denitrification potential [209]. In granules, their proportion reduced from 18% in Stage I to 8% in Stage II and 3% in Stage III. In flocs, their abundance decreased from 21% to 11% and down to 4% across the stages.

Among the core microorganisms, *Nitrosomonas* was the dominant genus responsible for ammonia oxidation. Although present in both granules and flocs, higher relative abundances *Nitrosomonas* were observed in flocs across all stages. In Stage I, its abundance was 0.7% in granules and 0.9% in flocs. As the C/N ratio decreased, the differences in the proportion of *Nitrosomonas* between granules and flocs became more pronounced, with 0.4% in Stage II granules, 1% in Stage II flocs, 0.8% in Stage III granules, and 2.5% in Stage III flocs. This observation aligns with the AAOB activity test results. The higher relative abundance of AAOB in Stage I granules compared to Stage III might be due to competition with heterotrophic bacteria at high C/N ratios, inducing AAOB attachment on granules to prevent washout. Without such stress, AAOB preferred to residing in flocs under low C/N ratios. Previous study has documented that higher C/N ratios can cause AAOB washout and reduce ammonia oxidation efficiency [210]. This highlights the beneficial role of granules in retaining AAOB and maintaining satisfactory ammonia oxidation in Stage I.

In addition to *Thauera*, *Paracoccus* is also a key denitrifying bacterium, which showed a considerable reduction when the reactor operation shifted from Stage II to III. In granules, its abundance decreased from 1% in Stages I and II to 0.1% in Stage III. In flocs, it changed from 1% in Stage I to 2% in Stage II, and to 0.3% in Stage III.

Genera *Truepera*, *Persicitalea*, *Leucobacter*, *Paludisphaera* and those affiliated with the family JG30-KF-CM45 are known for degrading a wide range of organic compounds [146, 211-213]. The abundance of these genera increased in granules and reduced in flocs as the C/N ratio reduced, likely due to the higher capacity of granular sludge to capture macromolecular organics. The abundance of *Truepera* in granules increased from 1% in Stages I and II to 2% in Stage III, while remaining around 1% in flocs. The abundance of *Persicitalea* in granules increased from 1.2% in Stage I to 1.5% in Stage III, while in flocs it decreased from 2.6% in Stage I to 1.2% in Stage III.

Similarly, the proportion of *Leucobacter* in granules increased from 1.2% (Stage I) to 2.5% (Stage III), while in flocs it reduced from 1.1% (Stage I) to 0.7% (Stage III). The abundance of genus affiliated with the family JG30-KF-CM45 increased in granules from 1% in Stage I to 2% in Stage II, and to 3% in Stage III. In flocs, while maintaining around 1% in flocs. In addition to COD degradation capabilities, *Paludisphaera* and the genus affiliated with the family JG30-KF-CM45, which belong to Chloroflexi and exhibit a filamentous structure, may also contribute to granule stability [213, 214].

Granule specific microorganisms

The genus affiliated with the family Dermatophilaceae was the most abundant microorganism among granule specific microorganisms, with relative abundance of 3% in Stage I granules, 13% in Stage II granules, and 8% in Stage III granules. These genera, including polyphosphate accumulating organisms (PAOs) and glycogen accumulating organisms (GAOs), likely support granule structure and stability during shifts in C/N ratios [215].

Candidatus Anammoximicrobium was the primary genus for nitrogen removal among the granule specific microorganisms, with a relative abundance of 1% in Stages I and II, increasing to 3% in Stage III. Genus *Limnobacter*, known for its role in partial denitrification and co-occurrence with anammox bacteria, increased in abundance in granules from 1% in Stages I and II to 2% in Stage III. Additionally, a genus associated with the family Caldilineaceae may also contribute to N removal, showing an elevated abundance in granules from 1% in Stage I to 3% in Stage III.

Both *Litorilinea* and an unknown genus associated with family Caldilineaceae have been reported as filamentous bacteria prevalent in anaerobic systems, potentially serving as the structural backbone for granular sludge. Regarding COD degradation, *Pirellula* and a genus within the family 67-14 are potent organic degraders in the granules [216]. The relative abundance of *Pirellula* elevated from less than 1% in Stage I granules to 3% in Stage III granules. Similarly, the genus within the family 67-14 rose from below 1% in Stage I to 5% in Stage III.

Floc specific microorganisms

The predominant genus among floc specific microorganisms was *Corynebacterium* in Stages I and II, which then shifted to *Thermus* in Stage III flocs. Genus *Corynebacterium*, known for N fixation and heterotrophic nitrification capabilities [181], exhibited a substantial reduction in abundance as the C/N ratio decreased, from 19% in Stage I granules to less than 1% in Stage III granules, and from 24% to below 1% in flocs. Conversely, *Pseudomonas*, which may participate in aerobic denitrification [185], increased in relative abundance in flocs from 1% in Stage I to 2% in Stage II, and to 7% in Stage III.

Genus *Thermus* was highly enriched in Stage III flocs, with a relative abundance of 38%. This enrichment could be attributed to its ability to secret a variety of enzymes and decompose macromolecular organics under aerobic condition [186]. This genus has been widely reported in geothermal systems, may perform incomplete denitrification, potentially resulting in N_2O production [205], warranting further investigation. *Taibaiella*, capable of degrading organics, showed a reduced relative abundance from 1% in Stage I flocs to below 1% in Stage III flocs.

Additionally, the genera *Coprothermobacter*, *Fervidobacterium* and *Arcobacter* were dominant among floc specific microorganisms. Genus *Coprothermobacter* and *Fervidobacterium*, known as fermentation bacteria [217, 218], might have been introduced with centrate containing residual biomass from previous stages.

7.3.4.4 C/N ratio impact on microbial community

Figure 7.4 elucidates the divergences between granule and flocs at different C/N ratios. The PCA results, shown in Figure 7.4a, illustrate a total variance of 83%, with PC1 explained 47% of the variance and PC2 explained 36%. Substantial separation was observed between Stage III granules and flocs, followed by Stage II, with Stage I granules being closest to Stage I flocs. These results imply that the divergences between granules and flocs enlarged as the C/N ratio decreased. Additionally, flocs showed higher divergence compared to granules from Stage I to III. The variance between Stage II and III flocs was more substantial than between Stage I and II flocs. In contrast, higher variance was observed between Stage I and II granules than between Stage II and III granules. Specifically, *Corynebacterium* and *Thermus* separated Stages I and II flocs from

Stage III flocs, while *Corynebacterium*, *Isosphaera*, *Thauera* and genera affiliated with the families Dermatophilaceae separated Stage I granules from Stages II and III granules.

STAMP analysis (Figure 7.4b) reveals a substantial difference in proportion was observed when comparing Stage I granules with Stage II granule and between Stage II and Stage III flocs. The proportion of *Corynebacterium* was over 15% more abundant in Stage I granules compared to Stage II. Substantial shifts were also seen in *Isosphaera* and genera associated with the families Comamonadaceae and Dermatophilaceae between Stage I and Stage II granules. These microorganisms, linked to heterotrophic nitrification and granule stability, showed significant abundance changes in granules during C/N ratio shifts from 6 (Stage I) to 4 (Stage II). In contrast, the level of differences between Stage II and Stage III granules were smaller, with a maximum 6% difference.

Comparing Stage I to Stage II flocs, differences were below 10%, with the highest in *Thauera*. In comparison, the highest difference of 40% was observed in the macromolecular organics degrading genus *Thermus* between Stage II and Stage III flocs. The second most significant difference was in the heterotrophic nitrification related genus *Corynebacterium*.

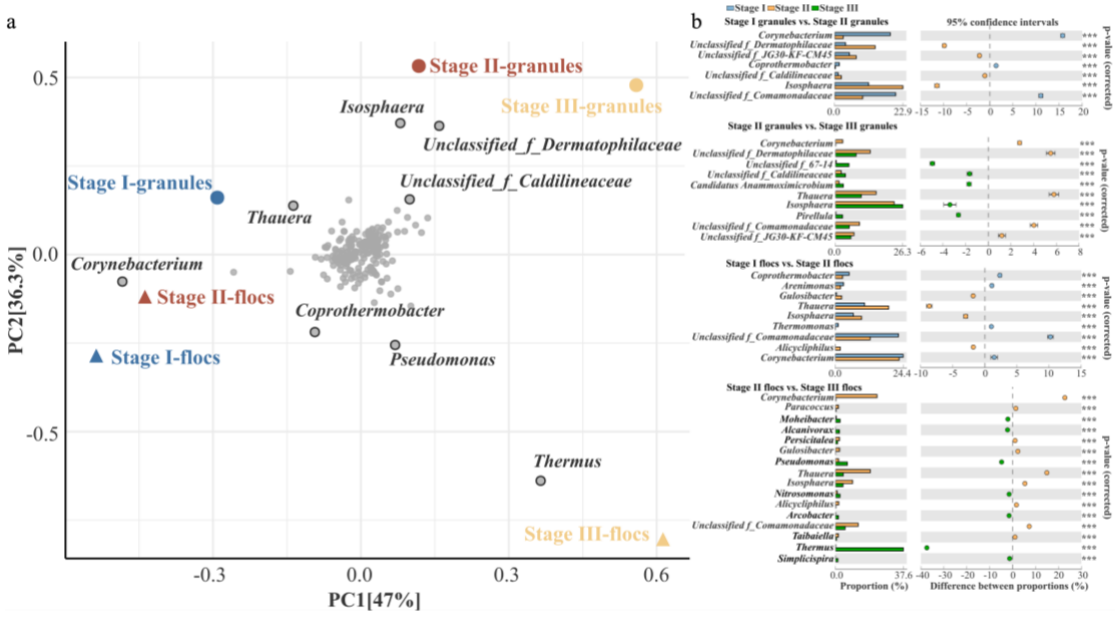

Figure 7.4 The similarities between granules and flocs under different C/N ratios, including a) principal component analysis (PCA) and b) comparative analysis of Stage I granules and Stage II granules, Stage II granules and Stage III granules, Stage I flocs and Stage II flocs, and Stage II flocs and Stage III flocs.

7.3.4.5 Functional variability across microbial groups

To investigate the correlation between reactor operation parameter and performance, as well as their associations with specific microbial groups (core, granule specific and floc specific microorganisms), Pearson's correlation analysis and the Mantel test were employed. The correlation plot (Figure 7.5) revealed a significant positive correlation between C/N ratios and ammonia and TIN removal efficiencies. Additionally, C/N ratios positive correlated with HAOB, denitritation, and denitrification activities. Sludge size exhibited a significant positive correlation with microbial diversity but negatively correlated with all specific microbial activities, particularly AAOB activity. Furthermore, ammonia removal efficiency significantly correlated with TIN removal efficiency, underscoring the importance of TIN removal for alkalinity recovery and complete ammonia removal.

The Mantel tests further revealed that core microorganisms were significantly correlated with AAOB activity and the removal efficiencies of ammonia and TIN. Similarly, floc specific microorganisms were significant correlated with AAOB, HAOB and denitritation activities, as well as ammonia and TIN removal efficiencies. In contrast, granule specific microorganisms were significantly correlated with denitrification activity and sludge size. These observations suggest that granules and flocs shared similar functionalities for N and COD removal. However, floc specific microorganisms presented a higher correlation with both N oxidation and reduction processes, while granule specific microorganisms, influenced by sludge size, primarily contribute to N reduction and granule formation and stability. Therefore, flocs are critical for N removal during the shift of C/N ratios from high to low.

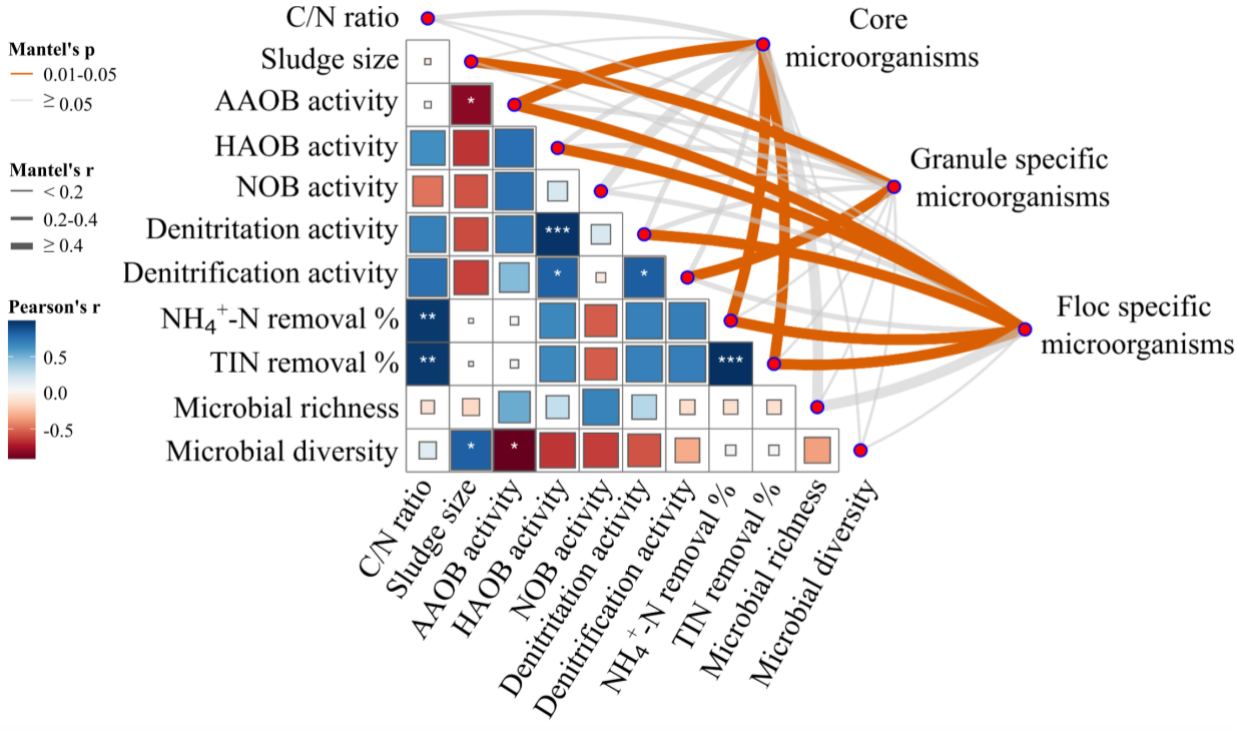

Figure 7.5 Pairwise comparisons of reactor operation parameters, microbial kinetics, and reactor performances metrics. The color gradient indicates Pearson's correlation coefficients, with statistical significance denotes as *** ($p<0.001$), ** ($p>0.01$) and * ($p<0.05$). The top 30 abundant genera in the microbial community, divided into three groups based on genus level analysis, were related to each operational factor and reactor performance result by Mantel tests. Edge color corresponds to the Mantel's p value, and edge width denotes the Mantel's r statistic for the distance correlation.

7.4 Discussion

7.4.1 Contributions of granules and flocs to N removal

Granules and flocs both contributed to N removal in the system. Activity tests consistently showed higher microbial activities in flocs compared to granules, but granules had higher biomass content in the reactor, which also affect their contributions to the N removal capacity. The results suggest granules were the main contributors to N oxidation, including autotrophic and heterotrophic ammonia oxidation and nitrite oxidation, at C/N ratio of 6 (Stage I) and 4 (Stage II). As the C/N ratio reduced to 2, the contributions from granules to these processes diminished, while flocs' contributions in Stage III became equal to or higher than granules. In contrast, granules consistently outperformed flocs in nitrite and nitrate reduction throughout the reactor operation. It is speculated that elevated N removal contribution from granules might associate with higher

C/N ratios, whereas flocs play a critical role under low C/N conditions. Specific anammox activity should be further investigated to better understand their contributions to the overall N removal.

7.4.2 Granule and floc specific microorganisms and responses to C/N ratios

Granules and flocs shared microorganisms involved in N removal, such as *Nitrosomonas* and *Thauera*, aerobic heterotrophic filamentous bacteria, like *Isosphaera*, and other microorganisms associated with the decomposition of complex organics. Granules predominantly contained anaerobic microorganisms (*Candidatus Anammoximicrobium*) and those have a filamentous structure, such as *Isosphaera*, *Litorilinea*, and genera involved in family Dermatophilaceae (PAOs and GAOs), which benefit granule stability. These microorganisms are crucial for granulation and maintaining structural stability during C/N ratio shifts. Flocs was dominated by aerobic microorganisms, including *Nitrosomonas*, *Corynebacterium*, *Thermus*, and genus associated with the family Comamonadaceae, which are likely capable of autotrophic/heterotrophic nitrification and organic degradation. Additionally, some microorganisms sourced from the influent wastewater were also present in the flocs.

As the C/N ratio reduced, the abundance of heterotrophic bacteria in both granules and flocs declined, while the abundance of microbes capable of degrading macromolecular organics increased. In granules, there was an increased abundance of filamentous and anammox bacteria, while flocs had more AAOB. The PCA results indicate a pronounced microbial shift occurred in granules when the C/N ratio shifted from 6 (Stage I) to 4 (Stage II), whereas flocs were more affected by the shift from 4 (Stage II) to 2 (Stage III). It is speculated that microbes in granules may detach and remain active in the bulk when the C/N ratio shifted from 6 to 4, possibly explaining the earlier microbial shift in granules compared to flocs.

7.5 Conclusion

This chapter investigated the N removal contributions and predominant microorganisms in granules and flocs under varying C/N ratios in an aerobic granular sludge reactor (AGS) for high ammonia centrate treatment. Results revealed that specific microbial activities in flocs consistently surpassed those in granules. However, granules contributed more to the N oxidation

and reduction at C/N ratios of 6 and 4. As C/N ratio reduced to 2, flocs showed higher contributions to N oxidation, while granules maintained their major role in N reduction. Granules and flocs shared most N and COD removal associated microorganisms, such as *Nitrosomonas* and *Thauera*. Granule specific microorganisms involved anammox bacteria (*Candidatus Anammoximicrobium*), filamentous bacteria and genus in family Dermatophilaceae. Flocs were dominated by aerobic microorganisms associated with organic and N degradation. As the C/N ratio decreased, the relative abundances of filamentous bacteria in granules and microorganisms capable for macromolecular organic degradation in both granules and flocs, and *Nitrosomonas* in flocs were increased. Denitrification related microorganisms showed reduced abundance with decreasing C/N ratios. A shift from a C/N ratio from 6 to 4 had a greater impact on the microbial community in granules, whereas a shift from 4 to 2 had a more pronounced effect on flocs. This chapter highlights the key role of granules and flocs in treating high ammonia waste streams, suggesting that the retention of granules is more critical for high ammonia, high C/N conditions, whereas retaining flocs is critical for high ammonia, low C/N waste streams.

Chapter 8. Newly Developed Granular Sludge Reactor (GSR) Enhances Nitrogen Removal from High Ammonia Waste Stream: Selection and Enrichment of Effective Microbial Community[5]

8.1 Introduction

Chapter 6 shows that the poor N removal from high ammonia, low C/N, low Alk/N centrate is primarily due to insufficient alkalinity in the centrate and inadequate denitrification, which recovers alkalinity. Although high N removal was observed under high C/N conditions (a ratio over 6), a significant proportion of COD was consumed by aerobic heterotrophs, which did not contribute to N removal. Therefore, AGS operation should be modified to enhance effective COD utilization to improve the denitrification process during the treatment of low C/N and low Alk/N waste streams. Further, Chapter 7 suggests the significant role of flocs or small granules in N removal under low C/N conditions. Therefore, AGS should be further modified to allow higher retention of small granules and flocs to improve the N removal capacity.

A range of high ammonia waste streams, such as anaerobically digested sludge supernatant and landfill leachate, contains up to 1000 mg N/L ammonia and very low biodegradable COD (< 300 mg/L), resulting in a C/N ratio of 0.25-0.5. This presents a scenario that has not been extensively explored in previous AGS studies for the treatment of ammonia rich waste streams. However, the feasibility of AGS reactors for treating high ammonia waste streams with low C/N ratios has not been well demonstrated, and optimization strategies for TIN removal and N loading have yet to be established. The paucity of studies in this area maybe due to granulation challenges arising from free ammonia inhibition and scarcity of readily biodegradable COD, which is essential for the synthesis of extracellular polymeric substance (EPS) required for microbial aggregation. Previous studies have documented that granulation processes tend to be slower under low C/N conditions. For instance, a study observed that it took 80 days to form granules in wastewater treatment systems where the C/N ratio was 5 [219]. Additionally, numerous investigations

[5] A version of this chapter has been published: Zou, X., Gao, M., Yao, Y., Zhang, Y., Guo, H., & Liu, Y. (2024). Efficient nitrogen removal from ammonia rich wastewater using aerobic granular sludge (AGS) reactor: Selection and enrichment of effective microbial community. *Environmental Research*, *251*, 118573. https://doi.org/10.1016/j.envres.2024.118573

reported compromised granular integrity when treating waste streams with C/N ratios over 10 or below 2 [45, 220].

In the present chapter, a newly developed GSR was introduced for the Nit/DNit of ammonia rich anaerobically digested sludge supernatant. Unlike previous AGS studies, which predominantly relied on continuous aeration, this study introduced an anoxic phase with additional COD to enhance nitrogen removal efficiency and optimize COD utilization in low C/N wastewater. The primary objectives are to demonstrate the innovative adaptation of GSR for low C/N, high ammonia wastewater treatment without the prerequisite of pretreatment, and optimize the TIN removal and the N loading capacity with a specific focus on selecting and enriching highly efficient N removing microbial consortium.

8.2 Methods and materials

8.2.1 Reactor setup and operation

A cylindrical GSR with a 4 L capacity was employed for the treatment of anaerobically digested sludge supernatant, which contains 800-1000 mg/L NH_4^+-N, 2500-3000 mg/L alkalinity as $CaCO_3$, and 100-300 mg/L BOD. Anaerobically digested sludge supernatant was biweekly sampled from a wastewater treatment facility in Alberta, Canada, and subsequently stored in a cold room until undergoing biotreatment. Due to the seasonal variation, varied influent wastewater characteristics were observed. The seed sludge was suspended solids that originated from a Nit/DNit reactor designed for high ammonia wastewater treatment [61]. The GSR operated in a sequencing batch manner, with a feed exchange rate of 50% at 20 ^oC. Both feed and air were introduced from the bottom of the reactor and the air provided an upflow superficial velocity at 1.4 cm/s. The reactor's operation involved 7 stages based on hydraulic retention time (HRT) and N loading. The HRT was progressively reduced from 48 hrs to 7 hrs based on the reactor capacity. Throughout the reactor operation, feeding and discharging duration were fixed at 10 min, and the settling duration was set at 30 min. The proportion of the aerobic phase within the cycle duration was progressively reduced from 68% to 43%, while the anoxic phase consistently occupied 30% of the cycle time. During the anoxic phase, a concentrated organic carbon source, sodium acetate anhydrous, with a

COD of 40 g/L was pulse added to a C/N ratio of 2 to aid in the removal of TIN. Reactor's operations were automatically controlled by timers.

8.2.2 Granular sludge characterization

Granular sludge retrieved from the GSR at Stage VII underwent characterization with X-ray powder diffraction (XRD, Rigaku Ultima IV, Japan) employing the Bragg Brentano reflection geometry. The acquired data was evaluated with JADE MDI 9.6 software, and phase identification was performed through DIFFRAC.EVA software using the 2021/2022 ICDD PDF 4+ and PDF 4+/Organics databases. Granule dimensions were ascertained using a digital image microscope (Axiovert100-Micro Injection), with subsequent image analysis executed via ImageJ software. Extracellular polymeric substances (EPS) were extracted from the seed sludge, as well as from samples collected at Stages III and VII.

8.2.3 DNA extraction and microbial analysis

Seed sludge and mixed liquor sludge samples gathered at the end of each stage were extracted for DNA. This extraction process was duplicated using the DNeasy PowerSoil Pro Kit (QIAGEN, Hilden, Germany). The extracted DNA was then amplified using the universal primer pair 515 F (GTGCCAGCMGCCGCGG) and 806 R (GGACTACHVGGGTWTCTAAT). Subsequently, these DNA samples were dispatched for sequencing on the Illumina Miseq PE250 platform at Genome Quebec (Montréal, QC, Canada). Analysis of the sequencing data employed the DADA2 algorithm in QIIME2 pipeline [77, 221]. Taxonomy assignments were made in accordance with the GreenGenes database (version 13_8) at a 97% similarity [79].

For the quantitative analysis of functional genes integral to N conversions, specifically ammonia monooxygenase (*amoA*), nitrite oxidoreductase (*NSR*) and nitrite reductase (*nirSK*), a quantitative polymerase chain reaction (qPCR) was utilized. Detailed primer information was presented in Table 8.1.

Table 8.1 Primer information for quantitative analysis of N conversion functional genes.

	Target gene	Primer	Sequence	Reference
Nitrification	*amoA*	*amoA-1F*	5'-GGGGTTTCTACTGGTGGT-3'	[222]
		amoA-2R	5'-CCCCTCKGSAAAGCCTTCTTC-3'	
	Nitrospira spp.	*NSR 1113f*	5'-CCTGCTTTCAGTTGCTACCG-3'	[223]
		NSR 1264r	5'-GTTTGCAGCGCTTTGTACCG-3'	
Denitrification	*nirS*	*nirS 2f*	5'-TACCACCCSGARCCGCGCGT-3'	[224]
		nirS 3r	5'-GCCGCCGTCRTGVAGGAA-3'	
	nirK	*nirK 876*	5'-ATYGGCGGVCAYGGCGA-3'	[225]
		nirK 1040	5'-GCCTCGATCAGRTTRTGGTT-3'	

8.2.4 Statistical analysis

T-test, executed in Microsoft® Excel® software, was used to determine statistical significance. Differences were reported significant at $P<0.05$.

8.3 Results and discussion

8.3.1 Nitrogen removal

Figure 8.1 presents the reactor performance over 450 days' continuous operation with an influent ammonia concentration of approximately 900 mg N/L. The reactor operation was divided into 7 stages with progressively reduced HRT from 48 hrs to 7 hrs. Within Figure 8.1a, Stage I is recognized as the start-up phase. During this phase, effluent NH_4^+-N and NO_2^--N concentrations fluctuated between 100 to 400 mg/L, achieving 40-85% NH_4^+-N and TIN removal (Figure 8.1b). The interruption in Stage I arose due to a facility shutdown. Beyond this phase, from Stages II to VII, effluent NH_4^+-N, NO_2^--N and NO_3^--N were consistently low, averaging 2 mg N/L, 20 mg N/L and 3 mg N/L, respectively. An exception was observed at the culmination of Stage III with a relatively higher effluent NO_2^--N (up to 55 mg/L) and NO_3^--N (up to 20 mg/L), likely attributed to the excessive aeration, suggesting the HRT could be further shortened. This prolonged aeration allowed AAOB to fully oxidize ammonia, while NOB further transformed nitrite to nitrate. The carbon source provided inadequate for the full conversion of nitrate to nitrogen gas, leading to observable leftover nitrite in Stage III's effluent. As depicted in Figure 8.1c, the inherent COD of the raw wastewater contained a readily biodegradable fraction of up to 200 mg/L. When combined with externally supplied COD during anoxic phase, the resultant C/N ratios varied between 2 and 2.5. These C/N values align with previously reported studies for nitrite denitrification [61, 226].

However, nitrate denitrification demands a higher COD input to complete. Figure 8.1b highlights impressive ammonia and total inorganic nitrogen (TIN) removal efficiencies at 99% and 95% respectively, from Stage II onward. In comparison to a previous study with a C/N ratio of 3, which achieved only a 31% nitrogen removal efficiency, the nitrogen removal efficiency observed in the current study is notably higher [227].

Meanwhile, Figure 8.1d details the N composition of wastewater before and after treatment at Stage VII. In the untreated wastewater, NH_4^+-N constituted 68.7% of the soluble total N and soluble organic N making up 31.1%. The remaining percentages were shared by NO_2^--N and NO_3^--N. In the GSR treated wastewater, the majority of soluble N was organic N, accounting for 76%. It's noteworthy that the soluble total N in the untreated wastewater was 1240 mg/L, which dramatically reduced to 64 mg/L in the treated effluent, that is a 95% reduction. The N loading rate achieved in present study was the highest at 4.2 kg N(m^3·d), compared to reported granular sludge studies treating industrial and municipal wastewaters, which reported rates ranging from 0.16 to 1.20 kg N/(m^3·d) [88, 228-231], or other technologies for high ammonia wastewater treatment, such as DEMON®, suspended SBR and ANITA™ Mox, reporting N loading rates of 0.03 to 2.2 kg N(m^3·d) [107, 232-234].

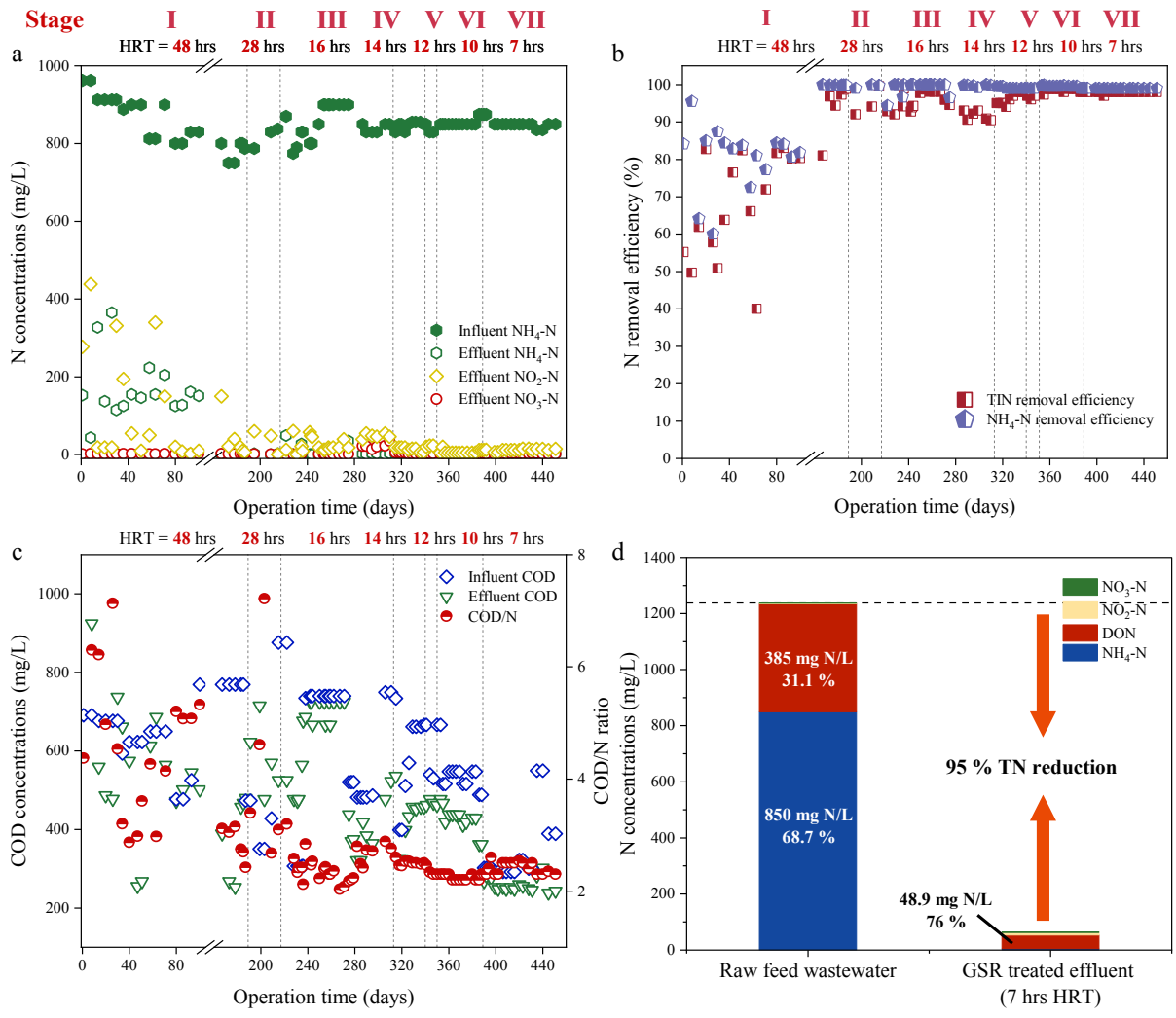

Figure 8.1 Granular sludge reactor (GSR) reactor performance for the treatment of ammonia rich digested sludge supernatant; a) influent and effluent NH_4^+-N concentrations and effluent NO_2^--N and NO_3^--N concentrations; b) NH_4^+-N and total inorganic nitrogen removal efficiencies; c) influent and effluent COD concentrations and $COD_{removed}/N_{removed}$ ratio; and d) proportion of different N (NH_4^+-N, NO_2^--N, NO_3^--N, and organic N) in raw wastewater and GSR treated effluent.

8.3.2 Sludge characteristics

8.3.2.1 Physical properties of granular sludge

At the commencement, the sludge concentration stood at roughly 4 g/L. As depicted in Figure 8.2a, during Stage I, the MLSS and MLVSS remained below 5 g/L. Subsequently, there was a gradual escalation in biomass concentration along with the diminishing HRT. By Stage VII, the MLSS and MLVSS peaked at 22 g/L and 17 g/L, respectively. Compared to conventional activated sludge (CAS) system, the biomass concentration in current study was about 4-5 folds higher,

which aligned with previously reported study [235]. The high biomass density might enhance the resilience of the reactor, resulted in stable treatment efficiencies across the operation period. The MLVSS/MLSS ratio experienced a decline from 0.84 to 0.76, potentially a consequence of the inorganic matter accumulation sourced from the raw wastewater or formed during the reaction.

As portrayed in Figure 8.2b, the SVI_{30} initially reached a high of 390 mL/g, with the SVI_5 also peaking at 260 mL/g during Stage I. These SVI values in Stage I signified that the seed sludge predominantly exhibited a floc form. As operations progressed, SVI values steadily decreased, with Stage VII recording the lowest SVI_{30} and SVI_5 values at 35 mL/g and 24 mL/g respectively. The low SVI values suggest high settleability of the granular sludge cultivated in current study.

This surge in biomass content and the decline in SVI values could be linked to the formation of granulated sludge, evident from Stage III onwards. This granulated sludge, characterized by its denser structure and lower SVI, led to enhanced sludge retention. Further, the longer settling time in current study facilitated greater biomass retention compared to traditional AGS reactor operation, which typically use shorter settling time to select for large granules.

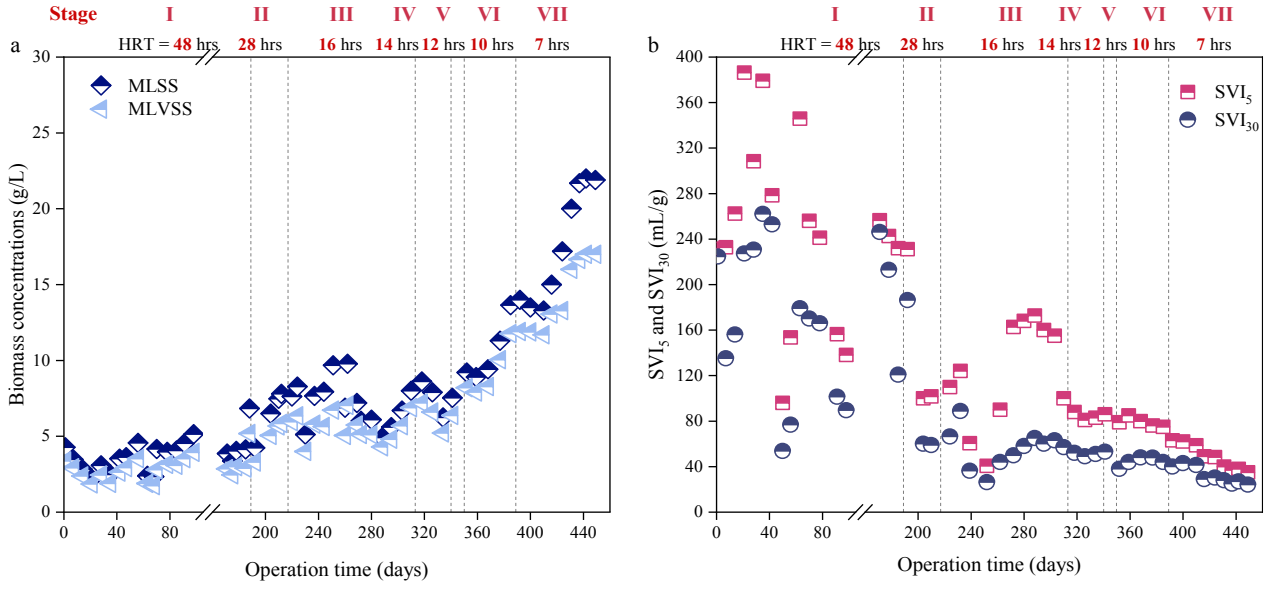

Figure 8.2 Sludge characteristics during bioreactor operation; a) mixed liquor suspended solids (MLSS) and mixed liquor volatile suspended solids (MLVSS) concentrations; and b) sludge volume index at 5 min and 30 min.

8.3.2.2 Granule composition and structure

Figure 8.3a illustrates the granule size distribution at Stage VII. An average size of 0.5 mm was observed, with a predominant distribution ranging from 0.3 to 0.6 mm (Figure 8.4). The dispersion of smaller granules was pronounced relative to the larger granules observed in previous AGS systems, ranging from 0.5 to 8 mm and even up to 2 cm [11, 38, 73, 236, 237]. During the reactor operation period, granular sludge was consistently observed. In current study, the slow granulation process observed might be due to a lack of EPS production. Instead, hydraulic force could have been the primary factor stimulating granule formation during the treatment of low C/N wastewater.

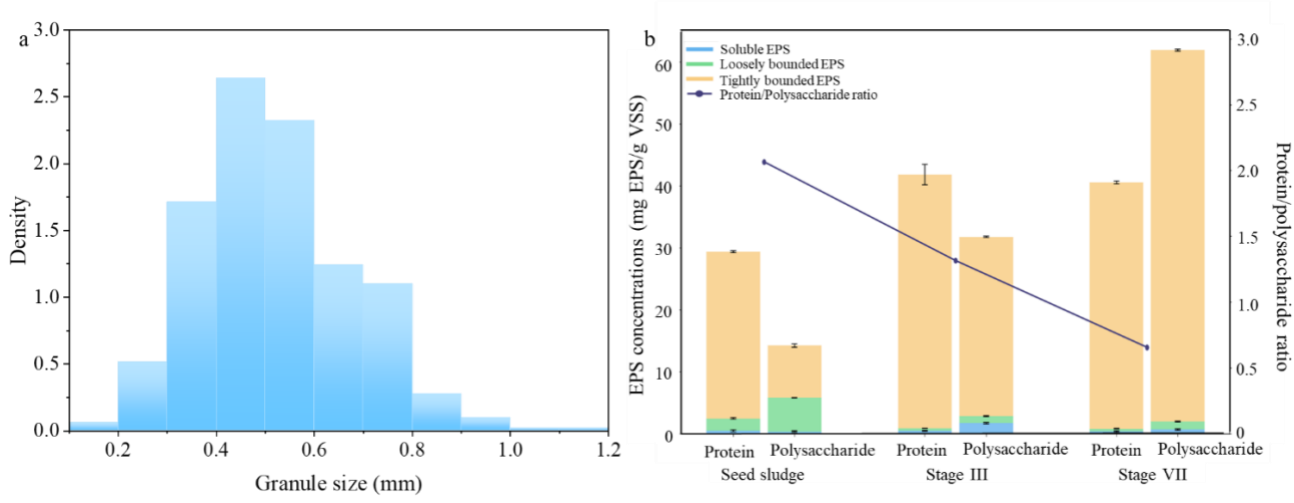

Figure 8.3 Characteristics of granular sludge: a) granule size distribution at Stage VII and b) dynamics of extracellular polymeric substances (EPS) in seed sludge samples and samples collected at Stage III and Stage VII.

Proteins and polysaccharides are reported as key components for the formation and integrity of granular sludge [238]. The dynamics of protein and polysaccharide concentrations in S-EPS, L-EPS and T-EPS were evaluated from seed sludge and samples collected in Stages III and VII, as shown in Figure 8.3b. Detailed information was listed in Table 8.2. Predominantly, T-EPS was observed in all the samples. While S-EPS content was comparable across the three samples, L-EPS showed the highest value in the seed sludge, and the highest T-EPS value was observed in the Stage VII sludge. T-EPS has been reported as the key for cell granulation, which supports the high T-EPS content in Stage VII sludge [239, 240]. Quantitively of the T-EPS, the seed sludge displayed 27 mg protein/g VSS and 8 mg polysaccharide/g VSS, while 41 mg protein/g VSS and 29 mg polysaccharide/g VSS in the Stage III T-EPS. Contrastingly, Stage VII sludge exhibited 40

mg protein/g VSS and 60 mg polysaccharide/g VSS in T-EPS. Protein and polysaccharide concentrations in T-EPS in the previously reported granular studies were higher than the values in current study [171, 241], which might be attributed to the low bCOD content in the raw wastewater, limiting the EPS secretion and granule growth. Notably, while proteins exceeded polysaccharide concentrations in the seed sludge and Stage III samples, Stage VII samples manifested a markedly elevated polysaccharide presence. Similar observation has been reported previously, observing higher polysaccharide content in the granular system [242].

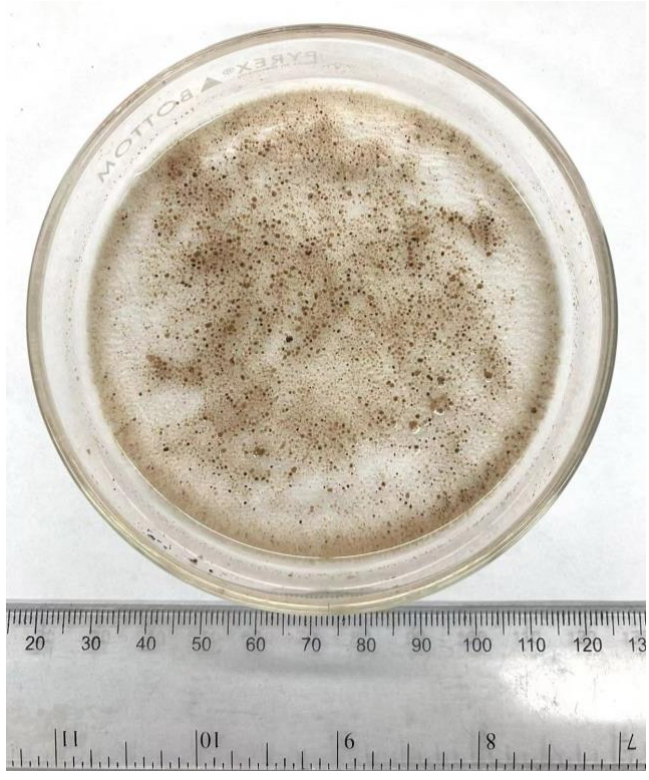

Figure 8.4 Image of granular sludge sampled at Stage VII.

Apart from protein and polysaccharide values, the protein to polysaccharide ratio (PN/PS) serves as a critical determination of granule structure regulation. Figure 8.3b illustrates a progressive decrease in PN/PS ratio throughout the granulation process, diminishing from 2.1 in the seed sludge to 1.3 in Stage III to 0.7 in Stage VII. The role of the PN/PS ratio in indicating granule structural stability and robustness remains debated in the literature. While some studies suggested that ratios less than 1 are indicative of stability [198, 237], others have predominantly reported ratio over 1 [171, 241, 243]. Multiple factors may influence the PN/PS ratio, such as the C/N ratio in feed water and the selection of COD source. Notably, a high PN/PS ratio has often associated

with a C/N ratio ranging between 5-20 [171, 241, 243]. In contrast, this study observed a low PN/PS ratio, which may be related to the specific wastewater characteristic (i.e., low C/N ratio at 0.25) and the utilization of sodium acetate as carbon source. The EPS content highlights the significant influence of polysaccharide in granulation, especially when treating wastewater with a low C/N ratio.

Table 8.2 Protein and polysaccharide concentrations in soluble extracellular polymeric substance (S-EPS), loosely bound EPS (L-EPS) and tightly bound EPS (T-EPS).

	Seed sludge (mg/L)		Stage III (mg/L)		Stage VII (mg/L)	
	Protein	Polysaccharide	Protein	Polysaccharide	Protein	Polysaccharide
S-EPS	0.47	0.33	0.49	1.71	0.36	0.67
L-EPS	1.98	5.46	0.36	1.13	0.45	1.28
T-EPS	26.92	8.44	40.93	28.93	39.77	59.94

XRD was applied to investigate the composition of the granular sludge, as shown in Figure 8.5, that monohydrocalcite was the predominant precipitate in the Stage VII sludge sample. Concurrently, the presence of variscite and SiO_2 were identified. The formation and accumulation of these precipitates might attribute to the reduced MLVSS/MLSS ratios.

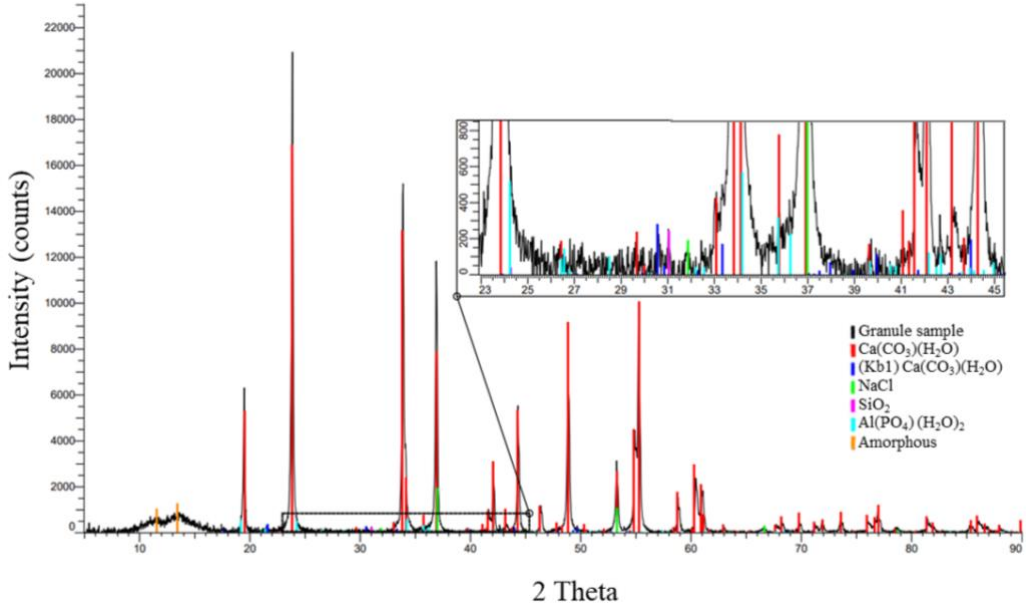

Figure 8.5 XRD analysis result for granular sludge collected at Stage VII.

8.3.3 Microbial kinetics

Specific microbial activities of AAOB, NOB, denitritation and denitrification were shown in Figure 8.6. The AAOB activities as shown in Figure 8.6a had the lowest value in Stage I at 0.18 g N/(g VSS·d), then increased with the shortened HRT and reached the highest value in Stage VII at 0.5 g N/(g VSS·d), which fitted at the high end of the reported AAOB activity values, ranging from 0.07 to 0.64 g N/(g VSS·d) [88, 90, 244-246]. The relatively high AAOB activity might be attributed to the selection of highly effective microbial community via enhanced N loading. As previous studies reported, the small-sized granular sludge might also contribute to the relatively high AAOB activity [90]. NOB activities were relatively low across the operation compared to AAOB activities. There was a significant ($p<0.05$) increment in NOB activity in Stage III, which aligns with the observation in reactor performance data in Stage III, where effluent nitrate was slightly higher compared to other stages.

The denitritation and denitrification specific activities were shown in Figure 8.6b. The denitritation activities increased progressively from 1.1 to 3.7 g N/(g VSS·d) and peaked at Stage VII. In contrast, the denitrification activities were stabilized at approximately 1 g N/(g VSS·d), which was 3-fold lower than the highest denitritation activities. Similar observation has been reported previously [88]. The nitrite reduction rate obtained in present study was the highest across the reported granular studies, which showed a value from 0.25 to 2 g N/(g VSS·d) [88, 244, 247]. Across all the samples, the specific activities of denitritation were considerably higher than denitrification, which has also been reported previously [88, 244, 246]. These results suggest that increased N loading also enhanced the denitritation activity in the GSR system.

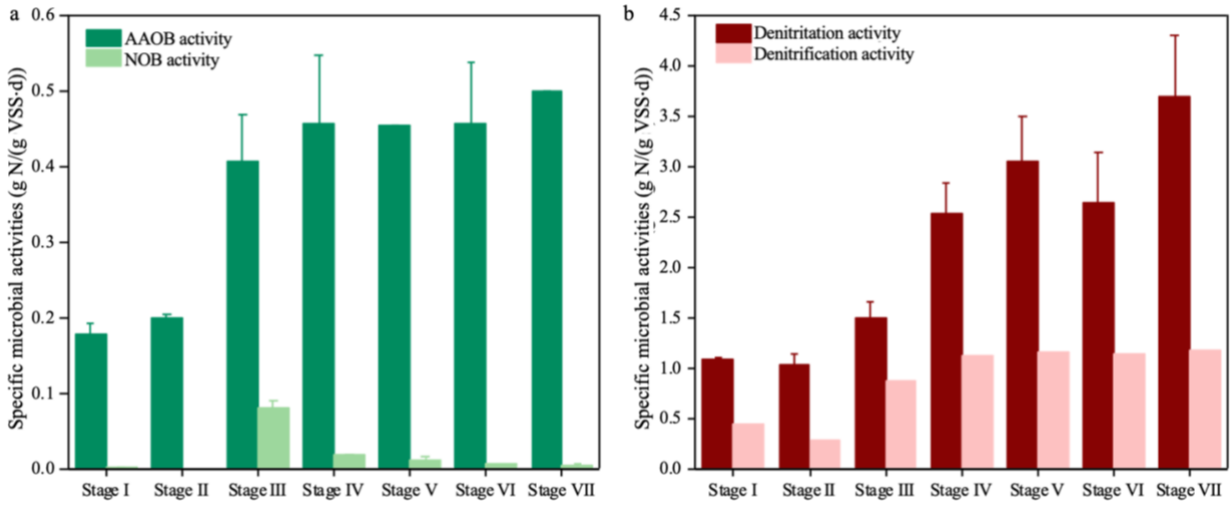

Figure 8.6 Specific microbial activities under each stage, including a) the specific activities of autotrophic ammonia oxidizing bacteria (AAOB) and nitrite oxidizing bacteria (NOB); b) the specific activities of denitritation and denitrification.

8.3.4 Microbial community dynamics

The relative abundance of bacteria at phylum level and genus level were depicted in Figure 8.7a and Figure 8.7b. As shown in Figure 8.7a, phylum Proteobacteria was dominated in sludge samples across all the stages, accounting for 68% in seed sludge and reached up to 98% in Stage VII. As previously reported, nitrogen removal related functional microbes are affiliated in phylum Proteobacteria [97]. Followed by Bacteroidetes, which reduced in relative abundance from 20% in seed sludge to 0.2% in Stage VII. Phylum [Thermi] is the third abundant group in microbial community, the relative abundance of which was increased from 6% in seed sludge to 10% in Stage I, then gradually reduced to 1% in Stage VII. This phylum has also been reported to be involved in ammonia removal process [248].

Figure 8.7b depicts the relative abundance of genus involved in nitrification and denitrification processes and genus constituted over 1% of the microbial communities. Genus *Nitrosomonas* was the primary ammonia oxidizing bacteria throughout the operational stages. This genus manifested a peak in its relative abundance during Stage III, registering at 14.4%, an increased from its previous concentrations in seed sludge (0.1%), Stage I (0.8%) and Stage II (1.4%). Thereafter, a decline was observed through Stage IV (10.3%), Stage V (11.2%), Stage VI (3.6%) to Stage VII (2.7%). Even though the relative abundance of *Nitrosomonas* reduced from Stage III onwards,

qPCR results in Figure 8.7c showed a statistically significant ($p<0.05$) increment in the copy number of functional ammonia monooxygenase gene (*amoA*) in the system, escalating from 6.4×10^9 copies/L in seed sludge to 4.3×10^{11} copies/L in last stage. The findings showed that the reduction in the relative abundance of *Nitrosomonas* was primarily attributed to the substantial growth of denitrifying bacteria. Despite this decrease in relative abundance, the quantitative abundance of the functional genes (*amoA*) increased along the reactor operation, fortifying specific ammonia oxidation rate and N removal capacity.

Genus *Nitrobacter* was the primary nitrite oxidizing bacteria in the reactor, marked a 0.1% in relative abundance during Stages III and IV, underscoring enhanced nitrite to nitrate conversions. The observation aligned with the performance data. Figure 8.7d, presenting quantifications of the nitrite oxidoreductase (*NSR*) gene throughout the operation, highlighting the highest *NSR* gene copy number in Stage III at 5.2×10^7 copies/L, which also matches the sequencing result. Outside these two stages, the relative abundance of *Nitrobacter* remained under 0.1%, implying effective inhibition of NOB by FA for the majority of the operation period. Remarkably, another identified genus within family Nitrosomonnadaceae was also detected in the seed sludge, albeit its prevalence reduced in subsequent GSR operations.

The most abundant denitrifiers was affiliated to *Thauera* and followed by *Paracoccus* (Figure 8.7b). The lowest relative abundance of *Thauera* was observed in the seed sludge at 32.7%, while peaked in Stage VII at 93.8%. In contrast, *Paracoccus* showed the highest relative abundance in Stage II at 3.3% and the lowest value in Stage VII at 0.1%. The domination of *Thauera* in the AGS system suggesting it is preferred for environments with high ammonia and low C/N condition, which also supported by previous study [249]. Further, the copy numbers of nitrite reductases (*nirSK*) increased gradually over time (Figure 8.7e), elevating from 4.7×10^{10} copies/L to 5.6×10^{11} copies/L, emphasizing the enhanced denitritation capacity in the GSR system.

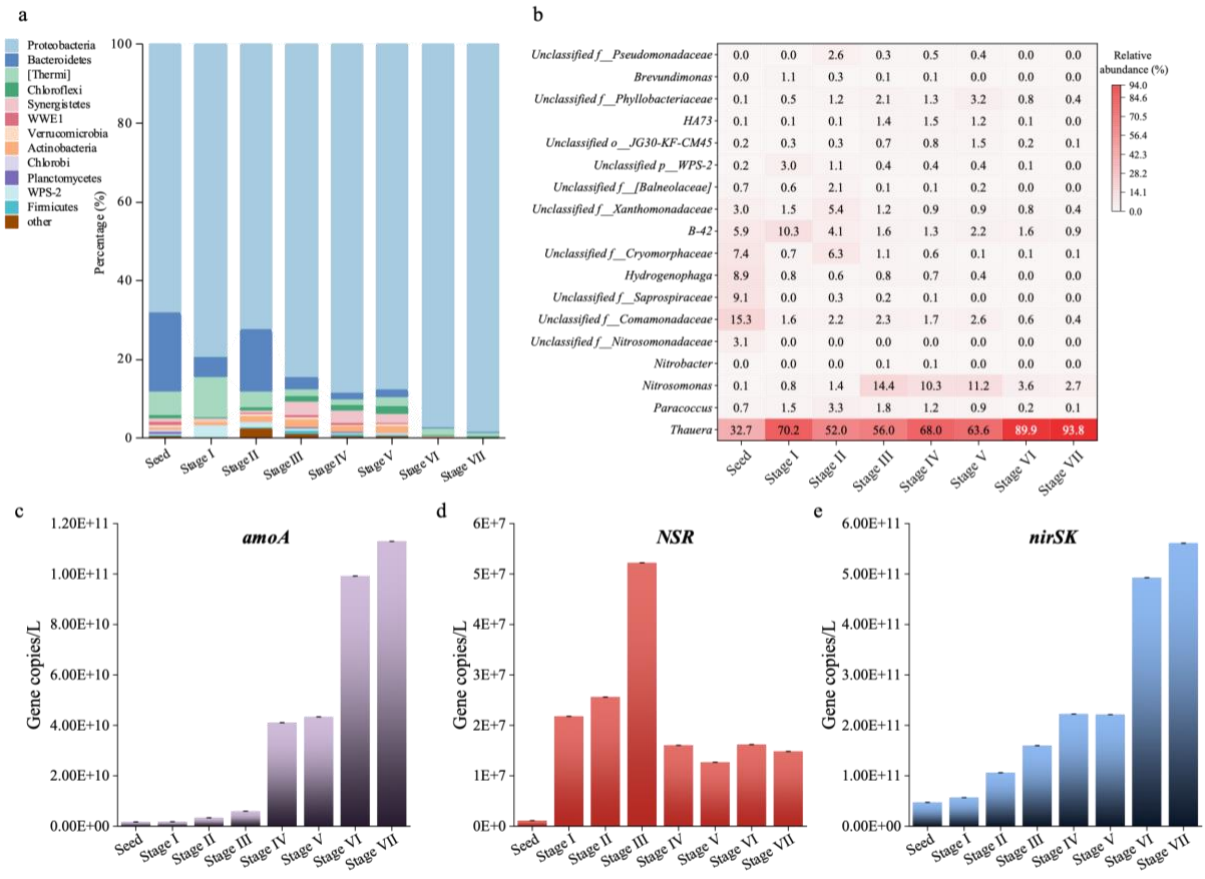

Figure 8.7 Microbial community analysis in seed sludge and sludge samples in Stage I to VII, including the relative abundance of bacteria in a) phylum and b) genus level, and qPCR analysis of functional genes involved in c) ammonia oxidation, ammonia monooxygenase (*amoA*), d) nitrite oxidation, nitrite oxidoreductase (*NSR*) and e) nitrite reduction, nitrite reductase (*nirSK*). Unidentified genera in b) are shown at family (Unclassified f_), order (Unclassified o_), and phylum (Unclassified p_) levels.

8.3.5 Key to the high nitrogen removal capacity

The remarkable nitrogen removal capacity obtained could be attributed to the synergist effect of multiple factors: i) the selectively enriched AAOB that demonstrated elevated specific microbial activities via incremental N loading; ii) the high biomass content attained with sufficient settling duration; iii) the formation of small-sized granular sludge, which not only exhibited an enhanced active microbial surface area but also mitigated diffusion constrains, encompassing substrate and oxygen diffusion dynamics within the granular sludge as well as; iv) the compact granule structure, which might also facilitate symbiotic interactions between AAOB and denitrifiers, recognizing as complimentary role in the N cycle. The enhanced specific microbial activities in line with the

reactor performance, suggesting a microbial adaptation and proliferation in response to operational conditions, fostering the proliferation of efficient nitrogen-transforming microorganisms. In summary, the high retention capacity of efficient functional bacteria underpins the exceptional N removal capacity of GSR system.

8.3.6 Implications and perspectives

Our work provides an insight for the application of granular sludge for the treatment of wastewater rich in ammonia and low in biodegradable COD. With the GSR, an impressive N treatment capacity at 4.2 kg N/(m^3·d) was achieved. This system not only reduces reactor size but also the demand of subsequent treatment units, such as settling tank, and minimizes the requirement for chemical and oxygen supplementation. The economical and sustainable attributes of GSR position it as a preferred alternative for wastewater treatment.

Other than the aforementioned merits, several areas require further research. As previous studies suggested, a moderate loading rate fostered a more stable granular sludge. It's observed that escalated substrate loading rates can amplify biomass growth, potentially compromising the structural integrity of microbial community [250]. While stable granular structure was consistently observed during the 450 days' operation, comprehensive assessment regarding the long-term stability and resilience of granular sludge under different N loading and shock conditions remain to be undertaken. Prior to large-scale applications, it is imperative to undertake a system scale-up to thoroughly evaluate the viability and effectiveness of the technology.

8.4 Conclusion

A high nitrogen treatment capacity at 4.2 kg N(m^3·d) was achieved in a GSR treating anaerobically digested sludge supernatant without any pretreatment. This chapter cultivated, selected, and enriched the highly efficient microbial community, especially the high AAOB and denitrifiers activities, showing the highest activity at 0.5 g N/(g VSS·d) and 3.7 g N/(g VSS·d), respectively. High biomass density at 17 g/L MLVSS was attained and small granular sludge (0.5 mm) was cultivated. At the genus level, *Nitrosomonas* was the dominated AAOB in ammonia oxidation process, while *Thauera* was the primary denitrifiers in nitrite reduction process. Quantitative PCR

analyses further revealed an increase in abundance of functional genes critical to the N cycle, namely, ammonia monooxygenase (*amoA*) and nitrite reductase (*nirSK*), as the operation progressed. This chapter showcased the efficacy of GSR in treating anaerobically digested sludge supernatant, attaining remarkable nitrogen removal capacity by selectively enriching a highly efficient microbial community and stably increased biomass density.

Chapter 9. Newly Developed Granular Sludge Reactor (GSR) for High Ammonia Mature Landfill Leachate Treatment[6]

9.1 Introduction

Chapter 8 has demonstrated the feasibility of the newly developed GSR for high ammonia, low C/N ratio anaerobically digested sludge supernatant treatment. Given that granules have higher resistance to toxic compounds, the newly developed GSR can be a superior alternative for treating high ammonia raw landfill leachate wastewater (LLW). LLW is particularly challenging due to its high toxicity and elevated concentrations of heavy metals, salinity, ammonia, and recalcitrant COD [251, 252]. Effective treatment of LLW is essential to prevent surface water and groundwater contamination [253].

To date, there are only limited studies on the application of granular sludge-based systems for LLW treatment. Studies using suspended sludge-based processes, such as conventional activated sludge (CAS) processes [254], or sequencing batch reactors (SBR) [255-257], reported poor treatment efficiencies, which was largely attributed to the poor sludge settleability, sludge bulking and low biomass concentration [258]. Studies using biofilm-based processes, such as rotating biological contactor (RBC), membrane aerated biofilm reactor (MABR) and moving bed biofilm reactor (MBBR) reported N loadings ranged from 0.1 to 2.3 kg N/(m^3·d) with HRTs ranged from 1-5 days [259-262]. In comparison, improved LLW ammonia removal efficiency and stability have been reported using granular sludge-based systems. For instance, Ren, Ferraz, Lashkarizadeh and Yuan [42] compared the nutrient removal performance between an activated sludge reactor and a granular sludge reactor for young landfill leachate wastewater treatment, and showed that the granular sludge reactor had significantly higher nutrient removal efficiency and tolerance to the toxic components. Previous study seeded granular sludge in a reactor treating LLW and achieved 95% ammonia removal and 83% total nitrogen removal at the relatively high nitrogen

[6] A version of this chapter has been published: Zou, X., Mohammed, A., Gao, M., & Liu, Y. (2022). Mature landfill leachate treatment using granular sludge-based reactor (GSR) via nitritation/denitritation: Process startup and optimization. *Science of the Total Environment*, *844*, 157078. https://doi.org/10.1016/j.scitotenv.2022.157078

loading rate of ~1.1 kg N/(m^3·d) [12]. Additionally, a reported study used AGS for landfill leachate treatment, and achieved 98% inorganic nitrogen removal with an HRT of 6 hrs [263].

Despite the promise reported in recent granular sludge based LLW studies, the biological treatment of LLW with no pretreatment, dilution or cotreatment with low strength streams requirements has rarely been demonstrated previously. The optimization of the treatment performance to achieve reduced HRT has yet to be demonstrated, and the impact of LLW on microbial activity, microbial communities, and functional gene abundance has not been evaluated.

In this chapter, Nit/DNit was applied to treat mature LLW in a GSR at 20 °C. Ammonia and TIN removal efficiencies, microbial activities and dynamics, and the relative abundance of functional genes related to the N cycle and heavy metals were assessed and compared at different stages in the treatment.

9.2 Materials and methods

9.2.1 Reactor setup and operation

A 4 L cylindrical reactor with an inner diameter of 9 cm and a height of 63 cm, was employed to treat mature landfill leachate at 20 °C. The reactor was operated in sequencing batch mode with a 50% feed exchange ratio. The seed sludge for the GSR was collected from a Nit/DNit based integrated fixed film activated sludge (IFAS) reactor treating high ammonia (~800 mg/L) digester effluent wastewater. Treatment performance of the IFAS reactor has been reported previously [61]. The initial seed sludge concentration was ~ 5.5 g/L mixed liquor volatile suspended solids (MLVSS).

Since the seed sludge originated from a reactor treating ammonia rich digestate, to minimize the potential adverse impacts of raw leachate on the microbes, the reactor was initially fed with ammonia rich digestate (collected from a wastewater treatment plant in Alberta, Canada) from the anaerobic digestion of primary and secondary sludge, and then was gradually replaced by landfill leachate using 10% additions and mixing well. Landfill leachate wastewater (LLW) was collected biweekly from a local landfill leachate (Alberta, Canada). The collected LLW and lagoon

supernatant were stored in a cold room (4 °C) before mixing together with different percentage (as shown in Table 9.1) and being treated by GSR. Detailed physicochemical characteristics of wastewaters are shown in Section 9.3.1.

During process optimization, the HRT in the GSR was gradually shortened from 16 hrs to 6 hrs, and the settling time was reduced from 30 min to 5 min, as the percentage landfill leachate increased. Conditions of reactor operation are depicted in Table 9.1. The operation sequences and duration were modified based on the cycle test results to prevent excessive aeration supply and eliminate nitrite oxidation. The feeding (10 min) and discharging (5 min) durations were consistent throughout the reactor operation. During the aerobic phase, a diffuser at the bottom of the reactor provided a superficial air upflow velocity of 1.4 cm/s and dissolved oxygen (DO) concentration at 0.6-1 mg/L. An external carbon source (sodium acetate anhydrous) at ~ 43 g COD/L was introduced into the reactor via pulse injection in the first 10 min of the anoxic phase to support the denitritation process, since the mature LLW was lack of biodegradable organic carbon. A recirculation rate of ~ 134 mL/min was provided during the anoxic phase to prevent sludge settling and to enhance COD mixing.

Table 9.1 Reactor operation conditions.

Stages	Landfill leachate %	NH_4^+-N concentration (mg/L)	HRT (hrs)	Operation sequences and duration (min)					
				Aeration	Anoxic	Aeration	Anoxic	Post-aeration	Settling
I	0	850	16	140	60	140	60	20	30
II	10	835	16	140	60	90	60	20	20
III	20	750	14	140	60	30	60	20	20
IV	30	632	10	120	90	-	-	20	20
V	40	594	8	120	90	-	-	20	15
VI	50	545	8	90	90	-	-	20	10
VII	60	510	7	90	90	-	-	20	10
VIII	70	458	6	60	75	-	-	20	5
IX	80	393	6	45	75	-	-	20	5
X	90	328	6	45	75	-	-	10	5
XI	100	300	6	45	75	-	-	10	5

9.2.2 Metal analysis

Metals in raw LLW and GSR treated LLW were digested based on the U.S, Environmental Protection Agency (EPA) 6010d method and analyzed with U.S. EPA 3051A using inductively coupled plasma optical emission spectroscopy (ICP-OES) (Thermo Icap6300 Duo ICP-OES).

9.2.3 DNA extraction

Seed sludge and sludge samples at 50% and 100% landfill leachate conditions were collected in duplicate to determine the microbial community dynamics in the granular sludge reactor (GSR). DNA was extracted from collected sludge samples using DNeasy PowerSoil® DNA Isolation Kits (QIAGEN, Hilden, Germany) according to the instructions provided. Extracted DNA was checked for quality with NanoDrop™ One (ThermoFisher Waltham, MA), then stored at -20 °C. Samples were sequenced on the Illumina Miseq PE250 platform at Genome Quebec (Montréal, QC, Canada).

9.2.4 Sequencing and analysis

The QIIME2 pipeline DADA2 algorithm was employed to process sequencing data and removing low quality sequences and chimeras [77, 221]. The taxonomy was assigned based on the GreenGenes database (version 13_8) with 99% similarity [79]. Alpha diversity was calculated in the RStudio (version 3.6.3) package "vegan" and "fossil" to assess the dynamics in richness and diversity of the microbial community as the landfill leachate loading increased. The Phylogenetic Investigation of Communities by Reconstruction of Unobserved States 2 (PICRUSt2) pipeline, based on the Kyoto Encyclopedia of Genes and Genomes (KEGG) database, was used to predict functional genes for nitrogen conversion and metal resistance in seed sludge and in sludge collected at 50% and 100% LLW [80]. Functional Annotation of Prokaryotic Taxa (FAPROTAX) was used to map the carbon and nitrogen metabolic functions in seed sludge and in the sludge at LLW percentages of 50% and 100% [264].

9.2.5 Statistical analysis

The results were expressed as a mean value ± standard deviation. The T-test in Microsoft® Excel® software (version 2109) was used to evaluate the significance of the results; $P<0.05$ was considered to be a significant difference.

9.3 Results and discussion

9.3.1 Main physicochemical characteristics of landfill leachate and lagoon supernatant

Raw landfill leachate wastewater (LLW) contained: 300.4 ± 5.8 mg/L NH_4^+-N, 4.5 ± 1.3 mg/L NO_2^--N, 2.7 ± 0.1 mg/L NO_3^--N, 480 ± 15 mg/L total nitrogen (TN), 479.7 ± 14.5 mg/L total Kjeldahl nitrogen (TKN), 2683.3 ± 49.3 mg/L alkalinity (as $CaCO_3$), 1078.2 ± 43.9 mg/L soluble COD, 106.8 ± 5.3 mg/L BOD, 8.4 ± 1.5 g/L total solids (TS), 1.6 ± 1.1 g/L total suspended solids (TSS) and pH 7.3 ± 0.3. The lagoon supernatant contained: 950 ± 100 mg/L NH_4^+-N, 4.0 ± 2.0 mg/L NO_2^--N, 2.0 ± 1.0 mg/L NO_3^--N, 2800-3000 mg $CaCO_3$/L alkalinity and 739.6 mg/L COD.

9.3.2 Granular sludge reactor (GSR) performance and cycle tests

The nitrogen (N) and COD removals over 50 days of sequencing batch operation of GSR are presented in Figure 9.1. The NH_4^+-N concentration in the feed gradually decreased as the landfill leachate wastewater (LLW) percentage increased, ranging from 850 (0% LLW) to 300 (100% LLW) mg/L (Figure 9.1a). At 10% LLW and 20% LLW, the removal efficiencies of ammonia and total inorganic nitrogen (TIN) dropped, then recovered in a short time, possibly due to sludge washout in the early stage of reactor operation and microbial acclimatization to the different feed characteristics. Effluent NH_4^+-N, NO_2^--N, and NO_3^--N stabilized at 2.5 ± 1.4, 15.1 ± 4.4, and 1.3 ± 0.9 mg/L, respectively (Figure 9.1a), and removal efficiencies of 99.1 ± 0.4 % NH_4^+-N and 92.6 ± 0.9 % total inorganic nitrogen (TIN) were consistently observed (Figure 9.1b), even at 100% LLW, with N loading at 1.2 ± 0.04 kg N/(m^3·d). The results suggest inorganic N removal from the GSR was not impacted by landfill leachate loading increase. The inorganic N removal from landfill leachate was superior in the present study, as compared to the results reported in previous studies, especially CAS systems [254-256]. Huang and Lee [255] reported an 86.4% TIN removal from landfill leachate at a 1.25 ± 0.04 kg N/(m^3·d) N loading rate, whereas Kulikowska and Bernat [256] reported a 78% TIN removal with an TIN loading of 0.42 ± 0.01 kg N/(m^3·d). With 480 ± 15 mg/L TN and 479.7 ± 14.5 mg/L TKN in the feed, the effluent TN and TKN concentrations were 110 and 95 mg/L, respectively, those were 77.1% TN removal and 80% TKN removal. The cycle test results at each LLW percentage (from 0% to 100%) are shown in Figure 9.2. The accumulated nitrite accounted for ~93% of the NO_x produced, indicating that nitritation was maintained in the GSR throughout the operation. Nit/DNit contributed 81-89% nitrogen removal

in each stage (as shown in Figure 9.3). Further research is needed to investigate the gas phase nitrogen compounds composition for a better understanding regards to N mass balance.

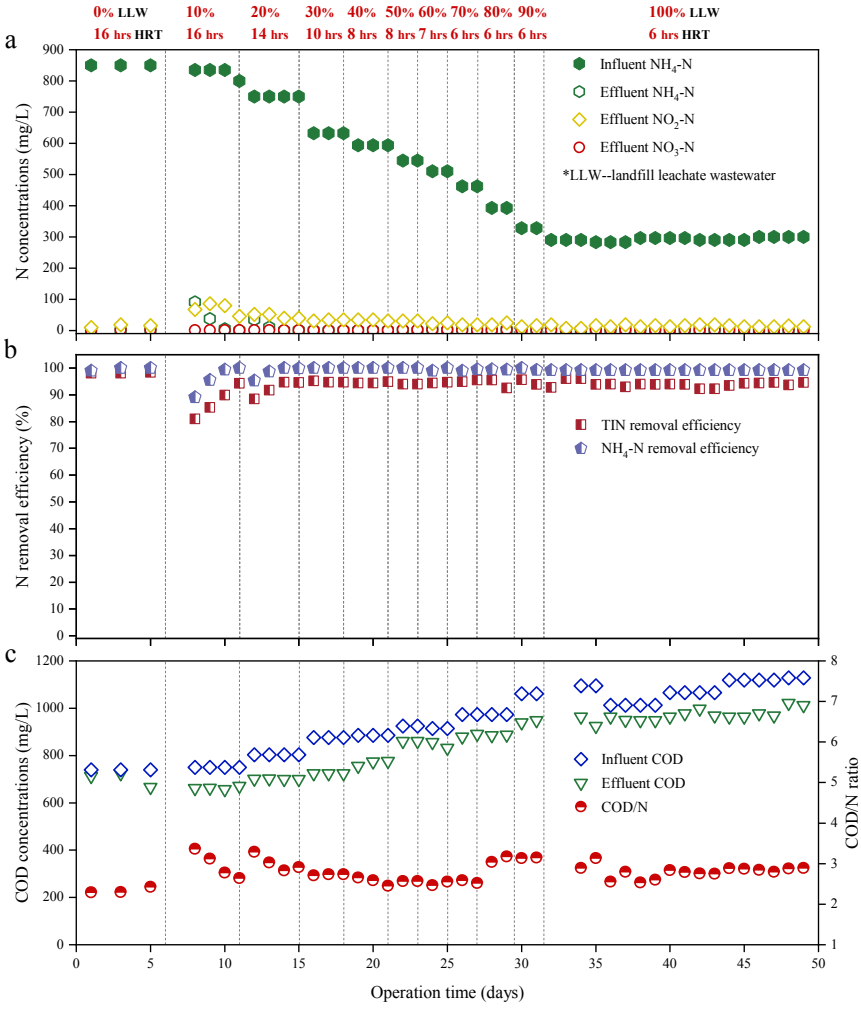

Figure 9.1 Granular sludge-based reactor (GSR) performance in the nitritation/denitritation (Nit/DNit) of landfill leachate over 50 days: (a) nitrogen (NH_4^+-N, NO_2^--N, NO_3^--N) concentrations in influent and effluent; (b) NH_4^+-N and total inorganic nitrogen (TIN) removal efficiencies; (c) COD concentrations in influent and effluent and $COD_{removed}/N_{removed}$ ratios.

The influent COD concentration gradually increased as the LLW loading increased, ranged from 739.6 to 1128.8 mg/L (Figure 9.1c), resulted in increased effluent COD concentration from 661.7 to 1021.8 mg/L (Figure 9.1c). At 100% LLW, the COD removal efficiency was 8.2 ± 1.4%. The high effluent COD concentration and the low COD removal efficiency were a result of the limited biodegradable COD in the mature landfill leachate. Similar observations have been reported previously [265, 266]. With external COD addition, the $COD_{removed}/N_{removed}$ ratio was maintained

at ~ 2.8 (Figure 9.1c), comparable to previously reported studies [226, 256, 267]. Further research is needed to investigate effective strategies for mature landfill leachate recalcitrant COD removal and thus achieve simultaneous N and COD removal. To further improve the environmental benefits of the LLW treatment process, incorporating the anammox based process in LLW treatment is promising to investigate in future studies.

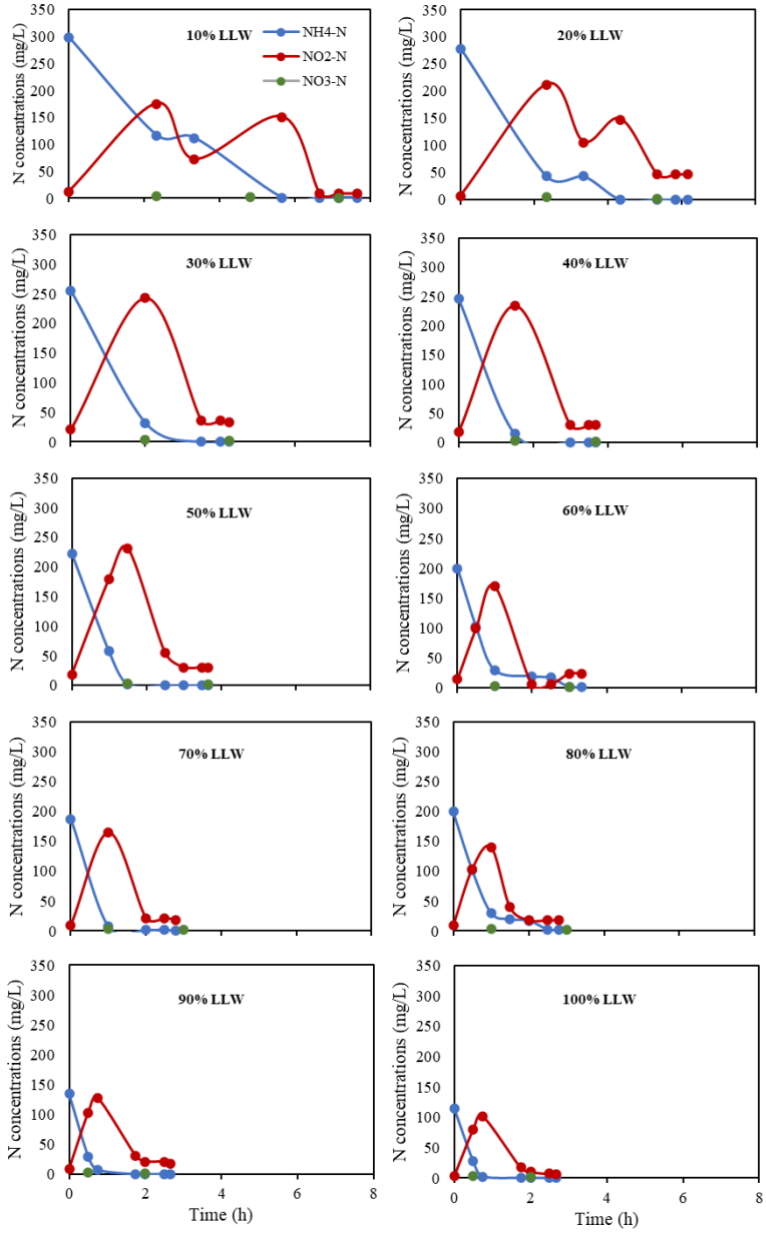

Figure 9.2 The nitrogen species concentrations in typical cycle tests at different landfill leachate percentages, from 10% to 100% with 10% interval.

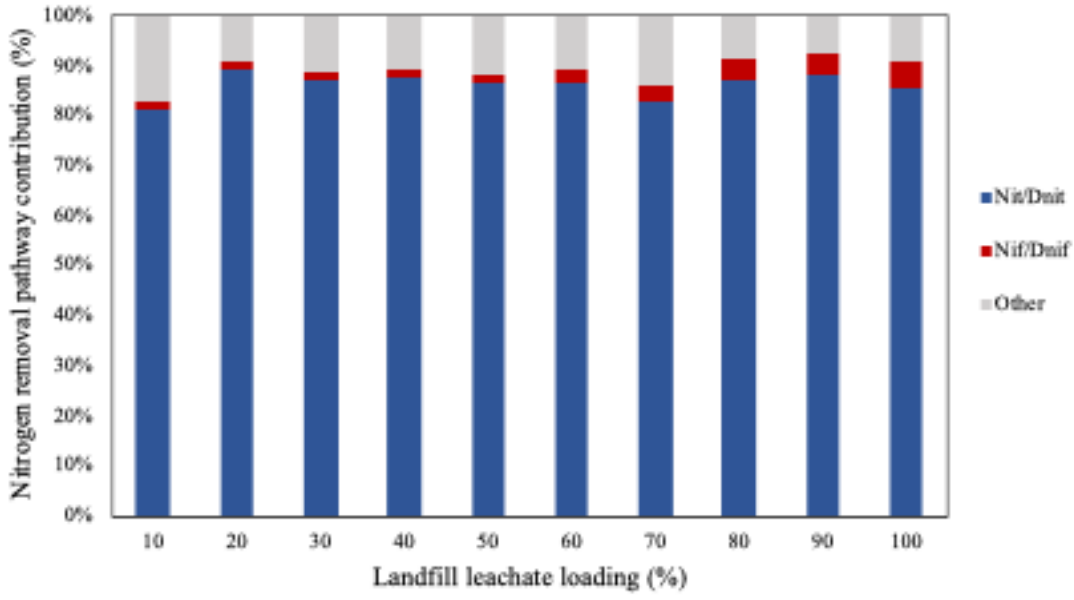

Figure 9.3 Contributions of nitrogen removal (%) from different pathways including nitritation/denitritation (Nit/DNit), nitrification/denitrification (Nif/DNif) and others (cell assimilation, simultaneous nitrogen oxidation and reduction).

9.3.3 Metal removal in the treatment of mature landfill leachate

Table 9.2 shows the average metal concentrations in the influent landfill leachate wastewater (LLW) and the effluent from the GSR with 100% LLW. The concentrations of most metals, especially Ca and Fe, were lower after granular sludge treatment. Although some of the metal levels were relatively low in Table 9.2, but since the metal precipitates accumulated in the system, therefore, analyzations related to metals were performed. Metal removal was likely carried out via biomineralization at pH ~8.6, through extracellular polymeric substances (EPS) adsorption and co-precipitation [268-270]. Potential microbes involved in biomineralization are discussed in following sections.

Table 9.2 Average metal concentrations in the landfill leachate influent and the effluent from the granular sludge reactor (GSR).

	Unit	Influent	Effluent
Ag	mg/L	*	*
Al	mg/L	0.70	0.40
As	mg/L	*	*
B	mg/L	25.15	24.54
Ba	mg/L	3.83	1.51
Be	mg/L	*	*
Ca	mg/L	300.87	111.11
Cd	mg/L	*	*
Cr	mg/L	0.07	0.04
Cu	mg/L	0.04	0.02
Fe	mg/L	42.66	27.52
K	mg/L	310.58	293.45
Li	mg/L	0.28	0.28
Mg	mg/L	242.35	223.63
Mn	mg/L	0.54	0.25
Mo	mg/L	*	*
Na	mg/L	1716.24	1625.71
Ni	mg/L	0.15	0.14
P	mg/L	2.46	13.29
Pb	mg/L	0.04	0.03
S	mg/L	15.51	15.47
Sb	mg/L	*	*
Se	mg/L	*	*
Si	mg/L	14.27	9.61
Sr	mg/L	5.31	2.97
Ti	mg/L	0.05	0.03
Tl	mg/L	*	*
V	mg/L	*	*
Zn	mg/L	0.17	0.10

*lower than the detection limit

9.3.4 Sludge concentrations and sludge settling

Increases in mixed liquor suspended solids (MLSS) and mixed liquor volatile suspended solids (MLVSS) in the GSR are shown in Figure 9.4a. Initial MLSS and MLVSS concentrations were 7.18 and 5.5 g/L, respectively, with a 0.77 MLVSS/MLSS ratio, commonly found in wastewater treatment systems [271]. After over 50 days of operation, the MLSS and MLVSS concentrations increased significantly to 60.7 and 22.5 g/L, respectively. The MLVSS is considerable higher than

the biomass content in CAS and biofilm systems and no biofilm/sludge control is required [92, 260, 261]. The final MLVSS/MLSS ratio of 0.37 was low because of the accumulation in the reactor of metal precipitates from the landfill leachate. Due to the high treatment performance maintained during the operation, no sludge wasting was conducted.

Figure 9.4b shows sludge volume index values, SVI_5 and SVI_{30}, that were used as an indicator of granulation and to evaluate the settling ability of the granular sludge [272]. A granular sludge reactor was commonly characterized by limited difference between SVI_5 and SVI_{30} and the SVI_5 and SVI_{30} were within the range from 35 to 70 mL/g [273, 274]. Initially, SVI_5 and SVI_{30} were 118.4 mL/g and 52.9 mL/g, respectively, which indicates that the seed sludge was in a flocculant form. SVI_5 and SVI_{30} decreased during reactor operation, to 37.7 and 34.2 mL/g, respectively, on day 11, with 30% LLW in the reactor feed. The sludge settling ability kept improving until the SVI_5 and SVI_{30} stabilized at 6.1 and 4.9 mL/g, respectively. The low SVI_5 and SVI_{30} enhanced the sludge retention capacity of the GSR, contributing to high effluent quality and the high MLSS and MLVSS contents in the reactor. The significant reduction in SVI values can be attributed to the selection pressures applied to the reactor—such as a short settling period and a high hydrodynamic shear force. Further, metal precipitates (Ca and Fe) introduced into the reactor from the LLW also contributed to the fast settling granular sludge, since the metal precipitates could enhance the production of extracellular polymeric substances (EPS) [275], contributing to the adsorption of metals to the negatively charged cell surface, thus enhancing sludge density and improving sludge settling ability [268, 269].

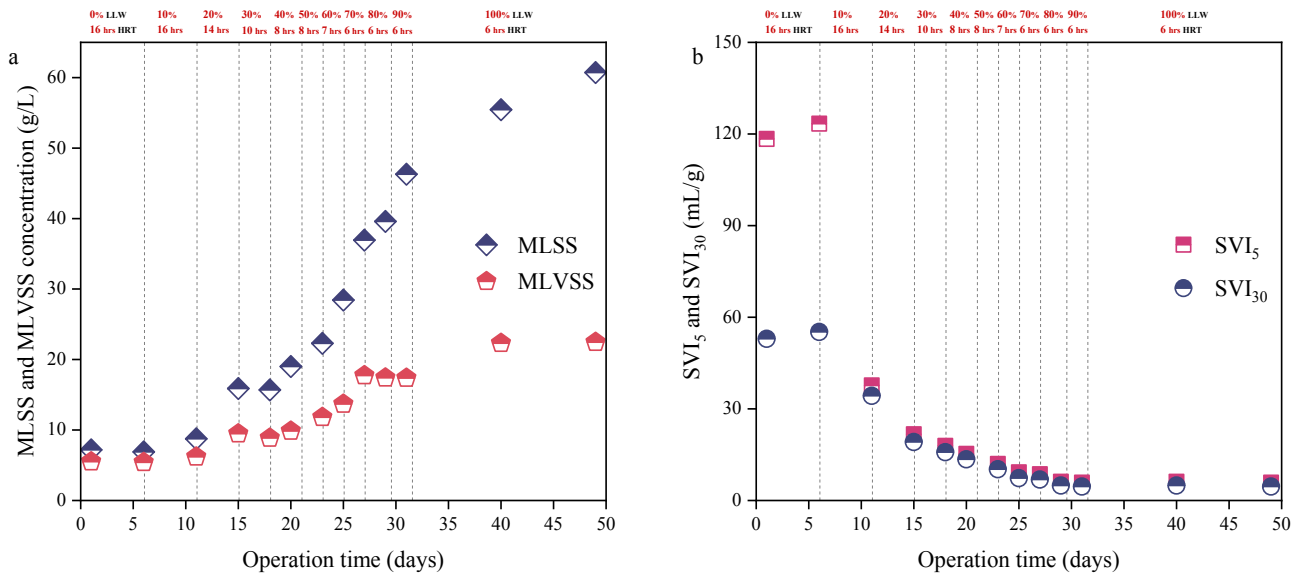

Figure 9.4 The dynamics of (a) concentrations of mixed liquor suspended solids (MLSS) and mixed liquor volatile suspended solids (MLVSS); (b) sludge volume index (SVI) over 50 days operation.

9.3.5 Nitrogen transformation kinetic tests

Batch tests were conducted to monitor the activity of specific microbes. Figure 9.5 indicates that AAOB activity (NH_4^+-N oxidation rates) was consistently higher than NOB activity (NO_3^--N production rates). NH_4^+-N oxidation rates increased from 0.24 ± 0.05 to 0.64 ± 0.11 g N/(g VSS·d) in the seed sludge (equally to the sludge at 0% LLW) and the sludge collected at 100% LLW, respectively. The highest NH_4^+-N oxidation rates obtained in this study were higher than the activity values previously reported in GSR systems [229, 244, 245, 247, 276-278]. The high NH_4^+-N oxidation rate was probably a result of the small granule size (~0.1-0.3 mm) in the GSR [90] and the relative high nitrogen loading rate. Granular size distribution under 100% LLW loading condition is shown in Figure 9.6. Negligible NO_3^--N production rates of 0.0028 ± 0.0004 (seed sludge) and 0.028 ± 0.0003 (100% LLW) g N/(g VSS·d) were obtained, indicating that NOB suppression was successfully maintained throughout the 50 days of reactor operation. The free ammonia (FA) concentrations in the GSR ranged from 7.61 to 21 mg/L, which was considerable higher than the reported FA for NOB inhibition (0.1-1 mg/L) [279]. The accumulated metal content in the GSR probably also contributed to the NOB inhibition. Operation parameters such as low dissolved oxygen (DO at 0.6-1 mg/L) and short aeration phase, which stopped once ammonia was depleted, favored the growth of AAOB over NOB. Trace NOB activities have been

reported in nitritation studies [61, 247, 278, 280]. However, the NO_3^--N production rate in 100% LLW sludge was slightly higher than the NO_3^--N production rate in the seed sludge, probably because of the lower FA concentration in 100% LLW) [279], which was attributed to the lower influent ammonia concentration at 100% LLW condition (reduced from 850 to 300 mg/L). Although the FA in the GSR was higher than the required FA for NOB inhibition, NOB may gradually become resistant to FA after long-term exposure [89].

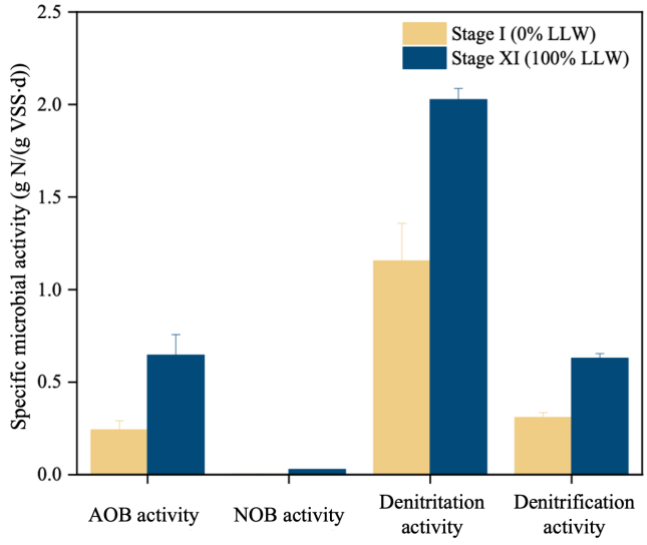

Figure 9.5 Microbial activity tests: oxidation of NH_4^+-N to NO_2^--N with autotrophic ammonia oxidizing bacteria (AAOB); oxidation of NO_2^--N to NO_3^--N with nitrite oxidizing bacteria (NOB); denitritation (NO_2^--N reduction) and denitrification (NO_3^--N reduction) in the seed sludge at Stage I and in the sludge at 100% LLW at Stage XI (error bars represent the standard deviation).

Figure 9.5 shows the denitritation and denitrification activities (NO_2^--N and NO_3^--N reduction rates, respectively) in the seed sludge and the 100% LLW sludge. NO_3^--N reduction rates in the seed sludge and the 100% LLW sludge were 0.31 ± 0.03 and 0.63 ± 0.02 g N/(g VSS·d), respectively. A significantly higher ($p<0.05$) NO_3^--N reduction rate was observed in the 100% LLW sludge compared to the seed sludge. NO_2^--N N reduction rates in 100% LLW sludge (2.03 ± 0.06 g N/(g VSS·d)) was significantly higher than the NO_2^--N reduction rate in the seed sludge (1.15 ± 0.20 g N/(g VSS·d)). Higher NO_2^--N reduction rates were obtained in this study compared to previous granular sludge based studies, which ranged between 0.25 and 1.27 g N/(g VSS·d) [244, 247]. NO_2^--N reduction rates were about 3-fold higher than NO_3^--N reduction rates. A similar study reported NO_2^--N reduction rates over 1.5 times higher than the NO_3^--N reduction rate [93].

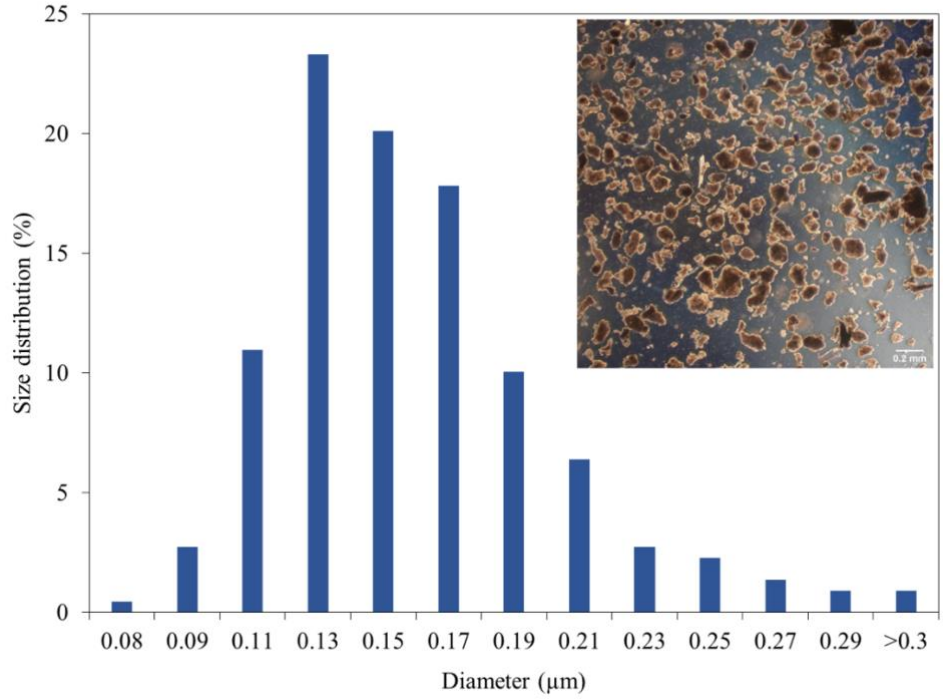

Figure 9.6 The granule size distribution and the structure of granular sludge with 100% landfill leachate loading.

9.3.6 Alpha diversity in the microbial community

Table 9.3 presents the microbial diversity indexes in the seed sludge and in the sludge at 50% and 100% LLW. Chao1 and ACE values refer to the richness of the microbial community, and Shannon and Simpson indexes represent the diversity of the microbial community. As the landfill leachate wastewater (LLW) loading increased to 50%, Chao1, ACE, and Shannon and Simpson values dropped, possibly due to inhibitory effects of compounds in the landfill leachate on the growth of microorganisms. Similar observations have been reported [281]. Although still smaller than those in the seed sludge, the values of all four parameters were slightly higher when 100% LLW was supplied to the reactor, possibly due to a gradual microbe acclimatization to the LLW.

Table 9.3 Microbial diversity indexes in the granular sludge reactor (GSR).

LLW%	Chao1	ACE	Shannon index	Simpson index
Seed	158.6	158.3	2.7	0.9
50% LLW	70.0	70.0	1.6	0.6
100% LLW	93.0	93.0	2.4	0.8

9.3.7 Microbial community dynamics and analysis

9.3.7.1 Microbial community dynamics at the phylum level with increased landfill leachate loading

In the seed sludge the dominant phyla (> 1%) were Proteobacteria (74.8%), Bacteroidetes (17.3%), Actinobacteria (2.1%), [Thermi] (1.8%) and Synergistetes (1.1%) (Figure 9.7a). In the sludge at 50% and 100% LLW, the phyla presented the following order of dominance: Proteobacteria, Bacteroidetes, [Thermi], Actinobacteria. An increase in relative abundances of Proteobacteria and [Thermi], and a reduction in relative abundances of Bacteroidetes and Synergistetes were observed in 50% and 100% LLW sludge. Proteobacteria, which includes species with nitrogen fixation capability [282], were predominant, with relative abundances of 90.3% in 50% LLW sludge and 84.4% in 100% LLW sludge. The relative abundance of Proteobacteria was slightly higher in 50% LLW sludge than in 100% LLW sludge, possibly due to a reduction in other dominant phyla in 50% LLW sludge, suggesting Proteobacteria potentially more tolerant to the environmental fluctuation and toxic compounds. Yan, Wang, Liu, Liu, Pu, Lin, … and Undefined [283] indicated that Proteobacteria and Actinobacteria contain the most metal resistant bacteria. A dominance of Proteobacteria in the microbial community has been reported in previous studies of landfill leachate treatment [282, 284]. Bacteroidetes accounted for 6.0% and 7.9%, respectively, of the microbial communities in 50% and 100% LLW sludge, and [Thermi] accounted for 1.6% and 2.6%, respectively, of the microbial communities in 50% and 100% LLW sludge. Actinobacteria had a relative abundance of 1.2% and 2.2% in 50% and 100% LLW sludge, respectively; and the relative abundance of Synergistetes was undetectable. Since the phylum Synergistetes is commonly found in wastewater treated with an up flow anaerobic sludge blanket (UASB) or in anaerobically treated wastewater effluent, it is reasonable that Synergistetes was detected in the seed originated from a reactor for anaerobic digestion effluent treatment, then disappeared during LLW treatment. Phylum level evolution similar to that described here has been observed during other leachate treatments [285].

9.3.7.2 Microbial dynamics at genus level with increased landfill leachate loading

Figure 9.7b shows the relative abundances (> 0.1%) of microorganisms at the genus level in the seed sludge, the 50% LLW sludge, and the 100% LLW sludge. Genera in the Pseudomonadaceae family, the Xanthomonadaceae family, and the Phyllobacteriaceae family, and the genera

Paracoccus, *Nitrosomonas*, and *Thauera* were dominant (> 1%) in the three sludge samples. Denitrifying microbes in the Pseudomonadaceae family have previously been shown to be involved in denitrification [286]. The relative abundance of microbes in the Pseudomonadaceae family indicated that a high denitrifying potential was achieved in the GSR. Members of the Xanthomonadaceae family and the *Paracoccus* genus have been reported to have the potential to conduct autotrophic Fe^{2+} oxidation/denitrification when the *nirS* gene abundance is higher than the *nirK* gene abundance [286, 287]. The relative abundance of the Xanthomonadaceae family decreased to 6.2% at 50% LLW, but was enriched to 11.9% at 100% LLW, similar to the level (12.3%) of the Xanthomonadaceae family in the seed sludge. The relative abundance of the *Paracoccus* genus decreased from 6.0% to 2.4% when leachate was introduced into the system. The existence of the Xanthomonadaceae family and the *Paracoccus* combined with the ICP results (Table 9.2), which showed a considerable amount of Fe in the landfill leachate, suggesting a potential of autotrophic Fe^{2+} oxidizing denitrification in the GSR. *Nitrosomonas*, a typical ammonia oxidizing bacterium, was relatively lower in abundance in 50% LLW sludge than in the seed sludge and in 100% LLW sludge. Possibly *Nitrosomonas* is sensitive to LLW, but became acclimatized by the time the LLW reached 100%. The lower relative abundance of *Nitrosomonas* in 50% LLW sludge did not impact ammonia removal performance. The microbial genera associated with nitrite oxidation was less than 0.1%, and therefore these organisms are not shown in Figure 9.7b. The negligible nitrite oxidation rate can be explained by the limited relative abundance of NOB, indicating a successful NOB suppression in the GSR. The genus *Thauera*, commonly found in Nit/DNit reactors [251, 280], is reported to be responsible for the high removal rate of N and organics at anoxic or low dissolved oxygen (DO) conditions [73, 234]. The relative abundance of *Thauera* enriched from 14.5% in the seed sludge to 22.5% in 100% LLW sludge, enhancing the removal of N and the reduction of organics in the GSR. Quantitative analysis of functional bacteria could be incorporated in future research to better understand the microbial community dynamics.

9.3.7.3 Microbial genera related to metal reduction

Biomineralization, in which living organisms produce minerals, is a potential pathway for metal precipitation [288]. For example, *Flavobacterium* are capable of precipitating calcium as calcite [269]. A relative abundance of *Flavobacterium* was detected only in 100% LLW sludge samples.

The relative abundance of *Leucobacter* increased gradually as the LLW percentage increased. *Leucobacter* was resistant to Cr (VI) and has been reported to reduce Cr (VI) to Cr (III) [289, 290]. Of note, the formation of insoluble Cr (III) could be absorbed by the negatively charged microbial cell [290], contributing to the slightly lower Cr concentration in the granular sludge reactor (GSR) effluent.

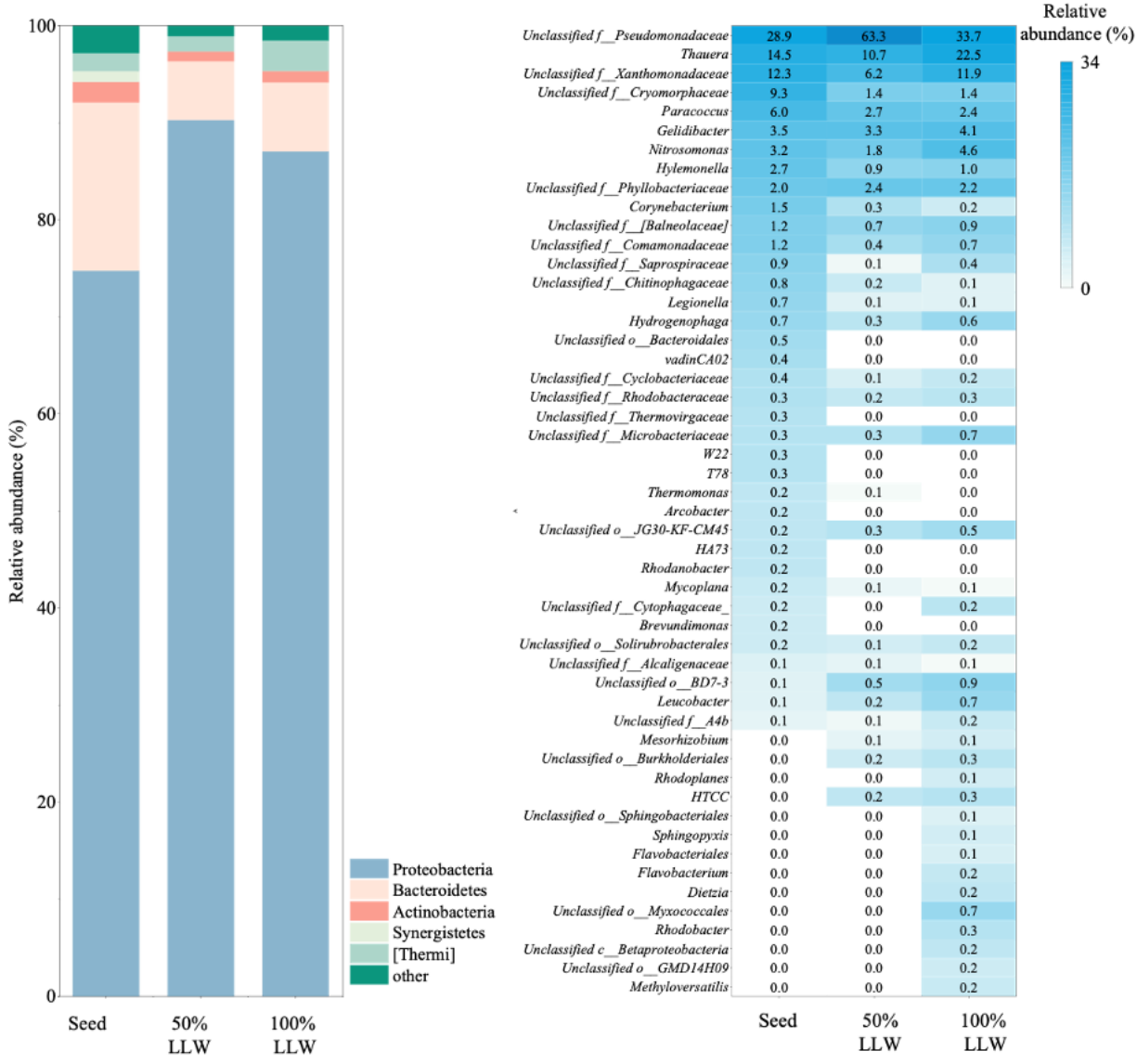

Figure 9.7 Relative abundances in the microbial community at (a) phylum (> 1%) and (b) up to genus (> 0.1%) levels. Unidentified genera are shown at family (Unclassified f_), order (Unclassified o_), or class (Unclassified c_) levels.

9.3.8 Functional gene prediction

To illustrate the evolution of N conversion and heavy metal related functional gene abundance during the feasibility test of landfill leachate treatment, PICRUSt2 was adopted to conduct the prediction analysis based on the KEGG database.

The relative abundance of functional genes associated with nitrification and denitrification are shown in Figure 9.8a. The relative abundance of functional genes in 50% LLW sludge was consistently lower than the relative abundance of functional genes in seed sludge and 100% LLW sludge, possibly this difference is due to microorganisms were acclimating to the landfill leachate. There are two functional genes involved in ammonia oxidation to nitrite, which are *amo* and *hao* genes, responsible for the ammonia oxidation to the hydroxylamine and the hydroxylamine oxidation to nitrite, respectively. The higher relative abundances of the *amo* and *hao* genes in 100% LLW sludge compared to seed sludge suggests an enhanced ammonia oxidation capacity in LLW sludge; this is consistent with the microbial results at the genus level and the enhanced AAOB activity test results. Both *nirS* and *nirK* were involved in nitrite reduction. As predicted, the *nirS* abundance prevailed over the *nirK* abundance; this observation supports the potential of autotrophic Fe^{2+} oxidation and denitrification during the LLW treatment (as mentioned in 8.3.7.1). As shown in Figure 9.8a, *nirS* and *nirK* genes were more abundant in 100% LLW sludge compared with the seed sludge. Compared to seed sludge, 100% LLW sludge showed similar or reduced relative abundances of nitrate reductases (reduce NO_3^- to NO_2^-), nitric oxide reductases (reduce NO to N_2O), and nitrous oxide reductases (reduce N_2O to N_2). The presence of *Nap* genes suggests some aerobic denitrification in the reactor [291] The depletion of nitric oxide and nitrous oxide reductases indicates a potential for NO and N_2O production [292] Further research is needed to address this point.

Genes associated with metal resistance or metal (Ni, Cr, Mg, Co, Zn, Hg, Cu, As) transport are abundant in Figure 9.8b. As the percentage of LLW increased, the abundance of genes that provide resistance to chromate, copper, arsenate, and heavy metals increased. The chromate related functional gene (*chrA*) increased at a higher percentage of LLW, as did the relative abundance of Leucobacter. An increase in heavy metal resistance genes is crucial for the survival of microbes in landfill leachate, which is contaminated with heavy metals [283]. The increase in heavy metal

resistance genes can partially account for the short acclimatization phase and the successful nitrogen removal in this study. This is the first study that has looked into the regulation of heavy metal related genes in landfill leachate treatment.

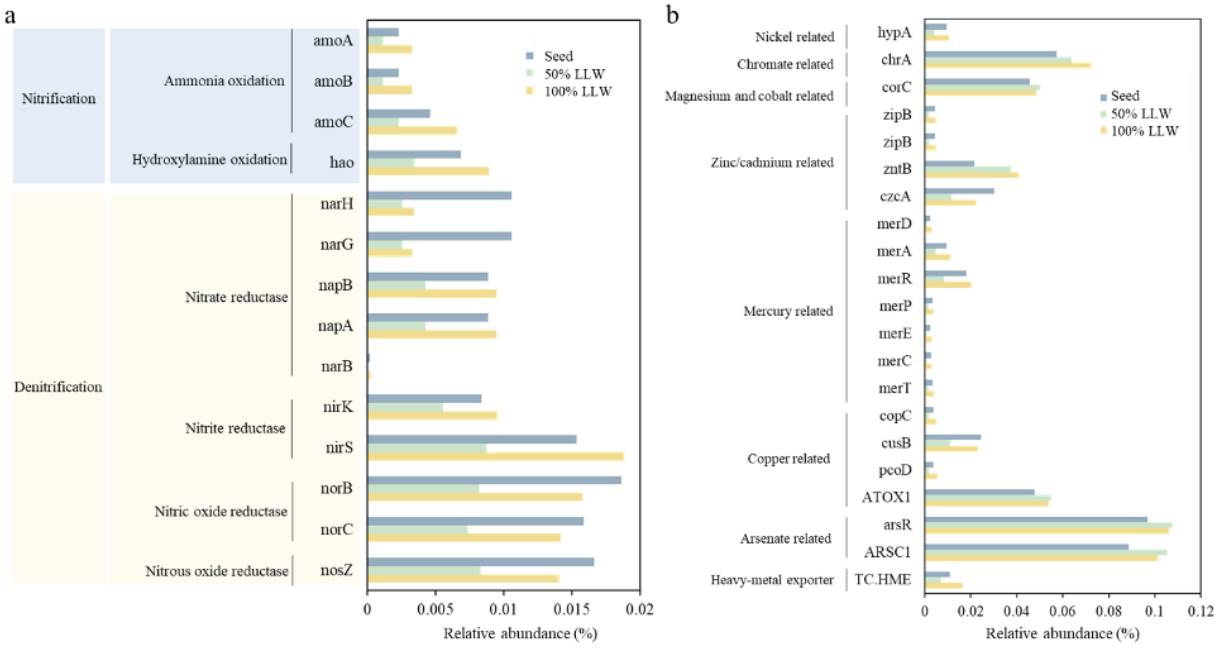

Figure 9.8 Predictions according to PICRUSt2 analysis of functional genes in the microbial community: (a) functional genes related to nitrogen removal by nitrification and denitrification; (b) functional genes related to heavy metal resistance and transport.

9.3.9 Prediction of metabolic annotations

Metabolic functional groups under heavy metal stress in microbial communities involved in carbon and nitrogen cycles were identified using FAPROTAX 1.1 (Figure 9.9). Approximately 32.2% operational taxonomic units (OTUs) were assigned to at least one group in the FAPROTAX analysis. The breadth of ecological functions involved in carbon and nitrogen cycles is shown in Figure 9.9. The relative abundance of the functions indicated in Figure 9.9 was mostly lower in 50% LLW sludge than in seed sludge, but recovered to the highest level in 100% LLW sludge. Chemoheterotroph (organisms that obtain energy from organic chemical substances) and aerobic chemoheterotroph were the major functionaries in the carbon cycle, and had the highest relative abundance in 100% LLW. Thus, biodegradation of carbon from LLW occurred in the granular sludge-based reactor (GSR) via Nit/DNit and external supplementation. Denitrification, nitrogen respiration, nitrate respiration, and nitrite respiration were enhanced at 50% LLW and 100% LLW,

indicating that nitrogen related functions were restored in the LLW treatment. The PICRUSt2 results indicate that increased denitrification was caused by an increase in the relative abundance of nitrite reductases encoded by *nirS* and *nirK* genes. The enhanced nitrification and aerobic ammonia oxidation functions at 100% LLW were in line with the dynamics of relative abundance of *Nitrosomonas*, indicating a capacity for ammonia oxidation in a GSR treating raw LLW. Although aerobic nitrite oxidation increased slightly in the last stage of LLW treatment (100% LLW), it was negligible compared to other functions according to the FAPROTAX analysis. This observation was consistent with the NOB activity test results, which showed a slightly higher NO_3^--N production rate in the 100% LLW sludge.

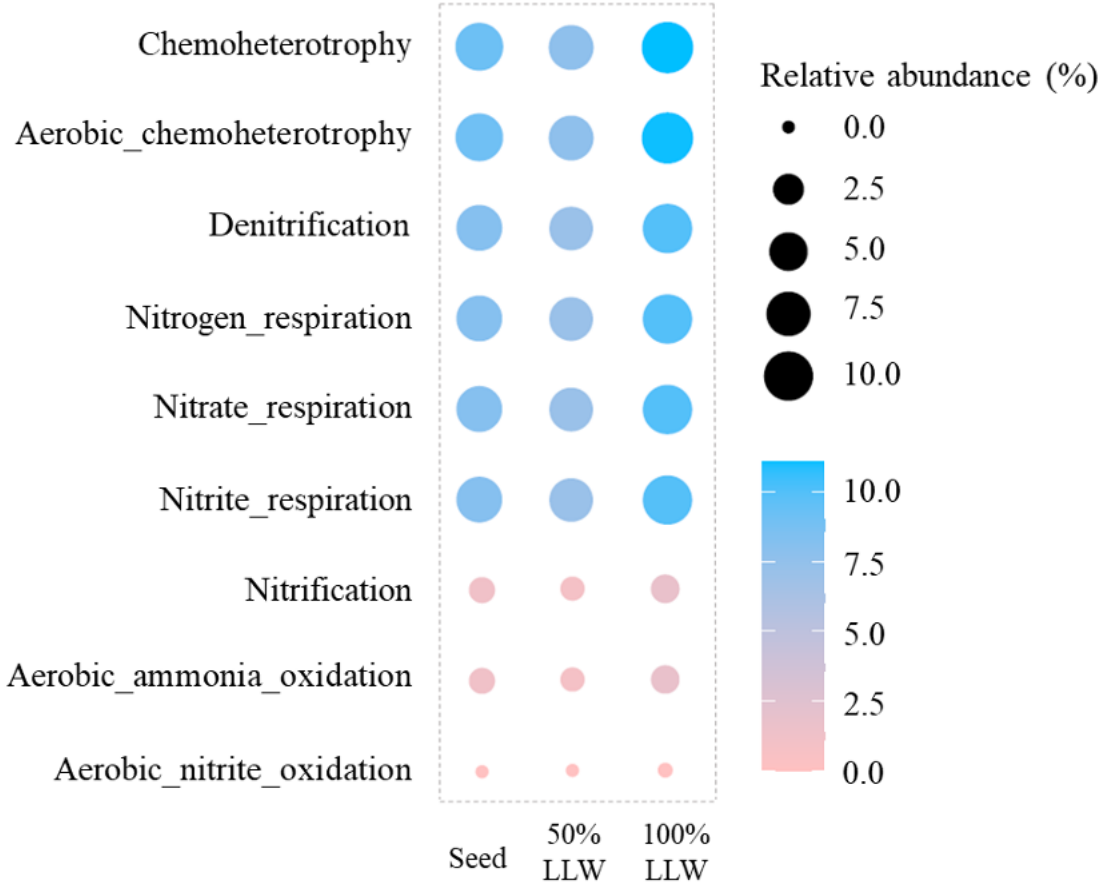

Figure 9.9 Metabolic annotations associated with carbon and nitrogen conversions in seed sludge, 50% landfill leachate wastewater (LLW) sludge, and 100% LLW sludge were predicted by FAPROTAX (Functional Annotation of Prokaryotic Taxa).

9.4 Conclusion

This chapter used the granular sludge reactor (GSR) to treat landfill leachate wastewater via nitritation/denitritation (Nit/DNit) at 20 °C. The microbial community dynamics, the functional genes associated with the N cycle, the prediction of heavy metal related resistance genes, and changes in the ecological functions were studied with increasing loading of landfill leachate. A short startup time (1 month) was needed to achieve stable ammonia and total inorganic nitrogen (TIN) removal efficiencies at 99% and 93%, respectively, with 100% raw landfill leachate feed. High MLVSS and MLSS concentrations were observed with the biomass development and the accumulation of metal precipitates. Small granules were formed in the GSR with high ammonia oxidation rate of 0.64 ± 0.11 g N/(g VSS·d), whereas the nitrite oxidation rate was negligible throughout reactor operation. The gradually acclimatized granular sludge microbes showed increased heavy metal resistance gene abundance as the LLW loading increased, ensuring the stable nitrogen removal efficiencies. The granular sludge in this chapter is featured by high microbial activities, treatment efficiencies, stability, settleability and heavy metal resistance genes abundance, which represents a feasible landfill leachate biological treatment process.

Chapter 10. Newly Developed Granular Sludge Reactor (GSR) for Enhanced Biological Dissolved Organic Nitrogen Removal in Landfill Leachate Wastewater: The Role of Sodium Acetate Co-Metabolism[7]

10.1 Introduction

Chapter 9 has examined the effectiveness of the newly developed GSR for treating landfill leachate wastewater (LLW), achieving high ammonia and TIN removal. Inorganic N and dissolved organic N (DON) are the two components of total dissolved N (TDN) in LLW. While extensive studies have focused on the removal of inorganic N in LLW [88, 258, 265], there is a notable gap in research on the removal of DON. DON is prevalently found in the environment and recent studies have highlighted its potential to stimulate algal growth and contribute to the formation of toxic disinfection by-products [1]. With increasingly stringent N discharge limits being imposed, there is a pressing need for effective strategies to remove organic N.

The major components of DON in wastewater are urea, amino acids, nucleic acids, humic acids and fulvic acids. Humic and fulvic acids are commonly considered as recalcitrant portion of DON, while other fractions are most likely labile [14, 15]. Most research on landfill leachate primarily concentrates on dissolved organic matter (DOM), covering its characterization, transformation, and removal through a combination of physicochemical and biological methods. These methods often include coagulation, nanofiltration, advanced oxidation, and adsorption [4, 29, 30]. Although dissolved organic nitrogen (DON) is recognized as one of the most problematic constituents in the discharge of leachate into wastewater treatment plants due to its recalcitrate nature, successful strategies for DON removal remain scarce. To date, reported approaches for DON removal rely on membrane filtration (i.e., ultrafiltration, and nanofiltration) [4], which can impose substantial operational and maintenance costs as well as significant energy requirements.

[7] A version of this chapter has been published: Zou, X., Zhang, Y., Gao, M., Yao, Y., Guo, H., & Liu, Y. (2024). Enhancing biological dissolved organic nitrogen removal in landfill leachate wastewater: The role of sodium acetate co-metabolism. *Chemical Engineering Journal*, *479*, 147714. https://doi.org/10.1016/j.cej.2023.147714

Co-metabolism is a biological approach utilized in degrading recalcitrant compounds when an easily biodegradable substrate is present. This differs from co-substrate, which refers to the addition of a substrate to complement the limited component in another substrate [293]. The underlying mechanism of co-metabolism is based on the consumption of easily biodegradable substrate, which induces the secretion of specific enzymes, aiding the degradation of recalcitrant compounds [294, 295]. It has been reported that N-containing organics can be degraded through hydrolysis and fermentation (decarboxylation and deamination) by extracellular enzymes. Major extracellular enzymes that involved in hydrolysis process are nuclease, urease, lysozyme, chitinase and protease, which are mainly targeting the degradation of nucleic acid, proteins and cell wall components [296]. The resulting N-containing organics from hydrolysis can be converted to ammonia or other organic acids by decarboxylase and deaminase [297]. In conventional biological nutrient removal (BNR) A^2O systems, the anaerobic zone has been identified as the primary contributor to DON removal, a process that generally involves hydrolysis and fermentation [2, 3]. However, an increase in DON concentration ranging from 5-20% has been observed in the aerobic zone of BNR systems [2, 3, 15].

Despite the numerous studies on DON transformations and removal in water, wastewater, and landfill leachate mainly via physicochemical approach [15, 298, 299], no effective biological strategy for DON degradation has been documented. This chapter explores the influence of readily biodegradable COD addition, specifically sodium acetate, on DON removal from LLW within the newly developed GSR. The primary aim of this chapter is to formulate an effective strategy for DON removal, to understand the molecular composition of DON, and to unravel the underlying mechanisms driving DON removal in the treatment of LLW. A thorough understanding of DON removal mechanisms from mature LLW could pave the way for strategies in larger-scale applications.

10.2 Materials and methods

10.2.1 Reactor operation

Mature landfill leachate wastewater (LLW) was treated in a 4 L cylindrical reactor (diameter: 9 cm, height: 63 cm) and operated with 50% exchange ratio. Sludge from a lab-scale landfill

leachate treatment GSR served as the reactor inoculum [88]. The raw LLW was collected regularly from a local landfill leachate storage facility and stored at 4 ^{o}C prior to the bioreactor treatment. The mature LLW contains NH_4^+-N at 322 ± 56 mg/L, NO_2^--N at 9 ± 3 mg/L, NO_3^--N at 0.7 ± 0.05 mg/L, dissolved Total Kjeldahl Nitrogen (DTKN) at 394 ± 68 mg/L, dissolved organic nitrogen (DON) at 75 ± 15 mg/L and COD at 1088 ± 100 mg/L. The reactor was operated with 10 min feeding, 60 min aerobic, 75 min anoxic, 10 min post-aerobic, 10 min settling, 10 min discharging and 5 min idling. During aerobic phase, 1.4 cm/s superficial air upflow velocity was provided through a fine bubble air diffuser at the bottom of the reactor. During anoxic phase, the aeration was stopped, and recirculation was provided for mixing, and external COD was pulse supplied in Stage I while no COD was supplied in Stage II. A concentrated sodium acetate solution with a COD at ~40 g/L was introduced via pulse injection to facilitate denitrification process. The external COD addition provided a C/N ratio at 2.5 for denitrification. The hydraulic retention time (HRT) was 6 hrs throughout the 134 days of operation.

10.2.2 Fourier-transform ion cyclotron resonance-mass spectrometry (FTICR-MS) analysis

Dissolved organic nitrogen (DON) was extracted from raw landfill leachate and GSR treated effluent samples in both stages following the protocol reported by Dittmar, Koch, Hertkorn and Kattner [300]. The sample with a volume of 50 mL was collected, filtered through 0.45µm filters and acidified to pH 2 prior to passing through the HLB tube (MilliporeSigma, USA). Briefly, the cartridges were pre-activated with one cartridge (12 mL) of methanol, then acidified samples were passed through the cartridge. Before elution, the cartridges were rinsed with 2 cartridge volumes (24 mL) of 0.01 M HCl to remove salts and dried with air. Dissolved organic matters were then eluted with 12 mL methanol and stored at -20 ^{o}C until proceeding the analysis on Bruker 9.4 T Apex-Qe FT-ICR (Bruker Daltonics, Billerica, MA, USA, 2007).

Raw data were processed using DataAnalysis software v.3.4. Categories of DON and corresponding zones based on elemental ratios have shown variations in prior studies, as summarized by Li, Li, Zhang, Chen, McKenna, Chen and Tang [301]. In this study, the DON formulae were delineated into 7 categories based on elemental ratios (O/C and H/C): i) lipid (H/C = 1.5-2.0, O/C = 0-0.3), ii) protein/amino sugar (H/C = 1.5-2.2, O/C = 0.3-0.67), iii) carbohydrates

(H/C = 1.5-2.2, O/C = 0.67-1.2), iv) unsaturated hydrocarbons (H/C = 0.7-1.5, O/C = 0-0.1), v) lignin and carboxylic rich alicyclic molecules (CRAM) (H/C = 0.7-1.5, O/C = 0.1-0.67), vi) tannins (H/C = 0.5-1.5, O/C = 0.67-1.2), and vii) condensed aromatics (H/C = 0.2-0.7, O/C = 0-0.67) [302, 303].

10.2.3 Microbial community analysis

At the end of each stage, duplicate biomass samples were collected from the GSR during aeration phase, centrifuged immediately at 4000 rpm for 5 min, and extracted the DNA from pellet using DNeasy PowerSoil® DNA Isolation Kits (QIAGEN, Hilden, Germany) following the protocol. DNA quality was checked with NanoDrop™ One (ThermoFisher Waltham, MA) and stored at -20 °C before future analysis. DNA samples were amplified using the universal primer pair 515 F (GTGCCAGCMGCCGCGG) and 806 R (GGACTACHVGGGTWTCTAAT), then sequenced on the Illumina Miseq PE250 platform at Genome Quebec (Montréal, QC, Canada). Sequencing data was processed using the DADA2 algorithm in QIIME2 pipeline [77, 221]. Taxonomy was assigned with 99% similarity using the GreenGenes database (version 13_8) [79]. The prediction of functional genes for nitrogen and organics metabolism was carried out through the Phylogenetic Investigation of Communities by Reconstruction of Unobserved States 2 (PICRUSt2) pipeline and the Kyoto Encyclopedia of Genes and Genomes (KEGG) database [80].

10.2.4 Statistical analysis

Significance of the results was evaluated using T-test in Microsoft® Excel® software (version 2109). Significant difference was determined when P-value was less than 0.05.

10.3 Results and discussion

10.3.1 Reactor performance

Inorganic and dissolved organic N concentrations and their removal efficiencies are shown in Figure 10.1. The variations in ammonia, DTKN and COD concentrations observed in Figure 10.1 could be attributed to seasonal and environmental factors such as rainfall, which influence the quality of landfill leachate. Figure 10.1a shows that with influent NH_4^+-N concentrations 322 ± 56 mg/L, only trace amounts of NH_4^+-N remained in the GSR effluent, and the ammonia removal

efficiencies were consistently observed at > 99% in both stages (Figure 10.1b). Low effluent NO_2^--N (< 18 mg/L) and NO_3^--N (< 2 mg/L) concentrations were noticed in Stage I when sodium acetate was provided to facilitate TIN removal, and under which 94% TIN removal was achieved, as shown in Figure 10.1b. In Stage II, without sodium acetate addition, effluent NO_2^--N and NO_3^--N were gradually accumulated, and the TIN removal efficiencies reduced substantially to ~10% and maintained at this level for the remaining operation days.

Figure 10.1c illustrates that DON was removed in Stage I and generated in Stage II. The influent DON level was 75 ± 15 mg/L. Effluent DON in Stage I was ~35 mg/L, which represents ~45% removal. In contrast, the DON concentration increased after GSR treatment in Stage II when sodium acetate addition was not conducted. After the treatment, an average DON increment of 22% was observed in the effluent, which can be attributed to the breakdown of particulate organic compounds and the microorganism-derived compounds from microbial metabolism, similar to other reported studies [32, 304].

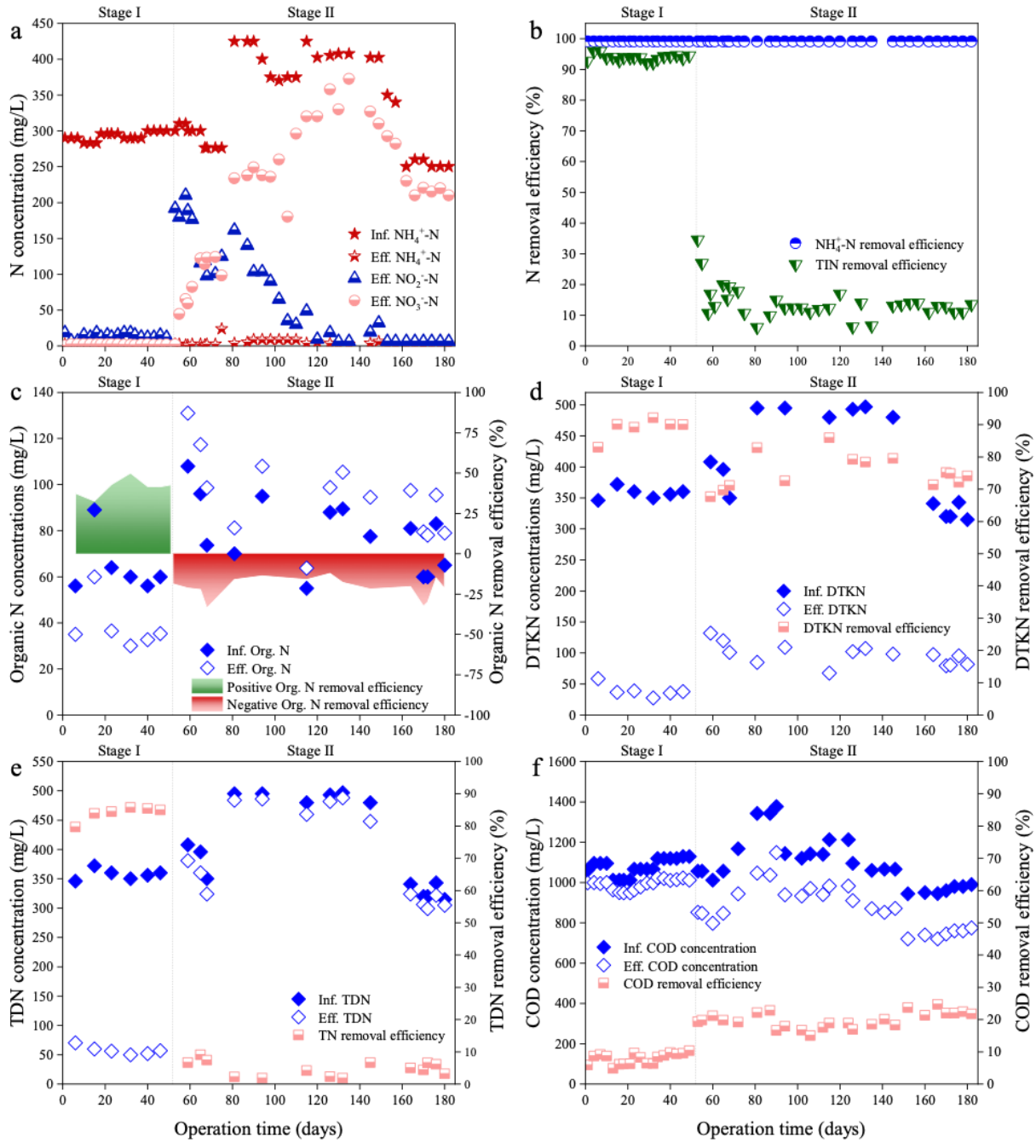

Figure 10.1 Granular sludge reactor (GSR) performance for landfill leachate wastewater treatment with (Stage I) or without (Stage II) COD supplementation: a) Influent NH_4^+-N, and effluent NH_4^+-N, NO_2^--N and NO_3^--N concentrations; b) NH_4^+-N removal efficiencies and total inorganic nitrogen (TIN) removal efficiencies; c) Influent and effluent dissolved organic nitrogen (DON) concentrations and DON removal efficiencies; d) influent and effluent dissolved Total Kjeldahl Nitrogen (DTKN) concentrations and DTKN removal efficiencies; e) influent and effluent total dissolved nitrogen (TDN) and TDN removal efficiencies; and f) influent and effluent COD concentrations and COD removal efficiencies.

As depicted in Figure 10.1d, with influent DTKN levels at 394 ± 68 mg/L, DTKN removal efficiencies were notably lower in Stage II compared to Stage I. This decrease can be primarily attributed to the substantial amount of DON that remained untreated in Stage II. Over 85% TDN removal was observed in Stage I (Figure 10.1e), while less than 10% removal was seen in Stage II without the addition of sodium acetate. Figure 10.2 shows the dissolved nitrogen mass balance before and after treatment in both stages. In each stage, ammonia constituted roughly 80% of the total dissolved nitrogen (TDN) in raw leachate, while DON comprised about 19%. The remaining percentages were attributed to nitrite and nitrate. In Stage I's effluent, DON was the predominant component of TDN (approximately 50 mg/L) making up 68%, followed by nitrite at 21%. In contrast, the effluent in Stage II was composed of 35% nitrite, 36% nitrate and 29% DON.

Further, as shown in Figure 10.1f, LLW COD removal, when comparing influent to effluent, was under 10% in Stage I, with a slightly higher removal observed in Stage II at around 20%. The limited COD removal can be attributed to the nature of mature landfill leachate, which contains minimal amount of biodegradable COD. The higher effluent COD in Stage I may be due to the leftover externally added COD after treatment, compared to Stage II.

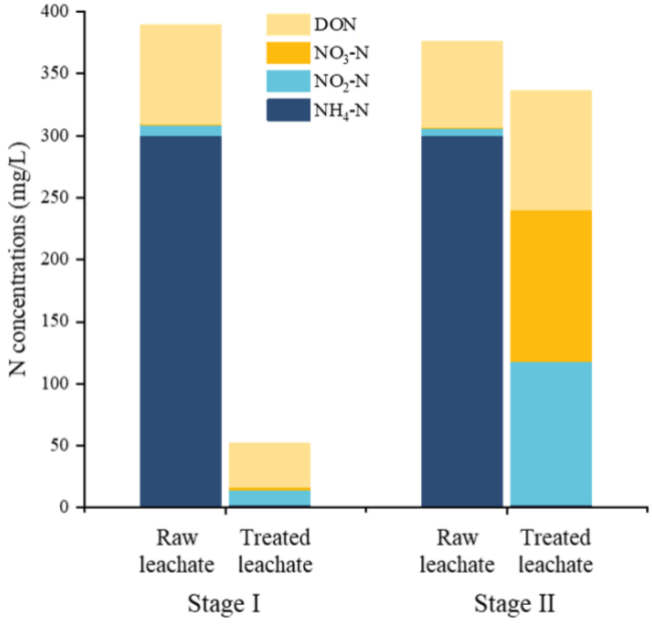

Figure 10.2 Nitrogen speciation and mass balance of raw and treated leachate samples in Stage I and Stage II.

10.3.2 Sludge properties

As indicated in Figure 10.3, the biomass concentration in Stage I was markedly high, with the Mixed Liquor Volatile Suspended Solids (MLVSS) stabilized between 20-25 g/L. In Stage II, the MLVSS gradually reduced, stabilizing at 13 g/L. The decrease in biomass concentration was likely due to the washout of heterotrophic bacteria and cell death, which can be attributed to the limited biodegradable COD available to support the growth of these bacteria.

In Figure 10.3, the SVI_{30} in Stage I was low, maintained at 5 mL/g. However, as the operation condition switched to Stage II, both the SVI_5 and SVI_{30} gradually increased to respective values of 30 and 20 mL/g. The reduced sludge settling capacity may be attributed to the reduced abundance of heterotrophic bacteria without COD addition. These bacteria play a key role as the primary producers of extracellular polymeric substances (EPS), which are crucial for the formation of granular sludge.

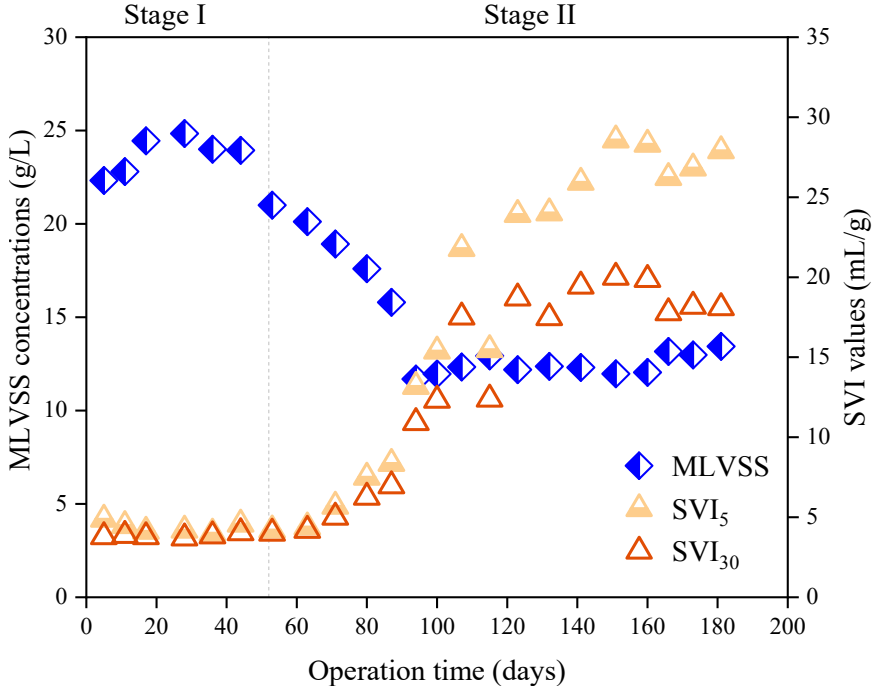

Figure 10.3 Sludge properties under different operation conditions in Stages I and II, including the concentration of mixed liquor volatile suspended solids (MLVSS) and sludge volume indexes at 5 min and 30 min.

10.3.3 Specific microbial activity --- inorganic nitrogen removal

The AAOB activity (Figure 10.4) was higher in Stage II, registering at 0.68 g N/(g VSS·d), compared to 0.64 g N/(g VSS·d) in Stage I. The AAOB activities obtained in this study were higher than previously reported studies, ranging from 0.14−0.64 g N/(g VSS·d) [88, 305-307]. Compared the NOB activity in Stage I, significant ($p<0.05$) increment was observed in Stage II, which could be attributed to the high residual nitrite in the bioreactor system when COD was not supplied. In Stage I, NOB activity was inhibited, likely due to free ammonia inhibition (FA>1 mg/L) and lack of nitrite. However, NOB has been reported to be resistant to free ammonia (FA) if it was exposed at the FA inhibition level for a long period [89, 246, 308]. On the other hand, as shown in Figure 10.4, the activities of denitritation and denitrification were significantly lower ($p<0.05$) in Stage II compared to Stage I, which might be due to the lack of organic carbon source to support the growth of heterotrophic denitrifying bacteria.

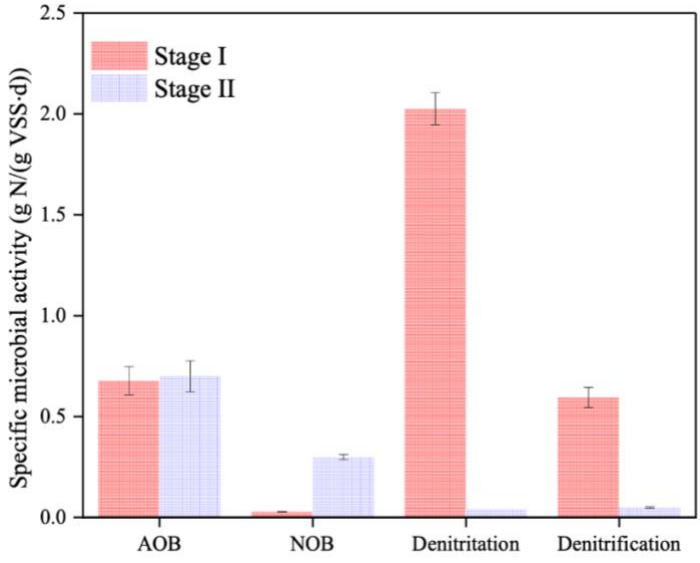

Figure 10.4 Specific microbial activity tests in Stages I and II, including the specific activity of autotrophic ammonia oxidizing bacteria (AAOB), nitrite oxidizing bacteria (NOB), and the activity of denitritation and denitrification.

10.3.4 Cycle tests

Cycle tests were carried out regularly along the bioreactor operation to decipher the impact of sodium acetate addition on N transformation. Figure 10.5 shows the N transformations during a typical cycle in Stage I (on day 50, Figure 10.5a) and Stage II (on day 175, Figure 10.5b).

10.3.4.1 Nitrogen transformation in cycle tests with sodium acetate addition

Figure 10.5a illustrates the N transformation, including NH_4^+-N, NO_2^--N, NO_3^--N and DON, within a typical cycle in Stage I with sodium acetate addition during the anoxic phase. According to Figure 10.5a, over 90% of NH_4^+-N was oxidized to NO_2^--N within an hour aeration. In the meantime, limited NO_3^--N concentration was observed throughout the cycle. During the anoxic phase, 90% TIN removal was achieved with sodium acetate addition at a C/N ratio of 2.5. Dissolved organic N (DON) decreased first and then increased during the aeration phase. During aerobic phase, the reduced DON concentration at the beginning of the phase might be attributed to the removal of biodegradable DON, such as protein and lipid like compounds [15]. Then, the increment in DON concentration was observed, which may be attributed to the hydrolysis of particulate to dissolved organic compounds as well as the production of soluble microbial products (SMPs). Previous studies reported the production of SMPs from the metabolism of nitrifying bacteria and the SMP is a significant source of DON in wastewater [15, 299]. The DON removal rate under the aerobic phase was lower than the ammonia oxidation rate. DON concentration slightly dropped during the anoxic phase from 55 mg/L to 44 mg/L. The DON that was removed during the anoxic phase may have been hydrolyzed to ammonia. However, an increase in ammonia concentration was not observed, which could be attributed to the activity of AAOB utilizing residual oxygen in the system from the previous aerobic phase or the oxygen introduced through recirculation.

10.3.4.2 Nitrogen transformation in cycle tests without sodium acetate addition

Figure 10.5b elucidates the dynamics of NH_4^+-N, NO_2^--N, NO_3^--N and DON in a typical cycle in the absence of sodium acetate. Different from the high NO_2^--N accumulation in Stage I, a large proportion of influent NH_4^+-N (70%) was completely oxidized to NO_3^--N and only a small proportion (30%) was partially oxidized to NO_2^--N. NO_3^--N accumulation indicated the enhanced NOB activity, as a result of the limited competition of NO_2^--N with denitrifiers. NO_3^--N concentration was consistent before and after the anoxic phase due to the lack of denitrification process. Similarly to the DON transformation observed during the aerobic phase in Stage I, DON concentration initially decreased and then increased. However, in contrast to Stage I, DON production was observed during the anoxic phase of Stage II. This DON production likely resulted from hydrolysis reactions and the production of SMPs. Without the addition of sodium acetate in

the anoxic phase, the microbial community was likely under starvation-induced stress, which might have stimulated the production of SMPs, thereby contributing to the increased DON concentration in the system [3].

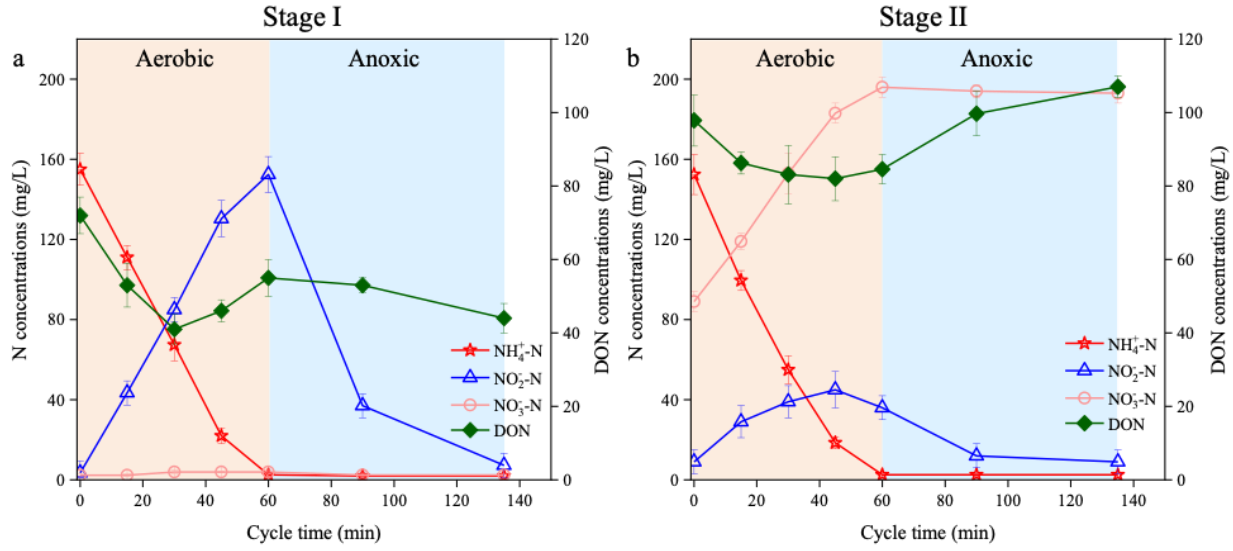

Figure 10.5 Inorganic and dissolved organic N transformation during typical cycle tests in a) Stage I and b) Stage II.

10.3.4.3 COD impact on nitrogen transformation

Under aerobic conditions, comparable reductions in DON were observed in both stages, with a decrease of 31 mg/L in Stage I and 26 mg/L in Stage II. Both stages exhibited similar DON trends under aerobic phase. Under anoxic conditions, however, DON was reduced in Stage I but increased in Stage II. The decrease in DON concentration in Stage I suggests that the addition of easily biodegradable COD in the form of sodium acetate likely induced co-metabolism, which enhances the degradation of recalcitrant organic compounds in the presence of easily biodegradable COD.

10.3.5 Transformation of dissolved organic nitrogen

The categories of DON in typical raw mature landfill leachate wastewater were shown in Figure 10.6a. The divergencies of DON categories in the effluent samples from Stage I and Stage II were depicted in Figure 10.6b and Figure 10.6c. Most identified DON were located in lignin and carboxylic rich alicyclic molecules (CRAM) region, accounting for 67-74% of the DON community, which was consistent with previous studies on mature landfill leachate wastewater

DON characteristics [4, 309]. Considering the recalcitrant nature of lignin and CRAM-type DON, it is likely that these compounds will persist in the treated effluent (Figure 10.6e and Figure 10.6f). As shown in Figure 10.1, the quality of raw leachate varied over time. While this study primarily focused on the DON results of a representative raw mature leachate sample, further studies on the characterization of raw leachate across different seasonal or environmental conditions should be performed.

Upon adding sodium acetate (Stage I), the number of DON formulae decreased slightly from 160 in the influent to 158 in the effluent (Figure 10.6d), with reductions in lipid, protein/amino sugar and unsaturated hydrocarbon-like DON. However, an increase in lignin, CRAM, and condensed aromatic-like DON was observed after GSR treatment. Most sulfur-containing DON (CHONS) were effectively removed with sodium acetate supplementation. As per the Venn diagram in Figure 10.6d, 79 DON formulae were common to both the influent and effluent in Stage I, with the effluent and influent each having 79 and 81 unique DON formulae respectively.

Contrastingly, without the addition of sodium acetate, the number of DON formulae rose from 160 in the influent to 200 in the effluent (Figure 10.6d), where most of the newly formed DON belonged to protein/amino sugar, lignin, CRAM, and condensed aromatics. It is worth noting that sulfur-containing DON were generated in the absence of an easily biodegradable carbon source. These sulfur-containing molecules (CHONS) are believed to originate from microbial metabolism [310] or the hydrolysis of particulates to soluble organics. These newly formed CHONS molecules were primarily found in the protein/amino sugar region, which are generally regarded as labile portions of dissolved organics [311]. Figure 10.6d showed that influent and Stage II effluent shared 74 DON formulae, with the effluent having 126 unique DON formulae and the influent having 86 unique DON formulae.

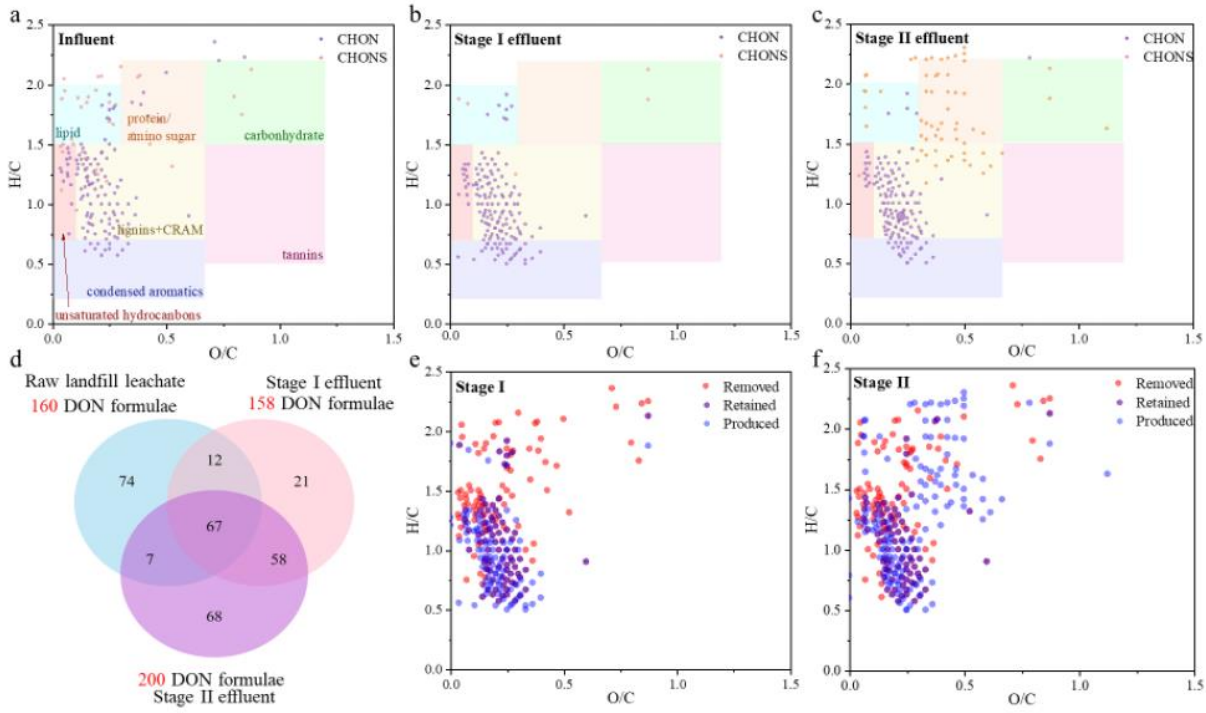

Figure 10.6 Van Krevelen diagrams of categories of identified dissolved organic nitrogen (DON) in a) influent (raw landfill leachate), and effluent samples after b) Stage I (with sodium acetate addition) and c) Stage II (without sodium acetate addition) GSR treatment. The number of shared and unique DON formulae in the influent and treated effluent in Stage I and Stage II were shown in d) Venn diagram. The production, persistence, and removal of DON compounds in e) Stage I and f) Stage II GSR treatment.

Moreover, the effluents from both Stage I and Stage II shared 125 DON formulae, some of which were only identified in the effluent samples. This implies that the degradation of leachate-originated DON by granular sludge might result in certain organic compounds that are particularly difficult for microorganisms to remove. The dynamics of DON compounds in both stages were illustrated in Figure 10.7. Within the raw leachate and treated effluent of both stages, the predominated DON molecular structures were identified as N_1O_2, N_1O_3 and N_1O_4. Together, these three compounds comprised 85% of the treated effluent in Stage I and 68% in Stage II. It is noticeable that most of the molecules in Stage I's influent wastewater containing N_2 and N_4 structures diminished during treatment. Instead, higher relative abundance of N_1O_3, N_1O_4 and N_1O_2 were observed, suggesting potential degradation of long chain molecules into shorter chain molecules. While the effluent from Stage II showed higher relative abundance of S-containing

molecules such as N_2O_7S, N_2O_6S, N_2O_5S, and $N_2O_1S_2$ after GSR treatment without the supplementation of easily biodegradable COD.

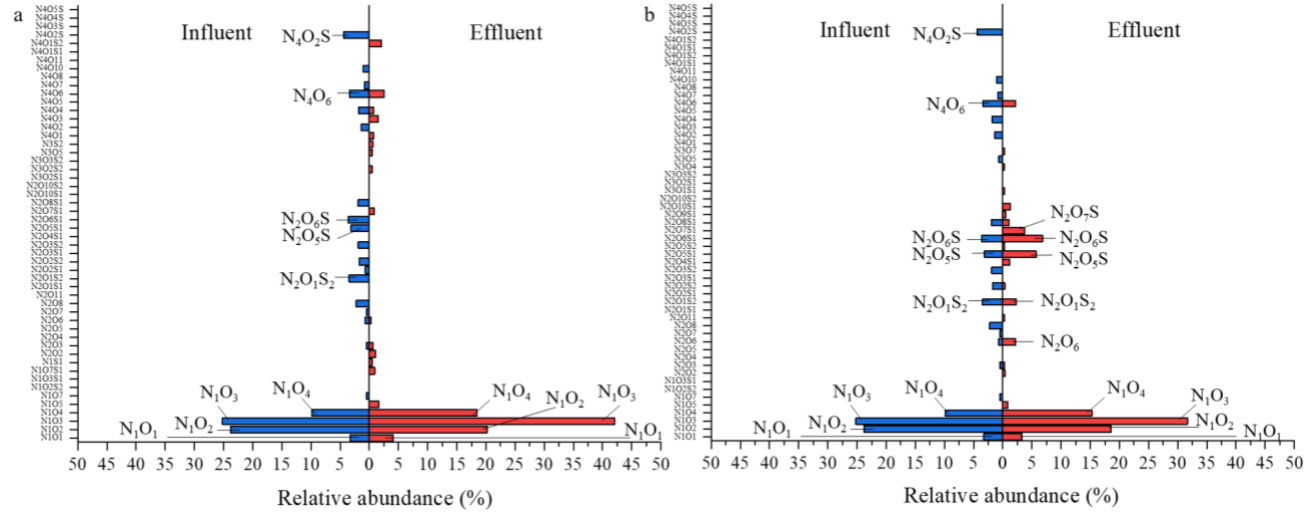

Figure 10.7 Dynamics of DON compounds in relative abundance of the raw leachate and treated effluent in a) Stage I and b) Stage II.

10.3.6 Microbial community dynamics

10.3.6.1 Microbial composition at phylum level

Microbial community composition at the phylum level in Stages I and II were shown in Figure 10.8a. Bacteria in phylum Proteobacteria was predominant in both stages and accounted for 84.4% in Stage I and 45.2% in Stage II. Bacteroidetes accounted for 7.9% in Stage I and 1.4% in Stage II. The reduction in the relative abundance of Proteobacteria and Bacteroidetes in Stage II might be attributed to the reduced abundance of denitrifiers. As previous study reported that microbes that take part in denitrification were most likely affiliated to phylum Proteobacteria and Bacteroidetes [312, 313]. Actinobacteria accounted for 2.2% in Stage I while increased to 24.2% in Stage II. Actinobacteria has been demonstrated to produce considerable secondary metabolites to help with the degradation of complex organics [314, 315]. Additionally, Actinobacteria also involves in the denitrifying process, which might be able to perform aerobic denitrification [315]. Chloroflexi accounted for 0.8% in Stage I and 13% in Stage II. Previous studies reported that Chloroflexi could uptake complex organic compounds. Its growth possesses the potential for the degradation of complex organics, amino acids and carbohydrate [316-318]. The relative abundances of Thermi and Planctomycetes were also increased from 2.9% in Stage I to 5.9% in

Stage II and 0.2% in Stage I to 6.7% in Stage II. Increased relative abundance of bacteria that belongs to Actinobacteria and Chloroflexi in Stage II, supporting the observation that lower effluent COD was achieved in Stage II.

10.3.6.2 Microbial composition at genus level

Microbial genera involved in nitrogen metabolism

Figure 10.8b depicts the microbial community development in genus level. In this study, nitrogen removal processes mainly consisted of nitritation, nitratation, denitritation and denitrification. Nitritation was mainly carried out by autotrophic ammonia oxidizing bacteria (AAOB), genus *Nitrosomonas*, which accounted for 4.6% in Stage I and 10.3% in Stage II. The relative abundance of *Nitrosomonas* increased from Stage I to II was probably due to the reduced abundance of heterotrophic bacteria in Stage II. The slightly higher specific AAOB activity in Stage II might be attributed to the higher relative abundance of AAOB in collected sludge. Nitratation was conducted by nitrite oxidizing bacteria (NOB), genus *Nitrobacter*, which was accounted for 0.1% in Stage I and 4.0% in Stage II. The limited relative abundance of *Nitrobacter* in Stage I was in agreement with the limited specific NOB activity in Figure 10.4. The relative abundance of *Nitrobacter* increased once COD supplementation was ceased in Stage II and that resulted in the accumulation of nitrite, which serves as the substrate for the growth of NOB. Genus *Thauera* and *Paracoccus* were widely reported denitrifiers that perform denitritation and denitrification processes [148, 319]. These two genera accounted for 22.5 and 11.9% in Stage I, while reduced in Stage II to 0.2 and 0.1%, respectively. The reduction of relative abundances of *Thauera* and *Paracoccus* in Stage II were attributed to the absence of bioavailable COD.

Microbial genera involved in organics removal

According to Figure 10.8b, the relative abundance of bacteria from family Pseudomonadaceae was reduced from 33.7% in Stage I to limited percentage in Stage II. Previous study reported that numerous genera in family Pseudomonadaceae were able to biodegrade organics, and this family was highly present in system with abundant easily biodegradable substrate, such as sodium acetate, therefore the abundance of bacteria from this family was dropped in Stage II [320]. Microbes that affiliated to family Xanthomonadaceae were also responsible for COD and N removal, as well as EPS production [321]; the relative abundance of which slightly reduced from 11.9% in Stage I to

8.5% in Stage II. In Stage II, increased relative abundances of genera that participated in the degradation of organics, humus substances and aromatic hydrocarbons, such as *Mycobacterium*, *Phycisphareae*, and *Rhodococcus* were noticed [322-325]. Current study showed that the growth of microbes that have the function of complex organics degradation was stimulated when easily biodegradable organics was limited.

10.3.6.3 Microbial function prediction

To gain insights into the influence of sodium acetate addition on microbial functions associated with N and organics degradation, the predicted relative abundance of N removal process involved functional genes, including *amoABC*, *hao*, *nxrAB*/*narGH*, *nirKS*, *norBC* and *nosZ* are presented in Figure 10.8c; and organics degradation process involved functional genes, including lysozyme, chitinase, urease, protease, decarboxylase and deaminase are presented in Figure 10.8d.

Nitrogen metabolism

The ammonia and nitrite oxidation related functional genes, including ammonia monooxygenase genes (*amoABC*), hydroxylamine dehydrogenase gene (*hao*) and nitrite oxidoreductase genes (*nxrAB*) are more abundant in Stage II compared to Stage I. Over 3 times higher *nxrAB* genes' relative abundance in Stage II emphasizing the increased activity of NOB under long term exposure to high FA condition. In contrast, the denitrifying process related functional genes, including nitrite oxidoreductase genes (*nirKS*), nitric oxide reductase genes (*norBC*) and nitrous oxide reductase gene (*nosZ*) were more abundant in Stage I. These results match the reactor performance and sequencing results.

Nitrogen-containing organics degradation

The extracellular enzymes found in current study includes urease, lysozyme, chitinase and protease, which are mainly targeting the degradation of proteins and cell wall components [296]. According to Figure 10.8d, the relative abundances of urease (*ureABC*), lysozyme, chitinase were limited compared to that of protease. The protease is a vital functional gene that involved in hydrolysis of protein. It functions in breaking down the peptide bonds, so that protein could be converted to amino acids [326]. The main group of protease found in our predicted functional genes was serine proteases, which has also been documented in other studies [296, 327]. Previous

study reported that the expression of serine proteases was dominated by phylum Proteobacteria [296], which was the predominant phylum in current study. Decarboxylase functions in breaking down the C-C bond, thus the products might be amine and CO_2 [328]. Deaminase functions in breaking down the C-N bond, and the products are mainly NH_3 and organic acids [328]. In both Stage I and Stage II, the protease has the highest relative abundance among those functional genes, followed by decarboxylase and deaminase. Higher relative abundance of decarboxylase compared to deaminase represented that decarboxylation was the dominated pathway for amino acid degradation. The predicted relative abundance of protease in Stage I and Stage II were at the same level, indicating both stages had comparable capacity to perform hydrolysis reaction. The abundance of deaminase was higher in Stage I compared to Stage II, indicating that the microbial community in Stage I had higher capacity to degrade nitrogen containing organics into ammonia. The results are in agreement with the higher DON removal in Stage I in Figure 10.1c.

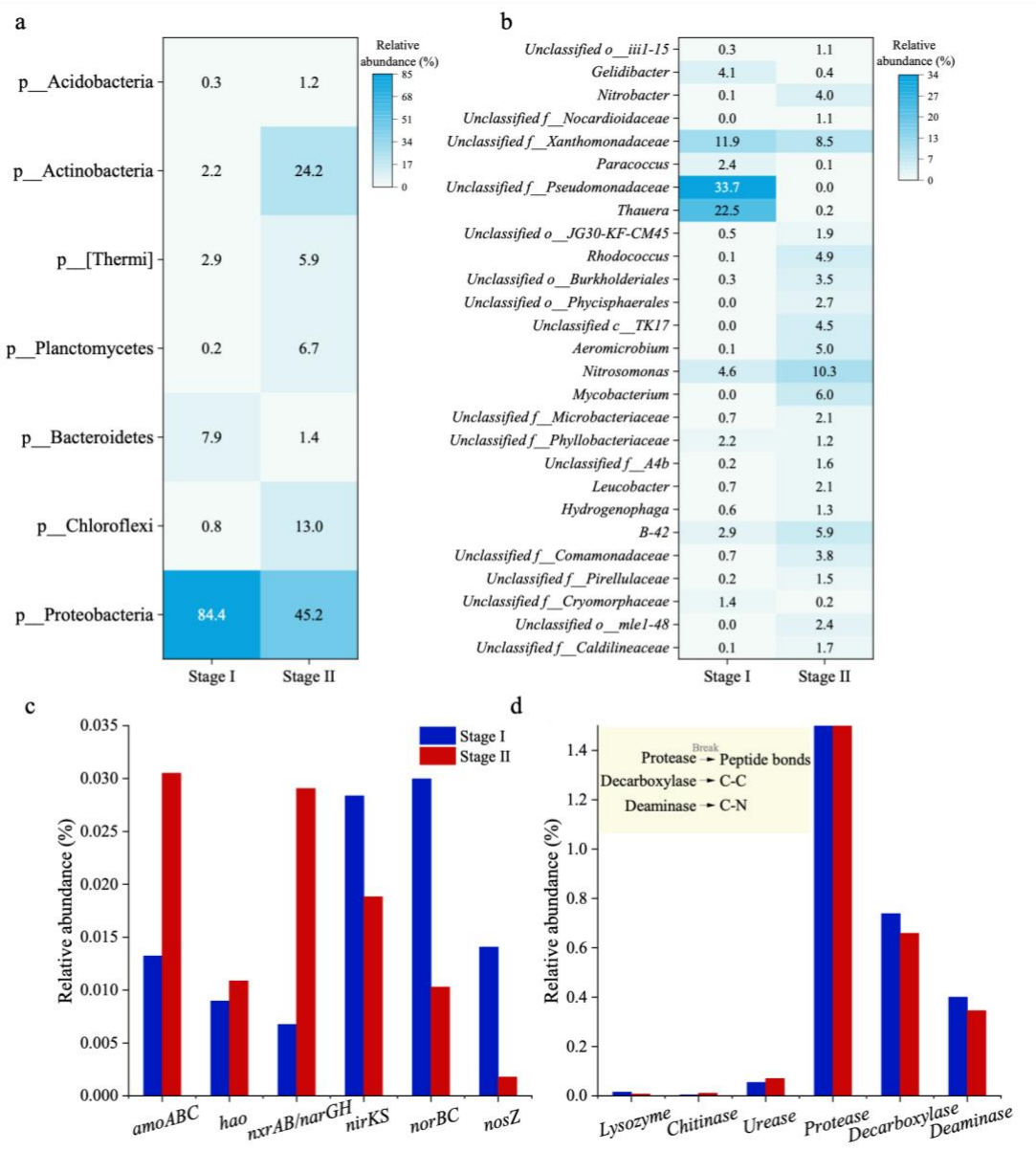

Figure 10.8 Microbial community structure in sludge samples collected in Stage I (with sodium acetate addition) and Stage II (without sodium acetate addition): a) microbial relative abundances at the phylum level; and b) microbial relative abundances at the genus level, and unidentified genera are shown at family (Unclassified f_), order (Unclassified o_), and class (Unclassified c_) levels. The relative abundance of predicted function genes associated with c) nitrogen oxidation and reduction and d) organics degradation in Stage I and Stage II.

10.3.7 Proposed mechanism for the removal of dissolved organic nitrogen

Cycle test results indicate that biodegradable DON could be diminished during the aerobic phase, whereas an increase in DON concentration was observed once the biodegradable DON had been

exhausted. The incorporation of sodium acetate was found to effectively decrease the number of DON formulae, the concentrations of DON, and the presence of sulfur-containing molecules.

Under aerobic conditions, DON degradation typically proceeds via a hydrolysis reaction which generates ammonia, subsequently utilized in nitrification and denitrification processes [3]. Under anoxic/anaerobic conditions, DON breakdown primarily occurs through hydrolysis and fermentation reactions. Here, larger molecular DON compounds such as proteins are broken down into smaller molecular DON compounds like amino acids. Subsequently, the amino acids can be deaminated, yielding ammonia [3, 296].

During the anoxic phase, hydrolysis and fermentation reactions likely occur concurrently. Our study showed that the addition of sodium acetate during the anoxic phase led to the upregulation of functional genes involved in releasing nitrogen from organics, such as decarboxylase and deaminase. This could explain the slight reduction in DON concentration observed in the anoxic phase during the Stage I cycle test. Conversely, in the Stage II cycle test, DON was generated during the anoxic phase, potentially due to limited fermentation reactions. Therefore, the combined production of DON from hydrolysis and microbial metabolism outweighed DON removal. Furthermore, the adsorption of hydrophobic DON could also contribute to DON removal. Higher DON adsorption capacity might have also occurred in Stage I, due to a higher potential for EPS production compared to Stage II [329].

We propose that the addition of easily biodegradable COD (sodium acetate) could induce co-metabolism by stimulating the secretion of extracellular hydrolytic enzymes, decarboxylases, deaminases, and other secondary metabolites. This enhancement could aid DON decomposition, particularly of protein/amino sugar and lipid-like CHONS during the biological nitrogen removal process, thereby lowering effluent DON concentrations. Future research should focus on characterizing DON produced and removed during the nitrogen removal process with different carbon sources to better understand the features of DON that can be effectively removed via the addition of easily biodegradable COD. Based on our findings, the addition of sodium acetate during the anoxic phase, as implemented in this study, could be applied in larger scale studies for effective DON and TIN removal, helping to meet stringent TKN discharge requirements. Further

research of various C/N ratios for DON removal is essential to offer economical solutions for large-scale studies. Additionally, the effectiveness of this approach for different types of LLW, like young leachate should also be investigated.

In the course of biotransformation, DON molecules were converted to less biodegradable organic nitrogen forms, which mitigate the potential for eutrophication in receiving water system. It is noteworthy that DON serves as a precursor for the formation of toxic nitrogenous disinfection by-products (N-DBPs). During chlorination or chloramination process, typical N-DBPs, including Dichloroacetonitrile (DCAN), N nitrosodimethylamine (NDMA) and trichloronitromethane (TCNM) are formed in the presence of DON [3]. These compounds pose significant risks to both aquatic ecosystems and human health [330]. However, the formation of N-DBPs is multifactorial, influenced not only by DON concentrations, but also by disinfectant quantities and temperature [3]. Further research to investigate the combined impact of DON and other factors on the formation of DBPs is needed. Consequently, maintaining low DON concentration is imperative to reduce the generation of DBPs.

10.4 Conclusion

The incorporation of sodium acetate significantly enhanced the removal of TIN and DON during the GSR nitrogen removal from mature landfill leachate wastewater. With the addition of sodium acetate, an impressive removal efficiency of 94% for TIN and 45% for DON were achieved. In contrast, without sodium acetate supplementation, only approximately 10% TIN removal was observed, and the effluent DON content increased by ~22% relative to the influent.

This chapter proposes that the supplementation of sodium acetate stimulates a co-metabolism process that contributes to the reduction of recalcitrant organics originating from mature landfill leachate. This co-metabolism process is likely facilitated by the secretion of extracellular enzymes and secondary metabolites that target the degradation of nitrogen and sulfur-containing compounds (CHONS). Decarboxylase and deaminase, major enzymes involved in the degradation of amino acids and the release of nitrogen from organics, had their corresponding genes upregulated in the presence of sodium acetate.

Moreover, the addition of sodium acetate resulted in improved sludge settling capacity, another critical aspect of effective wastewater treatment. Thus, our findings highlight the value of sodium acetate supplementation in enhancing both the efficiency and the overall functionality of N removal processes in wastewater treatment.

Chapter 11. Utilizing High COD Wastewater as Carbon Source for Enhanced Nitrogen Removal in High Ammonia Wastewater Using the Newly Developed Granular Sludge Reactor[8]

11.1 Introduction

In previous chapters, the newly developed GSR has achieved over 95% N removal from high ammonia wastewaters with the addition of an external carbon source, such as sodium acetate, during the anoxic phase [123, 164]. Compared to techniques like the Fenton process or a combination of post-denitrification and membrane filtration for enhanced N removal, supplementing external COD is a more cost-effective option, especially when utilizing high COD raw wastewaters as carbon source, which can save considerable chemical cost during large scale application.

In this chapter, the newly developed GSR was employed to treat high ammonia, low biodegradable COD (bCOD) anaerobically digested molasses wastewater. The raw molasses wastewater, prior to anaerobic digestion, which is rich in bCOD, was adopted to supply necessary organic carbon instead of commercial carbon sources. This chapter aims to investigate the feasibility and impact of supplementing high bCOD raw molasses wastewater on the performance of the GSR and the stability of the granular sludge. Furthermore, a microbial community analysis was conducted to identify potential nitrogen removal pathways. This is the first study demonstrating the utilization of raw high bCOD wastewater for enhancing denitrification in a GSR.

11.2 Methods and materials

11.2.1 Wastewater source and characteristics

In this study, two types of molasses wastewater were treated: pre- and post-anaerobic digestion, referred to here as raw and anaerobically digested molasses wastewater. The anaerobically

[8] A version of this chapter has been published: Zou, X., Yao, Y., Gao, M., Zhang, Y., Guo, H., & Liu, Y. (2024). Treatment of high ammonia anaerobically digested molasses wastewater using aerobic granular sludge reactor. *Bioresource Technology*, 131056. https://doi.org/10.1016/j.biortech.2024.131056

digested molasses wastewater, used as the influent, has a pH of 7.2, a high NH_4^+-N level ranging from 360 to 440 mg/L, a PO_4^--P concentration ranging from 10 to 22 mg/L and a salinity of 7800 mg/L. The raw molasses wastewater, utilized as the external carbon source, has a pH of 5.7 and limited amounts of ammonia, whereas the concentration of organic N was notably higher, approximately 1700 mg/L. The wastewater characteristics (Table 11.1) highlight significantly higher soluble COD (sCOD) and biodegradable soluble COD (bsCOD) concentrations in the raw molasses wastewater compared to its anaerobically digested counterpart. It is noted that the majority of the bCOD present in the raw wastewater is converted to methane through the anaerobic digestion process. The anaerobically digested wastewater was collected every three weeks, while the raw molasses wastewater was obtained in a single collection. Both wastewaters were collected from a yeast production industry in Alberta, Canada. Prior to the bioreactor treatment, all wastewater samples were stored at 4 ^oC in a cold room.

Table 11.1 Physiochemical characteristics of raw and anaerobically digested molasses wastewater.

Physiochemical parameters	Anaerobically digested molasses wastewater	Raw molasses wastewater
NH_4^+-N (mg/L)	406 ± 37	56 ± 10
NO_2^--N (mg/L)	9 ± 3	-
NO_3^--N (mg/L)	3 ± 1	-
PO_4^--P (mg/L)	17 ± 5	-
Alkalinity as $CaCO_3$ (mg/L)	3030 ± 85	-
Soluble COD (mg/L)	2464 ± 502	37150 ± 2450
Biodegradable soluble COD (mg/L)	340 ± 117	21000 ± 1879
Dissolved Ca (mg/L)	127 ± 35	920 ± 56
Dissolved Mg (mg/L)	31 ± 4	42 ± 11
Mixed liquor suspended solids (mg/L)	1800 ± 1000	-
Mixed liquor volatile suspended solids (mg/L)	1500 ± 900	-

11.2.2 Reactor setup and operation

A 3 L cylindrical GSR was employed for the treatment of anaerobically digested molasses wastewater at 20 ^oC. The inoculum was granular sludge (with a mean size of 0.6 mm) collected from a dual AGS designed for high ammonia wastewater treatment. The feed, primarily composed of supernatant, was introduced at the reactor's bottom with a 50% exchange ratio. Aeration was provided via a fine bubble air diffuser positioned at the bottom, achieving an upflow superficial velocity of 1.0 cm/s and dissolved oxygen values of 0.6 to 0.9 mg/L. The operation of the reactor was divided into two consecutive stages: Stage I, with a 4 h cycle time without the addition of high bCOD raw molasses wastewater, then switched to Stage II, with a 6 h cycle time

supplemented with high bCOD raw molasses wastewater, containing approximately 21000 mg/L bsCOD. The raw molasses wastewater was introduced in a pulsed manner during the first 10 min of the anoxic phase, with a volume of 34 mL. To enhance mixing during the anoxic phase, recirculation was provided at a rate of 130 mL/min. Programmable timers were utilized for automatically controlling the reactor operations. The feeding was conducted in a slow feeding mode for 1 hour to enhance granular stability, and the utilization of bCOD originated from the feed for N and P removal [53]. A consistent settling and decanting duration of 5 min was provided. Detailed sequence of the reactor operation can be found in Table 11.2. The solid retention time (SRT) in the system was not manually controlled, instead, sludge wasting occurred with the discharge of effluent.

Table 11.2 Granular sludge reactor operation sequence in Stage I and Stage II.

Stages	Feeding	Aerobic	Anoxic	Post-aerobic	Settling	Discharging
Stage I	1 h	2.75 h	-	-	5 min	5 min
Stage II	1 h	3 h	1.5 h	15 min	5 min	5 min

11.2.3 Sludge characterization

Sludge morphology and composition were analyzed using scanning electron microscopy (SEM) and energy dispersive X-ray (EDX) (ZEISS Sigma) [331]. The identification of chemical compounds within the granular sludge was performed using X-ray powder diffraction (XRD, Rigaku Ultima IV, Japan), employing the Bragg Brentano reflection geometry [332]. Data analysis was conducted using JADE MDI 9.6 software, and phase identification was based on the 2021/2022 ICDD PDF 4+ and PDF 4+/Organics databases, utilizing DIFFRAC.EVA software.

11.2.4 Microbial community analysis

DNA extraction was performed in duplicate from sludge samples collected at the steady state of each stage, using Dneasy PowerSoil Pro Kit (QIAGEN, Hilden, Germany). The extracted DNA was then amplified and sequenced using the Illumina Miseq PE250 platform at Genome Quebec (Montréal, QC, Canada). Subsequent sequence data processing employed the DADA2 algorithm in QIIME2 pipeline, with taxonomic assignments based on the GreenGenes database (version 13_8) at a 97% similarity [116]. Furthermore, the functional genes involved in nitrogen and sulfur metabolisms were predicted using the Phylogenetic Investigation of Communities by

Reconstruction of Unobserved States 2 (PICRUSt2) pipeline, aligned with the Kyoto Encyclopedia of Genes and Genomes (KEGG) database [333]. The raw sequencing data has been submitted to the National Center for Biotechnology Information (NCBI) GenBank (PRJNA1103104).

11.2.5 Statistical analysis

The statistical significance of the results was assessed using a T-test in Microsoft Excel. A p-value less than 0.05 was considered as significant.

11.3 Results and discussion

11.3.1 Reactor performance

The performance of the GSR in N and COD transformation in Stages I and II is illustrated in Figure 11.1. Figure 11.1a depicts the concentrations of influent NH_4^+-N, and effluent NH_4^+-N, NO_2^--N and NO_3^--N. The influent NH_4^+-N concentrations in both stages varied between 300 and 370 mg/L. In Stage I, without the addition of high bCOD raw molasses wastewater, the effluent NH_4^+-N concentration was approximately 1 mg/L, achieving a 99% ammonia removal efficiency (Figure 11.1b). The NO_3^--N was predominant in Stage I effluent, ranging from 260 to 330 mg/L, while a low NO_2^--N at 6 mg/L was observed. With the supplementation of high bCOD raw molasses wastewater in Stage II, the effluent NH_4^+-N concentration remained low at 1 mg/L, suggesting COD had no adverse impact on the ammonia oxidation process. Furthermore, a consistently low level of effluent NO_2^--N was observed in Stage II. In comparison to Stage I, the effluent NO_3^--N concentration in Stage II significantly decreased to less than 10 mg/L within 25 days and maintained low levels thereafter. Figure 11.1b reveals the TIN removal efficiency enhanced from approximately 10% in Stage I to 97% in Stage II. The increase in TIN removal could be attributed to the introduction of high bCOD raw molasses wastewater in the anoxic phase. The N loading rate obtained in Stage I was 3.6 kg N/(m^3·d) and in Stage II was 2.4 kg N/(m^3·d). In Stages I and II, the effluent contained solid concentrations ranging from 150 mg/L to 300 mg/L, resulting in an average SRT of 45 days. The effluent solid concentrations in this study were higher than the reported AGS studies, ranging from 5 to 20 mg/L [112, 272], likely due to the higher solid content in the influent wastewater.

As shown in Figure 11.1c, the sCOD removal in Stage I, without high bCOD raw molasses wastewater addition, was 13%. This represents a 90% bsCOD removal, calculated by dividing the removed sCOD at 300 mg/L by the feed bsCOD concentration of 340 mg/L. During anoxic phase in Stage II, a small volume of high bCOD raw molasses wastewater was added, resulting in a $COD_{removed}/N_{removed}$ ratio of 3. The influent sCOD concentration in Stage II was determined by adding up the externally supplied sCOD and the sCOD originated from the anaerobically digested molasses wastewater. A 36% sCOD removal was attained in Stage II, including the removal of biodegradable proportion of anaerobically digested molasses wastewater and externally added raw molasses wastewater. It is noticeable that the sCOD levels in the effluent from Stage II was at the same level as those in Stage I, suggesting the complete removal of externally added bsCOD. However, due to the high concentration of recalcitrant COD in the anaerobically digested molasses wastewater, a low COD removal efficiency was still observed. The remaining recalcitrant COD should be addressed through further treatment, potentially employing a combination of advanced oxidation processes or membrane technologies [334]. The provided C/N ratio in Stage II was slightly lower than the practical ratio of 3.5-3.8 required for denitrification [6]. This suggests the possible existence of an alternative pathway contributing to nitrate reduction. The soluble organic loading rate reached 7.4 kg/(m^3·d) in Stage I and 5.3 kg/(m^3·d) in Stage II, while the loading rate of biodegradable organics was 1 kg/(m^3·d) in Stage I and 1.6 kg/(m^3·d) in Stage II.

Figure 11.1d depicts the phosphorus (P) concentrations before and after GSR treatment in both stages. Notably, a reduction in P levels was observed in both stages: a decrease from 19 mg/L to 8 mg/L in Stage I, and a slightly higher reduction from 15 mg/L to 2 mg/L in Stage II. The P removal might be contributed by cell assimilation for growth, as well as activities of polyphosphate accumulating organisms (PAO) and denitrifying PAO (DPAO). The layer stratification of granular sludge and the slow plug flow feeding mode likely supported P removal via PAO and DPAO activities. The bCOD from the feed and raw molasses wastewater likely supports the biological phosphorus removal. Figure 11.1e illustrates the dissolved Ca concentrations in the influent wastewater and the treated effluent across both stages. During Stage I, there was a slight decrease in Ca concentration, with values dropping from an average of 127 mg/L in the influent to 122 mg/L in the effluent. In Stage II, a more substantial reduction in calcium levels was observed, where the effluent contained 136 mg/L Ca, down from 174 mg/L Ca

introduced to the reactor. This decrease in Stage II can potentially be linked to the increased initial Ca concentration due to the addition of high bCOD raw molasses wastewater, as well as the improved denitrification process. The latter may promote the secretion of extracellular polymeric substances (EPS) and certain enzymes, facilitating Ca precipitation in the wastewater [335].

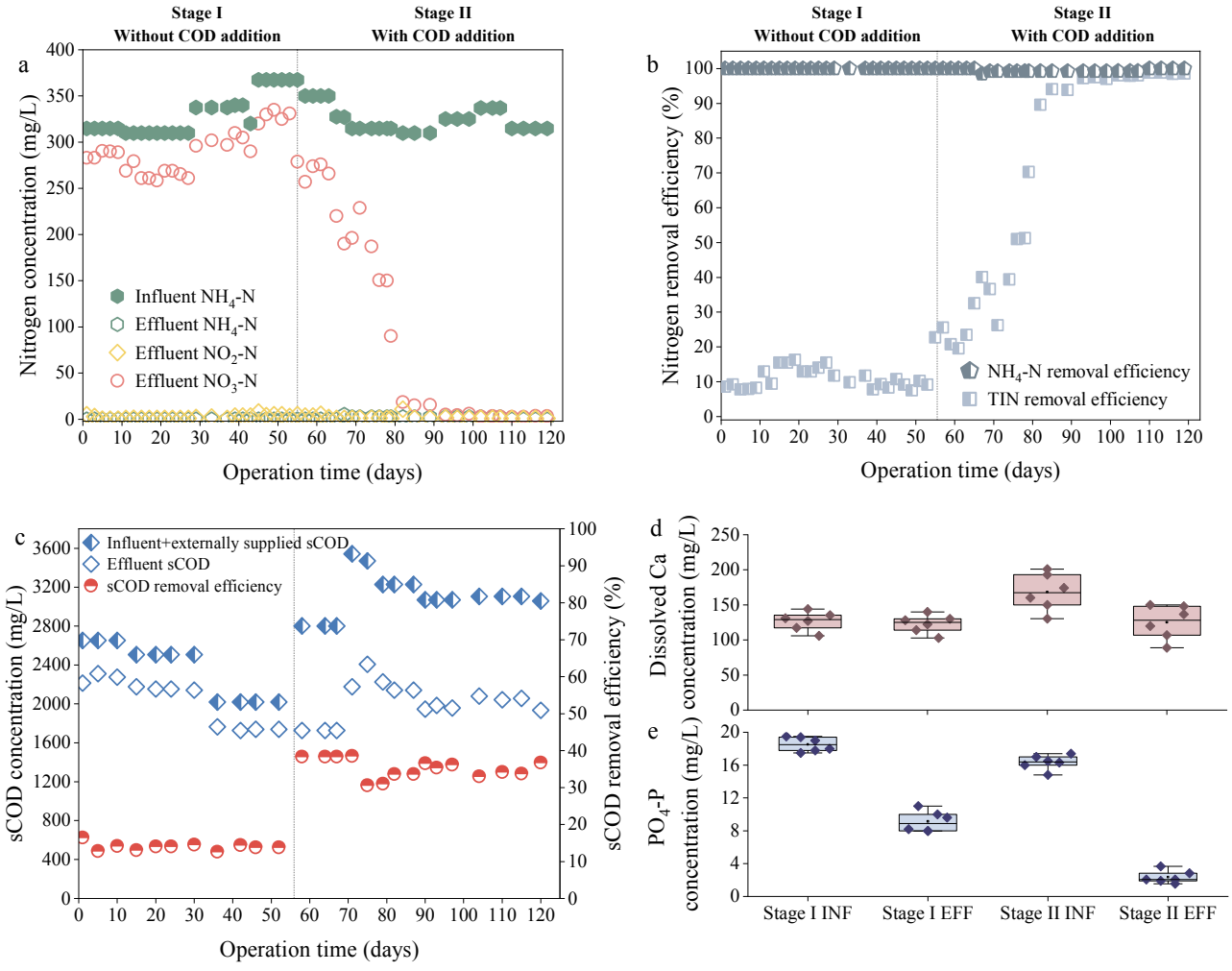

Figure 11.1 Performance of granular sludge reactor (GSR) in Stage I and Stage II, including a) nitrogen transformation (influent NH_4^+-N, and effluent NH_4^+-N, NO_2^--N and NO_3^--N); b) removal efficiencies of ammonia and total inorganic nitrogen (TIN); c) total sCOD inputs (sum of sCOD from digested molasses wastewater and externally added sCOD derived from raw molasses wastewater, normalized to influent volume), effluent sCOD and sCOD removal efficiency; d) PO_4^--P concentrations in influent (INF) and effluent (EFF); and e) dissolved Ca concentrations in influent (INF) and effluent (EFF). The bars in d) and e) represent the highest and lowest values in the data set, excluding any outliers. The lower edge of the box represents the 25th percentile, indicating 25% of the data fall below this line. The upper edge of the box marks the 75th percentile, showing that 75% of the data is below this point. The middle line denotes the median.

11.3.2 Cycle tests

A typical cycle test in each stage was presented to reveal the N transformations in the GSR (Figure 11.2). In both Stages I and II, ~155 mg/L ammonia was depleted within 150 min and nitrite accumulation was observed in the middle of the aeration phase, but mostly being converted to nitrate at the end of aeration phase. Without the addition of raw molasses wastewater (Figure 11.2a), elevated nitrate concentration at 264 mg/L was observed in Stage I's effluent, whereas low nitrate level at 21 mg/L was attained in Stage II's effluent (Figure 11.2b). Given a 50% feed exchange ratio, expected initial nitrate concentration was 132 mg/L for Stage I and 10 mg/L for Stage II. The actual measurements of initial nitrate level were lower, at 108 mg/L in Stage I and less than 6 mg/L in Stage II, indicating denitrification likely occurred during the feeding phase. However, the initial sCOD concentrations were around 2200 mg/L, consistent with theoretical expectations for a 50% exchange ratio, suggesting limited COD utilization in the feeding phase. This observation revealed that nitrate removal during feeding phase, possibly predominantly through autotrophic denitrification processes like sulfide-oxidizing autotrophic denitrification (SOAD), as sulfide likely existed in the anaerobically digested molasses wastewater. Due to the complexity of the process, additional research involving RNA level analysis and specific microbial activities is needed to characterize the contribution rate of autotrophic and heterotrophic denitrification to the TIN removal.

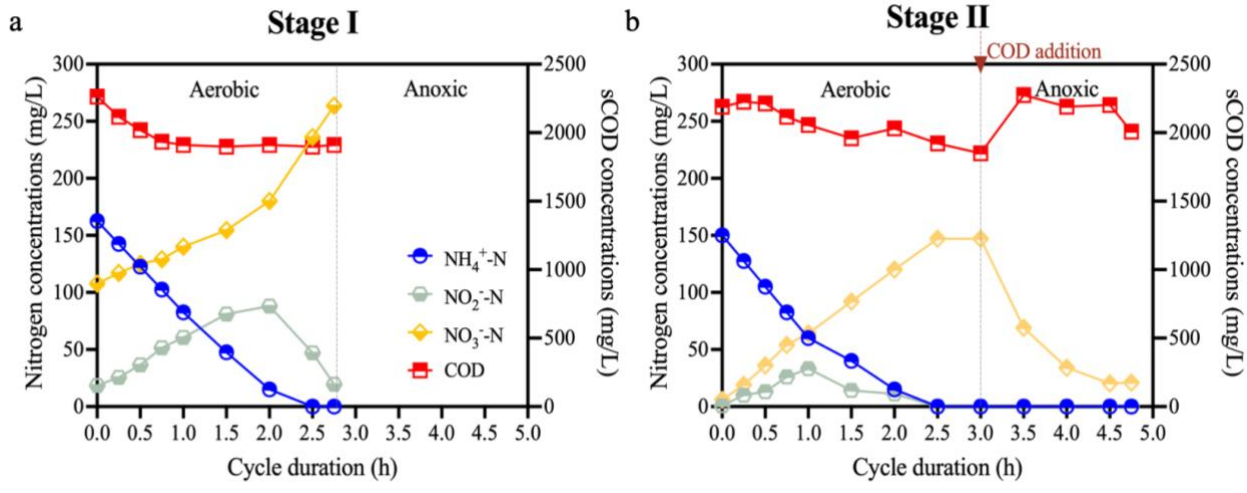

Figure 11.2 Typical cycle tests in a) Stage I without COD addition and b) Stage II with COD addition.

11.3.3 Sludge characteristics

11.3.3.1 Physical properties

The MLSS and MLVSS in Stage I stabilized at about 12 g/L and 9.4 g/L, respectively (Figure 11.3). During Stage II, MLSS levels gradually elevated to 18 g/L, while MLVSS slightly rose to approximately 11 g/L, resulting in a decrease in the MLVSS/MLSS ratio from 0.8 to 0.6. This reduction in the MLVSS/MLSS ratio, coinciding with the introduction of raw molasses wastewater, might be linked to the introduction of solids from raw wastewater or biologically induced chemical precipitation, as evidenced by the reduced Ca concentration in the treated effluent compared to the influent (Figure 11.1d). It is important to note that the wastewaters were predominantly settled before being introduced into the reactor, suggesting a minimal contribution to the reactor solids. Further, as indicated in Table 11.1, solids from the molasses wastewater were largely biomass, implying a limited impact on the reduction in MLVSS/MLSS ratio. The progressive buildup of inorganic solids within the granular sludge may improve granule stability, potentially acting as a nucleus for granular sludge.

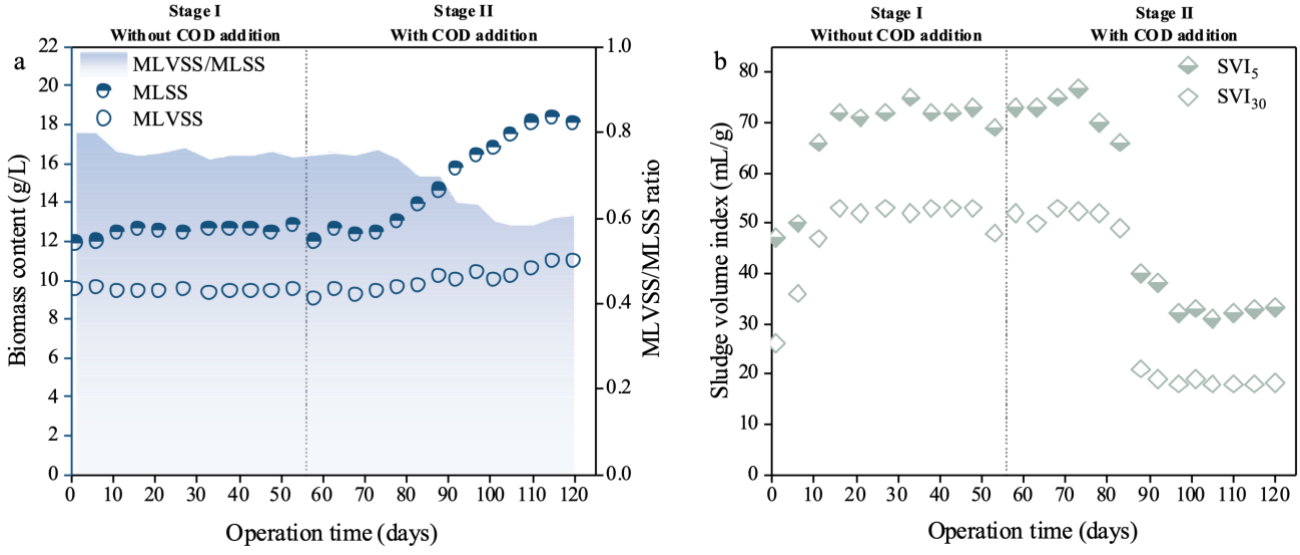

Figure 11.3 Biomass concentrations and properties across the reactor operation period: a) concentrations of mixed liquor suspended solids (MLSS) and mixed liquor volatile suspended solids (MLVSS), and the ratio of MLVSS/MLSS; b) sludge volume index (SVI) at 5 minutes and 30 minutes.

The SVI values in Stage I remained stable at 72 mL/g for SVI_5 and 53 mL/g for SVI_{30}. However, with the introduction of raw molasses wastewater, intended to enhance nitrate reduction, there

were significant reductions in SVI values, dropping from 72 to 32 mL/g for SVI_5 and from 53 to 18 mL/g for SVI_{30}. The dramatic decline in SVI may correlate with the decreased MLVSS/MLSS ratio. A progressive increase in the average size of granular sludge from Stage I (0.6 mm) to Stage II (0.7 mm) was observed (Figure 11.4), together with the improved settling capacity. This growth in granule size was likely attributed to the formation of inorganic compounds, which may enhance the microbial adhesion processes. The granule size in this study is at the lower end of the previously reported granule sizes (0.2-3 mm) [162, 336, 337]. The cultivation of small granular sludge in this study could be attributed to the limited availability of bCOD for aerobic heterotrophs [7]. Maintaining a stable granular structure in environments with low bCOD has traditionally been challenging. However, the current operational cycle of the reactor, which includes an anoxic phase, was expected to enhance the growth of heterotrophic bacteria, which are crucial for the secretion of EPS and supporting the granule structure.

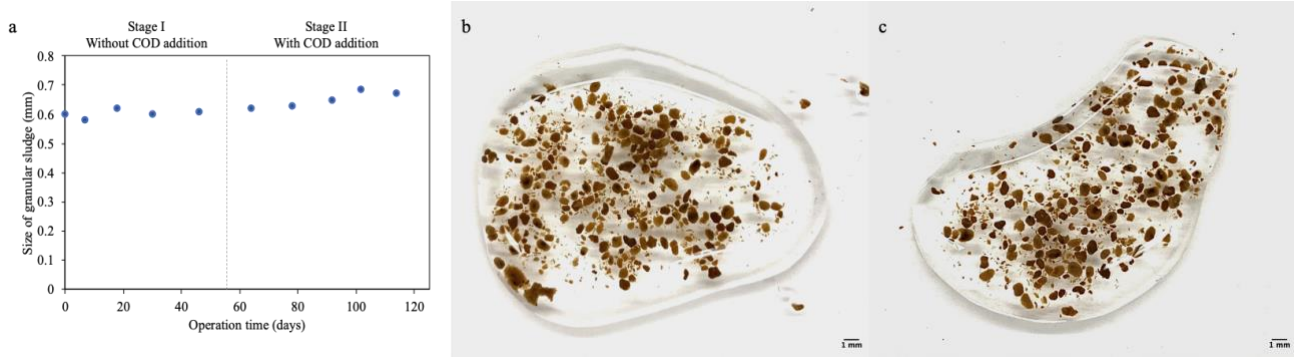

Figure 11.4 Granular sludge size and morphology, a) dynamics of granular sludge size, b) granular sludge morphology in Stage I, and c) granular sludge morphology in Stage II.

11.3.3.2 Chemical precipitation in sludge

Scanning electron microscopy (SEM, Figure 11.5) coupled with energy dispersive X-ray detector (EDX, Figure 11.5) analysis was performed on the sludge samples collected on day 115 to evaluate the formation and distribution of inorganic compounds within the granular sludge. The result reveals the presence of inorganic precipitates in the outer layer of the granules. The mineralized area exhibits a morphology clearly distinguishable from regions occupied by microorganisms. Diverse microbial shapes, including rod-shaped and spherical, were observed.

EDX spectrum shows the elemental composition of the granular sludge, demonstrating that oxygen, calcium and carbon were the dominant elements in the mineralized areas, constituting

40%, 27% and 24% of mass, respectively. Phosphorus accounted for about 2% of mass in the granular sludge, presenting a low elemental Ca/P ratio at 0.1 compared to the commonly reported 1.63 ± 5 in CaP precipitation studies [338]. This elemental composition suggests that calcium precipitate formation contributed to calcium removal, however, it is unlikely that CaP is the dominant precipitate involved. Multiple SEM and EDX analyses targeting various mineralized zones yielded similar spectra results.

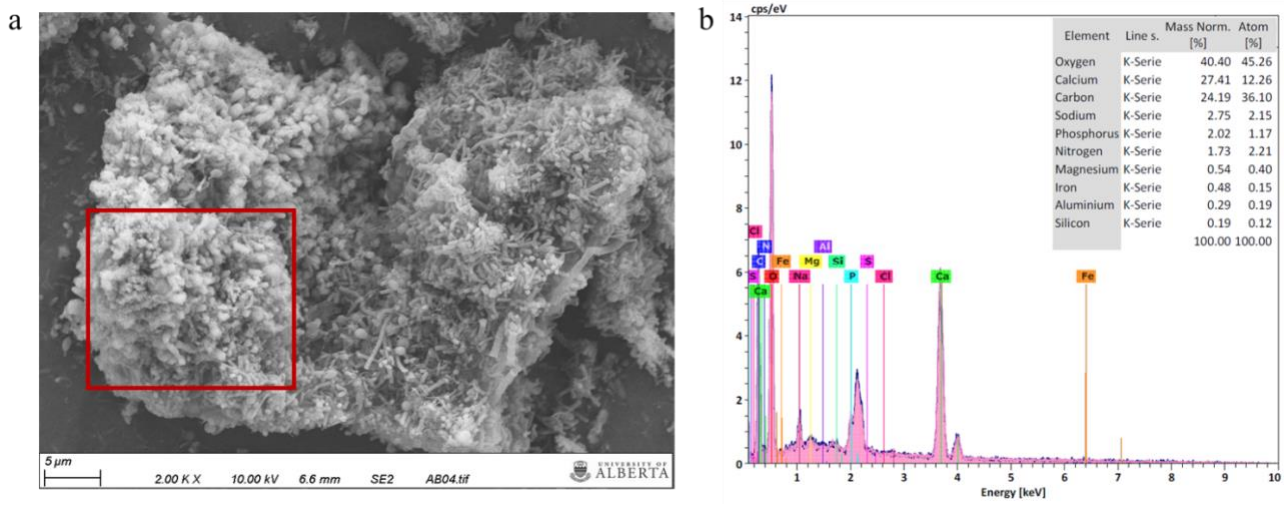

Figure 11.5 Granular sludge characterization a) scanning electron microscopy (SEM) images of granular sludge and b) energy dispersive X-ray detector (EDX) spectra.

According to the XRD analysis (Figure 11.6), calcite was the predominant precipitate in the granular sludge, given the high alkalinity levels in the wastewater. The occurrence of calcium precipitates was also documented in the context of an anaerobic membrane bioreactor treating raw molasses wastewater [339].

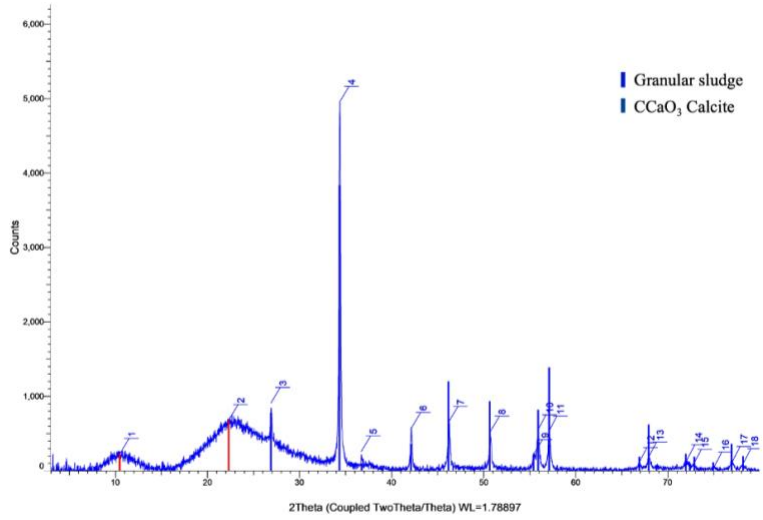

Figure 11.6 X-ray powder diffraction (XRD) result of the identification of chemical compounds within the granular sludge. (chapter 4)

11.3.4 Microbial kinetics

Figure 11.7 delineates the specific microbial activities evaluated in this study, including ammonia oxidation (AOB activity), nitrite oxidation (NOB activity), nitrite reduction (denitritation activity) and nitrate reduction (denitrification activity). The ammonia oxidation rate achieved in Stage I was 0.32 g N/(g VSS·d) and slightly reduced to 0.22 g N/(g VSS·d) in Stage II. These rates were within the previously reported range of 0.08 to 0.65 g N/(g VSS·d) [122, 123, 125, 340]. The NOB activities observed in both stages, at 0.31 (Stage I) and 0.28 g N/(g VSS·d) (Stage II), were higher than the previously reported range of 0.001 to 0.13 g N/(g VSS·d) [125, 197]. The elevated NOB activity in this study might be attributed to effective solid retention and high nitrite availability during the aeration phase. Additionally, the inoculum was originated from a dual AGS operated under similar free ammonia conditions (FA at ~7 mg/L), which likely contributed to the enrichment of NOB resistant to this level of FA.

In Stage II, there was a substantial increase in both denitritation and denitrification activities, reaching 0.18 and 0.11 g N/(g VSS·d), respectively, compared to 0.1 and 0.08 g N/(g VSS·d) in Stage I. These observed rates of denitritation and denitrification align with the ranges reported previously, varying from 0.02 to 2 g N/(g VSS·d) [123, 341]. The enhanced denitritation and denitrification activities in Stage II match with the improved performance results during this phase.

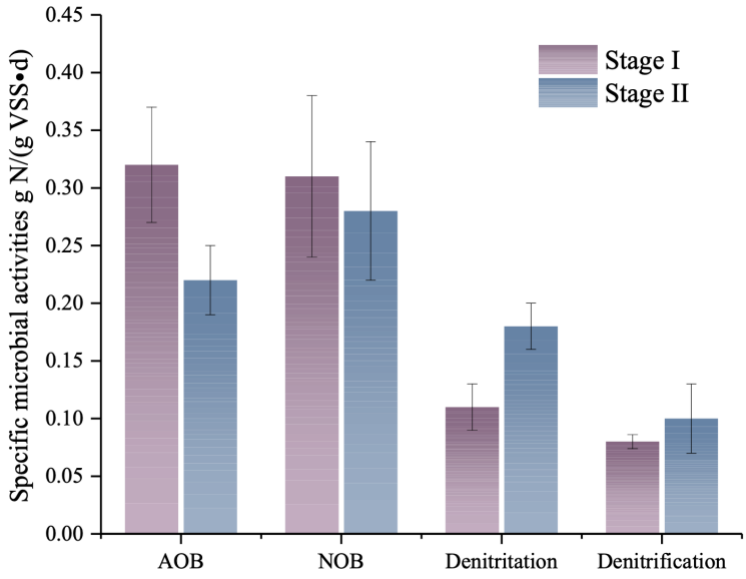

Figure 11.7 Specific microbial activities of autotrophic ammonia oxidizing bacteria (AAOB), nitrite oxidizing bacteria (NOB), denitritation bacteria and denitrification bacteria in Stage I and Stage II. Error bar represents the standard deviation of the results.

11.3.5 Development of microbial community

11.3.5.1 Microbial community at phylum level

Figure 11.8a illustrates the microbial community composition across Stages I and II. In Stage I, the dominant phyla were Proteobacteria (54%), Actinobacteria (13%) and Thermi (14%). In Stage II, Proteobacteria remained the most prevalent phylum, accounting 59% of the microbial community, followed by Chloroflexi at 15%, and Thermi at 7%. The consistent dominance of Proteobacteria in both stages indicates a stable capacity for nitrogen removal [342]. Compared to Stage I, Stage II showed a decrease in the relative abundances of Actinobacteria and Thermi to 5% and 7%, respectively, while Chloroflexi increased from 5% to 15%. This shift suggests an adaptation to the anoxic conditions introduced in Stage II, as Chloroflexi, known as facultative anaerobes, are well-suited to environments where oxygen is limited [248, 343]. Furthermore, the phylum Euryarchaeota, which includes methanogens, was observed at a relative abundance of 2% in Stage I and 1% in Stage II. The presence of Euryarchaeota in the reactor is likely due to the introduction of anaerobically digested molasses wastewater, which may have carried sludge from the anaerobic digestion process.

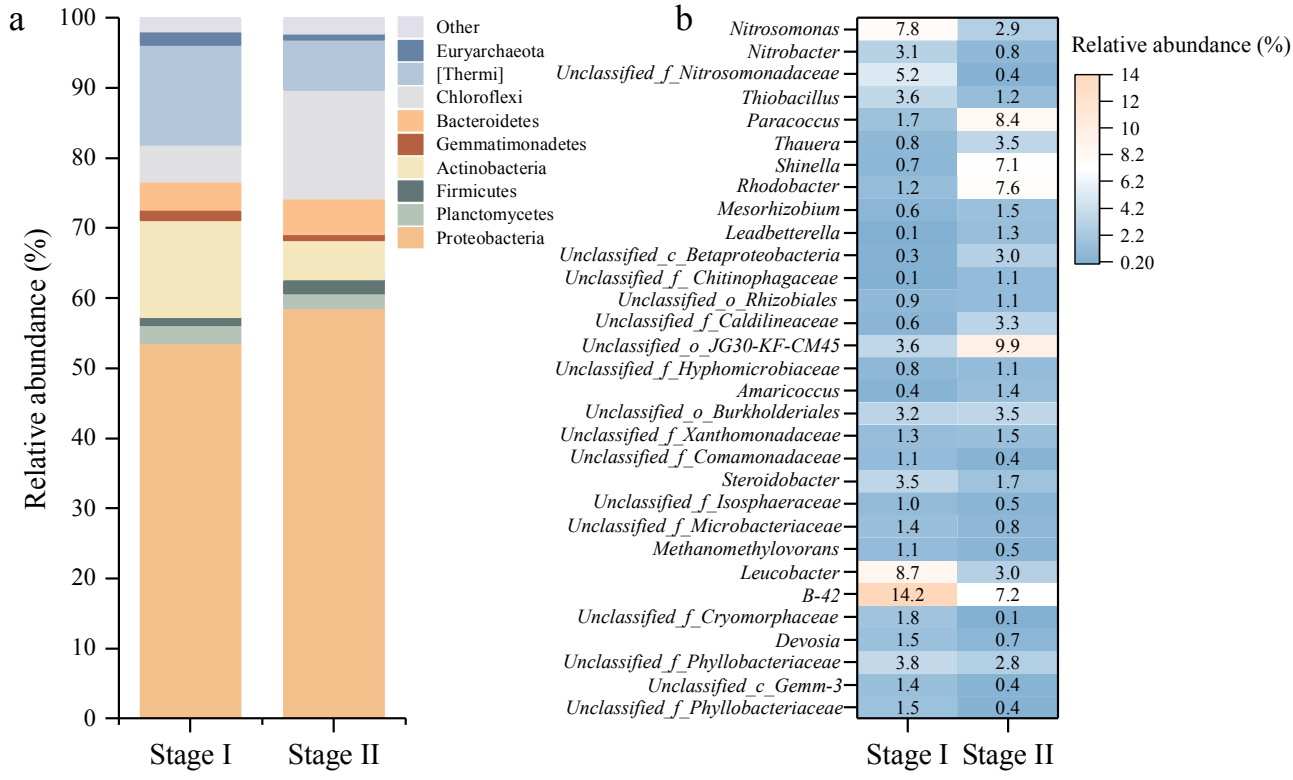

Figure 11.8 The development of microbial communities at a) phylum and b) genus level in both Stage I and Stage II. The unidentified genera were shown as family (Unclassified_f_), order (Unclassified_o_) or class (Unclassified_c_).

11.3.5.2 Microbial community at genus level

Figure 11.8b details the dynamics of the microbial community at the genus level, focusing on those with a relative abundance over 1%. Discrepancies in the microbial composition were observed between Stages I and II. In Stage I, the dominant genera included *B-42* (14%), *Leucobacter* (9%), and *Nitrosomonas* (8%). Both *Leucobacter* and *B-42* have been identified in other wastewater treatment systems operating under aerobic condition, while *Leucobacter* recognized for its capacity to degrade complex organics [149]. In contrast, Stage II showed an enrichment of genera known for their denitrification capabilities. This included a genus from the order JG30-KF-CM45, which accounted for 10% of the microbial population. Other significant denitrifying genera in Stage II were *Paracoccus* (8%), *Rhodobacter* (8%), *B-42* (7%) and *Shinella* (7%). Although the abundance of microorganisms belonging to PAO was below 0.1% in both stages, certain genera such as *Thauera*, *Paracoccus* and *Thiobacillus*, previously reported to be

capable of simultaneously removing N and P, may function as denitrifying PAO [344]. These microorganisms may reside in the granules and contribute to P removal in this study.

Genera associated with nitrogen oxidation

The N oxidation process includes ammonia oxidation and nitrite oxidation. For ammonia oxidation, the primary genera involved were *Nitrosomonas* and a genus within the family Nitrosomonadaceae. In Stage I, *Nitrosomonas* accounted 7.8% of the microbial community, but this decreased to 2.9% in Stage II. Similarly, the relative abundance of the genus from the family Nitrosomonadaceae declined from 5.2% in Stage I to 0.4% in Stage II. Regarding nitrite oxidation, the genus *Nitrobacter* was identified as the primary NOB. Its relative abundance also decreased, falling from 3.1% in Stage I to 0.8% in Stage II. This observed decrease in the relative abundance of both AAOB and NOB could be attributed to the enriched denitrifier population in Stage II, as a result of the addition of high bCOD raw molasses wastewater.

Genera associated with nitrogen reduction

I. Heterotrophic denitrification

The primary heterotrophic denitrifiers across both stages were identified as *Paracoccus*, *Thauera*, *Shinella* and *Rhodobacter*, all of which exhibited an increase in relative abundance from Stage I to Stage II. *Thauera* and *Paracoccus* were particularly notable, as they have been extensively documented in wastewater treatment for their ability to reduce nitrite and nitrate to nitrogen gas [134, 135]. Specifically, the relative abundance of *Paracoccus* surged from 1.7% in Stage I to 8.4% in Stage II, marking it as the most predominant heterotrophic denitrifier in Stage II. The relative abundance of *Thauera* grew from 0.8% in Stage I to 3.5% in Stage II, while *Shinella* increased from 1.2% in Stage I to 7.6% in Stage II. Additionally, the relative abundance of *Rhodobacter* rose from 0.7% to 7.1%. It is noteworthy that previous studies using a sole carbon source, such as sodium acetate, often reported *Thauera* or *Paracoccus* as the dominant genus with significantly high relative abundance (up to 83 %) compared to other genera [134, 345, 346]. In contrast, the denitrifying genera in this study displayed more comparable relative abundances. This variation may be attributed to the diversity of carbon sources present in the raw molasses wastewater. This indicates the redundancy and adaptability of the microbial community in treating a variety of

carbon sources, underscoring its resilience and functional versatility in the wastewater treatment process.

II. Autotrophic denitrification

The sulfide-oxidizing autotrophic denitrification (SOAD) process, which utilizes sulfide or thiosulfate as an electron donor for denitrification, may have been particularly relevant in this study, as sulfide likely existed in the anaerobically digested molasses wastewater. The SOAD process can be facilitated by genera such as *Thiobacillus*, *Sulfurimonas*, *Arcobacter*, *Thauera* and *Paracoccus* [122, 336]. Among these, only limited abundances of *Sulfurimonas* and *Arcobacter* were observed in this study, while *Thauera* and *Paracoccus* were dominant. In particular, the genus *Thiobacillus*, widely documented for its SOAD capabilities, was detected under both stages of current study. The SOAD process might have been particularly active during the feeding period when stored anaerobically digested molasses wastewater, potentially undergoing sulfate reduction to sulfide by sulfate reducing bacteria (SRB), was introduced. The sulfide could then serve as an electron donor for the SOAD process. Additionally, an hour-long feeding likely provided a conducive environment for SOAD processes. The relative abundances of *Thiobacillus* decreased from 3.6% in Stage I to 1.2% in Stage II, aligning with the cycle test results, showing lower contribution of autotrophic denitrification to the N removal in Stage II. This reduction could be due to the proliferation of heterotrophic denitrifying bacteria and a limitation of substrate (NO_3^--N) necessary for SOAD. The enhanced denitrification observed in Stage II might have led to a scarcity of nitrate or nitrite in the effluent, thereby limiting their availability for SOAD. This constraint could also explain the observed decline in *Thiobacillus* abundance. Further investigation is required to discern the individual contributions of *Thiobacillus*, *Thauera* and *Paracoccus* to autotrophic denitrification.

In the current study, two potential denitrification pathways, heterotrophic and autotrophic denitrification, might coexist and likely collaborate in nitrogen reduction. This mixotrophic approach could account for the observed lower C/N ratio requirement for nitrate denitrification. The coexistence of these pathways suggests a more efficient utilization of available carbon sources and electron donors for denitrification. Given the potential importance of SOAD in the treatment of anaerobically digested wastewater, further investigations are warranted. Specifically, RNA-

based studies could provide deeper insights into the functional roles and contributions of SOAD within the system.

11.3.6 Microbial functional genes analysis

To gain a comprehensive understanding of the microbial community composition and the associated metabolic functions crucial for the reactor's performance, the PICRUSt2 analysis was adopted [333]. PICRUSt2 predicts the functional potential of the microbial community using KEGG database to link known genomes to the marker gene in sequencing profile. Figure 11.9 depicts the relative abundance of functional genes involved in nitrogen metabolism, including both the oxidation and reduction of nitrogenous compounds. Additionally, the figure also highlights functional genes related to sulfur metabolism, including those responsible for sulfate reduction, and the oxidation of sulfide and thiosulfate.

11.3.6.1 Nitrogen metabolism

Nitrification associated functional genes

The nitrification process is primarily driven by two enzymes, ammonia monooxygenase and nitrite oxidoreductase. The relative abundances of the functional genes associated with these enzymes are depicted in Figure 11.9a. Specifically, the ammonia monooxygenases gene comprise three subunits, *amoA*, *amoB*, and *amoC*, referred to as *amoABC* in Figure 11.9a. During the study, it was observed that the *amoABC* genes were more prevalent in Stage I (0.030%) compared to Stage II (0.012%), aligning with the sequencing results. Additionally, nitrite oxidoreductase, which shares the *narG* gene with nitrate reductase, showed an increase in relative abundance, rising from 0.005% in Stage I to 0.011% in Stage II.

Denitrification associated functional genes

Denitrification process involves functional genes related to nitrate reductase (*narG*), nitrite reductases (*nirS* and *nirK*), nitric oxide reductases (*norB* and *norC*) and nitrous oxide reductase (*nosZ*). In this study, all genes associated with these enzymes were found to be upregulated in Stage II compared to Stage I. This upregulation is primarily attributed to the supplementation of high bCOD raw molasses wastewater during anoxic condition of Stage II.

More specifically, the functional genes *nirK* and *nirS*, which play a crucial role in denitrification, showed an increase from 0.023% to 0.029% and from 0.005% to 0.009%, respectively, between Stage I and Stage II. Similarly, the relative abundance of the *nosZ* gene, essential for reducing nitrous oxide emissions, also observed an increase from 0.02% in Stage I to 0.04% in Stage II. The ratio of the relative abundance of *nosZ* to *nirSK* increased from 0.85 in Stage I to 1.0 in Stage II, suggesting a reduced potential for nitrous oxide emissions [347]. The observed upregulation of these functional genes correlates with the enhanced TIN removal efficiencies achieved in Stage II.

11.3.6.2 Sulfur metabolism

Figure 11.9b illustrates the functional genes involved in sulfur metabolism. Sulfide oxidation, a key component of this process, primarily operates via two enzymatic pathways, the Sox pathway and sulfide: quinone oxidoreductase (Sqr) pathway [348]. The functional genes encoding the Sox system, including *soxC*, *soxY* and *soxZ*, maintained a consistent relative abundance of 0.2% across both stages. These genes are commonly reported in SOAD process [349, 350].

The *sqr* gene, pivotal for converting sulfide into elemental sulfur [351], showed an increase from 0.04% in Stage I to 0.05% Stage II. This upregulation suggests a heightened microbial capacity for sulfide conversion. Notably, the relative abundance of functional genes encoding the Sox system surpassed that of the Sqr pathway, suggesting the Sox system might be the dominant pathway for sulfide oxidation in the GSR.

The comparable relative abundances of functional genes in sulfide oxidation point to the coexistence of autotrophic and heterotrophic denitrifiers in both stages. Additionally, the similar sulfide oxidation capabilities observed in both stages imply the involvement of other microbial species in sulfur metabolism. This inference is supported by the noted reduced relative abundance of *Thiobacillus*. It is conceivable that other species, such as *Thauera* or others may complement the role of *Thiobacillus* in sulfur metabolism within the system, which require further investigations [122].

Moreover, genes involved in dissimilatory and assimilatory sulfate reduction were detected, exhibiting comparable abundance in both stages (0.3%). Functional genes such as *cysNC*, *cysN*,

cysH, *cysJ* and *cysI* were present in both stages, while the relative abundances of *sat*, *cysC* and *sir* functional genes fell below the detection limit in Stage II.

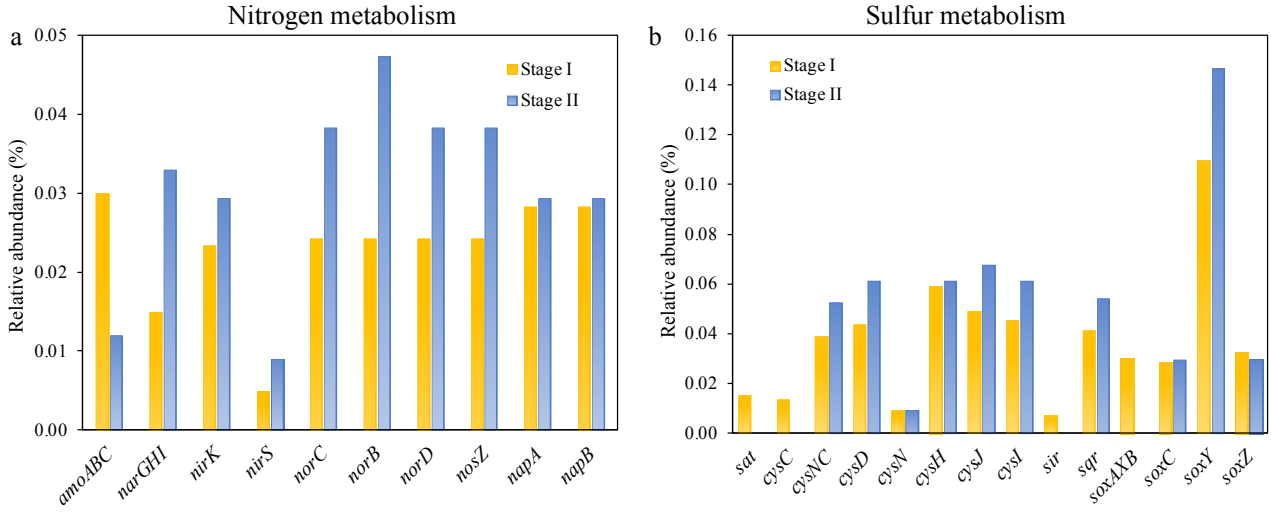

Figure 11.9 The prediction of relative abundance of functional genes involved in a) nitrogen and b) sulfur metabolism.

11.3.7 Impact of raw molasses wastewater supplementation and potential nitrogen removal pathways

High ammonia removal efficiencies were achieved with or without high bCOD raw molasses wastewater supplementation. Although the raw molasses wastewater contained 1700 mg/L organic N, the small volume added meant its impact on N removal was negligible. Adding high bCOD raw molasses wastewater as an external COD source significantly enhanced the denitrification process in Stage II, achieving over 97% TIN removal efficiency. This supplementation not only improved TIN removal but also positively affected sludge settleability. The introduction of raw molasses wastewater led to bio-induced calcium precipitation within the sludge, increasing the granular sludge density and thereby improving its settling properties. Based on these observations, adding raw molasses wastewater appears to be an effective approach for accelerating granule formation during reactor start-up.

Furthermore, the supply of high bCOD raw molasses wastewater during the anoxic phase of the reactor operation facilitated heterotrophic denitrification. The relatively low C/N ratio required for nitrate reduction is likely attributed to mixotrophic denitrification, indicating the possible co-

existence of autotrophic and heterotrophic denitrification. Autotrophic denitrification primarily utilizes inorganic carbon as the carbon source and sulfide as the electron donor for nitrate reduction. The final products of the SOAD process might be sulfate or elemental sulfur, which warrants further characterization of the sludge and identification of the SOAD pathway involved in this study. Under conditions of limited bCOD, the SOAD process might dominate nitrogen removal. However, with the addition of bCOD, heterotrophic denitrification tends to outcompete the SOAD process. The PICRUSt2 analysis revealed a comparable abundance of functional genes implicated in sulfide oxidation in both stages, suggesting that the introduction of high bCOD raw molasses wastewater exerted minimal adverse effects on SOAD microorganisms. This finding suggests a potentially enhanced synergy between autotrophic and heterotrophic bacteria in nitrate removal.

11.4 Conclusion

This chapter utilized the GSR to treat high ammonia, low bCOD anaerobically digested molasses wastewater, achieving a 99% ammonia removal efficiency, independent of bCOD levels. The introduction of high bCOD raw molasses wastewater improved TIN removal from 10% to 97% and sludge settleability. The study highlighted a synergistic interaction between autotrophic and heterotrophic denitrification pathways, significantly contributing to nitrogen removal. Key microorganisms included *Nitrosomonas* and *Nitrobacter* for ammonia and nitrite oxidation, respectively, with *Paracoccus* and *Thauera* serving as primary heterotrophic denitrifiers, and *Thiobacillus* leading sulfide-oxidizing autotrophic denitrification process. This study offers a more economically favorable GSR operation strategy for high N removal for upscaling.

Chapter 12. Conclusions and Recommendations

12.1 Conclusions of this thesis

This thesis comprehensively investigated the influence of C/N ratios and influent solid content on N removal pathways and the structural stability of granular sludge, revealing that high ammonia conditions are conducive to the enrichment of AAOB, which exhibit higher activity compared to HAOB. The influent solid content can lead to reduced SRT. According to the treatment of high ammonia wastewaters with varied C/N ratios, the limitation in N removal capacity often stems from insufficient denitrification due to a lack of alkalinity recovery. Furthermore, the study highlights the significant role of flocs and small granules, particularly those smaller than 0.2 mm, in achieving effective ammonia removal, especially under low C/N conditions. The retention of these small granules and flocs is essential as they harbor a considerable portion of active biomass that contributes to enhanced N removal.

Building on these findings, a new GSR was developed, introducing an anoxic phase with COD addition into the reactor operation—unlike conventional AGS systems operated with continuous aeration—and extended settling times to promote the retention of small granules and flocs. This novel GSR was tested for its ability to treat high ammonia, low C/N waste streams and heavy metal-contaminated wastewater, achieving a superior N removal capacity of 4.2 kg N/(m^3·d), which is approximately four times higher compared to existing commercial technologies. Additionally, the GSR demonstrated effectiveness in DON removal. The high biomass retention and the selection and enrichment of key N removal functional microbes, including AAOB and denitrifying bacteria, were the key in GSR technology. Prior to upscaling, the feasibility of using more cost-effective carbon sources for N removal in the GSR were tested, showing high N removal efficiency and improved sludge settling capacity. Main conclusions are shown below:

I. High ammonia and low C/N conditions are conducive to high ammonia removal in AGS system (Chapter 4). Elevated ammonia concentration with a low C/N ratio at 3 stimulated the growth of AAOB (*Nitrosomonas*), which enhanced ammonia removal efficiencies from 28% (C/N = 6) to 100%. Although the abundance of AAOB was low (0.3 %), their activity was 2.7-fold higher than that of HAOB. Heterotrophic nitrification was the

dominant nitrogen transformation pathway at high C/N ratios (12 and 6). Stable granular sludge was achieved throughout the operation, regardless of the shifts in C/N ratios. Current study believed that FA inhibition on heterotrophic bacteria and nitrogen competition between AAOB and heterotrophic bacteria played a key role for the development of autotrophic nitrogen transformation pathway.

II. Results obtained from Chapter 5 indicated that the introduction of AnGS with a concentration of 1.8 g/L had minimal impact on ammonia removal efficiency (99%). AnGS addition led to an increase in nitrite accumulation from 1% (the low AnGS condition) to 30% (the high AnGS condition), and an improvement in TIN removal efficiency from 8% to 11%. In contrast, elevated effluent sCOD concentration and increased effluent solid content were observed with high solid introduction. The AnGS introduction can support sludge granulation by acting as nucleus and promoting the formation of denser granular sludge.

III. Poor N removal under low C/N condition was primarily due to the limited denitrification process and insufficient alkalinity recovery potential (Chapter 6). Therefore, the key to enhancing N removal in low C/N and Alk/N ratio wastewaters is to improve the denitrification process in the reactor. The high ammonia induced selection and enrichment of slow growing autotrophic bacteria and heterotrophic bacteria might contribute to the integrity and stability of granules during C/N shifts. Enhanced AAOB and diminished HAOB, denitritation, denitrification activities were observed as the C/N ratio decreased.

IV. Results from Chapter 7 revealed that specific microbial activities in flocs consistently surpassed those in granules. However, granules contributed more to the N oxidation and reduction at C/N ratios of 6 and 4. As C/N ratio reduced to 2, flocs showed higher contributions to N oxidation, while granules maintained their major role in N reduction. Flocs were dominated by aerobic microorganisms associated with organic and N degradation. A shift of C/N ratio from 6 to 4 had a greater impact on the microbial community in granules, whereas a shift from 4 to 2 had a more pronounced effect on flocs. This result highlights the key role of granules and flocs in treating high ammonia wastewaters, suggesting that the retention of granules is more critical for high ammonia, high C/N conditions, whereas retaining flocs is critical for high ammonia, low C/N waste streams.

V. The newly developed GSR has been applied for inorganic and organic N removal from high ammonia, low COD wastewaters. Chapters 8 through 11 of this thesis highlight the exceptional treatment capabilities of the newly developed GSR across various challenging waste streams without requiring pretreatment. Specifically, Chapter 8 reports that a high N treatment capacity of 4.2 kg N/(m^3·d) was achieved in treating high ammonia, low C/N and low Alk/N anaerobically digested sludge supernatant. Chapter 9 details the GSR's rapid startup time of just one month, after which stable ammonia and total inorganic nitrogen (TIN) removal efficiencies of 99% and 93%, respectively, were maintained with a 100% raw landfill leachate feed. In Chapter 10, the addition of sodium acetate to the GSR significantly enhanced the removal efficiencies to 94% for TIN and 45% for dissolved organic nitrogen (DON) when treating mature landfill leachate wastewater. Furthermore, Chapter 11 demonstrated that introducing high bCOD raw molasses wastewater as an organic carbon source led to remarkable ammonia and TIN removal efficiencies of 99% and 97%, respectively. The outstanding performance and stability of the granular sludge within the GSR suggest anoxic COD supplementation is an effective strategy to enhance denitrification process with limited amount of chemical addition. Additionally, the high N removal capacity can be primarily attributed to the effective cultivation, selection, and enrichment of a highly efficient microbial community, and high biomass retention and the cultivation of small granular sludge.

12.2 Recommendations

This thesis demonstrated the feasibility of the newly developed GSR for high ammonia waste stream treatment. The high N loading rate and specific microbial activities unveil new opportunities to sidestream and industrial wastewater treatment. More future studies are anticipated before upscaling:

I. To validate the laboratory-scale findings, initiate pilot-scale studies to assess the GSR's performance under real-world conditions. These studies should focus on scalability, cost-effectiveness, and operational challenges that may arise at larger scales.

II. Investigate the patterns of nitrous oxide (N_2O) emissions within the GSR. Given its potent greenhouse effect, understanding the conditions that lead to N_2O production or

consumption is crucial. This can incorporate with modeling to quantify emissions and develop strategies to mitigate N_2O release during treatment processes.

III. This thesis has proposed the potential contribution of autotrophic denitrification in N removal such as SOAD, anammox and Feammox. To confirm the presence and fractionate the contributions of these processes to N removal, specific activities and RNA level studies need to be performed.

IV. The removal of inorganic and organic N from landfill leachate wastewater (LLW) was successfully demonstrated in this thesis. Considering that LLW often contains significant quantities of per- and polyfluoroalkyl substances (PFAS), further research is essential to explore and optimize the GSR's capability to effectively remove PFAS during LLW treatment.

V. This thesis primarily focused on N removal from waste streams; however, the phosphorus (P) content also requires treatment. Consequently, the GSR could be further optimized to enable simultaneous removal of both N and P.

VI. Assess the GSR's resilience to changes in wastewater characteristics, which can occur due to environmental factors like rainfall or seasonal variations. Conduct stress tests to evaluate the system's response to shock loadings and periods of starvation. This research is essential to ensure the GSR can operate reliably under fluctuating conditions typical of real-world applications.

Bibliography

[1] B. Liu, L. Gu, Q. Li, G. Yu, C. Zhao, H. Zhai, Effect of pre-ozonation-enhanced coagulation on dissolved organic nitrogen in municipal wastewater treatment plant effluent, Environmental Technology 40(20) (2018) 2684-2694. https://doi.org/10.1080/09593330.2018.1449897.
[2] H. Hu, C. Jiang, H. Ma, L. Ding, J. Geng, K. Xu, H. Huang, H. Ren, Removal characteristics of DON in pharmaceutical wastewater and its influence on the N-nitrosodimethylamine formation potential and acute toxicity of DOM, Water Research 109 (2017) 114-121. https://doi.org/10.1016/J.WATRES.2016.10.010.
[3] F. Zheng, J. Wang, R. Xiao, W. Chai, D. Xing, H. Lu, Dissolved organic nitrogen in wastewater treatment processes: Transformation, biosynthesis and ecological impacts, Environmental Pollution 273 (2021) 116436-116436. https://doi.org/10.1016/J.ENVPOL.2021.116436.
[4] L. Shao, Y. Deng, J. Qiu, H. Zhang, W. Liu, K. Bazienė, F. Lü, P. He, DOM chemodiversity pierced performance of each tandem unit along a full-scale "MBR+NF" process for mature landfill leachate treatment, Water Research 195 (2021) 117000-117000. https://doi.org/10.1016/J.WATRES.2021.117000.
[5] R. Hamza, A. Rabii, F.-z. Ezzahraoui, G. Morgan, O.T. Iorhemen, A review of the state of development of aerobic granular sludge technology over the last 20 years: Full-scale applications and resource recovery, Case Studies in Chemical and Environmental Engineering 5 (2022) 100173.
[6] Metcalf, Eddy, M. Abu-Orf, G. Bowden, F.L. Burton, W. Pfrang, H.D. Stensel, G. Tchobanoglous, R. Tsuchihashi, AECOM, Wastewater engineering: treatment and resource recovery, McGraw Hill Education2014.
[7] J. Luo, T. Hao, L. Wei, H.R. Mackey, Z. Lin, G.-H. Chen, Impact of influent COD/N ratio on disintegration of aerobic granular sludge, Water Research 62 (2014) 127-135. https://doi.org/https://doi.org/10.1016/j.watres.2014.05.037.
[8] W. Hu, Y. Zhou, X. Min, J. Liu, X. Li, L. Luo, J. Zhang, Q. Mao, L. Chai, Y.Y. Zhou, The study of a pilot-scale aerobic/Fenton/anoxic/aerobic process system for the treatment of landfill leachate, Environmental Technology 39(15) (2018) 1926-1936. https://doi.org/10.1080/09593330.2017.1344325.
[9] H.-Y. Ren, F. Kong, J. Ma, L. Zhao, G.-J. Xie, D. Xing, W.-Q. Guo, B.-F. Liu, N.-Q. Ren, Continuous energy recovery and nutrients removal from molasses wastewater by synergistic system of dark fermentation and algal culture under various fermentation types, Bioresource Technology 252 (2018) 110-117. https://doi.org/https://doi.org/10.1016/j.biortech.2017.12.092.
[10] E. Bardone, M. Bravi, T. Keshavarz, G. Di Bella, M. Torregrossa, Aerobic Granular Sludge for Leachate Treatment, 38 (2014). https://doi.org/10.3303/CET1438083.
[11] I. Othman, A.N. Anuar, Z. Ujang, N.H. Rosman, H. Harun, S. Chelliapan, Livestock wastewater treatment using aerobic granular sludge, Bioresource Technology 133 (2013) 630-634. https://doi.org/10.1016/J.BIORTECH.2013.01.149.
[12] Y. Wei, M. Ji, R. Li, F. Qin, Organic and nitrogen removal from landfill leachate in aerobic granular sludge sequencing batch reactors, Waste Management 32(3) (2012) 448-455. https://doi.org/10.1016/J.WASMAN.2011.10.008.
[13] S. Liu, N. Zhu, L.Y. Li, The one-stage autothermal thermophilic aerobic digestion for sewage sludge treatment, Chemical Engineering Journal 174(2) (2011) 564-570. https://doi.org/https://doi.org/10.1016/j.cej.2011.09.043.
[14] S. Chen, M. Wang, C. Asato, X. Mao, Characterization, Transformation, and Bioavailability

of Dissolved Organic Nitrogen in Biofilters Treating Domestic Onsite Wastewater, ACS ES and T Water 2(9) (2022) 1575-1583. https://doi.org/10.1021/ACSESTWATER.2C00228/ASSET/IMAGES/LARGE/EW2C00228_0005.JPEG.
[15] H. Eom, D. Borgatti, H.W. Paerl, C. Park, Formation of Low-Molecular-Weight Dissolved Organic Nitrogen in Predenitrification Biological Nutrient Removal Systems and Its Impact on Eutrophication in Coastal Waters, Environmental Science and Technology 51(7) (2017) 3776-3783. https://doi.org/10.1021/ACS.EST.6B06576/ASSET/IMAGES/LARGE/ES-2016-06576Y_0005.JPEG.
[16] C. Fux, S. Velten, V. Carozzi, D. Solley, J. Keller, Efficient and stable nitritation and denitritation of ammonium-rich sludge dewatering liquor using an SBR with continuous loading, Water Research 40(14) (2006) 2765-2775. https://doi.org/10.1016/j.watres.2006.05.003.
[17] S. Longo, B.M. d'Antoni, M. Bongards, A. Chaparro, A. Cronrath, F. Fatone, J.M. Lema, M. Mauricio-Iglesias, A. Soares, A. Hospido, Monitoring and diagnosis of energy consumption in wastewater treatment plants. A state of the art and proposals for improvement, Applied Energy 179 (2016) 1251-1268. https://doi.org/https://doi.org/10.1016/j.apenergy.2016.07.043.
[18] P. Wu, J. Chen, V.K. Garlapati, X. Zhang, F. Wani Victor Jenario, X. Li, W. Liu, C. Chen, T.M. Aminabhavi, X. Zhang, Novel insights into Anammox-based processes: A critical review, Chemical Engineering Journal 444 (2022) 136534. https://doi.org/https://doi.org/10.1016/j.cej.2022.136534.
[19] M. Gao, X. Zou, H. Dang, A.N. Mohammed, S. Yang, Y. Zhou, Y. Yao, H. Guo, Y. Liu, Exploring interactions between quorum sensing communication and microbial development in anammox membrane bioreactor, Journal of Environmental Chemical Engineering 11(2) (2023) 109339. https://doi.org/https://doi.org/10.1016/j.jece.2023.109339.
[20] D.-Q. Huang, J.-J. Fu, Z.-Y. Li, N.-S. Fan, R.-C. Jin, Inhibition of wastewater pollutants on the anammox process: A review, Science of The Total Environment 803 (2022) 150009. https://doi.org/https://doi.org/10.1016/j.scitotenv.2021.150009.
[21] D.R. de Graaff, M.C.M. van Loosdrecht, M. Pronk, Stable granulation of seawater-adapted aerobic granular sludge with filamentous Thiothrix bacteria, Water Research 175 (2020) 115683. https://doi.org/https://doi.org/10.1016/j.watres.2020.115683.
[22] J. Xie, M. Guo, J. Xie, Y. Chang, A. Mabruk, T.C. Zhang, C. Chen, COD inhibition alleviation and anammox granular sludge stability improvement by biochar addition, Journal of Cleaner Production 345 (2022) 131167. https://doi.org/https://doi.org/10.1016/j.jclepro.2022.131167.
[23] L.A. Robertson, E.W.J.v. Niel, R.A.M. Torremans, J.G. Kuenen, Simultaneous Nitrification and Denitrification in Aerobic Chemostat Cultures of Thiosphaera pantotropha, Applied and Environmental Microbiology 54(11) (1988) 2812-2818. https://doi.org/10.1128/AEM.54.11.2812-2818.1988.
[24] T. Song, X. Zhang, J. Li, X. Wu, H. Feng, W. Dong, A review of research progress of heterotrophic nitrification and aerobic denitrification microorganisms (HNADMs), Science of The Total Environment 801 (2021) 149319-149319. https://doi.org/10.1016/J.SCITOTENV.2021.149319.
[25] R. Pishgar, J.A. Dominic, J.H. Tay, A. Chu, Pilot-scale investigation on nutrient removal characteristics of mineral-rich aerobic granular sludge: Identification of uncommon mechanisms, Water Research 168 (2020) 115151-115151. https://doi.org/10.1016/J.WATRES.2019.115151.
[26] J. Huang, Y. Cui, J. Yan, Y. Cui, Occurrence of heterotrophic nitrification-aerobic

denitrification induced by decreasing salinity in a halophilic AGS SBR treating hypersaline wastewater, Chemical Engineering Journal 431 (2022) 134133.
[27] M. Arnaldos, K. Pagilla, Effluent dissolved organic nitrogen and dissolved phosphorus removal by enhanced coagulation and microfiltration, Water research 44(18) (2010) 5306-5315.
[28] S.P. Mallick, Z. Mallick, B.K. Mayer, Meta-analysis of the prevalence of dissolved organic nitrogen (DON) in water and wastewater and review of DON removal and recovery strategies, Science of The Total Environment 828 (2022) 154476. https://doi.org/https://doi.org/10.1016/j.scitotenv.2022.154476.
[29] Z.P. Liu, W.H. Wu, P. Shi, J.S. Guo, J. Cheng, Characterization of dissolved organic matter in landfill leachate during the combined treatment process of air stripping, Fenton, SBR and coagulation, Waste Management 41 (2015) 111-118. https://doi.org/10.1016/J.WASMAN.2015.03.044.
[30] Z. Gu, M. Bao, C. He, W. Chen, Transformation of dissolved organic matter in landfill leachate during a membrane bioreactor treatment, Science of The Total Environment 856 (2023) 159066-159066. https://doi.org/10.1016/J.SCITOTENV.2022.159066.
[31] H. Hu, S. Ma, X. Zhang, H. Ren, Characteristics of dissolved organic nitrogen in effluent from a biological nitrogen removal process using sludge alkaline fermentation liquid as an external carbon source, Water Research 176 (2020) 115741. https://doi.org/https://doi.org/10.1016/j.watres.2020.115741.
[32] J. Wang, F. Zheng, Z. Yu, J. Chen, H. Lu, Dissolved organic nitrogen derived from wastewater denitrification: Composition and nitrogenous disinfection byproduct formation, Journal of Hazardous Materials 440 (2022) 129775-129775. https://doi.org/10.1016/J.JHAZMAT.2022.129775.
[33] M. Pronk, E.J.H. van Dijk, M.C.M. van Loosdrecht, Aerobic granular sludge, Biological Wastewater Treatment: Principles, Modelling and Design, IWA Publishing, 2023, p. 0.
[34] J. Huang, Y. Cui, J. Yan, Y. Cui, Occurrence of heterotrophic nitrification-aerobic denitrification induced by decreasing salinity in a halophilic AGS SBR treating hypersaline wastewater, Chemical Engineering Journal 431 (2022) 134133-134133. https://doi.org/10.1016/J.CEJ.2021.134133.
[35] M.K.H. Winkler, J.P. Bassin, R. Kleerebezem, D.Y. Sorokin, M.C.M. Van Loosdrecht, Unravelling the reasons for disproportion in the ratio of AOB and NOB in aerobic granular sludge, Applied Microbiology and Biotechnology 94(6) (2012) 1657-1666. https://doi.org/10.1007/S00253-012-4126-9/FIGURES/6.
[36] M. Sarvajith, G.K.K. Reddy, Y.V. Nancharaiah, Textile dye biodecolourization and ammonium removal over nitrite in aerobic granular sludge sequencing batch reactors, Journal of Hazardous Materials 342 (2018) 536-543. https://doi.org/10.1016/J.JHAZMAT.2017.08.064.
[37] S. Zheng, H. Lu, G. Zhang, The recent development of the aerobic granular sludge for industrial wastewater treatment: a mini review, Environmental Technology Reviews 9(1) (2020) 55-66. https://doi.org/10.1080/21622515.2020.1732479.
[38] Y.V. Nancharaiah, G. Kiran Kumar Reddy, Aerobic granular sludge technology: Mechanisms of granulation and biotechnological applications, Bioresource Technology 247 (2018) 1128-1143. https://doi.org/10.1016/j.biortech.2017.09.131.
[39] A.A. Khan, M. Ahmad, A. Giesen, NEREDA®: an emerging technology for sewage treatment, Water Practice and Technology 10(4) (2015) 799-805.
[40] M. Zeng, Z. Li, Y. Cheng, Y. Luo, Y. Hou, J. Wu, B. Long, Stability of aerobic granular sludge for treating inorganic wastewater with different nitrogen loading rates, Environmental

Technology 45(19) (2024) 3898-3911.
[41] M. Figueroa, A. Val del Rio, J. Campos, A. Mosquera-Corral, R. Mendez, Treatment of high loaded swine slurry in an aerobic granular reactor, Water Science and Technology 63(9) (2011) 1808-1814.
[42] Y. Ren, F. Ferraz, M. Lashkarizadeh, Q. Yuan, Comparing young landfill leachate treatment efficiency and process stability using aerobic granular sludge and suspended growth activated sludge, Journal of Water Process Engineering 17 (2017) 161-167. https://doi.org/10.1016/J.JWPE.2017.04.006.
[43] J. Wang, Z. Zhang, F. Qian, Y. Shen, Z. Qi, X. Ji, E.M.L. Kajamisso, Rapid start-up of a nitritation granular reactor using activated sludge as inoculum at the influent organics/ammonium mass ratio of 2/1, Bioresource Technology 256 (2018) 170-177. https://doi.org/10.1016/j.biortech.2018.02.017.
[44] D. Gao, L. Liu, H. Liang, W.-M. Wu, Aerobic granular sludge: characterization, mechanism of granulation and application to wastewater treatment, Critical Reviews in Biotechnology 31(2) (2011) 137-152. https://doi.org/10.3109/07388551.2010.497961.
[45] L. Wang, X. Yu, W. Xiong, P. Li, S. Wang, A. Fan, H. Su, Enhancing robustness of aerobic granule sludge under low C/N ratios with addition of kitchen wastewater, Journal of Environmental Management 265 (2020) 110503-110503. https://doi.org/10.1016/J.JENVMAN.2020.110503.
[46] X. Wang, Z. Chen, J. Shen, X. Zhao, J. Kang, Impact of carbon to nitrogen ratio on the performance of aerobic granular reactor and microbial population dynamics during aerobic sludge granulation, Bioresource Technology 271 (2019) 258-265.
[47] Z. Zhang, Z. Yu, J. Dong, Z. Wang, K. Ma, X. Xu, P.J.J. Alvarezc, L. Zhu, Stability of aerobic granular sludge under condition of low influent C/N ratio: Correlation of sludge property and functional microorganism, Bioresource Technology 270 (2018) 391-399. https://doi.org/10.1016/J.BIORTECH.2018.09.045.
[48] O.T. Iorhemen, Y. Liu, Effect of feeding strategy and organic loading rate on the formation and stability of aerobic granular sludge, Journal of Water Process Engineering 39 (2021) 101709-101709. https://doi.org/10.1016/J.JWPE.2020.101709.
[49] B. Zhang, H. Tang, D. Huang, C. Liu, W. Shi, Y. Shen, Effect of superficial gas velocity on membrane fouling behavior and evolution during municipal wastewater treatment, Separation and Purification Technology 315 (2023) 123665. https://doi.org/https://doi.org/10.1016/j.seppur.2023.123665.
[50] Q. He, W. Zhang, S. Zhang, H. Wang, Enhanced nitrogen removal in an aerobic granular sequencing batch reactor performing simultaneous nitrification, endogenous denitrification and phosphorus removal with low superficial gas velocity, Chemical Engineering Journal 326 (2017) 1223-1231. https://doi.org/https://doi.org/10.1016/j.cej.2017.06.071.
[51] Y. Zhang, X. Dong, M. Nuramkhaan, Z. Lei, K. Shimizu, Z. Zhang, Y. Adachi, D.-J. Lee, J.H. Tay, Rapid granulation of aerobic granular sludge: A mini review on operation strategies and comparative analysis, Bioresource Technology Reports 7 (2019) 100206. https://doi.org/https://doi.org/10.1016/j.biteb.2019.100206.
[52] R.D.G. Franca, H.M. Pinheiro, M.C.M. van Loosdrecht, N.D. Lourenço, Stability of aerobic granules during long-term bioreactor operation, Biotechnology Advances 36(1) (2018) 228-246. https://doi.org/https://doi.org/10.1016/j.biotechadv.2017.11.005.
[53] O.T. Iorhemen, M.S. Zaghloul, R.A. Hamza, J.H. Tay, Long-term aerobic granular sludge stability through anaerobic slow feeding, fixed feast-famine period ratio, and fixed SRT, Journal

of Environmental Chemical Engineering 8(2) (2020) 103681. https://doi.org/https://doi.org/10.1016/j.jece.2020.103681.
[54] M.-K.H. Winkler, C. Meunier, O. Henriet, J. Mahillon, M.E. Suárez-Ojeda, G. Del Moro, M. De Sanctis, C. Di Iaconi, D.G. Weissbrodt, An integrative review of granular sludge for the biological removal of nutrients and recalcitrant organic matter from wastewater, Chemical Engineering Journal 336 (2018) 489-502.
[55] S.L.d.S. Rollemberg, L.Q. de Oliveira, A.R.M. Barros, V.M.M. Melo, P.I.M. Firmino, A.B. dos Santos, Effects of carbon source on the formation, stability, bioactivity and biodiversity of the aerobic granule sludge, Bioresource Technology 278 (2019) 195-204. https://doi.org/https://doi.org/10.1016/j.biortech.2019.01.071.
[56] C. Wan, S. Chen, L. Wen, D.-J. Lee, X. Liu, Formation of bacterial aerobic granules: Role of propionate, Bioresource Technology 197 (2015) 489-494. https://doi.org/https://doi.org/10.1016/j.biortech.2015.08.137.
[57] J. Lin, H. He, J. Zou, Y. Yang, J. Li, Effects of high-concentration influent suspended solids on aerobic granulation in sequencing batch reactors treating real textile wastewater, Journal of Water Process Engineering 57 (2024) 104609. https://doi.org/https://doi.org/10.1016/j.jwpe.2023.104609.
[58] E. Cetin, E. Karakas, E. Dulekgurgen, S. Ovez, M. Kolukirik, G. Yilmaz, Effects of high-concentration influent suspended solids on aerobic granulation in pilot-scale sequencing batch reactors treating real domestic wastewater, Water Research 131 (2018) 74-89. https://doi.org/https://doi.org/10.1016/j.watres.2017.12.014.
[59] S. Wang, Q. Yang, W. Shi, S. Yu, Y. Wang, J. Li, Nitrifier augmentation for high ammonia nitrogen removal by aerobic granular sludge at low temperatures, CLEAN–Soil, Air, Water 44(5) (2016) 525-531.
[60] V.E. P.S.G. da Silva, S.L. de Sousa Rollemberg, A. Bezerra dos Santos, Impact of feeding strategy on the performance and operational stability of aerobic granular sludge treating high-strength ammonium concentrations, Journal of Water Process Engineering 44 (2021) 102378. https://doi.org/https://doi.org/10.1016/j.jwpe.2021.102378.
[61] X. Zou, Y. Zhou, M. Gao, S. Yang, A. Mohammed, Y. Liu, Effective N2O emission control during the nitritation/denitritation treatment of ammonia rich wastewater, Journal of Environmental Chemical Engineering 10(2) (2022) 107234-107234. https://doi.org/10.1016/J.JECE.2022.107234.
[62] I. Owusu-Agyeman, B. Bedaso, C. Laumeyer, C. Pan, A. Malovanyy, C. Baresel, E. Plaza, Z. Cetecioglu, Volatile fatty acids production from municipal waste streams and use as a carbon source for denitrification: The journey towards full-scale application and revealing key microbial players, Renewable and Sustainable Energy Reviews 175 (2023) 113163. https://doi.org/https://doi.org/10.1016/j.rser.2023.113163.
[63] P. Roots, A.F. Rosenthal, Q. Yuan, Y. Wang, F. Yang, J.A. Kozak, H. Zhang, G.F. Wells, Optimization of the carbon to nitrogen ratio for mainstream deammonification and the resulting shift in nitrification from biofilm to suspension, Environmental Science: Water Research & Technology 6(12) (2020) 3415-3427.
[64] A. Lacroix, C. Mentzer, K.R. Pagilla, Full-scale N removal from centrate using a sidestream process with a mainstream carbon source, Water Environment Research 92(11) (2020) 1922-1934.
[65] APHA, E.W. Rice, L. Bridgewater, Standard methods for the examination of water and wastewater, American public health association Washington, DC2012.
[66] D. Li, S. Zhang, S. Li, H. Zeng, J. Zhang, The nitrogen removal of autotrophic and

heterotrophic bacteria in aerobic granular reactors with different feast/famine ratio, Bioresource Technology 272 (2019) 370-378. https://doi.org/10.1016/J.BIORTECH.2018.10.046.
[67] H. Liu, H.H.P. Fang, Extraction of extracellular polymeric substances (EPS) of sludges, Journal of Biotechnology 95(3) (2002) 249-256. https://doi.org/10.1016/S0168-1656(02)00025-1.
[68] B. Fr/olund, T. Griebe, P.H. Nielsen, Enzymatic activity in the activated-sludge floc matrix, Applied Microbiology and Biotechnology 43(4) (1995) 755-761. https://doi.org/10.1007/BF00164784/METRICS.
[69] M. DuBois, K.A. Gilles, J.K. Hamilton, P.t. Rebers, F. Smith, Colorimetric method for determination of sugars and related substances, Analytical chemistry 28(3) (1956) 350-356.
[70] X. Song, F. Kong, B.F. Liu, Q. Song, N.Q. Ren, H.Y. Ren, Combined transcriptomic and metabolomic analyses of temperature response of microalgae using waste activated sludge extracts for promising biodiesel production, Water Research 251 (2024) 121120-121120. https://doi.org/10.1016/J.WATRES.2024.121120.
[71] X. Song, B.F. Liu, F. Kong, Q. Song, N.Q. Ren, H.Y. Ren, New insights into rare earth element-induced microalgae lipid accumulation: Implication for biodiesel production and adsorption mechanism, Water Research 251 (2024) 121134-121134. https://doi.org/10.1016/J.WATRES.2024.121134.
[72] X. Zhang, S. Zheng, H. Zhang, S. Duan, Autotrophic and heterotrophic nitrification-anoxic denitrification dominated the anoxic/oxic sewage treatment process during optimization for higher loading rate and energy savings, Bioresource Technology 263 (2018) 84-93. https://doi.org/10.1016/J.BIORTECH.2018.04.113.
[73] Y. Zhao, J. Huang, H. Zhao, H. Yang, Microbial community and N removal of aerobic granular sludge at high COD and N loading rates, Bioresource Technology 143 (2013) 439-446. https://doi.org/10.1016/J.BIORTECH.2013.06.020.
[74] S.F. Yang, J.-H.H. Tay, Y. Liu, Respirometric Activities of Heterotrophic and Nitrifying Populations in Aerobic Granules Developed at Different Substrate N/COD Ratios, Current Microbiology 2004 49:1 49(1) (2004) 42-46.
[75] R.A. Hamza, M.S. Zaghloul, O.T. Iorhemen, Z. Sheng, J.H. Tay, Optimization of organics to nutrients (COD:N:P) ratio for aerobic granular sludge treating high-strength organic wastewater, Science of The Total Environment 650 (2019) 3168-3179. https://doi.org/10.1016/J.SCITOTENV.2018.10.026.
[76] O. Terna Iorhemen, S. Ukaigwe, H. Dang, Y. Liu, Phosphorus Removal from Aerobic Granular Sludge: Proliferation of Polyphosphate-Accumulating Organisms (PAOs) under Different Feeding Strategies, Processes 2022, Vol. 10, Page 1399 10(7) (2022) 1399-1399. https://doi.org/10.3390/PR10071399.
[77] B.J. Callahan, P.J. McMurdie, M.J. Rosen, A.W. Han, A.J.A. Johnson, S.P. Holmes, DADA2: High-resolution sample inference from Illumina amplicon data, Nature Methods 13(7) (2016) 581-583. https://doi.org/10.1038/nmeth.3869.
[78] D. McDonald, M.N. Price, J. Goodrich, E.P. Nawrocki, T.Z. Desantis, A. Probst, G.L. Andersen, R. Knight, P. Hugenholtz, An improved Greengenes taxonomy with explicit ranks for ecological and evolutionary analyses of bacteria and archaea, The ISME Journal 2012 6:3 6(3) (2011) 610-618. https://doi.org/10.1038/ismej.2011.139.
[79] J.J. Werner, O. Koren, P. Hugenholtz, T.Z. Desantis, W.A. Walters, J.G. Caporaso, L.T. Angenent, R. Knight, R.E. Ley, Impact of training sets on classification of high-throughput bacterial 16s rRNA gene surveys, ISME Journal 6(1) (2012) 94-94.

https://doi.org/10.1038/ismej.2011.82.
[80] G.M. Douglas, V.J. Maffei, J.R. Zaneveld, S.N. Yurgel, J.R. Brown, C.M. Taylor, C. Huttenhower, M.G.I. Langille, PICRUSt2 for prediction of metagenome functions, Nature Biotechnology 2020 38:6 38(6) (2020) 685-688. https://doi.org/10.1038/s41587-020-0548-6.
[81] I. González, S. Déjean, CCA: Canonical correlation analysis, (R package version 1) (2012).
[82] P. Bucci, B. Coppotelli, I. Morelli, N. Zaritzky, A. Caravelli, Micronutrients and COD/N ratio as factors influencing granular size and SND in aerobic granular sequencing batch reactors operated at low organic loading, Journal of Water Process Engineering 46 (2022) 102625-102625. https://doi.org/10.1016/J.JWPE.2022.102625.
[83] S. Yang, J. Tay, Y. Liu, Effect of Substrate Nitrogen/Chemical Oxygen Demand Ratio on the Formation of Aerobic Granules, Journal of Environmental Engineering 131(1) (2005) 86-92. https://doi.org/10.1061/(ASCE)0733-9372(2005)131:1(86).
[84] S.F. Yang, J.H. Tay, Y. Liu, Inhibition of free ammonia to the formation of aerobic granules, Biochemical Engineering Journal 17(1) (2004) 41-48. https://doi.org/10.1016/S1369-703X(03)00122-0.
[85] Y. Liu, Q.S. Liu, Causes and control of filamentous growth in aerobic granular sludge sequencing batch reactors, Biotechnology Advances 24(1) (2006) 115-127. https://doi.org/10.1016/J.BIOTECHADV.2005.08.001.
[86] W. Metcalf, C. Eddy, Wastewater engineering: treatment and recovery reuse, Wastewater Engineering: Treatment and Reuse McGraw Hill. New York, NY. (2013).
[87] Y. Sun, L. Feng, A. Li, X. Zhang, J. Yang, F. Ma, Ammonium assimilation: An important accessory during aerobic denitrification of Pseudomonas stutzeri T13, Bioresource Technology 234 (2017) 264-272. https://doi.org/10.1016/J.BIORTECH.2017.03.053.
[88] X. Zou, A. Mohammed, M. Gao, Y. Liu, Mature landfill leachate treatment using granular sludge-based reactor (GSR) via nitritation/denitritation: Process startup and optimization, Science of The Total Environment 844 (2022) 157078-157078. https://doi.org/10.1016/J.SCITOTENV.2022.157078.
[89] Z. An, T.R. Kent, Y. Sun, C.B. Bott, Z.W. Wang, Free ammonia resistance of nitrite-oxidizing bacteria developed in aerobic granular sludge cultivated in continuous upflow airlift reactors performing partial nitritation, Water Environment Research 93(3) (2021) 421-432. https://doi.org/10.1002/WER.1440.
[90] B. Nguyen Quoc, S. Wei, M. Armenta, R. Bucher, P. Sukapanpotharam, D.A. Stahl, H.D. Stensel, M.K.H. Winkler, Aerobic granular sludge: Impact of size distribution on nitrification capacity, Water Research 188 (2021) 116445-116445. https://doi.org/10.1016/J.WATRES.2020.116445.
[91] G. Xu, Z. Zhang, F. Gao, Effect of COD/N ratios and DO concentrations on the NOB suppression in a multi-cycle SBR, Journal of Environmental Chemical Engineering 9(4) (2021) 105735-105735. https://doi.org/10.1016/J.JECE.2021.105735.
[92] Y. Shao, S. Yang, A. Mohammed, Y. Liu, Impacts of ammonium loading on nitritation stability and microbial community dynamics in the integrated fixed-film activated sludge sequencing batch reactor (IFAS-SBR), International Biodeterioration and Biodegradation 133 (2018) 63-69. https://doi.org/10.1016/j.ibiod.2018.06.002.
[93] Y.Z. Peng, G.B. Zhu, Biological nitrogen removal with nitrification and denitrification via nitrite pathway, Applied Microbiology and Biotechnology 73(1) (2006) 15-26. https://doi.org/10.1007/s00253-006-0534-z.
[94] Q. Chen, J. Ni, T. Ma, T. Liu, M. Zheng, Bioaugmentation treatment of municipal wastewater

with heterotrophic-aerobic nitrogen removal bacteria in a pilot-scale SBR, Bioresource Technology 183 (2015) 25-32. https://doi.org/10.1016/J.BIORTECH.2015.02.022.
[95] B. Ji, K. Yang, L. Zhu, Y. Jiang, H. Wang, J. Zhou, H. Zhang, Aerobic denitrification: A review of important advances of the last 30 years, Biotechnology and Bioprocess Engineering 2015 20:4 20(4) (2015) 643-651. https://doi.org/10.1007/S12257-015-0009-0.
[96] M. Zheng, D. He, T. Ma, Q. Chen, S. Liu, M. Ahmad, M. Gui, J. Ni, Reducing NO and N2O emission during aerobic denitrification by newly isolated Pseudomonas stutzeri PCN-1, Bioresource Technology 162 (2014) 80-88. https://doi.org/10.1016/J.BIORTECH.2014.03.125.
[97] Y. Luo, J. Yao, X. Wang, M. Zheng, D. Guo, Y. Chen, Efficient municipal wastewater treatment by oxidation ditch process at low temperature: Bacterial community structure in activated sludge, Science of The Total Environment 703 (2020) 135031-135031. https://doi.org/10.1016/J.SCITOTENV.2019.135031.
[98] P. Świątczak, A. Cydzik-Kwiatkowska, Performance and microbial characteristics of biomass in a full-scale aerobic granular sludge wastewater treatment plant, Environmental Science and Pollution Research 25(2) (2018) 1655-1669. https://doi.org/10.1007/S11356-017-0615-9/FIGURES/6.
[99] Y. Guo, W. Shi, B. Zhang, W. Li, P.N.L. Lens, Effect of voltage intensity on the nutrient removal performance and microbial community in the iron electrolysis-integrated aerobic granular sludge system, Environmental Pollution 274 (2021) 116604-116604. https://doi.org/10.1016/J.ENVPOL.2021.116604.
[100] Y. Wang, J. Geng, Z. Ren, G. Guo, C. Wang, H. Wang, Effect of COD/N and COD/P ratios on the PHA transformation and dynamics of microbial community structure in a denitrifying phosphorus removal process, Journal of Chemical Technology & Biotechnology 88(7) (2013) 1228-1236. https://doi.org/10.1002/JCTB.3962.
[101] E.R. Coats, C.K. Brinkman, S. Lee, Characterizing and contrasting the microbial ecology of laboratory and full-scale EBPR systems cultured on synthetic and real wastewaters, Water Research 108 (2017) 124-136. https://doi.org/10.1016/J.WATRES.2016.10.069.
[102] S. Chen, S. Li, T. Huang, S. Yang, K. Liu, B. Ma, Y. Shi, Y. Miao, Nitrate reduction by Paracoccus thiophilus strain LSL 251 under aerobic condition: Performance and intracellular central carbon flux pathways, Bioresource Technology 308 (2020) 123301-123301. https://doi.org/10.1016/J.BIORTECH.2020.123301.
[103] C. Fall, L.M. Barrón-Hernández, V.E. Gonzaga-Galeana, M.T. Olguín, Ordinary heterotrophic organisms with aerobic storage capacity provide stable aerobic granular sludge for C and N removal, Journal of Environmental Management 308 (2022) 114662-114662. https://doi.org/10.1016/J.JENVMAN.2022.114662.
[104] M.G.E. Albuquerque, G. Carvalho, C. Kragelund, A.F. Silva, M.T. Barreto Crespo, M.A.M. Reis, P.H. Nielsen, Link between microbial composition and carbon substrate-uptake preferences in a PHA-storing community, The ISME Journal 2013 7:1 7(1) (2012) 1-12. https://doi.org/10.1038/ismej.2012.74.
[105] A. Sarkar, B. Reinhold-Hurek, Transcriptional Profiling of Nitrogen Fixation and the Role of NifA in the Diazotrophic Endophyte Azoarcus sp. Strain BH72, PLOS ONE 9(2) (2014) e86527-e86527. https://doi.org/10.1371/JOURNAL.PONE.0086527.
[106] M. Geng, S. You, H. Guo, F. Ma, X. Xiao, J. Zhang, Impact of fungal pellets dosage on long-term stability of aerobic granular sludge, Bioresource Technology 332 (2021) 125106-125106. https://doi.org/10.1016/j.biortech.2021.125106.
[107] P. Regmi, M.W. Miller, B. Holgate, R. Bunce, H. Park, K. Chandran, B. Wett, S. Murthy,

C.B. Bott, Control of aeration, aerobic SRT and COD input for mainstream nitritation/denitritation, Water Research 57 (2014) 162-171. https://doi.org/10.1016/J.WATRES.2014.03.035.
[108] L. Xia, X. Li, W. Fan, J. Wang, Heterotrophic nitrification and aerobic denitrification by a novel Acinetobacter sp. ND7 isolated from municipal activated sludge, Bioresource Technology 301 (2020) 122749-122749. https://doi.org/10.1016/J.BIORTECH.2020.122749.
[109] Y. Zhang, Y. Wang, Y. Yan, H. Han, M. Wu, Characterization of CANON reactor performance and microbial community shifts with elevated COD/N ratios under a continuous aeration mode, Frontiers of Environmental Science & Engineering 2019 13:1 13(1) (2018) 1-13. https://doi.org/10.1007/S11783-019-1095-6.
[110] Y. Liu, H.H. Ngo, W. Guo, L. Peng, D. Wang, B. Ni, The roles of free ammonia (FA) in biological wastewater treatment processes: A review, Environment International 123 (2019) 10-19. https://doi.org/10.1016/J.ENVINT.2018.11.039.
[111] L. Zhang, A. Mou, B. Guo, H. Sun, M.N. Anwar, Y. Liu, Simultaneous Phosphorus Recovery in Energy Generation Reactor (SPRING): High Rate Thermophilic Blackwater Treatment, Resources, Conservation and Recycling 164 (2021) 105163. https://doi.org/https://doi.org/10.1016/j.resconrec.2020.105163.
[112] J. Ekholm, F. Persson, M. de Blois, O. Modin, M. Pronk, M.C. van Loosdrecht, C. Suarez, D.J. Gustavsson, B.-M. Wilén, Full-scale aerobic granular sludge for municipal wastewater treatment–granule formation, microbial succession, and process performance, Environmental Science: Water Research & Technology 8(12) (2022) 3138-3154.
[113] L. Lei, J.-c. Yao, Y.-d. Liu, W. Li, Performance, sludge characteristics and microbial community in a salt-tolerant aerobic granular SBR by seeding anaerobic granular sludge, International Biodeterioration & Biodegradation 163 (2021) 105258. https://doi.org/https://doi.org/10.1016/j.ibiod.2021.105258.
[114] S. Cao, W. Yan, L. Yu, L. Zhang, W. Lay, Y. Zhou, Challenges of THP-AD centrate treatment using partial nitritation-anammox (PN/A) – inhibition, biomass washout, low alkalinity, recalcitrant and more, Water Research 203 (2021) 117555. https://doi.org/https://doi.org/10.1016/j.watres.2021.117555.
[115] O.T. Iorhemen, Y. Liu, Effect of feeding strategy and organic loading rate on the formation and stability of aerobic granular sludge, Journal of Water Process Engineering 39 (2021) 101709.
[116] J.J. Werner, O. Koren, P. Hugenholtz, T.Z. DeSantis, W.A. Walters, J.G. Caporaso, L.T. Angenent, R. Knight, R.E. Ley, Impact of training sets on classification of high-throughput bacterial 16s rRNA gene surveys, The ISME Journal 6(1) (2012) 94-103. https://doi.org/10.1038/ismej.2011.82.
[117] B. Guo, Z. Sheng, Y. Liu, Evaluation of influent microbial immigration to activated sludge is affected by different-sized community segregation, npj Clean Water 4(1) (2021) 20.
[118] R. Mei, T. Narihiro, M.K. Nobu, K. Kuroda, W.-T. Liu, Evaluating digestion efficiency in full-scale anaerobic digesters by identifying active microbial populations through the lens of microbial activity, Scientific reports 6(1) (2016) 34090.
[119] E. Pasciucco, F. Pasciucco, R. Iannelli, I. Pecorini, A Fenton-based approach at neutral and un-conditioned pH for recalcitrant COD removal in tannery wastewater: Experimental test and sludge characterization, Science of The Total Environment 926 (2024) 172070. https://doi.org/https://doi.org/10.1016/j.scitotenv.2024.172070.
[120] Q.Q. Cai, B.C.Y. Lee, S.L. Ong, J.Y. Hu, Fluidized-bed Fenton technologies for recalcitrant industrial wastewater treatment–Recent advances, challenges and perspective, Water Research 190 (2021) 116692. https://doi.org/https://doi.org/10.1016/j.watres.2020.116692.

[121] J.-h. Zhou, Z.-m. Zhang, H. Zhao, H.-t. Yu, P.J. Alvarez, X.-y. Xu, L. Zhu, Optimizing granules size distribution for aerobic granular sludge stability: effect of a novel funnel-shaped internals on hydraulic shear stress, Bioresource Technology 216 (2016) 562-570.
[122] C. Huang, Q. Liu, Z.-L. Li, X.-d. Ma, Y.-N. Hou, N.-Q. Ren, A.-J. Wang, Relationship between functional bacteria in a denitrification desulfurization system under autotrophic, heterotrophic, and mixotrophic conditions, Water Research 188 (2021) 116526. https://doi.org/https://doi.org/10.1016/j.watres.2020.116526.
[123] X. Zou, A. Mohammed, M. Gao, Y. Liu, Mature landfill leachate treatment using granular sludge-based reactor (GSR) via nitritation/denitritation: Process startup and optimization, Science of The Total Environment 844 (2022) 157078.
[124] X. Zou, Y. Zhang, M. Gao, Y. Yao, H. Guo, Y. Liu, Enhancing biological dissolved organic nitrogen removal in landfill leachate wastewater: The role of sodium acetate co-metabolism, Chemical Engineering Journal (2023) 147714. https://doi.org/https://doi.org/10.1016/j.cej.2023.147714.
[125] C. Kao, J. Li, R. Gao, W. Li, X. Li, Q. Zhang, Y. Peng, Advanced nitrogen removal from real municipal wastewater by multiple coupling nitritation, denitritation and endogenous denitritation with anammox in a single suspended sludge bioreactor, Water Research 221 (2022) 118749. https://doi.org/https://doi.org/10.1016/j.watres.2022.118749.
[126] H. Liu, X. Zhou, W. Ding, Z. Zhang, L.D. Nghiem, J. Sun, Q. Wang, Do Microplastics Affect Biological Wastewater Treatment Performance? Implications from Bacterial Activity Experiments, ACS Sustainable Chemistry & Engineering 7(24) (2019) 20097-20101. https://doi.org/10.1021/acssuschemeng.9b05960.
[127] X. Gu, Y. Huang, Y. Hu, W. Huang, M. Zhang, Impact of nitrite on partial nitrification in aerobic sewage treatment reactors under mainstream conditions, Journal of Environmental Chemical Engineering 10(5) (2022) 108414. https://doi.org/https://doi.org/10.1016/j.jece.2022.108414.
[128] A. Alvarez, J.M. Saez, J.S. Davila Costa, V.L. Colin, M.S. Fuentes, S.A. Cuozzo, C.S. Benimeli, M.A. Polti, M.J. Amoroso, Actinobacteria: Current research and perspectives for bioremediation of pesticides and heavy metals, Chemosphere 166 (2017) 41-62. https://doi.org/https://doi.org/10.1016/j.chemosphere.2016.09.070.
[129] H. Zhang, W. Yang, B. Ma, X. Liu, T. Huang, L. Niu, K. Zhao, Y. Yang, H. Li, Aerobic denitrifying using actinobacterial consortium: Novel denitrifying microbe and its application, Science of The Total Environment 859 (2023) 160236. https://doi.org/https://doi.org/10.1016/j.scitotenv.2022.160236.
[130] M. Gao, B. Guo, L. Li, Y. Liu, Role of syntrophic acetate oxidation and hydrogenotrophic methanogenesis in co-digestion of blackwater with food waste, Journal of Cleaner Production 283 (2021) 125393. https://doi.org/https://doi.org/10.1016/j.jclepro.2020.125393.
[131] C. Mao, Y. Wang, X. Wang, G. Ren, L. Yuan, Y. Feng, Correlations between microbial community and C:N:P stoichiometry during the anaerobic digestion process, Energy 174 (2019) 687-695. https://doi.org/https://doi.org/10.1016/j.energy.2019.02.078.
[132] M. Ali, Z. Wang, K.W. Salam, A.R. Hari, M. Pronk, M.C. van Loosdrecht, P.E. Saikaly, Importance of species sorting and immigration on the bacterial assembly of different-sized aggregates in a full-scale aerobic granular sludge plant, Environmental science & technology 53(14) (2019) 8291-8301.
[133] Q. Yin, Y. Sun, B. Li, Z. Feng, G. Wu, The r/K selection theory and its application in biological wastewater treatment processes, Science of The Total Environment 824 (2022) 153836.

https://doi.org/https://doi.org/10.1016/j.scitotenv.2022.153836.
[134] X. Zou, M. Gao, A. Mohammed, Y. Liu, Responses of various carbon to nitrogen ratios to microbial communities, kinetics, and nitrogen metabolic pathways in aerobic granular sludge reactor, Bioresource Technology 367 (2023) 128225. https://doi.org/https://doi.org/10.1016/j.biortech.2022.128225.
[135] Y.-T. Lv, Y. Su, M. Li, L. Lin, X. Wang, L. Wang, Achievement of partial denitrification in SBR treating acidic wastewater: Performance and mechanism of nitrite accumulation, Journal of Water Process Engineering 55 (2023) 104251. https://doi.org/https://doi.org/10.1016/j.jwpe.2023.104251.
[136] J. Hu, T. Li, Y. Zhao, X. Zhang, H. Ren, H. Huang, A novel in-situ enhancement strategy of denitrification biofilter for simultaneous removal of steroid estrogens and total nitrogen from low C/N wastewater, Chemical Engineering Journal 452 (2023) 138896. https://doi.org/https://doi.org/10.1016/j.cej.2022.138896.
[137] S. Zheng, X. Liu, X. Yang, H. Zhou, J. Fang, S. Gong, J. Yang, J. Chen, T. Lu, M. Zeng, Y. Qin, The nitrogen removal performance and microbial community on mixotrophic denitrification process, Bioresource Technology 363 (2022) 127901. https://doi.org/https://doi.org/10.1016/j.biortech.2022.127901.
[138] L. Yang, Y. Qin, X. Liu, Z. Liu, S. Zheng, J. Chen, S. Gong, J. Yang, T. Lu, The performance and microbial communities of Anammox and Sulfide-dependent autotrophic denitrification coupling system based on the gel immobilization, Bioresource Technology 356 (2022) 127287. https://doi.org/https://doi.org/10.1016/j.biortech.2022.127287.
[139] F. Chen, Z.-L. Li, M. Lv, C. Huang, B. Liang, Y. Yuan, X.-Q. Lin, X.-Y. Gao, A.-J. Wang, Recirculation ratio regulates denitrifying sulfide removal and elemental sulfur recovery by altering sludge characteristics and microbial community composition in an EGSB reactor, Environmental Research 181 (2020) 108905. https://doi.org/https://doi.org/10.1016/j.envres.2019.108905.
[140] H.-J. Yan, Y.-W. Cui, S.-C. Han, Promoting enrichment of sulfur-oxidizing autotrophic denitrifiers via static magnetic fields: Performance and mechanism of magnetic biological effects, Bioresource Technology 347 (2022) 126388. https://doi.org/https://doi.org/10.1016/j.biortech.2021.126388.
[141] Z. Xia, Q. Wang, Z. She, M. Gao, Y. Zhao, L. Guo, C. Jin, Nitrogen removal pathway and dynamics of microbial community with the increase of salinity in simultaneous nitrification and denitrification process, Science of The Total Environment 697 (2019) 134047. https://doi.org/https://doi.org/10.1016/j.scitotenv.2019.134047.
[142] C.M. Spirito, S.E. Daly, J.J. Werner, L.T. Angenent, Redundancy in Anaerobic Digestion Microbiomes during Disturbances by the Antibiotic Monensin, Applied and Environmental Microbiology 84(9) (2018) e02692-17. https://doi.org/doi:10.1128/AEM.02692-17.
[143] M. Wang, H. Chen, S. Chang, Linkage among the combined temperature–retention time condition, microbial interaction, community structure, and process performance in the hydrolysis of waste activated sludge, Bioresource Technology 331 (2021) 125029. https://doi.org/https://doi.org/10.1016/j.biortech.2021.125029.
[144] M.L.B. Da Silva, M.E. Cantão, M.P. Mezzari, J. Ma, C.W. Nossa, Assessment of Bacterial and Archaeal Community Structure in Swine Wastewater Treatment Processes, Microbial Ecology 70(1) (2015) 77-87. https://doi.org/10.1007/s00248-014-0537-8.
[145] J.X. Lim, Y. Zhou, V.M. Vadivelu, Enhanced volatile fatty acid production and microbial population analysis in anaerobic treatment of high strength wastewater, Journal of Water Process

Engineering 33 (2020) 101058. https://doi.org/https://doi.org/10.1016/j.jwpe.2019.101058.
[146] M.-h. Zhong, L. Yang, K. Xiong, H.-l. Yang, X.-l. Wang, Exploring the mechanism of Self-Consistent balance between microbiota and high efficiency in wastewater treatment, Bioresource Technology 374 (2023) 128785. https://doi.org/https://doi.org/10.1016/j.biortech.2023.128785.
[147] M. Custodio, R. Peñaloza, C. Espinoza, W. Espinoza, J. Mezarina, Treatment of dairy industry wastewater using bacterial biomass isolated from eutrophic lake sediments for the production of agricultural water, Bioresource Technology Reports 17 (2022) 100891. https://doi.org/https://doi.org/10.1016/j.biteb.2021.100891.
[148] L. Li, G. Qian, L. Ye, X. Hu, X. Yu, W. Lyu, Research on the enhancement of biological nitrogen removal at low temperatures from ammonium-rich wastewater by the bio-electrocoagulation technology in lab-scale systems, pilot-scale systems and a full-scale industrial wastewater treatment plant, Water Research 140 (2018) 77-89. https://doi.org/10.1016/J.WATRES.2018.04.036.
[149] S. Zhu, H. Wu, C. Wu, G. Qiu, C. Feng, C. Wei, Structure and function of microbial community involved in a novel full-scale prefix oxic coking wastewater treatment O/H/O system, Water Research 164 (2019) 114963. https://doi.org/https://doi.org/10.1016/j.watres.2019.114963.
[150] T.R. Kent, Y. Sun, Z. An, C.B. Bott, Z.-W. Wang, Mechanistic understanding of the NOB suppression by free ammonia inhibition in continuous flow aerobic granulation bioreactors, Environment International 131 (2019) 105005. https://doi.org/https://doi.org/10.1016/j.envint.2019.105005.
[151] Y. Zhou, C. Wang, X. Xu, L. Liu, G. Zhang, F. Yang, Advance nitrogen removal from anaerobic sludge digestion liquor using partial nitrification and denitrification coupled with simultaneous partial nitrification, anammox, and denitrification process, Bioresource Technology 393 (2024) 130117. https://doi.org/https://doi.org/10.1016/j.biortech.2023.130117.
[152] C. Reino, J. Carrera, Impact of the nitrifying community dynamics on the partial nitritation process performed by an AOB-enriched culture in a granular sludge airlift reactor, Journal of Environmental Chemical Engineering 9(6) (2021) 106691. https://doi.org/https://doi.org/10.1016/j.jece.2021.106691.
[153] M. Zhi, Z. Zhou, C. Yang, Y. Chen, Y. Xiao, F. Meng, Solid retention time regulates partial nitrification by algal-bacterial consortia in wastewater treatment: Performance and mechanism, Chemical Engineering Journal 452 (2023) 139537. https://doi.org/https://doi.org/10.1016/j.cej.2022.139537.
[154] X. Zou, Y. Zhou, M. Gao, S. Yang, A. Mohammed, Y. Liu, Effective N2O emission control during the nitritation/denitritation treatment of ammonia rich wastewater, Journal of Environmental Chemical Engineering 10(2) (2022) 107234. https://doi.org/https://doi.org/10.1016/j.jece.2022.107234.
[155] X. Han, Y. Jin, J. Yu, Rapid formation of aerobic granular sludge by bioaugmentation technology: A review, Chemical Engineering Journal 437 (2022) 134971. https://doi.org/https://doi.org/10.1016/j.cej.2022.134971.
[156] B. Zhang, W. Li, Y. Guo, Z. Zhang, W. Shi, F. Cui, P.N.L. Lens, J.H. Tay, A sustainable strategy for effective regulation of aerobic granulation: Augmentation of the signaling molecule content by cultivating AHL-producing strains, Water Research 169 (2020) 115193. https://doi.org/https://doi.org/10.1016/j.watres.2019.115193.
[157] G. Yang, N. Zhang, J. Yang, Q. Fu, Y. Wang, D. Wang, L. Tang, J. Xia, X. Liu, X. Li, Q. Yang, Y. Liu, Q. Wang, B.-J. Ni, Interaction between perfluorooctanoic acid and aerobic granular sludge, Water Research 169 (2020) 115249.

https://doi.org/https://doi.org/10.1016/j.watres.2019.115249.
[158] M. Pronk, M. De Kreuk, B. De Bruin, P. Kamminga, R.v. Kleerebezem, M. Van Loosdrecht, Full scale performance of the aerobic granular sludge process for sewage treatment, Water research 84 (2015) 207-217.
[159] X. Liu, D. Wang, Z. Chen, W. Wei, G. Mannina, B.-J. Ni, Advances in pretreatment strategies to enhance the biodegradability of waste activated sludge for the conversion of refractory substances, Bioresource Technology 362 (2022) 127804. https://doi.org/https://doi.org/10.1016/j.biortech.2022.127804.
[160] Z. Wang, M. Zheng, Y. Xue, J. Xia, H. Zhong, G. Ni, Y. Liu, Z. Yuan, S. Hu, Free ammonia shock treatment eliminates nitrite-oxidizing bacterial activity for mainstream biofilm nitritation process, Chemical Engineering Journal 393 (2020) 124682. https://doi.org/https://doi.org/10.1016/j.cej.2020.124682.
[161] J. Meng, Z. Hu, Z. Wang, S. Hu, Y. Liu, H. Guo, J. Li, Z. Yuan, M. Zheng, Determining Factors for Nitrite Accumulation in an Acidic Nitrifying System: Influent Ammonium Concentration, Operational pH, and Ammonia-Oxidizing Community, Environmental Science & Technology 56(16) (2022) 11578-11588. https://doi.org/10.1021/acs.est.1c07522.
[162] Y.V. Nancharaiah, M. Sarvajith, Aerobic granular sludge process: a fast growing biological treatment for sustainable wastewater treatment, Current Opinion in Environmental Science & Health 12 (2019) 57-65. https://doi.org/https://doi.org/10.1016/j.coesh.2019.09.011.
[163] Y. Liu, S.-F. Yang, J.-H. Tay, Improved stability of aerobic granules by selecting slow-growing nitrifying bacteria, Journal of Biotechnology 108(2) (2004) 161-169. https://doi.org/https://doi.org/10.1016/j.jbiotec.2003.11.008.
[164] X. Zou, M. Gao, Y. Yao, Y. Zhang, H. Guo, Y. Liu, Efficient nitrogen removal from ammonia rich wastewater using aerobic granular sludge (AGS) reactor: Selection and enrichment of effective microbial community, Environmental Research (2024) 118573. https://doi.org/https://doi.org/10.1016/j.envres.2024.118573.
[165] M.R. McLaren, B.J. Callahan, Silva 138.1 prokaryotic SSU taxonomic training data formatted for DADA2, Zenodo (2021).
[166] K.S. Andersen, R.H. Kirkegaard, S.M. Karst, M. Albertsen, ampvis2: an R package to analyse and visualise 16S rRNA amplicon data, BioRxiv (2018) 299537.
[167] J. Wang, J. Song, F. Yin, Y. Shen, D. Yang, W. Liu, Insight into how high dissolved oxygen favors the startup of nitritation with aerobic granules, Chemosphere 270 (2021) 128643. https://doi.org/https://doi.org/10.1016/j.chemosphere.2020.128643.
[168] L. Wu, C. Peng, Y. Peng, L. Li, S. Wang, Y. Ma, Effect of wastewater COD/N ratio on aerobic nitrifying sludge granulation and microbial population shift, Journal of Environmental Sciences 24(2) (2012) 234-241. https://doi.org/https://doi.org/10.1016/S1001-0742(11)60719-5.
[169] T. Peng, Y. Wang, J. Wang, F. Fang, P. Yan, Z. Liu, Effect of different forms and components of EPS on sludge aggregation during granulation process of aerobic granular sludge, Chemosphere 303 (2022) 135116. https://doi.org/https://doi.org/10.1016/j.chemosphere.2022.135116.
[170] Y. Wang, J. Wang, Z. Liu, X. Huang, F. Fang, J. Guo, P. Yan, Effect of EPS and its forms of aerobic granular sludge on sludge aggregation performance during granulation process based on XDLVO theory, Science of The Total Environment 795 (2021) 148682. https://doi.org/https://doi.org/10.1016/j.scitotenv.2021.148682.
[171] M. Basuvaraj, J. Fein, S.N. Liss, Protein and polysaccharide content of tightly and loosely bound extracellular polymeric substances and the development of a granular activated sludge floc,

Water Research 82 (2015) 104-117. https://doi.org/https://doi.org/10.1016/j.watres.2015.05.014.
[172] C.S. Laspidou, B.E. Rittmann, A unified theory for extracellular polymeric substances, soluble microbial products, and active and inert biomass, Water Research 36(11) (2002) 2711-2720. https://doi.org/https://doi.org/10.1016/S0043-1354(01)00413-4.
[173] J. Liu, X. Han, X. Zhu, J. Li, D. Zhong, L. Wei, H. Liang, A systemic evaluation of aerobic granular sludge among granulation, operation, storage, and reactivation processes in an SBR, Environmental Research 235 (2023) 116594. https://doi.org/https://doi.org/10.1016/j.envres.2023.116594.
[174] J. Luo, H. Chen, X. Han, Y. Sun, Z. Yuan, J. Guo, Microbial community structure and biodiversity of size-fractionated granules in a partial nitritation–anammox process, FEMS Microbiology Ecology 93(6) (2017). https://doi.org/10.1093/femsec/fix021.
[175] Y. Zhang, Z. Ji, Y. Pei, Nutrient removal and microbial community structure in an artificial-natural coupled wetland system, Process Safety and Environmental Protection 147 (2021) 1160-1170. https://doi.org/https://doi.org/10.1016/j.psep.2021.01.036.
[176] Y. Zhao, Q. Lu, Y. Wei, H. Cui, X. Zhang, X. Wang, S. Shan, Z. Wei, Effect of actinobacteria agent inoculation methods on cellulose degradation during composting based on redundancy analysis, Bioresource technology 219 (2016) 196-203.
[177] D. Dodd, R.I. Mackie, I.K. Cann, Xylan degradation, a metabolic property shared by rumen and human colonic Bacteroidetes, Molecular microbiology 79(2) (2011) 292-304.
[178] J. Wang, H. Wang, R. Zhang, L. Wei, R. Cao, L. Wang, Z. Lou, Variations of nitrogen-metabolizing enzyme activity and microbial community under typical loading conditions in full-scale leachate anoxic/aerobic system, Bioresource Technology 351 (2022) 126946. https://doi.org/https://doi.org/10.1016/j.biortech.2022.126946.
[179] C. Wang, M. Wu, C. Peng, F. Yan, Y. Jia, X. Li, M. Li, B. Wu, H. Xu, Z. Qiu, Bacterial dynamics and functions driven by a novel microbial agent to promote kitchen waste composting and reduce environmental burden, Journal of Cleaner Production 337 (2022) 130491. https://doi.org/https://doi.org/10.1016/j.jclepro.2022.130491.
[180] Z. Yang, S. Shi, X. He, M. Cao, H. Lin, J. Fu, J. Zhou, High-efficient nutrient removal in a single-stage electrolysis-integrated sequencing batch biofilm reactor (E-SBBR) for low C/N sanitary sewage treatment, Journal of Environmental Management 351 (2024) 119848. https://doi.org/https://doi.org/10.1016/j.jenvman.2023.119848.
[181] C. Ospina-Betancourth, K. Acharya, B. Allen, J. Entwistle, I.M. Head, J. Sanabria, T.P. Curtis, Enrichment of Nitrogen-Fixing Bacteria in a Nitrogen-Deficient Wastewater Treatment System, Environmental Science & Technology 54(6) (2020) 3539-3548. https://doi.org/10.1021/acs.est.9b05322.
[182] D. Li, W. Li, D. Zhang, K. Zhang, L. Lv, G. Zhang, Performance and mechanism of modified biological nutrient removal process in treating low carbon-to-nitrogen ratio wastewater, Bioresource Technology 367 (2023) 128254. https://doi.org/https://doi.org/10.1016/j.biortech.2022.128254.
[183] N. Yang, H. Luo, X. Xiong, M. Liu, G. Zhan, X. Jin, W. Tang, Z. Chen, Y. Lei, Deciphering three-dimensional bioanode configuration for augmenting power generation and nitrogen removal in air–cathode microbial fuel cells, Bioresource Technology 379 (2023) 129026. https://doi.org/https://doi.org/10.1016/j.biortech.2023.129026.
[184] Z. Yang, L. Zhang, C. Nie, Q. Hou, S. Zhang, H. Pei, Multiple anodic chambers sharing an algal raceway pond to establish a photosynthetic microbial fuel cell stack: Voltage boosting accompany wastewater treatment, Water Research 164 (2019) 114955.

https://doi.org/https://doi.org/10.1016/j.watres.2019.114955.
[185] H. Shu, H. Sun, W. Huang, Y. Zhao, Y. Ma, W. Chen, Y. Sun, X. Chen, P. Zhong, H. Yang, X. Wu, M. Huang, S. Liao, Nitrogen removal characteristics and potential application of the heterotrophic nitrifying-aerobic denitrifying bacteria Pseudomonas mendocina S16 and Enterobacter cloacae DS'5 isolated from aquaculture wastewater ponds, Bioresource Technology 345 (2022) 126541. https://doi.org/https://doi.org/10.1016/j.biortech.2021.126541.
[186] J. Che, Y. Bai, X. Li, J. Ye, H. Liao, P. Cui, Z. Yu, S. Zhou, Linking microbial community structure with molecular composition of dissolved organic matter during an industrial-scale composting, Journal of hazardous materials 405 (2021) 124281.
[187] L. de Almeida Fernandes, A.D. Pereira, C.D. Leal, R. Davenport, D. Werner, C.R. Mota Filho, T. Bressani-Ribeiro, C.A. de Lemos Chernicharo, J.C. de Araujo, Effect of temperature on microbial diversity and nitrogen removal performance of an anammox reactor treating anaerobically pretreated municipal wastewater, Bioresource technology 258 (2018) 208-219.
[188] X. Huang, P.-H. Lee, Shortcut nitrification/denitrification through limited-oxygen supply with two extreme COD/N-and-ammonia active landfill leachates, Chemical Engineering Journal 404 (2021) 126511. https://doi.org/https://doi.org/10.1016/j.cej.2020.126511.
[189] L. Cheng, H. Liang, W. Yang, T. Yang, T. Chen, D. Gao, The biochar/Fe-modified biocarrier driven simultaneous NDFO and Feammox to remove nitrogen from eutrophic water, Water Research 243 (2023) 120280. https://doi.org/https://doi.org/10.1016/j.watres.2023.120280.
[190] L. Qiao, Y. Yuan, C. Mei, W. Yin, C. Zou, Y. Yin, Q. Guo, T. Chen, C. Ding, Reinforced nitrite supplement by cathode nitrate reduction with a bio-electrochemical system coupled anammox reactor, Environmental Research 204 (2022) 112051. https://doi.org/https://doi.org/10.1016/j.envres.2021.112051.
[191] N. Ward, J.T. Staley, J.A. Fuerst, S. Giovannoni, H. Schlesner, E. Stackebrandt, The order planctomycetales, including the genera planctomyces, pirellula, gemmata and Isosphaera and the candidatus genera brocadia, kuenenia and scalindua, Prokaryotes 7 (2006) 757-793.
[192] T. Song, X. Zhang, J. Li, The formation and distinct characteristics of aerobic granular sludge with filamentous bacteria in low strength wastewater, Bioresource Technology 360 (2022) 127409. https://doi.org/https://doi.org/10.1016/j.biortech.2022.127409.
[193] M. Geng, S. You, H. Guo, F. Ma, X. Xiao, X. Ma, Co-existence of flocs and granules in aerobic granular sludge system: Performance, microbial community and proteomics, Chemical Engineering Journal 451 (2023) 139011. https://doi.org/https://doi.org/10.1016/j.cej.2022.139011.
[194] B. Li, Y. Wang, X. Li, Z. Zhang, H. Wang, Y. Li, L. Wu, J. Li, Comparing the nitrogen removal performance and microbial communities of flocs-granules hybrid and granule-based CANON systems, Science of The Total Environment 703 (2020) 134949. https://doi.org/https://doi.org/10.1016/j.scitotenv.2019.134949.
[195] M.-K.H. Winkler, M.C.M. van Loosdrecht, Intensifying existing urban wastewater, Science 375(6579) (2022) 377-378. https://doi.org/doi:10.1126/science.abm3900.
[196] D. Wu, B. Zhao, P. Zhang, Q. An, Insight into the effect of nitrate on AGS granulation: Granular characteristics, microbial community and metabolomics response, Water Research 236 (2023) 119949. https://doi.org/https://doi.org/10.1016/j.watres.2023.119949.
[197] S.P. Wei, H.D. Stensel, R.M. Ziels, S. Herrera, P.-H. Lee, M.-K.H. Winkler, Partitioning of nutrient removal contribution between granules and flocs in a hybrid granular activated sludge system, Water Research 203 (2021) 117514. https://doi.org/https://doi.org/10.1016/j.watres.2021.117514.
[198] B. Long, X. Xuan, C. Yang, L. Zhang, Y. Cheng, J. Wang, Stability of aerobic granular

sludge in a pilot scale sequencing batch reactor enhanced by granular particle size control, Chemosphere 225 (2019) 460-469. https://doi.org/10.1016/J.CHEMOSPHERE.2019.03.048.
[199] X. Gu, J. Leng, J. Zhu, K. Zhang, J. Zhao, P. Wu, Q. Xing, K. Tang, X. Li, B. Hu, Influence mechanism of C/N ratio on heterotrophic nitrification- aerobic denitrification process, Bioresource Technology 343 (2022) 126116. https://doi.org/https://doi.org/10.1016/j.biortech.2021.126116.
[200] D.H. Parks, G.W. Tyson, P. Hugenholtz, R.G. Beiko, STAMP: statistical analysis of taxonomic and functional profiles, Bioinformatics 30(21) (2014) 3123-3124.
[201] Y. Liu, T. Zhao, Z. Su, T. Zhu, B.-J. Ni, Evaluating the roles of coexistence of sludge flocs on nitrogen removal and nitrous oxide production in a granule-based autotrophic nitrogen removal system, Science of The Total Environment 730 (2020) 139018. https://doi.org/https://doi.org/10.1016/j.scitotenv.2020.139018.
[202] Z. Pan, J. Zhou, Z. Lin, Y. Wang, P. Zhao, J. Zhou, S. Liu, X. He, Effects of COD/TN ratio on nitrogen removal efficiency, microbial community for high saline wastewater treatment based on heterotrophic nitrification-aerobic denitrification process, Bioresource Technology 301 (2020) 122726. https://doi.org/https://doi.org/10.1016/j.biortech.2019.122726.
[203] J.-L. Zhuang, X. Sun, W.-Q. Zhao, X. Zhang, J.-J. Zhou, B.-J. Ni, Y.-D. Liu, J.P. Shapleigh, W. Li, The anammox coupled partial-denitrification process in an integrated granular sludge and fixed-biofilm reactor developed for mainstream wastewater treatment: Performance and community structure, Water Research 210 (2022) 117964. https://doi.org/https://doi.org/10.1016/j.watres.2021.117964.
[204] F.O. Ajibade, W.-X. Yin, A. Guadie, T.F. Ajibade, Y. Liu, M.N. Kumwimba, W.-Z. Liu, J.-L. Han, H.-C. Wang, A.-J. Wang, Impact of biochar amendment on antibiotic removal and ARGs accumulation in constructed wetlands for low C/N wastewater treatment, Chemical Engineering Journal 459 (2023) 141541. https://doi.org/https://doi.org/10.1016/j.cej.2023.141541.
[205] C.C. Mefferd, E. Zhou, C.O. Seymour, N.A. Bernardo, S. Srivastava, A.J. Bengtson, J.-Y. Jiao, H. Dong, W.-J. Li, B.P. Hedlund, Incomplete denitrification phenotypes in diverse Thermus species from diverse geothermal spring sediments and adjacent soils in southwest China, Extremophiles 26(2) (2022) 23. https://doi.org/10.1007/s00792-022-01272-1.
[206] Z. Feng, G. Wu, Start-up of anammox systems with different feeding patterns: System performance, microbial community and potential microbial interactions, Journal of Water Process Engineering 39 (2021) 101694. https://doi.org/https://doi.org/10.1016/j.jwpe.2020.101694.
[207] M. Song, L. Jiang, D. Zhang, C. Luo, H. Yin, Y. Li, G. Zhang, Identification of biphenyl-metabolising microbes in activated biosludge using cultivation-independent and -dependent approaches, Journal of Hazardous Materials 353 (2018) 534-541. https://doi.org/https://doi.org/10.1016/j.jhazmat.2018.04.028.
[208] R.A. Hamza, Z. Sheng, O.T. Iorhemen, M.S. Zaghloul, J.H. Tay, Impact of food-to-microorganisms ratio on the stability of aerobic granular sludge treating high-strength organic wastewater, Water Research 147 (2018) 287-298. https://doi.org/https://doi.org/10.1016/j.watres.2018.09.061.
[209] M. Atasoy, W.T. Scott Jr, K. van Gijn, J.J. Koehorst, H. Smidt, A.A.M. Langenhoff, Microbial dynamics and bioreactor performance are interlinked with organic matter removal from wastewater treatment plant effluent, Bioresource Technology 372 (2023) 128659. https://doi.org/https://doi.org/10.1016/j.biortech.2023.128659.
[210] Y. Guo, Q. Niu, T. Sugano, Y.-Y. Li, Biodegradable organic matter-containing ammonium wastewater treatment through simultaneous partial nitritation, anammox, denitrification and COD

oxidization process, Science of The Total Environment 714 (2020) 136740. https://doi.org/https://doi.org/10.1016/j.scitotenv.2020.136740.
[211] S.-P. Wang, L. Wang, Z.-Y. Sun, S.-T. Wang, C.-H. Shen, Y.-Q. Tang, K. Kida, Biochar addition reduces nitrogen loss and accelerates composting process by affecting the core microbial community during distilled grain waste composting, Bioresource Technology 337 (2021) 125492. https://doi.org/https://doi.org/10.1016/j.biortech.2021.125492.
[212] C. Sanchez-Huerta, L. Fortunato, T. Leiknes, P.Y. Hong, Influence of biofilm thickness on the removal of thirteen different organic micropollutants via a Membrane Aerated Biofilm Reactor (MABR), Journal of Hazardous Materials 432 (2022) 128698. https://doi.org/https://doi.org/10.1016/j.jhazmat.2022.128698.
[213] I.S. Kulichevskaya, A.A. Ivanova, N.E. Suzina, W.I.C. Rijpstra, J.S. Sinninghe Damsté, S.N. Dedysh, Paludisphaera borealis gen. nov., sp. nov., a hydrolytic planctomycete from northern wetlands, and proposal of Isosphaeraceae fam. nov, International Journal of Systematic and Evolutionary Microbiology 66(2) (2016) 837-844.
[214] H. Zhao, Y. Guo, Z. Zhang, H. Sun, X. Wang, S. Li, J. Liao, Y.-Y. Li, Q. Wang, The stable operation of nitritation process with the continuous granular sludge-type reactor and microbial community analysis, Chemosphere 345 (2023) 140527. https://doi.org/https://doi.org/10.1016/j.chemosphere.2023.140527.
[215] C.N. Freeman, J.N. Russell, C.K. Yost, Temporal metagenomic characterization of microbial community structure and nitrogen modification genes within an activated sludge bioreactor system, Microbiology Spectrum 12(1) (2024) e02832-23.
[216] W. Lin, F. Fan, G. Xu, K. Gong, X. Cheng, X. Yuan, C. Zhang, Y. Gao, S. Wang, H.Y. Ng, Y. Dong, Microbial community assembly responses to polycyclic aromatic hydrocarbon contamination across water and sediment habitats in the Pearl River Estuary, Journal of Hazardous Materials 457 (2023) 131762. https://doi.org/https://doi.org/10.1016/j.jhazmat.2023.131762.
[217] P. Wang, H. Peng, S. Adhikari, B. Higgins, P. Roy, W. Dai, X. Shi, Enhancement of biogas production from wastewater sludge via anaerobic digestion assisted with biochar amendment, Bioresource Technology 309 (2020) 123368. https://doi.org/https://doi.org/10.1016/j.biortech.2020.123368.
[218] Z. Liu, Y. Zhu, C. Zhao, C. Zhang, J. Ming, A. Sharma, G. Chen, Y. Yang, Light stimulation strategy for promoting bio-hydrogen production: Microbial community, metabolic pathway and long-term application, Bioresource Technology 350 (2022) 126902. https://doi.org/https://doi.org/10.1016/j.biortech.2022.126902.
[219] D. Liang, W. Guo, D. Li, F. Ding, P. Li, Z. Zheng, J. Li, Enhanced aerobic granulation for treating low-strength wastewater in an anaerobic-aerobic-anoxic sequencing batch reactor by selecting slow-growing organisms and adding carriers, Environmental Research 205 (2022) 112547-112547. https://doi.org/10.1016/J.ENVRES.2021.112547.
[220] Y.Q. Liu, J.H. Tay, Fast formation of aerobic granules by combining strong hydraulic selection pressure with overstressed organic loading rate, Water Research 80 (2015) 256-266. https://doi.org/10.1016/J.WATRES.2015.05.015.
[221] E. Bolyen, J.R. Rideout, M.R. Dillon, N.A. Bokulich, C.C. Abnet, G.A. Al-Ghalith, H. Alexander, E.J. Alm, M. Arumugam, F. Asnicar, Y. Bai, J.E. Bisanz, K. Bittinger, A. Brejnrod, C.J. Brislawn, C.T. Brown, B.J. Callahan, A.M. Caraballo-Rodríguez, J. Chase, E.K. Cope, R. Da Silva, C. Diener, P.C. Dorrestein, G.M. Douglas, D.M. Durall, C. Duvallet, C.F. Edwardson, M. Ernst, M. Estaki, J. Fouquier, J.M. Gauglitz, S.M. Gibbons, D.L. Gibson, A. Gonzalez, K. Gorlick, J. Guo, B. Hillmann, S. Holmes, H. Holste, C. Huttenhower, G.A. Huttley, S. Janssen, A.K.

Jarmusch, L. Jiang, B.D. Kaehler, K.B. Kang, C.R. Keefe, P. Keim, S.T. Kelley, D. Knights, I. Koester, T. Kosciolek, J. Kreps, M.G.I. Langille, J. Lee, R. Ley, Y.X. Liu, E. Loftfield, C. Lozupone, M. Maher, C. Marotz, B.D. Martin, D. McDonald, L.J. McIver, A.V. Melnik, J.L. Metcalf, S.C. Morgan, J.T. Morton, A.T. Naimey, J.A. Navas-Molina, L.F. Nothias, S.B. Orchanian, T. Pearson, S.L. Peoples, D. Petras, M.L. Preuss, E. Pruesse, L.B. Rasmussen, A. Rivers, M.S. Robeson, P. Rosenthal, N. Segata, M. Shaffer, A. Shiffer, R. Sinha, S.J. Song, J.R. Spear, A.D. Swafford, L.R. Thompson, P.J. Torres, P. Trinh, A. Tripathi, P.J. Turnbaugh, S. Ul-Hasan, J.J.J. van der Hooft, F. Vargas, Y. Vázquez-Baeza, E. Vogtmann, M. von Hippel, W. Walters, Y. Wan, M. Wang, J. Warren, K.C. Weber, C.H.D. Williamson, A.D. Willis, Z.Z. Xu, J.R. Zaneveld, Y. Zhang, Q. Zhu, R. Knight, J.G. Caporaso, Reproducible, interactive, scalable and extensible microbiome data science using QIIME 2, Nature Biotechnology 2019 37:8 37(8) (2019) 852-857. https://doi.org/10.1038/s41587-019-0209-9.
[222] N. Risgaard-Petersen, M.H. Nicolaisen, N.P. Revsbech, B.A. Lomstein, Competition between ammonia-oxidizing bacteria and benthic microalgae, Applied and Environmental Microbiology 70(9) (2004) 5528-5537. https://doi.org/10.1128/AEM.70.9.5528-5537.2004.
[223] H.M. Dionisi, A.C. Layton, G. Harms, I.R. Gregory, K.G. Robinson, G.S. Sayler, Quantification of Nitrosomonas oligotropha-like ammonia-oxidizing bacteria and nitrospira spp. from full-scale wastewater treatment plants by competitive PCR, Applied and Environmental Microbiology 68(1) (2002) 245-253. https://doi.org/10.1128/AEM.68.1.245-253.2002.
[224] G. Braker, A. Fesefeldt, K.P. Witzel, Development of PCR primer systems for amplification of nitrite reductase genes (nirK and nirS) to detect denitrifying bacteria in environmental samples, Applied and Environmental Microbiology 64(10) (1998) 3769-3775. https://doi.org/10.1128/AEM.64.10.3769-3775.1998.
[225] S. Henry, E. Baudoin, J.C. López-Gutiérrez, F. Martin-Laurent, A. Brauman, L. Philippot, Quantification of denitrifying bacteria in soils by nirK gene targeted real-time PCR, Journal of Microbiological Methods 59(3) (2004) 327-335. https://doi.org/10.1016/J.MIMET.2004.07.002.
[226] A.I. Gomes, S.G.S. Santos, T.F.C.V. Silva, R.A.R. Boaventura, V.J.P. Vilar, Treatment train for mature landfill leachates: Optimization studies, Science of The Total Environment 673 (2019) 470-479. https://doi.org/10.1016/J.SCITOTENV.2019.04.027.
[227] R. Campo, S. Sguanci, S. Caffaz, L. Mazzoli, M. Ramazzotti, C. Lubello, T. Lotti, Efficient carbon, nitrogen and phosphorus removal from low C/N real domestic wastewater with aerobic granular sludge, Bioresource Technology 305 (2020) 122961-122961. https://doi.org/10.1016/J.BIORTECH.2020.122961.
[228] Y.V. Nancharaiah, M. Sarvajith, Granular stability, nitrogen and phosphorus removal pathways of aerobic granular sludge treating real municipal wastewater at different temperatures, Journal of Environmental Chemical Engineering 11(5) (2023) 110769-110769. https://doi.org/10.1016/J.JECE.2023.110769.
[229] L. Yan, S. Zhang, G. Hao, X. Zhang, Y. Ren, Y. Wen, Y. Guo, Y. Zhang, Simultaneous nitrification and denitrification by EPSs in aerobic granular sludge enhanced nitrogen removal of ammonium-nitrogen-rich wastewater, Bioresource Technology 202 (2016) 101-106. https://doi.org/10.1016/J.BIORTECH.2015.11.088.
[230] G. Yilmaz, R. Lemaire, J. Keller, Z. Yuan, Simultaneous nitrification, denitrification, and phosphorus removal from nutrient-rich industrial wastewater using granular sludge, Biotechnology and Bioengineering 100(3) (2008) 529-541. https://doi.org/10.1002/BIT.21774.
[231] W. Zhang, Y. Peng, L. Zhang, X. Li, Q. Zhang, Simultaneous partial nitritation and denitritation coupled with polished anammox for advanced nitrogen removal from low C/N

domestic wastewater at low dissolved oxygen conditions, Bioresource Technology 305(123045) (2020). https://doi.org/10.1016/j.biortech.2020.123045.
[232] D.M. Graham, D. Jolis, Pilot-Scale Evaluation of pH-Based Control of Single Stage Deammonification Processes for Sidestream Treatment, Water Environment Research 89(2) (2017) 99-104. https://doi.org/10.2175/106143016X14798353399377.
[233] F. Veuillet, S. Lacroix, A. Bausseron, E. Gonidec, J. Ochoa, M. Christensson, R. Lemaire, Integrated fixed-film activated sludge ANITA™Mox process - A new perspective for advanced nitrogen removal, Water Science and Technology 69(5) (2014) 915-922. https://doi.org/10.2166/wst.2013.786.
[234] X. Zhou, Z. Zhang, X. Zhang, Y. Liu, A novel single-stage process integrating simultaneous COD oxidation, partial nitritation-denitritation and anammox (SCONDA) for treating ammonia-rich organic wastewater, Bioresource Technology 254 (2018) 50-55. https://doi.org/10.1016/j.biortech.2018.01.057.
[235] Y.V.S.M. Nancharaiah, T.V.K. Mohan, Aerobic granular sludge: the future of wastewater treatment, Current Science 117(3) (2019) 395-404.
[236] H. Vashi, O.T. Iorhemen, J.H. Tay, Extensive studies on the treatment of pulp mill wastewater using aerobic granular sludge (AGS) technology, Chemical Engineering Journal 359 (2019) 1175-1194. https://doi.org/10.1016/J.CEJ.2018.11.060.
[237] X.T. Wang, H. Yang, Y. Su, X.Y. Liu, Characteristics and mechanism of anammox granular sludge with different granule size in high load and low rising velocity sewage treatment, Bioresource Technology 312 (2020). https://doi.org/10.1016/J.BIORTECH.2020.123608.
[238] X. Li, J. Luo, G. Guo, H.R. Mackey, T. Hao, G. Chen, Seawater-based wastewater accelerates development of aerobic granular sludge: A laboratory proof-of-concept, Water Research 115 (2017) 210-219. https://doi.org/10.1016/J.WATRES.2017.03.002.
[239] X.M. Liu, G.P. Sheng, H.W. Luo, F. Zhang, S.J. Yuan, J. Xu, R.J. Zeng, J.G. Wu, H.Q. Yu, Contribution of extracellular polymeric substances (EPS) to the sludge aggregation, Environmental Science and Technology 44(11) (2010) 4355-4360. https://doi.org/10.1021/ES9016766/SUPPL_FILE/ES9016766_SI_001.PDF.
[240] Y. Wang, J. Wang, Z. Liu, X. Huang, F. Fang, J. Guo, P. Yan, Effect of EPS and its forms of aerobic granular sludge on sludge aggregation performance during granulation process based on XDLVO theory, Science of The Total Environment 795 (2021) 148682-148682. https://doi.org/10.1016/J.SCITOTENV.2021.148682.
[241] T. Peng, Y. Wang, J. Wang, F. Fang, P. Yan, Z. Liu, Effect of different forms and components of EPS on sludge aggregation during granulation process of aerobic granular sludge, Chemosphere 303 (2022) 135116-135116. https://doi.org/10.1016/J.CHEMOSPHERE.2022.135116.
[242] Q. He, H. Wang, L. Chen, S. Gao, W. Zhang, J. Song, J. Yu, Robustness of an aerobic granular sludge sequencing batch reactor for low strength and salinity wastewater treatment at ambient to winter temperatures, Journal of Hazardous Materials 384 (2020) 121454-121454. https://doi.org/10.1016/J.JHAZMAT.2019.121454.
[243] L. Zhu, J. Zhou, M. Lv, H. Yu, H. Zhao, X. Xu, Specific component comparison of extracellular polymeric substances (EPS) in flocs and granular sludge using EEM and SDS-PAGE, Chemosphere 121 (2015) 26-32. https://doi.org/10.1016/J.CHEMOSPHERE.2014.10.053.
[244] S.F. Corsino, M. Capodici, F. Di Pippo, V. Tandoi, M. Torregrossa, Comparison between kinetics of autochthonous marine bacteria in activated sludge and granular sludge systems at different salinity and SRTs, Water Research 148 (2019) 425-437.

https://doi.org/10.1016/J.WATRES.2018.10.086.
[245] M. Layer, M.G. Villodres, A. Hernandez, E. Reynaert, E. Morgenroth, N. Derlon, Limited simultaneous nitrification-denitrification (SND) in aerobic granular sludge systems treating municipal wastewater: Mechanisms and practical implications, Water Research X 7 (2020) 100048-100048. https://doi.org/10.1016/J.WROA.2020.100048.
[246] X. Zou, M. Gao, A. Mohammed, Y. Liu, Responses of various carbon to nitrogen ratios to microbial communities, kinetics, and nitrogen metabolic pathways in aerobic granular sludge reactor, Bioresource Technology 367 (2023) 128225-128225. https://doi.org/10.1016/J.BIORTECH.2022.128225.
[247] N. Frison, E. Katsou, S. Malamis, D. Bolzonella, F. Fatone, Biological nutrients removal via nitrite from the supernatant of anaerobic co-digestion using a pilot-scale sequencing batch reactor operating under transient conditions, Chemical Engineering Journal 230 (2013) 595-604. https://doi.org/10.1016/J.CEJ.2013.06.071.
[248] H. Liang, D. Ye, P. Li, T. Su, J. Wu, L. Luo, Evolution of bacterial consortia in an integrated tannery wastewater treatment process, RSC Advances 6(90) (2016) 87380-87388. https://doi.org/10.1039/C6RA19603A.
[249] J. Luo, T. Hao, L. Wei, H.R. Mackey, Z. Lin, G.H. Chen, Impact of influent COD/N ratio on disintegration of aerobic granular sludge, Water Research 62 (2014) 127-135. https://doi.org/10.1016/J.WATRES.2014.05.037.
[250] A. Carucci, G. Cappai, G. Erby, S. Milia, Aerobic granular sludge formation in a sequencing batch reactor treating agro-industrial digestate, Environmental Technology 42(25) (2021) 3932-3941. https://doi.org/10.1080/09593330.2020.1769742.
[251] S. Ren, Z. Wang, H. Jiang, J. Qiu, X. Li, Q. Zhang, Y. Peng, Stable nitritation of mature landfill leachate via in-situ selective inhibition by free nitrous acid, Bioresource Technology 340 (2021) 125647-125647. https://doi.org/10.1016/J.BIORTECH.2021.125647.
[252] B. Wang, M. Zhao, Y. Guo, Y. Peng, Y. Yuan, Long-term partial nitritation and microbial characteristics in treating low C/N ratio domestic wastewater, Environmental Science: Water Research & Technology 4(6) (2018) 820-827. https://doi.org/10.1039/C8EW00009C.
[253] P. Wijekoon, P.A. Koliyabandara, A.T. Cooray, S.S. Lam, B.C.L. Athapattu, M. Vithanage, Progress and prospects in mitigation of landfill leachate pollution: Risk, pollution potential, treatment and challenges, Journal of Hazardous Materials 421 (2022). https://doi.org/10.1016/J.JHAZMAT.2021.126627.
[254] Z. Chen, X. Wang, Y.Y. Yang, M.W. Mirino, Y. Yuan, Partial nitrification and denitrification of mature landfill leachate using a pilot-scale continuous activated sludge process at low dissolved oxygen, Bioresource Technology 218 (2016) 580-588. https://doi.org/10.1016/J.BIORTECH.2016.07.008.
[255] X. Huang, P.H. Lee, Shortcut nitrification/denitrification through limited-oxygen supply with two extreme COD/N-and-ammonia active landfill leachates, Chemical Engineering Journal 404 (2021) 126511-126511. https://doi.org/10.1016/J.CEJ.2020.126511.
[256] D. Kulikowska, K. Bernat, Nitritation-denitritation in landfill leachate with glycerine as a carbon source, Bioresource Technology 142 (2013) 297-303. https://doi.org/10.1016/j.biortech.2013.04.119.
[257] J. Li, Q. Du, H. Peng, Y. Zhang, Y. Bi, Y. Shi, Y. Xu, T. Liu, Optimization of biochemical oxygen demand to total nitrogen ratio for treating landfill leachate in a single-stage partial nitrification-denitrification system, Journal of Cleaner Production 266 (2020) 121809-121809. https://doi.org/10.1016/J.JCLEPRO.2020.121809.

[258] D. Bove, S. Merello, D. Frumento, S.A. Arni, B. Aliakbarian, A. Converti, A Critical Review of Biological Processes and Technologies for Landfill Leachate Treatment, Chemical Engineering & Technology 38(12) (2015) 2115-2126. https://doi.org/10.1002/CEAT.201500257.
[259] D. Kulikowska, T. Jóźwiak, P. Kowal, S. Ciesielski, Municipal landfill leachate nitrification in RBC biofilm – Process efficiency and molecular analysis of microbial structure, Bioresource Technology 101(10) (2010) 3400-3405. https://doi.org/10.1016/J.BIORTECH.2009.12.050.
[260] N. Remmas, P. Melidis, I. Zerva, J.B. Kristoffersen, S. Nikolaki, G. Tsiamis, S. Ntougias, Dominance of candidate Saccharibacteria in a membrane bioreactor treating medium age landfill leachate: Effects of organic load on microbial communities, hydrolytic potential and extracellular polymeric substances, Bioresource Technology 238 (2017) 48-56. https://doi.org/10.1016/J.BIORTECH.2017.04.019.
[261] E. Syron, M.J. Semmens, E. Casey, Performance analysis of a pilot-scale membrane aerated biofilm reactor for the treatment of landfill leachate, Chemical Engineering Journal 273 (2015) 120-129. https://doi.org/10.1016/J.CEJ.2015.03.043.
[262] J. Xiong, Z. Zheng, X. Yang, J. He, X. Luo, B. Gao, Mature landfill leachate treatment by the MBBR inoculated with biocarriers from a municipal wastewater treatment plant, Process Safety and Environmental Protection 119 (2018) 304-310. https://doi.org/10.1016/J.PSEP.2018.08.019.
[263] R. De Freitas Bueno, J.K. Faria, D. Pinheiro, U. Vitor, S. Liduino, D.P. Uliana, V.S. Liduino, Simultaneous removal of organic matter and nitrogen compounds from landfill leachate by aerobic granular sludge, Environmental Technology 42(24) (2020) 3756-3770. https://doi.org/10.1080/09593330.2020.1740798.
[264] S. Louca, L.W. Parfrey, M. Doebeli, Decoupling function and taxonomy in the global ocean microbiome, Science 353(6305) (2016) 1272-1277. https://doi.org/10.1126/SCIENCE.AAF4507/SUPPL_FILE/LOUCA.SM.PDF.
[265] H. Jiang, P. Yang, Z. Wang, S. Ren, J. Qiu, H. Liang, Y. Peng, X. Li, Q. Zhang, Efficient and advanced nitrogen removal from mature landfill leachate via combining nitritation and denitritation with Anammox in a single sequencing batch biofilm reactor, Bioresource Technology 333 (2021) 125138-125138. https://doi.org/10.1016/J.BIORTECH.2021.125138.
[266] F. Zhang, Y. Peng, Z. Wang, H. Jiang, S. Ren, J. Qiu, New insights into co-treatment of mature landfill leachate with municipal sewage via integrated partial nitrification, Anammox and denitratation, Journal of Hazardous Materials 415 (2021) 125506-125506. https://doi.org/10.1016/J.JHAZMAT.2021.125506.
[267] J.A. Torà, J.A. Baeza, J. Carrera, J.A. Oleszkiewicz, Denitritation of a high-strength nitrite wastewater in a sequencing batch reactor using different organic carbon sources, Chemical Engineering Journal 172(2-3) (2011) 994-998. https://doi.org/10.1016/J.CEJ.2011.07.013.
[268] Y. Guo, Z. Zhang, W. Shi, B. Zhang, W. Li, F. Cui, P.N.L. Lens, Evolution of the sludge mineral composition enhances operation performance of the aerobic granular sludge reactor coupled with iron electrolysis, Journal of Cleaner Production 295 (2021) 126394-126394. https://doi.org/10.1016/J.JCLEPRO.2021.126394.
[269] Y.C. Juang, S.S. Adav, D.J. Lee, J.H. Tay, Stable aerobic granules for continuous-flow reactors: Precipitating calcium and iron salts in granular interiors, Bioresource Technology 101(21) (2010) 8051-8057. https://doi.org/10.1016/J.BIORTECH.2010.05.078.
[270] K. Naka, H. Cölfen, K. Naka, T. Okamura, A. Onoda, Biomineralization II: Mineralization Using Synthetic Polymers and Templates, (2007).
[271] M. Ahnert, T. Schalk, H. Brückner, J. Effenberger, V. Kuehn, P. Krebs, Organic matter

parameters in WWTP – a critical review and recommendations for application in activated sludge modelling, Water Science and Technology 84(9) (2021) 2093-2112. https://doi.org/10.2166/WST.2021.419.
[272] E.J.H. van Dijk, M. Pronk, M.C.M. van Loosdrecht, Controlling effluent suspended solids in the aerobic granular sludge process, Water Research 147 (2018) 50-59. https://doi.org/10.1016/J.WATRES.2018.09.052.
[273] M. Pronk, M.K. de Kreuk, B. de Bruin, P. Kamminga, R. Kleerebezem, M.C.M. van Loosdrecht, Full scale performance of the aerobic granular sludge process for sewage treatment, Water Research 84 (2015) 207-217. https://doi.org/10.1016/J.WATRES.2015.07.011.
[274] A. Sharaf, B. Guo, Y. Liu, Impact of the filamentous fungi overgrowth on the aerobic granular sludge process, Bioresource Technology Reports 7 (2019) 100272-100272. https://doi.org/10.1016/J.BITEB.2019.100272.
[275] X. Ren, Y. Chen, L. Guo, Z. She, M. Gao, Y. Zhao, M. Shao, The influence of Fe2+, Fe3+ and magnet powder (Fe3O4) on aerobic granulation and their mechanisms, Ecotoxicology and Environmental Safety 164 (2018) 1-11. https://doi.org/10.1016/J.ECOENV.2018.07.072.
[276] B. Nguyen Quoc, M. Armenta, J.A. Carter, R. Bucher, P. Sukapanpotharam, S.J. Bryson, D.A. Stahl, H.D. Stensel, M.K.H. Winkler, An investigation into the optimal granular sludge size for simultaneous nitrogen and phosphate removal, Water Research 198 (2021) 117119-117119. https://doi.org/10.1016/J.WATRES.2021.117119.
[277] D. Scaglione, G. Tornotti, A. Teli, L. Lorenzoni, E. Ficara, R. Canziani, F. Malpei, Nitrification denitrification via nitrite in a pilot-scale SBR treating the liquid fraction of co-digested piggery/poultry manure and agro-wastes, Chemical Engineering Journal 228 (2013) 935-943. https://doi.org/10.1016/j.cej.2013.05.075.
[278] Y. Shi, G. Wells, E. Morgenroth, Microbial activity balance in size fractionated suspended growth biomass from full-scale sidestream combined nitritation-anammox reactors, Bioresource Technology 218 (2016) 38-45. https://doi.org/10.1016/J.BIORTECH.2016.06.041.
[279] S. Aslan, M. Dahab, Nitritation and denitritation of ammonium-rich wastewater using fluidized-bed biofilm reactors, Journal of Hazardous Materials 156(1-3) (2008) 56-63. https://doi.org/10.1016/j.jhazmat.2007.11.112.
[280] X. Zou, Y. Zhou, B. Guo, Y. Shao, S. Yang, A. Mohammed, Y. Liu, Single reactor nitritation-denitritation for high strength digested biosolid thickening lagoon supernatant treatment, Biochemical Engineering Journal 160 (2020) 107630-107630. https://doi.org/10.1016/J.BEJ.2020.107630.
[281] W. Yin, K. Wang, J. Xu, D. Wu, C. Zhao, The performance and associated mechanisms of carbon transformation (PHAs, polyhydroxyalkanoates) and nitrogen removal for landfill leachate treatment in a sequencing batch biofilm reactor (SBBR), RSC Advances 8(74) (2018) 42329-42336. https://doi.org/10.1039/C8RA07839D.
[282] X. Wen, J. Zhou, J. Wang, X. Qing, Q. He, Effects of dissolved oxygen on microbial community of single-stage autotrophic nitrogen removal system treating simulating mature landfill leachate, Bioresource Technology 218 (2016) 962-968. https://doi.org/10.1016/J.BIORTECH.2016.07.023.
[283] C. Yan, F. Wang, H. Liu, H. Liu, S. Pu, F. Lin, H.G.E. …, Undefined, Deciphering the toxic effects of metals in gold mining area: Microbial community tolerance mechanism and change of antibiotic resistance genes, Environmental Research 189 (2020) 109869-109869.
[284] Q.Q. Zhang, B.H. Tian, X. Zhang, A. Ghulam, C.R. Fang, R. He, Investigation on characteristics of leachate and concentrated leachate in three landfill leachate treatment plants,

Waste Management 33(11) (2013) 2277-2286. https://doi.org/10.1016/J.WASMAN.2013.07.021.
[285] J.Y. Wang, X.L. An, F.Y. Huang, J.Q. Su, Antibiotic resistome in a landfill leachate treatment plant and effluent-receiving river, Chemosphere 242 (2020) 125207-125207. https://doi.org/10.1016/J.CHEMOSPHERE.2019.125207.
[286] S.S. Adav, D.J. Lee, J.Y. Lai, Microbial community of acetate utilizing denitrifiers in aerobic granules, Applied Microbiology and Biotechnology 85(3) (2010) 753-762. https://doi.org/10.1007/S00253-009-2263-6/FIGURES/7.
[287] Y. Pang, J.-L. Wang, S. Li, G. Ji, Activity of Autotrophic Fe(II)-Oxidizing Denitrifiers in Freshwater Lake Sediments, ACS ES&T Water 1(7) (2021) 1566-1576. https://doi.org/10.1021/ACSESTWATER.1C00075.
[288] P.M. Dove, J.J.D. Yoreo, S. Weiner, Biomineralization, 2018.
[289] Y. Hu, T. Liu, N. Chen, C. Feng, Changes in microbial community diversity, composition, and functions upon nitrate and Cr(VI) contaminated groundwater, Chemosphere 288 (2022) 132476-132476. https://doi.org/10.1016/J.CHEMOSPHERE.2021.132476.
[290] G. Sturm, S. Brunner, E. Suvorova, F. Dempwolff, J. Reiner, P. Graumann, R. Bernier-Latmani, J. Majzlan, J. Gescher, Chromate resistance mechanisms in Leucobacter chromiiresistens, Applied and Environmental Microbiology 84(23) (2018). https://doi.org/10.1128/AEM.02208-18/SUPPL_FILE/ZAM023188877S1.PDF.
[291] X. Chen, Q. Zhang, Y. Zhu, T. Zhao, Response of rotating biological contactor started up by heterotrophic nitrification-aerobic denitrification bacteria to various C/N ratios, Chemosphere 291 (2022) 133048-133048. https://doi.org/10.1016/J.CHEMOSPHERE.2021.133048.
[292] M. Conthe, P. Lycus, M. Arntzen, A. Ramos da Silva, Å. Frostegård, L.R. Bakken, R. Kleerebezem, M.C.M. van Loosdrecht, Denitrification as an N2O sink, Water Research 151 (2019) 381-387. https://doi.org/10.1016/j.watres.2018.11.087.
[293] G. Mohanakrishna, I.M. Abu-Reesh, D. Pant, Enhanced bioelectrochemical treatment of petroleum refinery wastewater with Labaneh whey as co-substrate, Scientific Reports 2020 10:1 10(1) (2020) 1-11. https://doi.org/10.1038/s41598-020-76668-0.
[294] D. Xu, H. Liu, Z. Yin, K. He, S. Song, Y. Chen, Y. Hu, C. Liu, Oxytetracycline co-metabolism with denitrification/desulfurization in SRB mediated system, Chemosphere 298 (2022) 134256-134256. https://doi.org/10.1016/J.CHEMOSPHERE.2022.134256.
[295] H. Lu, G. Zhang, Y. Lu, Y. Zhang, B. Li, W. Cao, Using co-metabolism to accelerate synthetic starch wastewater degradation and nutrient recovery in photosynthetic bacterial wastewater treatment technology, Environmental Technology 37(7) (2016) 775-784. https://doi.org/10.1080/09593330.2015.1084050.
[296] E.T. Sieradzki, E.E. Nuccio, J. Pett-Ridge, M.K. Firestone, Expression of macromolecular organic nitrogen degrading enzymes identifies potential mediators of soil organic N availability to an annual grass, The ISME Journal 2023 (2023) 1-9. https://doi.org/10.1038/s41396-023-01402-3.
[297] X. He, J. Yin, J. Liu, T. Chen, D. Shen, Characteristics of acidogenic fermentation for volatile fatty acid production from food waste at high concentrations of NaCl, Bioresource Technology 271 (2019) 244-250. https://doi.org/10.1016/J.BIORTECH.2018.09.116.
[298] H. Zhang, K. Zhang, H. Jin, L. Gu, X. Yu, Variations in dissolved organic nitrogen concentration in biofilters with different media during drinking water treatment, Chemosphere 139 (2015) 652-658. https://doi.org/10.1016/J.CHEMOSPHERE.2014.10.092.
[299] B.J. Ni, B.E. Rittmann, H.Q. Yu, Soluble microbial products and their implications in mixed culture biotechnology, Trends in Biotechnology 29(9) (2011) 454-463.

https://doi.org/10.1016/J.TIBTECH.2011.04.006.
[300] T. Dittmar, B. Koch, N. Hertkorn, G. Kattner, A simple and efficient method for the solid-phase extraction of dissolved organic matter (SPE-DOM) from seawater, Limnology and Oceanography: Methods 6(6) (2008) 230-235. https://doi.org/10.4319/LOM.2008.6.230.
[301] R. Li, L. Li, Z. Zhang, H. Chen, A.M. McKenna, G. Chen, Y. Tang, Speciation and conversion of carbon and nitrogen in young landfill leachate during anaerobic biological pretreatment, Waste Management 106 (2020) 88-98. https://doi.org/10.1016/J.WASMAN.2020.03.011.
[302] Y. Sun, X. Li, X. Li, J. Wang, Deciphering the Fingerprint of Dissolved Organic Matter in the Soil Amended with Biodegradable and Conventional Microplastics Based on Optical and Molecular Signatures, Environmental Science and Technology 56(22) (2022) 15746-15759. https://doi.org/10.1021/ACS.EST.2C06258/ASSET/IMAGES/LARGE/ES2C06258_0007.JPEG.
[303] X. Li, X. Huang, C. Zhao, X. Wang, B. Dong, A. Goonetilleke, K.H. Kim, Characterizing molecular transformation of dissolved organic matter during high-solid anaerobic digestion of dewatered sludge using ESI FT-ICR MS, Chemosphere 320 (2023) 138101-138101. https://doi.org/10.1016/J.CHEMOSPHERE.2023.138101.
[304] H. Eom, C. Park, Investigation of characteristics of effluent DON derived from conventional activated sludge (CAS) and predenitrification biological removal (BNR): In terms of proteins and humic substances, Environmental Research 196 (2021) 110912-110912. https://doi.org/10.1016/J.ENVRES.2021.110912.
[305] J. Gao, R. Wang, Y. Li, H. Huang, X. Su, Z. An, W. Yin, L. Yang, L. Rong, F. Sun, Effect of aeration modes on nitrogen removal and N2O emission in the partial nitrification and denitrification process for landfill leachate treatment, Science of The Total Environment 853 (2022) 158424-158424. https://doi.org/10.1016/J.SCITOTENV.2022.158424.
[306] Y. Zhang, J. Zhou, J. Zhang, S. Yuan, An innovative membrane bioreactor and packed-bed biofilm reactor combined system for shortcut nitrification-denitrification, Journal of Environmental Sciences 21(5) (2009) 568-574. https://doi.org/10.1016/S1001-0742(08)62309-8.
[307] A. Eldyasti, M. Andalib, H. Hafez, G. Nakhla, J. Zhu, Comparative modeling of biological nutrient removal from landfill leachate using a circulating fluidized bed bioreactor (CFBBR), Journal of Hazardous Materials 187(1-3) (2011) 140-149. https://doi.org/10.1016/J.JHAZMAT.2010.12.115.
[308] S. Li, H. Duan, Y. Zhang, X. Huang, Z. Yuan, Y. Liu, M. Zheng, Adaptation of nitrifying community in activated sludge to free ammonia inhibition and inactivation, Science of The Total Environment 728 (2020) 138713-138713. https://doi.org/10.1016/J.SCITOTENV.2020.138713.
[309] Z. Yuan, C. He, Q. Shi, C. Xu, Z. Li, C. Wang, H. Zhao, J. Ni, Molecular Insights into the Transformation of Dissolved Organic Matter in Landfill Leachate Concentrate during Biodegradation and Coagulation Processes Using ESI FT-ICR MS, Environmental Science and Technology 51(14) (2017) 8110-8118. https://doi.org/10.1021/ACS.EST.7B02194/ASSET/IMAGES/LARGE/ES-2017-02194M_0005.JPEG.
[310] G. Tang, B. Li, B. Zhang, C. Wang, G. Zeng, X. Zheng, C. Liu, Dynamics of dissolved organic matter and dissolved organic nitrogen during anaerobic/anoxic/oxic treatment processes, Bioresource Technology 331 (2021) 125026-125026. https://doi.org/10.1016/J.BIORTECH.2021.125026.
[311] H. Chen, K. Wang, S. She, X. Yu, L. Yu, G. Xue, X. Li, Insight into dissolved organic nitrogen transformation and characteristics: Focus on printing and dyeing wastewater treatment

process, Journal of Hazardous Materials 450 (2023) 131086-131086. https://doi.org/10.1016/J.JHAZMAT.2023.131086.
[312] H. Lu, K. Chandran, D. Stensel, Microbial ecology of denitrification in biological wastewater treatment, Water Research, Pergamon, 2014, pp. 237-254.
[313] C. Wang, Y. Liu, W. Lv, S. Xia, J. Han, Z. Wang, X. Yu, L. Cai, Enhancement of nitrogen removal by supplementing fluidized-carriers into the aerobic tank in a full-scale A2/O system, Science of The Total Environment 660 (2019) 817-825. https://doi.org/10.1016/J.SCITOTENV.2019.01.046.
[314] S. Sharma, A.B. Fulke, A. Chaubey, Bioprospection of marine actinomycetes: recent advances, challenges and future perspectives, Acta Oceanologica Sinica 2019 38:6 38(6) (2019) 1-17. https://doi.org/10.1007/S13131-018-1340-Z.
[315] H. Zhang, B. Ma, T. Huang, Y. Shi, Nitrate reduction by the aerobic denitrifying actinomycete Streptomyces sp. XD-11-6-2: Performance, metabolic activity, and micro-polluted water treatment, Bioresource Technology 326 (2021) 124779-124779. https://doi.org/10.1016/J.BIORTECH.2021.124779.
[316] M. Nierychlo, A. Miłobędzka, F. Petriglieri, B. McIlroy, P.H. Nielsen, S.J. McIlroy, The morphology and metabolic potential of the Chloroflexi in full-scale activated sludge wastewater treatment plants, FEMS Microbiology Ecology 95(2) (2019). https://doi.org/10.1093/FEMSEC/FIY228.
[317] B. Ji, Y. Shi, M. Yılmaz, Microalgal-bacterial granular sludge process for sustainable municipal wastewater treatment: Simple organics versus complex organics, Journal of Water Process Engineering 46 (2022) 102613-102613. https://doi.org/10.1016/J.JWPE.2022.102613.
[318] X.X. Li, X.S.X.S. Shi, M.Y.M.Y. Lu, Y.Z.Y.Z. Zhao, X.X. Li, H.P.B. Technology, Undefined, H. Peng, R.B. Guo, Succession of the bacterial community and functional characteristics during continuous thermophilic composting of dairy manure amended with recycled ceramsite, Bioresource Technology 294 (2019) 122044-122044. https://doi.org/10.1016/J.BIORTECH.2019.122044.
[319] H. Yuan, S. Huang, J. Yuan, Y. You, Y. Zhang, Characteristics of microbial denitrification under different aeration intensities: Performance, mechanism, and co-occurrence network, Science of The Total Environment 754 (2021) 141965-141965. https://doi.org/10.1016/J.SCITOTENV.2020.141965.
[320] B. Herzog, A. Dötsch, H. Lemmer, H. Horn, E. Müller, Profiling 5-tolyltriazole biodegrading sludge communities using next-generation sequencing and denaturing gradient gel electrophoresis, Systematic and Applied Microbiology 40(8) (2017) 508-515. https://doi.org/10.1016/J.SYAPM.2017.09.007.
[321] W. Xiong, L. Wang, N. Zhou, A. Fan, S. Wang, H. Su, High-strength anaerobic digestion wastewater treatment by aerobic granular sludge in a step-by-step strategy, Journal of Environmental Management 262 (2020) 110245-110245. https://doi.org/10.1016/J.JENVMAN.2020.110245.
[322] Y. Jiang, X. Shi, H.Y. Ng, Aerobic granular sludge systems for treating hypersaline pharmaceutical wastewater: Start-up, long-term performances and metabolic function, Journal of Hazardous Materials 412 (2021) 125229-125229. https://doi.org/10.1016/J.JHAZMAT.2021.125229.
[323] S. Li, S. Wang, M.H. Wong, M. Zaynab, K. Wang, L. Zhong, L. Ouyang, Changes in the composition of bacterial communities and pathogen levels during wastewater treatment, Environmental Science and Pollution Research 30(1) (2023) 1232-1243.

https://doi.org/10.1007/S11356-022-21947-8/FIGURES/5.
[324] X. Wang, M. Wang, J. Zhang, Z. Kong, X. Wang, D. Liu, Q. Shen, Contributions of the biochemical factors and bacterial community to the humification process of in situ large-scale aerobic composting, Bioresource Technology 323 (2021) 124599-124599. https://doi.org/10.1016/J.BIORTECH.2020.124599.
[325] J. Guo, J. Liu, Y. Yang, Y. Zhou, S. Jiang, C. Chen, Fermentation and kinetics characteristics of a bioflocculant from potato starch wastewater and its application OPEN, Scientific Reports 8(1) (2018) 1-11. https://doi.org/10.1038/s41598-018-21796-x.
[326] Q. Zhang, X. Zhao, W. Li, H. Chen, X. Zhu, H. Zhu, P. Zhang, Responses of short-chain fatty acids production to the addition of various biocarriers to sludge anaerobic fermentation, Bioresource Technology 304 (2020) 122989-122989. https://doi.org/10.1016/J.BIORTECH.2020.122989.
[327] C. Hui, R. Wei, H. Jiang, Y. Zhao, L. Xu, Characterization of the ammonification, the relevant protease production and activity in a high-efficiency ammonifier Bacillus amyloliquefaciens DT, International Biodeterioration & Biodegradation 142 (2019) 11-17. https://doi.org/10.1016/J.IBIOD.2019.04.009.
[328] J. Huang, Y. Pan, L. Liu, J. Liang, L. Wu, H. Zhu, P. Zhang, High salinity slowed organic acid production from acidogenic fermentation of kitchen wastewater by shaping functional bacterial community, Journal of Environmental Management 310 (2022) 114765-114765. https://doi.org/10.1016/J.JENVMAN.2022.114765.
[329] S. Gur-Reznik, I. Katz, C.G. Dosoretz, Removal of dissolved organic matter by granular-activated carbon adsorption as a pretreatment to reverse osmosis of membrane bioreactor effluents, Water Research 42(6-7) (2008) 1595-1605. https://doi.org/10.1016/J.WATRES.2007.10.004.
[330] H. Chang, C. Chen, G. Wang, Identification of potential nitrogenous organic precursors for C-, N-DBPs and characterization of their DBPs formation, Water Research 45(12) (2011) 3753-3764. https://doi.org/10.1016/J.WATRES.2011.04.027.
[331] R. Pishgar, J.A. Dominic, J.H. Tay, A. Chu, Pilot-scale investigation on nutrient removal characteristics of mineral-rich aerobic granular sludge: Identification of uncommon mechanisms, Water Research 168 (2020) 115151. https://doi.org/https://doi.org/10.1016/j.watres.2019.115151.
[332] C. Moragaspitiya, J. Rajapakse, G.J. Millar, Effect of Ca:Mg ratio and high ammoniacal nitrogen on characteristics of struvite precipitated from waste activated sludge digester effluent, Journal of Environmental Sciences 86 (2019) 65-77. https://doi.org/https://doi.org/10.1016/j.jes.2019.04.023.
[333] G.M. Douglas, V.J. Maffei, J.R. Zaneveld, S.N. Yurgel, J.R. Brown, C.M. Taylor, C. Huttenhower, M.G.I. Langille, PICRUSt2 for prediction of metagenome functions, Nature Biotechnology 38(6) (2020) 685-688. https://doi.org/10.1038/s41587-020-0548-6.
[334] W. Hu, Y. Zhou, X. Min, J. Liu, X. Li, L. Luo, J. Zhang, Q. Mao, L. Chai, Y. Zhou, The study of a pilot-scale aerobic/Fenton/anoxic/aerobic process system for the treatment of landfill leachate, Environmental technology 39(15) (2018) 1926-1936.
[335] J. Liu, A. Ali, J. Su, Z. Wu, R. Zhang, R. Xiong, Simultaneous removal of calcium, fluoride, nickel, and nitrate using microbial induced calcium precipitation in a biological immobilization reactor, Journal of Hazardous Materials 416 (2021) 125776. https://doi.org/https://doi.org/10.1016/j.jhazmat.2021.125776.
[336] W. Yang, H. Lu, S.K. Khanal, Q. Zhao, L. Meng, G.-H. Chen, Granulation of sulfur-oxidizing bacteria for autotrophic denitrification, Water Research 104 (2016) 507-519. https://doi.org/https://doi.org/10.1016/j.watres.2016.08.049.

[337] Y. Chen, J. Ge, S. Wang, H. Su, Insight into formation and biological characteristics of Aspergillus tubingensis-based aerobic granular sludge (AT-AGS) in wastewater treatment, Science of The Total Environment 739 (2020) 140128. https://doi.org/https://doi.org/10.1016/j.scitotenv.2020.140128.
[338] A. Mañas, B. Biscans, M. Spérandio, Biologically induced phosphorus precipitation in aerobic granular sludge process, Water Research 45(12) (2011) 3776-3786. https://doi.org/https://doi.org/10.1016/j.watres.2011.04.031.
[339] M. Turker, R.K. Dereli, Long term performance of a pilot scale anaerobic membrane bioreactor treating beet molasses based industrial wastewater, Journal of Environmental Management 278 (2021) 111403. https://doi.org/https://doi.org/10.1016/j.jenvman.2020.111403.
[340] Z. Lei, J. Xue, Y. Feng, Y.-Y. Li, Z. Kong, R. Chen, Sludge granulation in PN/A enhances nitrogen removal from mainstream anaerobically pretreated wastewater, Science of The Total Environment 895 (2023) 165048. https://doi.org/https://doi.org/10.1016/j.scitotenv.2023.165048.
[341] X. Gong, F. Hou, H. Pang, Y. Guo, Q. Zhang, X. Li, L. Zhang, Y. Peng, Robust and high-efficient nitrogen removal from real sewage and waste activated sludge (WAS) reduction in zero-external carbon PN/A combined with in-situ fermentation-denitrification process under decreased temperatures, Journal of Environmental Management 345 (2023) 118761. https://doi.org/https://doi.org/10.1016/j.jenvman.2023.118761.
[342] J. Guo, B.-J. Ni, X. Han, X. Chen, P. Bond, Y. Peng, Z. Yuan, Unraveling microbial structure and diversity of activated sludge in a full-scale simultaneous nitrogen and phosphorus removal plant using metagenomic sequencing, Enzyme and Microbial Technology 102 (2017) 16-25. https://doi.org/https://doi.org/10.1016/j.enzmictec.2017.03.009.
[343] C. Chen, M. Zhang, X. Yu, J. Mei, Y. Jiang, Y. Wang, T.C. Zhang, Effect of C/N ratios on nitrogen removal and microbial communities in the anaerobic baffled reactor (ABR) with an anammox-coupling-denitrification process, Water Science and Technology 78(11) (2018) 2338-2348.
[344] R. Diaz, B. Mackey, S. Chadalavada, J. kainthola, P. Heck, R. Goel, Enhanced Bio-P removal: Past, present, and future – A comprehensive review, Chemosphere 309 (2022) 136518. https://doi.org/https://doi.org/10.1016/j.chemosphere.2022.136518.
[345] D. Zeng, J. Miao, G. Wu, X. Zhan, Nitrogen removal, microbial community and electron transport in an integrated nitrification and denitrification system for ammonium-rich wastewater treatment, International Biodeterioration & Biodegradation 133 (2018) 202-209. https://doi.org/https://doi.org/10.1016/j.ibiod.2018.07.014.
[346] S. Cao, Y. Lan, R. Du, Y. Peng, Robustness and stability of acetate-driven partial denitrification (PD) in response to high COD/NO3−-N, Chemosphere 322 (2023) 138213. https://doi.org/https://doi.org/10.1016/j.chemosphere.2023.138213.
[347] R. Bian, Y. Sun, W. Li, Q. Ma, X. Chai, Co-composting of municipal solid waste mixed with matured sewage sludge: The relationship between N2O emissions and denitrifying gene abundance, Chemosphere 189 (2017) 581-589. https://doi.org/10.1016/J.CHEMOSPHERE.2017.09.070.
[348] Y. Zhao, Y. Dong, X. Chen, Z. Wang, Z. Cui, S.-Q. Ni, Using sulfide as nitrite oxidizing bacteria inhibitor for the successful coupling of partial nitrification-anammox and sulfur autotrophic denitrification in one reactor, Chemical Engineering Journal 475 (2023) 146286. https://doi.org/https://doi.org/10.1016/j.cej.2023.146286.
[349] Y. Bai, S. Wang, A. Zhussupbekova, I.V. Shvets, P.-H. Lee, X. Zhan, High-rate iron sulfide and sulfur-coupled autotrophic denitrification system: Nutrients removal performance and

microbial characterization, Water Research 231 (2023) 119619. https://doi.org/https://doi.org/10.1016/j.watres.2023.119619.
[350] W. Li, J. Gao, J.-l. Zhuang, G.-j. Yao, X. Zhang, Q.-k. Liu, J.P. Shapleigh, L. Ma, Metagenomics and metatranscriptomics uncover the microbial community associated with high S0 production in a denitrifying desulfurization granular sludge reactor, Water Research 203 (2021) 117505.
[351] K. Wang, M. Qaisar, B. Chen, J. Xiao, J. Cai, Metagenomic analysis of microbial community and metabolic pathway of simultaneous sulfide and nitrite removal process exposed to divergent hydraulic retention times, Bioresource Technology 354 (2022) 127186. https://doi.org/https://doi.org/10.1016/j.biortech.2022.127186.